UNIVERSIDAD COMPLUTENSE DE MADRID
FACULTAD DE CIENICAS QUÍMICAS
Departamento de Química Orgánica

TESIS DOCTORAL

Selectivity in fullerenes chemistry: catalytic and photovoltaic applications

Selectividad en química de fullerenos: aplicaciones catalíticas y fotovoltaicas

MEMORIA PARA OPTAR AL GRADO DE DOCTOR

PRESENTADA POR

Sara Vidal Estremera

Directores

Nazario Martín León
Salvatore Filippone

Madrid, 2018

UNIVERSIDAD COMPLUTENSE DE MADRID
FACULTAD DE CIENCIAS QUÍMICAS
Departamento de Química Orgánica

SELECTIVITY IN FULLERENES CHEMISTRY: CATALYTIC AND PHOTOVOLTAIC APPLICATIONS

SELECTIVIDAD EN QUÍMICA DE FULLERENOS: APLICACIONES CATALÍTICAS Y FOTOVOLTAICAS

TESIS DOCTORAL

Sara Vidal Estremera

Madrid, 2017

SELECTIVITY IN FULLERENES CHEMISTRY: CATALYTIC AND PHOTOVOLTAIC APPLICATIONS

SELECTIVIDAD EN QUÍMICA DE FULLERENOS: APLICACIONES CATALÍTICAS Y FOTOVOLTAICAS

Directores:

Dr. Nazario Martín León

Dr. Salvatore Filippone

Memoria que para optar al grado de

DOCTOR EN CIENCIAS QUÍMICAS

presenta

Sara Vidal Estremera

MADRID

Mayo, 2017

D. Nazario Martín León, Catedrático del Departamento de Química Orgánica de la Universidad Complutense de Madrid y D. Salvatore Filippone, Investigador del Departamento de Química Orgánica de la Universidad Complutense de Madrid.

CERTIFICAN:

Que la presente Memoria titulada “Selectivity in Fullerenes Chemistry: Catalytic and Photovoltaic Applications” se ha realizado bajo su dirección en el Departamento de Química Orgánica de la Universidad Complutense de Madrid, por la licenciada en Ciencias Químicas Dña. Sara Vidal Estremera y autorizan su presentación para ser calificada como tesis doctoral.

Y para que conste firmo el presente certificado en Madrid a 25 de Mayo de 2017.

Fdo. Dr. Nazario Martín

Fdo. Dr. Salvatore Filippone

The results presented in this thesis have been published and listed below:

1) D. Fernández, A. Viterisi, J. W. Ryan, F. Gispert-Guirado, S. Vidal, S. Filippone, N. Martín and E. Palomares, "Small molecule BHJ solar cells based on DPP(TBFu)2 and diphenylmethanofullerenes (DPM): linking morphology, transport, recombination and crystallinity" *Nanoscale*, **2014**, *6*, 5871-5878.

2) S. Vidal, M. Izquierdo, S. Filippone, F. G. Brunetti and N. Martín, "Reaction of diazocompounds with C_{70}: unprecedented synthesis and characterization of isomeric [5,6]-fulleroids" *Chem. Commun*. **2015**, *51*, 16774-16777.

3) S. Vidal, M. Izquierdo, W. K. Law, K. Jiang, S. Filippone, J. Perles, H. Yan and N. Martín, "Photochemical site-selective synthesis of [70]methanofullerenes" *Chem. Commun*. **2016**, *52*, 12733-12736.

4) J. Marco-Martínez, S. Vidal, I. Fernández, S. Filippone and N. Martín, "Stereodivergent-at-Metal Synthesis of [60]Fullerene Hybrids" *Angew. Chem. Int. Ed*. **2017**, *56*, 1–5.

5) S. Vidal, J. Marco-Martínez, S. Filippone and N. Martín, "Fullerenes for Catalysis: Metallofullerenes in Hydrogen Transfer Reactions" *Chem. Commun*. **2017**, DOI: 10.1039/C7CC01267E.

6) S. Vidal, M. Izquierdo, S. Alom, M. Garcia-Borràs, S. Filippone, S. Osuna, Miquel Solà, R. J. Whitby and N. Martín, "Effect of Incarcerated HF on the Chemical Reactivity of Endohedral HF@C_{60}" **submitted to *JACS***.

A mi madre

Acknowledgments

El presente trabajo ha sido realizado en el Departamento de Química Orgánica de la Universidad Complutense de Madrid bajo la dirección del Profesor Nazario Martín y el Dr. Salvatore Filippone.

En primer lugar me gustaría dar las gracias a mis directores,

Nazario, gracias por darme la oportunidad de formar parte de tu grupo de investigación. Gracias por tu confianza y por tu dedicación admirable en este trabajo. Como jefe eres increíble pero como persona eres aún mejor.

Salvo, muchísimas gracias por todo, no me imagino estar en un laboratorio sin ti. Gracias por sacar lo mejor de mí siempre, por tu paciencia y por tu ayuda incondicional. No creo que nunca tenga unos jefes tan increíbles como vosotros, he sido muy afortunada y ha sido un honor aprender de vosotros.

También me gustaría destacar a otros miembros del grupo que han contribuido en parte del trabajo descrito en esta memoria: Marta y Juan.

Martita, soy incapaz de escribir estas palabras sin que se me salten las lágrimas. Millones de gracias por todo, eres una persona increíble y un ejemplo para mí tanto en lo personal como en lo profesional. Gracias por todo lo que me has enseñado y por estar siempre a mi lado, te debo muchísimo, eres como una hermana para mí.

Juan, poder trabajar contigo y aprender de ti ha sido una suerte. Muchísimas gracias por tu paciencia y amistad, es imposible reflejar en unas líneas lo que significáis para mí. Ha sido un placer trabajar con vosotros.

En la realización de este trabajo han participado otros grupos de investigación, a los que agradezco enormemente su contribución:

Al grupo de investigación del profesor He Yan, Hong Kong University of Science and Technology, por los estudios sobre dispositivos fotovoltaicos que se recogen en la Memoria.

Al profesor Israel Fernández de la Universidad Complutense de Madrid, por los estudios teóricos sobre los híbridos quirales metal/fullereno.

Al grupo de investigación del profesor Richard J. Whitby, University of Southampton, por el suministro del endoédrico HF@C_{60}.

Al profesor Miquel Solà y su grupo de la Universidad de Girona por los estudios teóricos sobre la reactividad de la molécula HF@C_{60}.

Así mismo, quiero agradecer al personal de los diferentes CAIs de la Facultad de Ciencias Químicas de la UCM, en especial al CAI de RMN, a Lola, Elena y Ángel, su gran ayuda y dedicación.

Al CAI de Masas de la Facultad de Ciencias Geológicas de la Universidad Complutense, especialmente a Lina, por su enorme implicación y simpatía, y al CAI de Difracción de Rayos X de Monocristal de la Facultad de Ciencias de la Universidad Autónoma de Madrid, en especial a Josefina, por su atención, su amabilidad y sus consejos para obtener cristales.

A continuación me gustaría dar las gracias a todos mis amigos y compañeros del laboratorio y del departamento, por su gran ayuda y apoyo en todo momento. Ir cada día al laboratorio ha sido un auténtico placer.

Mª Ángeles, Beti, Carmencita, Ángel, Andreas, Luis, David, Margarita, muchísimas gracias por estar siempre dispuestos a ayudar. Virginia, gracias por ser como eres y por tu sonrisa permanente. Ana y Helena, gracias por vuestra constante ayuda.

Al resto de mis compañeros, Inés, Rafa, Javi, José, Agus, Laura, Sonia, Marina, Rosa, Antonio, Valentina, Alfonso, Mikiko, Paul, Alicita, Adrián, Esther, Marta, Jesús, y los que ya se fueron, Raúl, Helena, María, Toni, Andreíta, Enrique, Vanesa, André, Jaime, “Muchachito”, Simona y Silvia. De todos y cada uno de vosotros me llevo algo bueno, gracias por haberme hecho vivir tan buenos momentos, sois los mejores.

Fulvio, gracias por todo lo que me enseñaste en tan poco tiempo, eres una gran persona. Luismo y Javi, muchas gracias por demostrarme tanto cariño siempre.

Carmen, muchísimas gracias por todo, has sido una gran compañera y amiga. Son muchos los buenos momentos que me llevo conmigo.

A los que han pasado por el laboratorio de Imdea, Matteo, Joe, Adrián, muchas gracias por todos los momentos divertidos, sin vosotros no hubiera sido lo mismo.

Por último Andrés, mi hermanito, que siempre ha estado apoyándome y animándome, muchísimas gracias por todo. Eres el mejor amigo y compañero que se puede tener.

A Sandra, vecina de enfrente, muchas gracias por todo tu cariño. A mis compañeras de máster, Paula y Julia, sois geniales, y a Alberto y Jorge, sin vosotros el departamento no sería lo mismo.

A la profesora Mª Luz del Departamento de Analítica, muchísimas gracias por todo tu cariño y tu ayuda, ha sido una suerte poder contar con alguien como tú.

Finalmente quiero dar las gracias a todas las personas que me han apoyado durante todo este tiempo y que forman parte de mi vida fuera de la universidad.

A mis amigas de toda la vida Pilar y Elena, soy muy afortunada por teneros, muchas gracias por vuestro apoyo, no sé qué haría sin vosotras.

A mis amigos Ramón y Sara, sois fundamentales en mi vida, no tengo palabras para agradeceros todo lo que hacéis por mí.

Al resto de mis amigos Lydia, Santi, Josu, Mercedes, Chechu, Alvarito, Dani, María, gracias por hacerme sentir tan querida y apoyarme durante todo este camino.

Por último, quiero dar las gracias a las personas más importantes de mi vida, a toda mi familia, a mi abuelo, a mi madre, a mis hermanas, a Paco, a mis tíos y mis primos Alejandro y Silvia, por vuestro cariño y apoyo incondicional.

Mamá, te debo todo lo que soy, muchísimas gracias por sacrificar tu vida para darme lo mejor, por apoyarme siempre y hacerme creer que podía con todo. Eres una gran inspiración para mí, te quiero muchísimo.

Mery, gracias por existir y por saber que siempre puedo contar contigo para todo, no habría conseguido nada de esto sin vosotras.

Alberto, sin ti esto habría sido imposible, gracias por estar siempre a mi lado y apoyarme en todo, por tu cariño, por tu ayuda y por hacerme las cosas más fáciles siempre. Son muchos años creciendo juntos y me siento muy afortunada por tenerte.

ABBREVIATIONS AND ACRONYMS

References, abbreviations and acronyms

Bibliographic citations have been placed as footnotes in the pages where they were first cited in the section and at the end of this manuscript.

In addition to the standard abbreviations and acronyms in organic chemistry (as defined by the *J. Org. Chem*. Author Guidelines) the following terms have been used in this manuscript:

Anh	Anhydrous
BHJ	Bulk Heterojunction
BPE	1,2-Bis(2,5-dimethylphospholano)ethane
CD	Circular Dichroism
CNT	Carbon Nanotube
Cp^*	Pentamethylcyclopentadienyl
CV	Cyclic Voltammetry
CVD	Chemical Vapor Deposition
CS_2	Carbon disulphide
DBU	1,8-Diazabicyclo[5.4.0]undec-7-ene
DCM	Dichloromethane
DHL	Dehydrolinalool
DFT	Density Functional Theory
DMF	*N*,*N*-Dimethylformamide
DPM	Diphenylmethanofullerene
DPPE	1,2-Bis(diphenylphosphino)ethane
(*R*)-DTBM-SegPhos	(*R*)-5,5′-Bis[di(3,5-di-*tert*-butil-4-metoxifenil)fosfino]-4,4′-bi-1,3-benzodioxol, [(4*R*)-(4,4′-bi-1,3-benzodioxol)-5,5′-diil]bis[bis(3,5-di-*tert*-butil-4-metoxyfenil)fosfina]
ee	Enantiomeric excess
EQE	External Quantum Efficiency
E_{red}	Reduction Potential
ESI	Electrospray Ionization

Et_3N	Triethylamine
Fc	Ferrocene
FF	Fill Factor
(*R*)-FeSulPhos	(*R*)-2-(*tert*-Butylthio)-1-(diphenylphosphino)ferrocene
FTIR	Fourier Transform Infrared Spectroscopy
GCE	Glassy Carbon Electrode
HF	Hydrogen Fluoride
HOMO	Highest Occupied Molecular Orbital
HPLC	High Performance Liquid Chromatography
HRMS	High Resolution Mass Spectrometry
IPA	Isopropyl alcohol
IPR	Isolated Pentagon Rule
IUPAC	International Union of Pure and Applied Chemistry
ITO	Indium Tin Oxide
J_{sc}	Short Circuit Current
KBr	Potassium Bromide
LN	Linalool
LUMO	Lowest Unoccupied Molecular Orbital
MALDI	Matrix Assisted Laser Desorption/Ionization
(*S*)-Me-f-KetalPhos	1,1-Bis[(2*S*,3*S*,4*S*,5*S*)-2,5-dimethyl-3,4-O-isopropylidene-3,4-dihydroxyphospholanyl]ferrocene
MeOH	Methanol
NaH	Sodium Hydride
NHC	N-Heterocyclic Carbene
NMR	Nucler Magnetic Resonance
NOE	Nuclear Overhauser Effect
***o*-DCB**	*Ortho*-Dichlorobencene
OPV	Organic Photovoltaic
PCE	Power Conversion Efficiency

PEDOT	Poly-3,4-ethylenedioxythiophene
P3HT	Poly-3-hexylthiophene
PCBM	[6,6]-phenyl-C_{61}-butyric acid methyl ester
PSC	Perovskite Solar Cell
PK	Pauson-Khand
PV	Photovoltaic
RT	Room temperature
SEM	Scanning Electron Microscopy
$TBAPF_6$	Tetrabutylammonium hexafluorophosphate
TFA	Trifluoroacetic acid
THF	Tetrahydrofuran
TLC	Thin Layer Chromatography
TTF	Tetrathiafulvalene
Tol	Toluene
Py	Pyridine
UV-vis	Ultraviolet Visible Spectroscopy
V_{oc}	Open Circuit Voltage

Table of Contents

SUMMARY

"Selectivity in Fullerenes Chemistry: Catalytic and Photovoltaic Applications"

Introduction

Fullerenes, firstly discovered by H. W. Kroto, R. F. Curl and R. E. Smalley in 1985, have received a great attention by the scientific community due to their remarkable electronic and photophysical properties, becoming one of the most intensively investigated molecules. Considering their unique properties derived from well-defined chemical constitution, fullerenes have emerged as promising materials for many potential applications.

Objectives

Synthesis of Chiral Metal/Fullerene Hybrids

Design and synthesis of new chiral fullerene hybrids endowed with different metals, with a complete control over the new stereogenic centers, specifically with a metal-centered chirality.

Catalytic Activity of Chiral Metal/Fullerene Hybrids

Evaluate the efficiency of these new hybrid catalysts in fundamental hydrogen transfer reactions and the ability to be reused maintaining efficiency.

Selectivity in Higher Fullerenes

Development of new synthetic methodologies based on mild conditions for obtaining [70]fullerene derivatives with a high degree of selectivity.

Chemical Reactivity on Endohedral Fullerenes

Synthesis of enantiomerically enriched HF@C_{60} pyrrolidines and study of the effect of the incarcerated molecule on the *cis-trans* isomerization process.

Results and Discussion

1. Synthesis of Chiral Metal/Fullerene Hybrids

We have carried out the synthesis of a new family of chiral fullerene–metal hybrids namely, iridium, rhodium, and ruthenium pyrrolidino[3,4:1,2][60]fullerene half-sandwich complexes, with a good control over the new stereogenic centers, including the metal atom (Scheme S1).

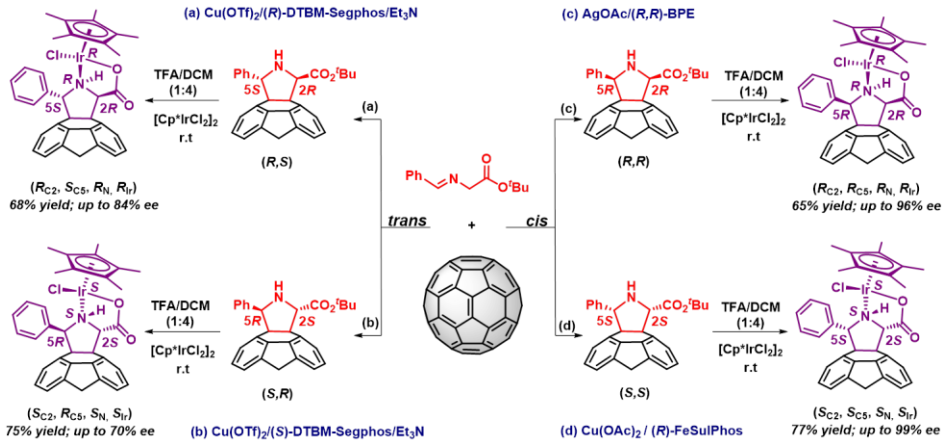

Scheme S1. Enantioselective synthesis of iridium-fullerene hybrids.

Despite the metal center can adopt two different configurations (*R* or *S*), only one product is formed. In contrast to related complexes based on a prolinate ligand, no evidence of diastereomeric mixture or epimerization process at the metal center has been found. This can be explained by the diastereospecific addition of the metal fragment where its configuration is determined by the chirality of the C-2 of the pyrrolidine ring, without any loss of optical purity.

The presence of a repulsive interaction between the lone pair of the chloride ligand and the π-electrons of the adjacent phenyl ring, as well as the stabilizing CH-π interaction between two methyl groups of the Cp^* ligand and the phenyl substituent lead to an exclusive isomer avoiding epimerization processes at the metal. DFT calculations support the observed configurational stability at the metal center.

Therefore, the stereochemistry of the four chiral centers formed during [60]fullerene functionalization is the result of both the chiral catalysts employed and the diastereoselective addition of the metal complexes used (iridium, rhodium, or ruthenium).

2. Catalytic Activity of Chiral Metal/Fullerene Hybrids

As a first approximation, we tested the catalytic activity of these metal-fullerene hybrids in a fundamental hydrogen transfer reaction, such as the reduction of ketones with isopropanol as hydrogen donor solvent, with the aim to evaluate the efficiency and the ability to be reused maintaining efficiency and enantioselectivity.

The results revealed a strong increase of the catalytic efficiency in the reduction of acetophenone by transfer hydrogenation with respect to the iridium dimer complex, being among the most efficient iridium-based catalysts. This high efficiency was the result of a synergic effect of the metal and the hydrogen borrowing ability of C_{60} carbon cage (Scheme S2).

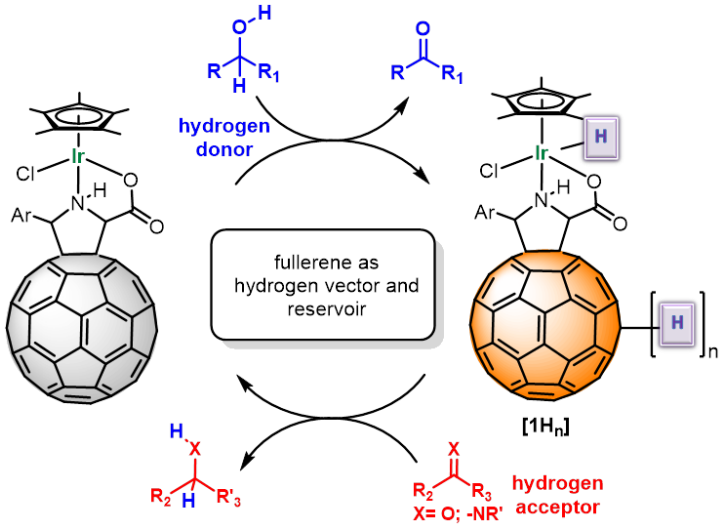

Scheme S2. Iridium-fullerene hybrid catalyzed hydrogen transfer reactions.

Furthermore, these hybrid catalysts present important advantages compared to other catalysts. As result of the very poor solubility of fullerene cage in polar solvents, once carried out the reaction, the catalyst could be removed from the

solution after centrifugation and recovered for a further use, keeping the product pure without any further purification but solvent elimination. Therefore, they merge the advantages of the molecular homogeneous catalyst with those of heterogeneous catalysts.

Encouraged by the excellent results obtained, we have evaluated the efficiency of these new hybrid catalysts in the *N*-alkylation of amines with alcohols. Finally, enantioenriched metal-fullerene hybrids have also proven their efficiency in hydrogen and chirality transfer in ketones reduction.

3. Selectivity in Higher Fullerenes

Chemoselectivity [5,6] *vs* [6,6]

In the search for new methods to achieve selectivity on C_{70}, we describe a new approach for selectively obtaining the [5,6]-derivative as the principal product of the reaction.

In the reaction of diazocompound with C_{70}, of the 15 possible isomers that could be formed (a, b, c, d), (α, β, δ, λ), fulleroid-a was formed predominantly (Scheme S3).

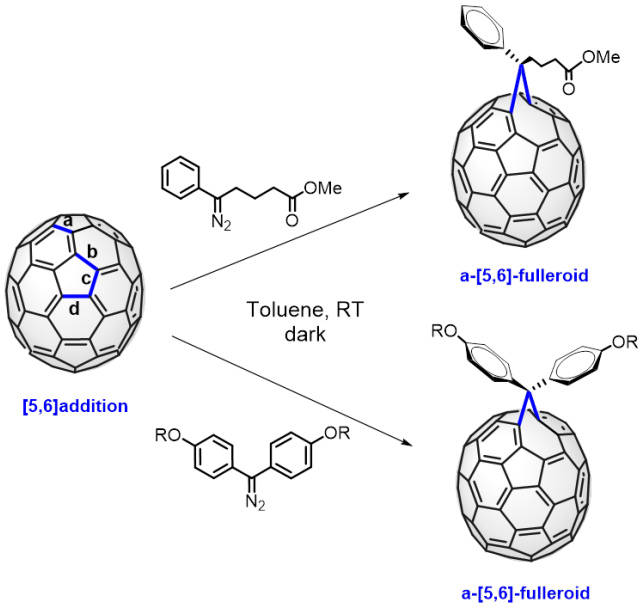

Scheme S3. Chemoselective synthesis of [70]fullerene derivatives.

The quantitative preparation of three [70]PCBM [5,6]-fulleroids was carried out with a high degree of selectivity (99%), as well as for their analogues of [70]DPM (89%). The control of light was a critical factor, since the [5,6] isomer gives rise to the formation of the [6,6] isomer by the action of light. UV-vis spectroscopy and CV electrochemical data clearly confirmed their [5,6]-fulleroid nature.

Based on the isomers obtained in the photochemical isomerization from the [5,6]-fulleroids to their respective [6,6]-methanofullerenes, the nature of the fulleroids obtained in the reaction was unambiguously assigned.

Siteselectivity [6,6]: α>β

On the other hand, we have developed a new methodology based on mild conditions, such as low temperature and light irradiation, for achieving selectively the α-siteisomer on C_{70}.

This unprecedented approach avoids time- and solvent-consuming HPLC separations that are usually employed to obtain these products. In this regard, we have successfully prepared, isolated, and characterized [70]fullerene derivatives with a remarkable high isomeric purity in two different systems (Scheme S4).

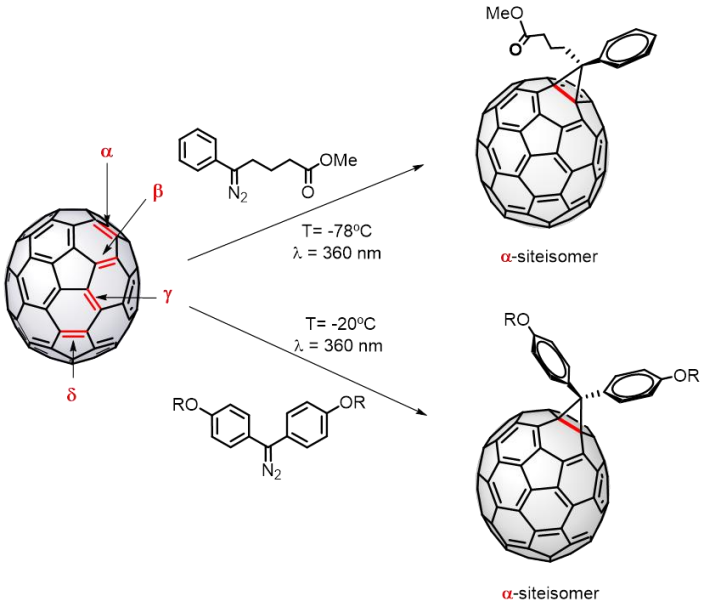

Scheme S4. Siteselective synthesis of [70]fullerene derivatives.

Thus, control on the isomeric purity of [70]fullerene derivatives, may be crucial to improve the power conversion efficiency of organic photovoltaic devices. As preliminary results, some organic devices were fabricated with two different fullerene samples, from pure α-[70]PCBM isomer and its isomeric mixture, in order to determine how the purity of the organic sample affects the device efficiency. According to the results, α-siteisomer showed better efficiency but no significant differences in the photovoltaic parameters were observed.

4. Chemical Reactivity on Endohedral Fullerenes

It is known that the encapsulated molecules in endofullerenes can affect the exohedral reactivity of the fullerenes carbon cage. In this sense, we have carried out the first exohedral functionalization on the novel HF@C_{60}, using an efficient methodology to obtain enantiomerically enriched fulleropyrrolidines.

The isomerization process from optically pure (2*S*,5*S*)-*cis*- to the (2*S*,5*R*)-*trans* pyrrolidinofullerene, has been studied and compared with empty C_{60} and endohedral $H_2O@C_{60}$. Interestingly, the incarcerated HF molecule contributes to increase the isomerization rate, showing the existence of a hydrogen bonding assistance of the trapped molecule without affecting the final *cis*-*trans* ratio or promoting the loss of enantioselective control.

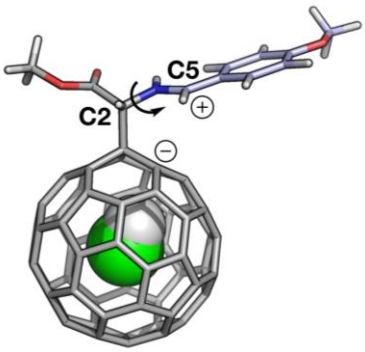

Figure S1. Zwitterionic intermediate formed by a carbanion on the C_{60} cage and a benzylic cation on the former pyrrolidine ring.

Conclusions

For the first time, a new family of chiral fullerene–metal hybrids, iridium, rhodium, and ruthenium pyrrolidino[3,4:1,2][60]fullerene with a configurationally stable stereogenic metal center, have been synthesized.

The novel C_{60}-based catalysts showed high efficiencies in fundamental hydrogen transfer reactions and presented important advantages. These hybrid catalysts are recovered by mechanical means and reused without losing efficiency.

We have developed new methodologies based on mild conditions, for a chemoselective and siteselective control on [70]fullerene.

The first chemical modification on the recently reported HF@C_{60} endohedral was carried out. In the isomerization process from the *cis*- to the *trans*-pyrrolidino[60]fullerene, the encapsulated HF molecule contributes to increase the isomerization rate through a weak hydrogen bonding assistance.

RESUMEN

"Selectividad en Química de Fullerenos: Aplicaciones Catalíticas y Fotovoltaicas"

Introducción

Los fullerenos, descubiertos por H. W. Kroto, R. F. Curl y R. E. Smalley en 1985, han recibido una gran atención por parte de la comunidad científica debido a sus notables propiedades electrónicas y fotofísicas, convirtiéndose en una de las moléculas más intensamente investigadas. Teniendo en cuenta sus propiedades únicas derivadas de una constitución química bien definida, los fullerenos se consideran un material prometedor para diversas aplicaciones.

Objetivos

Síntesis de Híbridos Quirales Metal-Fullereno

Diseño y síntesis de nuevos híbridos quirales de fullereno dotados con diferentes metales, con un completo control sobre los nuevos centros estereogénicos creados, con la quiralidad centrada en el metal.

Actividad Catalítica de Híbridos Quirales Metal-Fullereno

Se pretende evaluar la eficiencia de estos nuevos híbridos en reacciones fundamentales de transferencia de hidrógeno y su capacidad para ser reutilizados manteniendo la eficiencia.

Selectividad en Fullerenos Superiores

Se pretende desarrollar nuevas metodologías sintéticas basadas en condiciones suaves para obtener isómeros puros de [70]fullereno con un alto grado de selectividad.

Reactividad Química en Fullerenos Endohédricos

Síntesis de pirrolidinas enantioméricamente enriquecidas de HF@C_{60} y estudio del efecto que produce la mólecula de dentro en el proceso de isomerización *cis-trans*.

Resultados y Discusión

1. Síntesis de Híbridos Quirales Metal-Fullereno

Se llevó a cabo la síntesis de una nueva familia de híbridos quirales metal-fullereno, iridio-, rodio- y rutenio-pirrolidino[3,4:1,2][60]fullereno con un buen control sobre los nuevos centros estereogénicos, incluyendo el átomo de metal (Esquema S1).

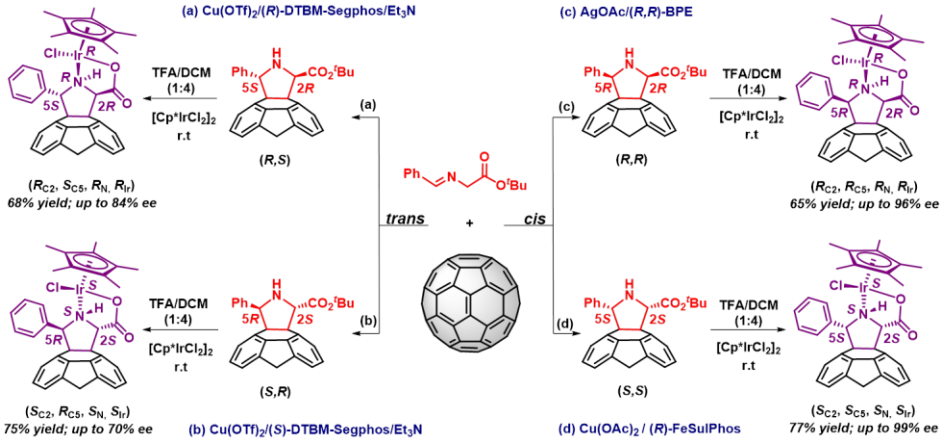

Esquema S1. Síntesis enantioselectiva de híbridos iridio-fullereno.

A pesar de que el centro metálico puede adoptar dos configuraciones diferentes (*R* o *S*), sólo se forma un producto, ya que no se han encontrado evidencias de mezclas diastereoméricas o procesos de epimerización en el metal. Esto puede explicarse por la adición diastereoespecífica del fragmento metálico cuya configuración viene determinada por la quiralidad del C-2 del anillo de pirrolidina, sin pérdida de pureza óptica.

La existencia de una interacción repulsiva entre el par solitario del ligando cloruro y los electrones π del anillo de fenilo adyacente, así como la interacción estabilizadora CH-π entre dos grupos metilo del ligando Cp^* y el fenilo, da lugar exclusivamente a un isómero, evitando procesos de epimerización en el metal. Los cálculos DFT apoyan la estabilidad configuracional observada en el centro metálico.

Por lo tanto, la estereoquímica de los cuatro centros quirales formados durante la funcionalización del [60]fullereno es el resultado, tanto de los catalizadores quirales empleados, como de la adición diastereoselectiva de los complejos metálicos utilizados (iridio, rodio o rutenio).

2. Actividad Catalítica de Híbridos Quirales Metal-Fullereno

Como primera aproximación, evaluamos la actividad catalítica de estos híbridos en reacciones fundamentales de transferencia de hidrógeno, como la reducción de cetonas en isopropanol (dador de hidrógeno), y la capacidad de ser reutilizados manteniendo la eficiencia y la enantioselectividad.

Los resultados revelaron un fuerte aumento de la eficiencia catalítica en la reducción de acetofenona con respecto al dímero de iridio comercial, pasando a ser uno de los catalizadores de iridio más eficientes. Esta alta eficiencia fue el resultado combinado de un efecto sinérgico del metal y la capacidad de donación de hidrógeno de la jaula de carbono del C_{60} (Esquema S2).

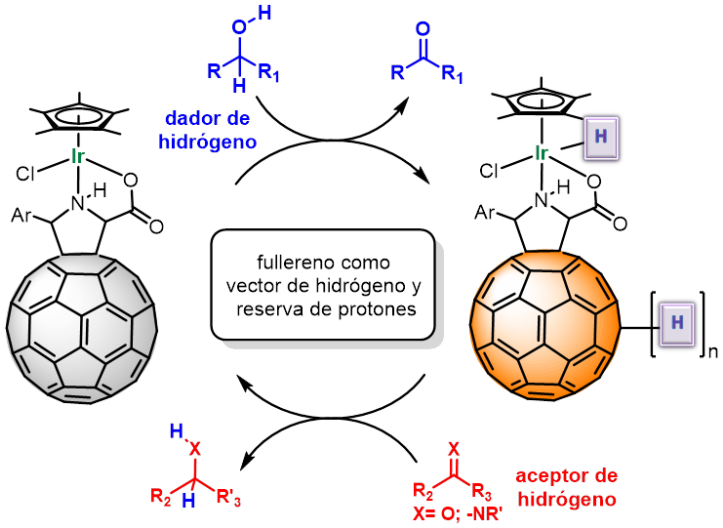

Esquema S2. Reacciones de transferencia de hidrógeno catalizadas por híbridos de iridio-fullereno.

Además, estos catalizadores híbridos presentan importantes ventajas en comparación con otros catalizadores. Como resultado de la baja solubilidad del fullereno en disolventes polares, una vez llevada a cabo la reacción, el

catalizador se puede retirar de la solución por centrifugación y recuperarse para un uso adicional, manteniendo el producto puro sin ninguna purificación adicional más que la eliminación del disolvente. Por lo tanto, se combinan las ventajas de los catalizadores homogéneos con las de los catalizadores heterogéneos. Alentados por los excelentes resultados obtenidos, se evaluó la eficiencia de estos catalizadores híbridos en la *N*-alquilación de aminas con alcoholes. Finalmente, los híbridos de metal-fullereno enriquecidos también han demostrado su eficiencia en la transferencia de quiralidad en la reducción de cetonas.

3. Selectividad en Fullerenos Superiores

Quimioselectividad [5,6] *vs* [6,6]

En la búsqueda de nuevos métodos para lograr selectividad en el C_{70}, describimos una nueva aproximación para obtener selectivamente el derivado [5,6] como producto principal de la reacción. En la reacción del diazocompuesto con el C_{70}, de los 15 posibles isómeros que podrían formarse (a, b, c, d), (α, β, δ, λ), logramos obtener predominantemente el isómero [5,6]-abierto correspondiente al sitio de enlace a (Esquema S3).

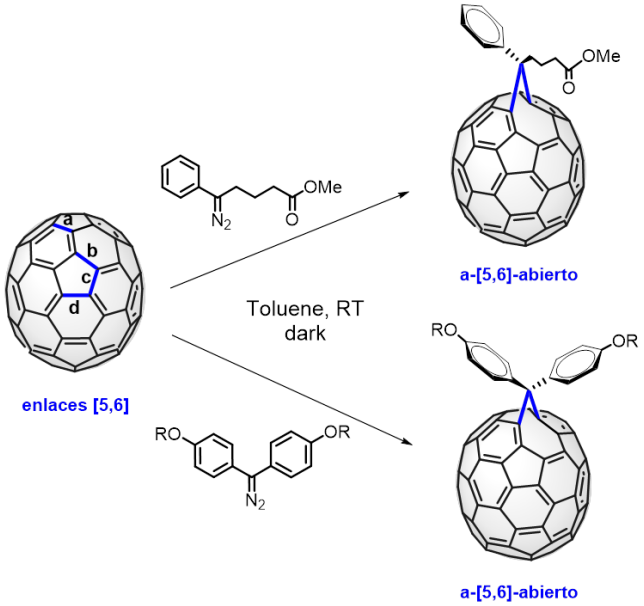

Esquema S3. Síntesis quimioselectiva de derivados de [70]fullereno.

La síntesis de derivados [5,6]-abiertos de [70]PCBM se llevó a cabo con un alto grado de selectividad (99%), así como para los derivados de [70]DPM (89%), obteniendo tres isómeros [5,6] diferentes en cada caso dependiendo del sitio de enlace. La ausencia de luz fue un factor crítico, ya que el isómero [5,6] da lugar a la formación del isómero [6,6] por la acción de la luz. La espectroscopia UV-vis y los datos de voltamperometría cíclica confirmaron claramente la naturaleza [5,6] de los derivados.

Basándonos en los loco-isómeros obtenidos en la isomerización fotoquímica de los [5,6]-abiertos a los respectivos [6,6]-cerrados, la naturaleza de los tres isómeros [5,6]-abiertos obtenidos en la reacción se asignó inequívocamente.

Locoselectividad [6,6]: α>β

Por otro lado, hemos desarrollado una nueva metodología sintética basada en condiciones suaves, como son baja temperatura e irradiación de luz, para lograr obtener selectivamente el locoisómero α en el C_{70}. Este enfoque sin precedentes evita las tediosas separaciones de HPLC, que consumen tiempo y disolvente, usualmente empleadas para obtener estos productos. En este sentido, hemos preparado con éxito derivados de [70]fullereno con una alta pureza isomérica en dos sistemas diferentes (Esquema S4).

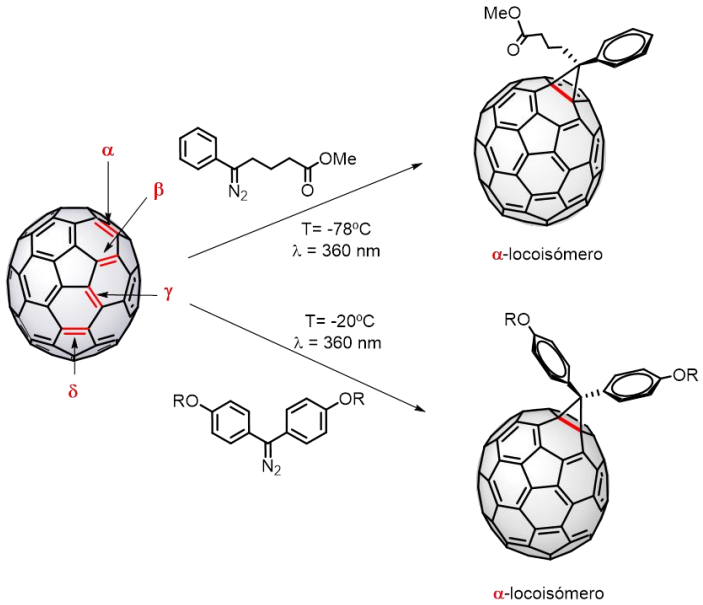

Esquema S4. Síntesis locoselectiva de derivados de [70]fullereno.

El control sobre la pureza isomérica de los derivados de [70]fullereno, puede ser crucial para mejorar la eficiencia de conversión de los dispositivos fotovoltaicos orgánicos.

Como resultados preliminares, se fabricaron algunos dispositivos orgánicos con dos muestras de fullereno diferentes, a partir del isómero puro α-[70] PCBM y su mezcla isomérica, con el fin de determinar cómo la pureza de la muestra afecta a la eficiencia del dispositivo. De acuerdo con los resultados obtenidos, el isómero puro α mostró una mejor eficiencia, pero sin diferencias significativas en los parámetros fotovoltaicos con respecto a la mezcla.

4. Reactividad Química en Fullerenos Endoédricos

Es conocido que las moléculas encapsuladas dentro de los fullerenos pueden afectar a su reactividad química. En este sentido, hemos llevado a cabo la primera funcionalización sobre la nueva molécula de HF@C_{60}, empleando una metodología eficiente para obtener pirrolidinas enantioméricamente enriquecidas.

Se ha estudiado el proceso de isomerización de la pirrolidina pura (2*S*,5*S*)-*cis* a la pirrolidina (2*S*,5*R*)-*trans*, y se ha comparado con la mólecula de C_{60} y el endoédrico de H_2O. Curiosamente, la molécula de HF encarcelada contribuye a incrementar la isomerización, debido a una asistencia por enlace de hidrógeno, sin afectar a la relación *cis*-*trans* final ni perder enantioselectividad.

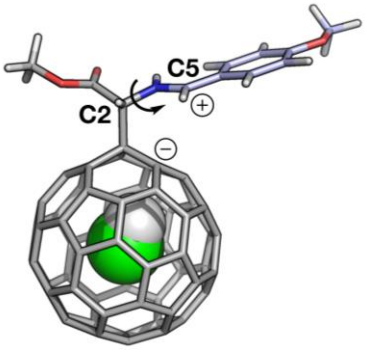

Figura S1. Intermedio formado por un carbanión en la jaula de C_{60} y un catión bencílico en el anillo de pirrolidina.

Conclusiones

Se ha sintetizado una nueva familia de híbridos quirales metal-fullereno, iridio-, rodio- y rutenio-pirrolidino[3,4:1,2][60]fullereno, con un centro metálico estereogénico estable.

Los nuevos catalizadores basados en C_{60} mostraron altas eficiencias en reacciones fundamentales de transferencia de hidrógeno y presentaron ventajas importantes. Estos catalizadores híbridos se recuperan por medios mecánicos y se reutilizan sin perder eficiencia.

Hemos desarrollado nuevas metodologías sintéticas basadas en condiciones suaves, para un control quimio- y locoselectivo en el C_{70}.

Se ha llevado a cabo la primera modificación química sobre la molécula HF@C_{60}. En el proceso de isomerización de *cis*- a *trans*-pirrolidino[60]fullereno, la molécula de HF encapsulada contribuye a aumentar la tasa de isomerización a través de una ligera asistencia por enlace de hidrógeno.

INTRODUCTION

1. INTRODUCTION

Fullerenes are a family of molecules constituted exclusively by carbon atoms. In contrast to the other carbon allotropes, graphite and diamond, with extended reticular structures, fullerenes present a precise number of carbon atoms, spatially disposed in high symmetric closed cages with defined shape and geometry. Since its discovery by H. W. Kroto, R. F. Curl and R. E. Smalley in 1985,[1] who were awarded with the Nobel Prize of Chemistry in 1996, and his later preparation at multigram scale,[2] C_{60} rapidly became one of the most intensively investigated molecules. These carbon allotropes maintain an unabated interest in a large number of studies, review articles and books about their chemical reactivity and properties, in the search for practical applications.

The discovery of fullerenes has been followed by other carbon nanostructures, which have also been given preferential attention by scientists from different areas. Since the discovery of carbon nanotubes by S. Iijima in 1991,[3] and more recently graphene by A. K. Geim and K. S. Novoselov in 2004,[4] who also received the Nobel Prize in 2010, these carbon nanoforms have been the focus of intense research, especially in the field of materials science, nanotechnology, and biomedical applications.[5] Although many other forms of carbon are known, namely endohedral fullerenes,[6] carbon nanohorns,[7] carbon

1. H. W. Kroto, J. R. Heath, S. C. O'Brien, R. F. Curl, R. E. Smalley, *Nature*, **1985**, *318*, 162.
2. W. Krätschmer, L. D. Lamb, K. Fostiropoulos, D. R. Huffman, *Nature*, **1990**, *347*, 354.
3. a) Multi-wall carbon nanotubes: S. Iijima, *Nature*, **1991**, *354*, 56. Single-wall carbon nanotubes: b) S. Iijima, T. Ichihashi, *Nature*, **1993**, *363*, 603. c) D. S. Bethune, C. H. Klang, M. S. de Vries, G. Gorman, R. Savoy, J. Vasquez, R. Beyers, *Nature*, **1993**, *363*, 605.
4. a) K. S. Novoselov, A. K. Geim, S. V. Morozov, D. Jiang, Y. Zhang, S. V. Dubonos, I. V. Grigorieva, A. A. Firsov, *Science*, **2004**, *306*, 666. b) A. K. Geim, K. S. Novoselov, *Nat. Mater.*, **2007**, *6*, 183.
5. J. L. Delgado, M. A. Herranz, N. Martín, *J. Mater. Chem.*, **2008**, *18*, 1417.
6. a) T. Akasaka, S. Nagase, *Endofullerenes: A New Family of Carbon Clusters*, Ed. Kluver Academic Publishers, Dordrecht, The Netherlands, **2002**. b) L. Dunsch, S. Yang, *Small*, **2007**, *3*, 1298. c) M. N. Chaur, F. Melin, A. L. Ortíz, L. Echegoyen, *Angew. Chem. Int. Ed.*, **2009**, *48*, 7514.
7. S. Iijima, M. Yudasaka, R. Yamada, S. Bandow, K. Suenaga, F. Kokai, K. Takahashi, *Chem. Phys. Lett.*, **1999**, *309*, 165.

nanoonions,[8] etc, C_{60} with its singular spherical shape, its size in the nanometre scale (~1nm) and their remarkable electronic and photophysical properties, has emerged as a promising material for many potential applications. In this introduction we will mention two of the most realistic applications.

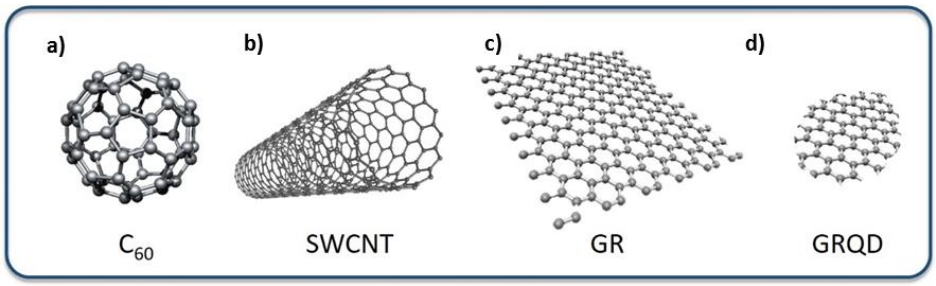

Figure 1. Chemical structure of the main carbon nanoforms, (a) C_{60}, (b) single-wall carbon nanotube, (c) graphene and (d) graphene quantum dot.

1.1. Carbon Materials for Energy

The increase in energy consumption is one of the great problems of the twenty-first century. A huge fraction of our electricity depends on non-renewable fossil fuels, which are currently starting to disappear after years of massive consumption. It is estimated that in the next few decades the world population will exceed 8 billion people, leading to higher energy consumption, which requires more energy (Figure 2).[9] As a solution to this growing energy demand and high environmental impact, the development of renewable, clean and inexpensive energy is a priority.

The Sun is the most powerful source of energy available in our Solar System. Therefore, one of the scientific challenges of this century will be the development of highly efficient, renewable and sustainable strategies for using Sun energy. Currently, the highest level of development in solar energy production is achieved with solar cells silicon technology with efficiencies around 25% in a laboratory setting. However, this technology has a great limitation due to the high energy required for the fabrication process, making

8. D. Ugarte, *Nature*, **1992**, *359*, 707.
9. D. Larcher, J-M. Tarascon, *Nat. Chem.*, **2015**, *7*, 19.

the cost of photovoltaic electricity greater than the conventional generation, which leads to the development of new alternative materials.

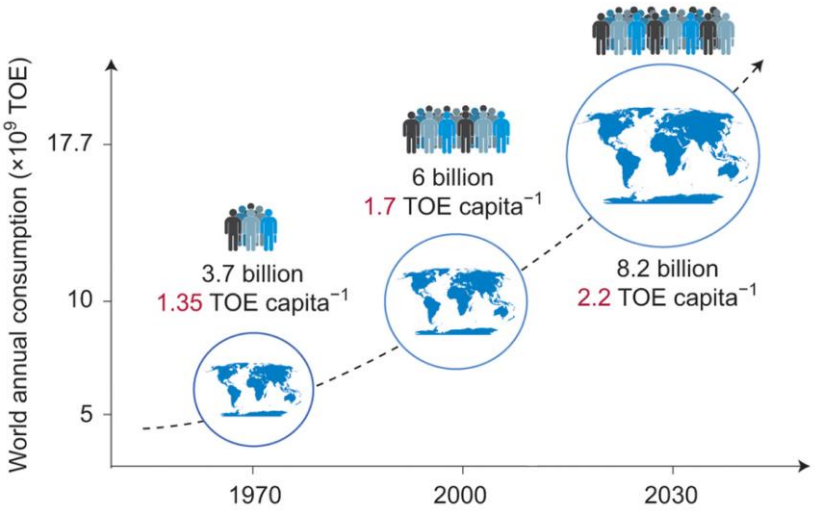

Figure 2. World energy consumption in 1970, 2000, and 2030. (Power unit, TOE: ton oil equivalent).

In general, organic materials are appealing for photovoltaics (PV) due to some properties such as the ability for solution processing, affording flexible, lighter and cheaper PV devices. These aforementioned features[10] confer advantages to these organic materials compared with the most commonly used silicon based devices. In this regard, some of the known carbon nanoforms, fullerenes, carbon nanotubes as well as graphene and graphene quantum dots, are appealing materials of choice for addressing this issue by efficiently harvesting sunlight and transforming it into other useful forms of energy. In particular, photovoltaic is currently among the most realistic applications of fullerene derivatives.

In the field of organic solar cells, the most widely studied materials have been those based on blends of electron-donor semiconducting polymer and chemically modified fullerenes as the electron-acceptor component. In this regard, based on their electronic (moderate electron-acceptor) and geometric

10. Z. Zhang, L. Wei, X. Qin, Y. Li, *Nano Energy*, **2015**, *15*, 490.

(singular sphere shape) properties, fullerenes have proved to be the ideal electron conducting material to form a bicontinous phase network with π-conjugated polymers.[11]

The plastic solar cell idea brings photovoltaic solar energy to a new level. This technology will not only decrease the cost of produced energy (which is still the major target), but also engage many applications of solar electricity into low cost consumer goods which are not accessible up to now due to the high cost of integration. The use of available solar energy can be increased by integration of solar cells in articles such as toys, chip-cards and electronic equipment with low energy consumption or to supply the power for small portable devices such as cell phones and players, as well as for recharging surfaces for laptops.

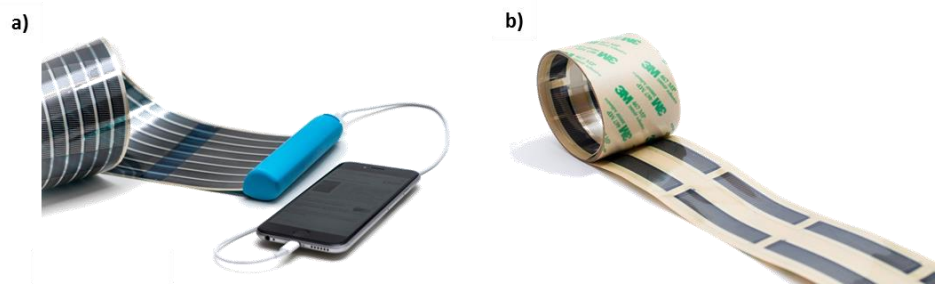

Figure 3. (a) Flexible display made of organic materials for recharging cellphones. (b) Printed organic solar cells available as solar tape.

The use of carbon nanostructures for photovoltaic applications is becoming a reality not only from the scientific viewpoint, most importantly, from a social point of view since the companies have been able to implement this technology to producing high tech devices paving the way for a safer and sustainable future.[12]

11. A. J. Heeger, *Adv. Mater*., **2014**, *26*, 10.
12. N. Martín, *Adv. Energy Mater*., **2016**, 1601102.

1.2. Carbon Materials as Catalysts

Despite transition-metal based catalysts have been successfully and widely employed in many organic transformation, their use is considered not "sustainable" due to the limited available resources. As a result, "carbocatalysis"[13] has emerged as a new research field devoted to the development of metal-free catalysts or, at least, to catalysts with low metal content. Other factors besides sustainability that may also favor carbon materials as catalysts are economic considerations, since the price of some precious metals is considerably higher than carbon materials.

Carbocatalysis is also associated to a new term, namely "*pseudohomogeneous*" catalysis.[14] It means that for reactions carried out using suspended materials as catalyst, the visual appearance of the system is like that of a homogeneous catalytic process with the added advantage of being recoverable at the end of the reaction. Even though the carbocatalyst is in a single phase with reactants, the carbonaceous material can be easily separated from the mixture after the reaction and recovered by filtration or centrifugation as is a typical feature in heterogeneous catalysis.[15]

In the last decades there has been a continued growing interest in the application of carbon nanoforms in catalysis, as a logical evolution of the continued use of active carbons (ACs),[16] for the preparation of heterogeneous catalysts since their structure is much better defined than ACs. Carbon materials, including amorphous carbon, graphite/graphene (oxide) and carbon nanotubes, have widely been applied in many catalytic transformations in modern organic chemistry.[17]

13. a) S. Navalon, A. Dhakshinamoorthy, M. Alvaro, H. García, *Chem. Rev.*, **2014**, *114*, 6179. b) D. R. Dreyer, C. W. Bielawski, *Chem. Sci.*, **2011**, *2*, 1233. c) D. S. Su, S. Perathoner, G. Centi, *Chem. Rev.*, **2013**, *113*, 5782. d) C. Su, K. P. Loh, *Acc. Chem. Res*., **2013**, *46*, 2275. e) J. Pyun, *Angew. Chem. Int. Ed*., **2011**, *50*, 46. f) X. Liu, L. Dai, *Nat. Rev. Mater*., **2016**, *1*, 16064.
14. A. Tiwari, S. Titinchi, Advanced Catalytic Materials, Wiley, **2015**.
15. M. Boronat, A. Corma, *Journal of Catalysis*, **2011**, *284*, 138.
16. R. Schloegl, *Advances in Catalysis*, **2013**, *56*, 103.
17. a) D. Haag, H. H. Kung, *Top. Catal*., **2014**, *57*, 762. b) C. J. Shearer, A. Cherevan, D. Eder, *Adv. Mater*., **2014**, *26*, 2295. c) X. K. Kong, C. L. Chen, Q. W. Chen, *Chem. Soc. Rev*., **2014**, *43*, 2841.

In this regard, fullerenes, among the different carbon nanoforms, result to be very promising carbocatalysts for their peculiar molecular structure and higher solubility with respect to graphene or carbon nanotubes. Properties of C_{60}, namely its thermal stability, high capacity in hydrogen store, a wide absorption spectrum and acceptor properties allow fullerene to be considered, for example, as a possible multifunctional ligand in reactions of transition metal complexes with hydrocarbons. Such a ligand would be able to perform as an electron and/or hydrogen acceptor in reactions with hydrogen donors.[18]

Accompanying the great advances in materials science and nanotechnology, a variety of carbon-based nanostructured materials, including graphene and CNTs, have been successfully developed as low-cost, highly efficient, metal free catalysts for photocatalytic and/or electrocatalytic water splitting.[19] Despite considerable progress has been achieved in this field, many issues and challenges are still yet to be addressed.

Considering the availability of new allotropic nanostructured carbon materials and their unique properties derived from well-defined morphologies, high surface area, and predictable interactions, it can be anticipated that their use in catalysis will grow in the near future.[20] The advances in the development of carbon-based metal free catalysts will certainly lead to significant economic, environmental and social benefits.

18. N. F. Goldshleger, A. P. Moravsky, *Russ. Chem. Rev*., **1997**, *66*, 323.
19. Y. Xu, M. Kraft, R. Xu, *Chem. Soc. Rev*., **2016**, *45*, 3039.
20. a) D. R. Dreyer, H.-P. Jia, C. W. Bielawski, *Angew. Chem. Int. Ed*., **2010**, *49*, 6813. b) C. Huang, C. Li, G. Shi, *Energy Environ. Sci.*, **2012,** *5*, 8848.

BACKGROUND

2. BACKGROUND

2.1. Fullerenes: Structure and Properties

Fullerenes are carbon structures built up of fused pentagons and hexagons. The pentagons, absent in graphite, provide curvature, since a network consisting only by hexagons is planar. The smallest and most studied stable fullerene, C_{60}, with an outer diameter of 10.34 Å,[21] presents an icosahedral structure with twelve pentagonal rings isolated by 20 hexagonal rings and two different bonds in the molecule. The bonds at the junctions of two hexagons, [6,6] bonds are shorter (1.37 Å) than the bonds at the junctions of a hexagon and a pentagon [5,6] bonds (1.45 Å). This bond-length alternation in C_{60} shows that the double bonds are located in the [6,6] bonds and there are no double bonds in the pentagonal rings. Due to the curvature of the molecule, each carbon atom presents peculiar $sp^{2.3}$ hybridization[22] and fullerene behave as an electron deficient polyene, with the most reactive positions placed in the [6,6] bonds. The driving force of the reactivity of fullerene is due to the release of strain energy that comes out from the saturation of one or more double bonds.

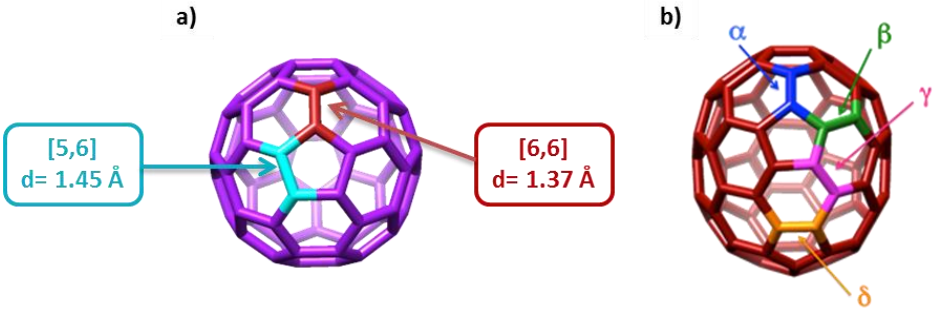

Figure 4. Schematic representation of (a) [60]fullerene with the lengths of the two different bonds in the molecule and (b) [70]fullerene with four different double bonds.

21. a) C. S. Yannoni, P. P. Bernier, D. S. Bethune, G. Meijer, J. R. Salem, *J. Am. Chem. Soc*., **1991**, *113*, 3190. b) M. S. Dresselhaus, G. Dresselhaus, P. C. Eklund, *Science of Fullerenes and Carbon Nanotubes*, Academic Press, San Diego, **1996**.
22. R. C. Haddon, *Acc. Chem. Res*., **1992**, *25*, 127.

The stability of C_{60} has been demonstrated through the isolated pentagon rule (IPR), developed by H. Kroto in 1987.[23,24] It says that the local tension enhances with the number of shared bonds between two pentagon rings (pentalene), leading to less stable molecules. Owing to this rule, the easier fullerenes to be formed will be those in which two pentagons must be separated by hexagonal rings.[24] The presence of pentagons not only produces a major tension of the bond angle of the molecule, also a destabilization of the π-electron cloud.[23] In this regard, a spherical shape distributes the strain as evenly as possible and minimizes the anisotropic contribution to the strain energy.

The next more stable fullerene is [70]fullerene. It is a cage formed by 12 pentagonal rings and 25 hexagonal rings which structure resembles a rugby ball. Unlike C_{60}, C_{70} molecule presents D_{5h} symmetry and is constituted by four non-equivalent double bonds, namely: α, β, γ and δ (Figure 4b).

The geometry at the poles (highest curvature) of [70]fullerene is very similar to that of [60]fullerene. The corannulene subunits have the same type of bond length alternation. In contrast to C_{60}, this fullerene has an equatorial belt consisting of fused hexagons with different reactivity compared with the more reactive polar region. This aspect will be explained in more detail in following sections (2.3. Higher Fullerenes).

23. T. G. Schmalz, W. A. Seitz, D. J. Klein, G. E. Hite, *Chem. Phys. Lett*., **1986**, *130*, 203.
24. H. W. Kroto, *Nature*, **1987**, *329*, 529.

2.1.1. Electronic Properties

C_{60} absorbs strongly in the UV region, and weakly in the visible spectrum. Although fullerenes present some forbidden transitions in the visible range, these are produced with low absorption coefficients, and are responsible for the purple color of C_{60} and the red color of C_{70} in solution.[25] The absorption spectrum of C_{60} is characterized by a strong absorption at 320-350 nm and also a weak sharp absorption peak at 408-410 nm.

Higher fullerenes, like C_{70}, present a stronger absorption in the visible region of the electronic spectrum as a consequence of the loss of symmetry. Absorption in the visible region of C_{70} begins with a weak band at 650 nm, followed by a series of peaks (637, 624, 610, 600, and 594 nm) on a gradually rising that leads to a broad absorption band at 469-544 nm. Maximun absorption appears at 378, 359, and 331 nm in the UV region (Figure 5).

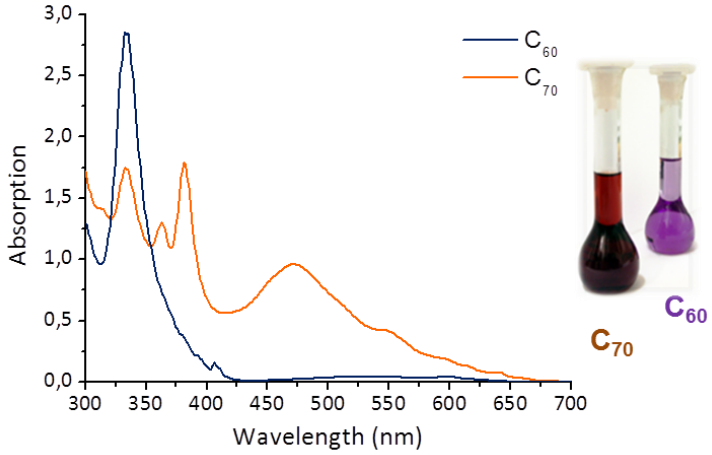

Figure 5. UV-vis spectra of the molecules C_{60} (blue) and C_{70} (orange) in chlorobenzene at room temperature ($5 \cdot 10^{-5}$M).

25. H. Ajie, M. M. Alvarez, S. J. Anz, R. D. Beck, F. Diederich, K. Fostiropoulos, D. R. Huffman, W. Krätschmer, Y. Rubin, K. E. Shriver, D. Sensharma, R. L. Whetten, *J. Phys. Chem*., **1990**, *94*, 8630.

2.1.2. Electrochemical Properties

Fullerene C_{60} is a good electron acceptor.[26,27,28] Theoretical calculations of the molecular orbital levels of C_{60} exhibit a LUMO comparatively low in energy which is triply degenerated.[29] It allows the reversible addition of up to six electrons in solution.[30] This was also supported by cyclic voltammetry (CV)[31] measurements carried out with C_{60}, which shows its facile and stepwise reversible reduction (Figure 6). All the reductions are one-electron transfer processes and are favored by the low reorganization energy of these species.[26] The reduction potentials are strongly dependent on the nature of the solvent, the electrolyte and the temperature. The six electron acceptor reversible capability of [60]fullerene came out in experiments at -10°C in a solution of Acetonitrile:Toluene.[32]

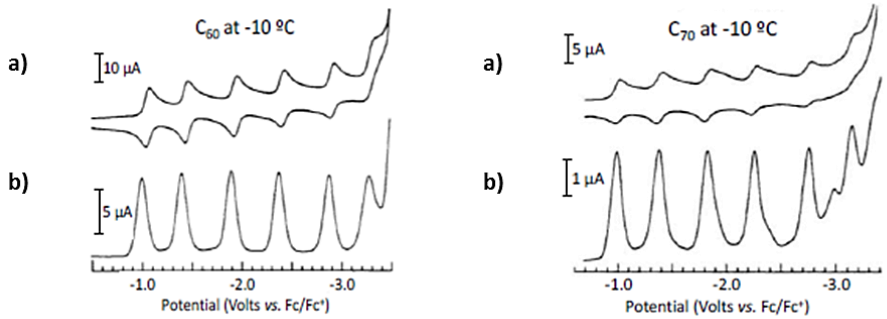

Figure 6. (a) Cyclic voltammogram and (b) square wave voltammogram of C_{60} and C_{70} with $TBAPF_6$ as supporting electrolyte at –10ºC in Toluene:Acetonitrile 4:1 at 100 mV/s (V *vs* Fc/Fc^+).

26. D. M. Guldi, *Chem. Commun*., **2000**, *5*, 321.
27. D. M. Guldi, M. Prato, *Acc. Chem. Res*., **2000**, *33*, 695.
28. N. Martín, L. Sánchez, B. Illescas, I. Pérez, *Chem. Rev*., **1998**, *98*, 2527.
29. a) C. A. Reed, R. D. Bolskar, *Chem. Rev*., **2000**, *100*, 1075. b) A. D. J. Haymet, *Chem. Phys. Lett*., **1985**, *122*, 421. c) P. D. Hale, *J. Am. Chem. Soc*., **1986**, *108*, 6087.
30. a) F. Arias, Q. Xie, Y. Wu, Q. Lu, S. R. Wilson, L. Echegoyen, *J. Am. Chem. Soc*., **1994**, *116*, 6388. b) P.-M. Allemand, A. Koch, F. Wudl, Y. Rubin, F. Diederich, M. M. Alvarez, S. J. Anz, R. L. Whetten, *J. Am. Chem. Soc*., **1991**, *113*, 1050.
31. R. E. Haufler, J. Conceicao, L. P. F. Chibante, Y. Chai, N. E. Byrne, S. Flanagan, M. M. Haley, S. C. O'Brien, C. Pan, *J. Phys. Chem*., **1990**, *94*, 8634.
32. Q. Xie, E. Pérez-Cordero, L. Echegoyen, *J. Am. Chem. Soc*., **1992**, *114*, 3978.

The higher homologue C_{70} exhibits analogous behaviour, six reduction waves at comparable potentials have been observed.[32] The electrochemistry of C_{60} derivatives has also been widely investigated.[33] As observed by electrochemical reduction, derivatization usually decreases the electron affinity of the C_{60}-sphere. Typically, cathodically (more negative) shifted waves have been observed by cyclic voltammetry.[34]

The oxidation process, as Haddon *et al*. predicted,[35] is an extremely difficult process. In 1993 Echegoyen and col. were able to measure the first electrochemically irreversible oxidation of C_{60} at 1.26 V (*vs* Fc/Fc^+, $TBAPF_6$, 1,1,2,2-tetrachloroethane, 100 mV/s).[36]

These properties have led to the synthesis of a large number of donor-acceptor systems in which C_{60} acts as an electron acceptor. Remarkably, small reorganization energies are associated with the reduction of C_{60} and its derivatives. Under optimal conditions, small reorganization energy leads to optimal charge-separation kinetics, and a deceleration of charge-recombination rates. That is, charge-recombination in these systems occurs more slowly than photoinduced charge separation which results in the generation of relatively long-lived charge-separated states. Thus, donor-acceptor arrays containing fullerene have been proposed as models for photosynthesis and as energy storage systems.[37] Thanks to this property, C_{60} or its derivatives may be employed as acceptor component in photovoltaic devices as well as in organic electronics.

33. L. Echegoyen, L. E. Echegoyen, *Acc. Chem. Res*., **1998**, *31*, 593.
34. a) T. Suzuki, Q. Li, K. C. Khemani, F. Wudl, Ö. Almarsson, *Science*, **1991**, *254*, 1186. b) D. M. Guldi, N. Martín, M. A. Herranz, L. Echegoyen, Chapter 9, *Fullerenes: From Synthesis to Optoelectronic Properties*, Kluwer Academic Publishers, Dordrecht, The Netherlands, **2002**.
35. R. C. Haddon, L. E. Brus, K. Raghavachari, *Chem. Phys. Lett*., **1986**, *125*, 459.
36. Q. Xie, F. Arias, L. Echegoyen, *J. Am. Chem. Soc*., **1993**, *115*, 9818.
37. H. Imahori, Y. Sakata, *Eur. J. Org. Chem*., **1999**, *1999*, 2445.

2.2. Chemical Reactiviy of Fullerenes

As aforementioned, [60]fullerene, differently from the other allotropic carbon forms, presents a discrete composition and can be functionalised to obtain new compounds with higher solubility in organic solvents. Because [60]fullerene does not have any kind of functionalization, but double bonds, its reactivity becomes peculiar and it is driven by the transformation of sp^2 into sp^3 carbon atoms. This simple consideration shows the great difference between the reactivity of fullerenes and the classical planar aromatic systems.

The [60]fullerene chemical behaviour is comparable to an electron poor polyolefin, being the nucleophilic addition the typical reaction experimented by fullerenes. The driving force of the chemical reactivity of the fullerenes stems from the energy release in the saturation of a double bond. This aspect is pronounced in the C_{70} molecule where the more planar equatorial region has different reactivity compared with the most reactive polar region. Among all known organic reactions, the nucleophilic addition and the cycloaddition reactions have been widely employed to modify fullerenes for their practical applications.

Fullerenes are soluble in aromatic solvents and in carbon disulfide. In polar and H-bonding solvents such as acetone, tetrahydrofuran or methanol, C_{60} is essentially insoluble.

2.2.1. Nucleophilic Addition

Fullerenes undergo a wide variety of nucleophilic addition reactions with carbon, nitrogen, phosphorous and oxygen nucleophiles. By the initial attack of a nucleophile to C_{60}, the intermediate $Nu_nC_{60}^{n-}$ is formed. This intermediate is stabilized by: (a) the addition of electrophiles E^+, for example H^+ or carbocations to give $C_{60}E_nNu_n$ (b) the addition of neutral electrophiles EX such as alkylhalogenides to give $C_{60}E_nNu_n$ (c) intramolecular addition to yield methanofullerenes and cyclohexenofullerenes, or by (d) oxidation to obtain compounds $C_{60}Nu_2$.

Although many isomers are possible for additions, the preferred mode of addition is 1,2. The addition pattern changes according to the size of the added groups. For a combination of sterically addends, 1,4 additions and even 1,6

additions can take place alternatively or exclusively.[38] Given the large number of reactive double bonds in the molecule, polyadditions are frequent in the chemistry of fullerenes.

2.2.1.1. Fullerene Hydrides

Hydrogenated fullerenes, also termed fullerene hydrides[39] or "fulleranes",[40] may be interesting for applications such as hydrogen storage[41] (the storage capacity of for example $C_{60}H_{36}$ is 4.8%). As a rule, mixtures of fullerene hydrides are obtained in all the hydrogenations and the main product is usually $C_{60}H_{36}$, the most stable according to theoretical calculations.[42] Polyhydrofullerenes were observed up to a degree of hydrogenation of about 44 H atoms per C_{60} or even higher. But at this high hydrogen content, bond breaking in the C_{60}-cage usually takes place and the fullerene loses its structural integrity. An increasing degree of hydrogenation introduces considerable strain into the framework of the sphere.

Henderson and Cahill reported the synthesis of $C_{60}H_2$, the simplest fullerene hydride, in 1993.[43] Hydrolysis of the borane resulting from addition of BH_3 in THF to a solution of C_{60} in dry toluene gave the dihydride in 10-30% yield. Another synthetic method was soon published, in which Zn/HCl in refluxing toluene was used to synthesize $C_{60}H_2$.[44]

38. a) M. S. Meier, R. G. Bergosh, M. E. Gallagher, H. P. Spielmann, Z. Wang, *J. Org. Chem*., **2002**, *67*, 5946. b) A. Hirsch, *Top. Curr. Chem*., **1999**, *199*, 1.
39. J. Nossal, R. K. Saini, L. B. Alemany, M. Meier, W. E. Billups, *Eur. J. Org. Chem*., **2001**, 4167.
40. F. Cataldo, S. Iglesias-Groth, *Fulleranes: The Hydrogenated Fullerenes*, Springer: Dordrecht, The Netherlands, **2010**.
41. R. M. Baum, *Chem. Eng. News*, **1993**, *22*, 8.
42. R. Taylor, *J. Chem. Soc. Perkin Trans*, **1994**, *2*, 2497.
43. C. C. Henderson, P. A. Cahill, *Science*, **1993**, *259*, 1885.
44. M. S. Meier, P. S. Corbin, V. K. Vance, M. Clayton, M. Mollman, M. Poplawska, *Tetrahedron Lett*., **1994**, *35*, 5789.

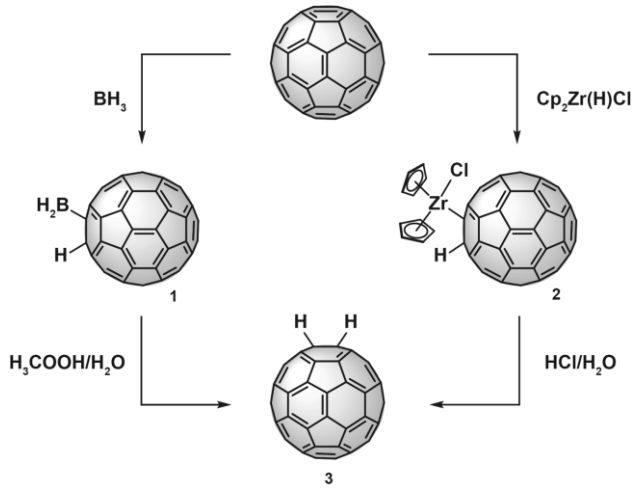

Scheme 1. Synthesis of $C_{60}H_2$ via hydroboration and hydrozirconation.

Various sources in the literature describe hydrogenated fullerenes as sensitive to air and light,[45] especially in solution.[46] The air sensitivity of hydrogenated fullerenes also complicates their chemical analysis. Samples quickly degrade, even if precautions are taken to deoxygenate samples or solvents because oxygen is often caught in the cage of fullerene structures.[47] C_{60} was hydrogenated in deuterated solvents to minimize the rapid oxidation process.[48]

2.2.1.2. Cycloadditions

The most employed reaction in fullerenes chemistry is the cycloaddition reaction since it leads to very stable cycloadducts avoiding the formation of isomeric mixtures, very frequent in nucleophilic addition reactions.

A large variety of cycloaddition reactions have been carried out with C_{60} and the complete characterization of the products, mainly monoadducts, have greatly increased our knowledge of fullerenes chemistry. These chemical

45. L. Becker, T. P. Evans, J. L. Bada, *J. Org. Chem*., **1993**, *58*, 7630.
46. A. S. Lobach, A. A. Perov, A. I. Rebrov, O. S. Roschupkina, V. A. Tkacheva, A. N. Stepanov, *Russ. Chem. Bull*., **1997**, *46*, 641.
47. A. D. Darwish, A. K. Abdul-Sada, G. J. Langley, H. W. Kroto, R. Taylor, D. R. M. Walton, *Synth. Met*., **1996**, *77*, 303.
48. A. D. Darwish, A. K. Abdul-Sada, G. J. Langley, H. W. Kroto, R. Taylor, D. R. M. Walton, *J. Chem. Soc. Perkin Trans*., **1995**, *2*, 2359.

transformations also provide a powerful tool for the functionalization of the fullerene sphere. Almost any functional group can be covalently linked to C_{60} by the cycloaddition of suitable addends.

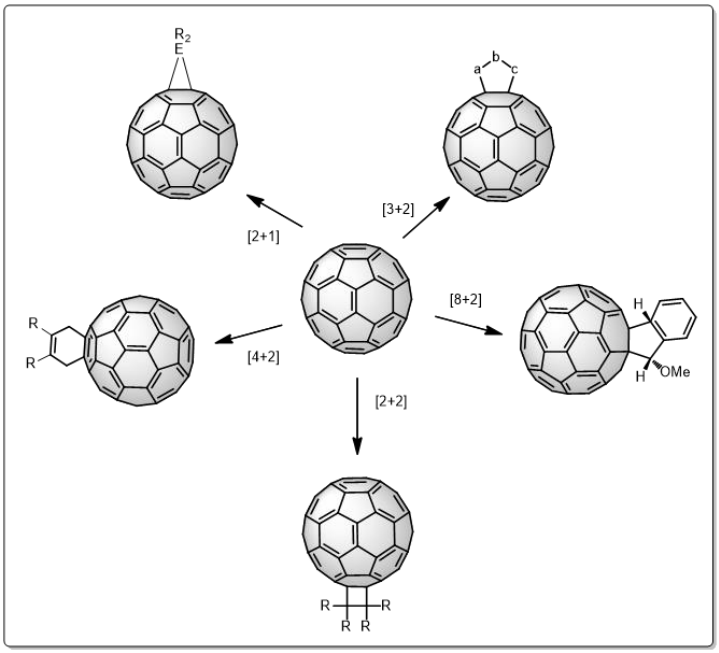

Scheme 2. Cycloadditions reactions carried out on C_{60}.

In the following sections, a brief introduction to the best known and most useful cycloaddition reactions will be presented in order to have a better knowledge on the chemical reactivity of fullerenes.

[3+2] Cycloadditions

Addition of azomethine ylides

Azomethine ylides, which exhibit 1,3-dipole character, react smoothly and in good yields with C_{60} to give fulleropyrrolidines.[49,50,51] This reaction was

49. M. Maggini, G. Scorrano, M. Prato, *J. Am. Chem. Soc*., **1993**, *115*, 9798.
50. a) N. Tagmatarchis, M. Prato, *Synlett*, **2003**, 768. b) M. Prato, M. Maggini, *Acc. Chem. Res*., **1998**, *31*, 519.

introduced by Prato and Maggini[49] and was evolved in one of the most used methods of fullerene functionalization. The broad acceptance of this method is explained by the good selectivity (only the [6,6] bond is attacked) and the wide range of addends and functional groups that are tolerated.

Azomethine ylides can be generated *in situ* from various readily accessible starting materials. One of the easiest approaches to produce 1,3-dipoles involves the decarboxylation of immonium salts derived from condensation of α-amino acids with aldehydes or ketones.[49,50] The versatility of this reaction arises from the possibility of introducing different substituents into three different positions of the pyrrolidine ring depending on the used aldehyde/ketone and respective amino acid.

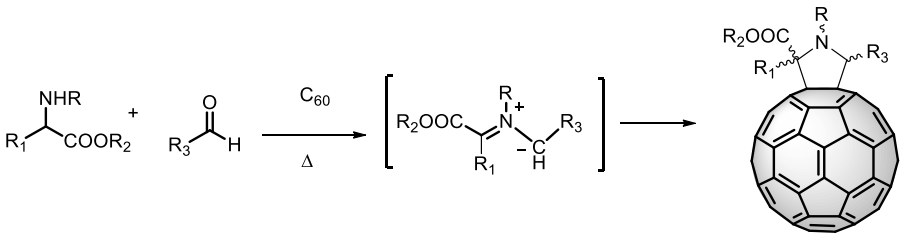

Scheme 3. 1,3-Dipolar cycloaddition of azomethine ylides to C_{60}.

An established procedure for attaching any functional molecule with aldehyde or ketone functionality to C_{60} is the original Prato reaction using sarcosine (*N*-methylglycine) as the amino acid component.[49] It has been used to append molecules such as porphyrins,[52] and TTF.[53] Most of the obtained fullerene

51. Although fulleropyrrolidines is usually used, the IUPAC name for these compounds is pyrrolidino[3,4:1,2][60]fullerene.
52. a) P. A. Liddell, D. Kuciauskas, J. P. Sumida, B. Nash, D. Nguyen, A. L. Moore, T. A. Moore, D. Gust, *J. Am. Chem. Soc*., **1997**, *119*, 1400. b) L. Sánchez, M. Sierra, N. Martín, A. J. Myles, T. J. Dale, J. Rebek, W. Seitz, D. M. Guldi, *Angew. Chem. Int. Ed*., **2006**, *45*, 4637.
53. a) J. L. Segura, E. Priego, N. Martín, C. Luo, D. M. Guldi, *Org. Lett*., **2000**, *2*, 4021. b) N. Martín, L. Sánchez, D. M. Guldi, *Chem. Commun*., **2000**, 113. c) M. Segura, L. Sánchez, N. Martín, J. De Mendoza, D. M. Guldi, *Org. Lett*., **2003**, *5*, 557. d) S. González, N. Martín, J. De Mendoza, D. M. Guldi, *Chem. Eur. J*., **2003**, *9*, 2457. e) F. Giacalone, J. L. Segura, N. Martín, D. M. Guldi, *J. Am. Chem. Soc*., **2004**, *126*, 5340. f) F. Giacalone, J. L. Segura, N. Martín, J. Ramey, D. M. Guldi, *Chem. Eur. J*., **2005**, *11*, 4819.

derivatives were used to examine the interaction between donors (e.g. porphyrin, TTF, conducting polymers etc.) and C_{60}, which acts as an electron acceptor. Our research group has shown that the Prato reaction can be quantitatively reversible (Scheme 4), which increases the versatility of this reaction, since it can also be used as a protection-deprotection protocol.[54]

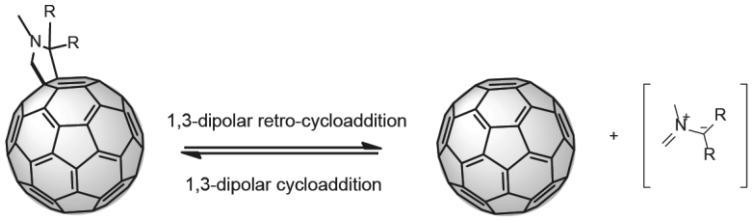

Scheme 4. Reversibility of the process cycloaddition retro-cycloaddition 1,3-dipolar of azomethine ylides to [60]fullerene.

Although retro-cycloadditions of other fullerene derivatives such as Diels-Alder cycloadducts[55] or Bingel methanofullerenes[56] have been known for years, fulleropyrrolidines had always been considered as stable cycloadducts. It is known that the pyrrolidines revert back,[57] leading to the formation of the alkene and the azomethine ylide. Nevertheless, the lower basicity of the fulleropyrrolidinic amino group due to the electronegative character of the fullerene unit, made this process unlikely.

However, by heating fulleropyrrolidines at reflux of 1,2-dichlorobenzene in the presence of a dipolarophile (maleic anhydride), able of trapping the formed

54. a) N. Martín, M. Altable, S. Filippone, A. Martín-Domenech, L. Echegoyen, C. M. Cardona, *Angew. Chem. Int. Ed*., **2006**, *45*, 110. b) O. Lukoyanova, C. M. Cardona, M. Altable, S. Filippone, A. M. Domenech, N. Martín, L. Echegoyen, *Angew. Chem. Int. Ed*., **2006**, *45*, 7430. c) S. Filippone, M. Izquierdo, A. Martín-Domenech, S. Osuna, M. Solá, N. Martín, *Chem. Eur. J*., **2008**, *14*, 5198.
55. a) N. Martín, F. Giacalone, *Fullerene Polymers. Synthesis, Properties and Applications*, Wiley-VCH, **2009**. b) F. Langa, J.-F. Nierengarten, *Fullerenes. Principles and Applications*, RSC, Cambridge, **2011**. c) N. Martín, J. F. Nierengarten, *Supramolecular Chemistry of Fullerenes and Carbon Nanotubes*, Wiley-VCH, **2012**.
56. N. N. P. Moonen, C. Thilgen, L. Echegoyen, F. Diederich, *Chem. Commun*., **2000**, 335.
57. S. Sinbandhit, J. Hamelin, *J. Chem. Soc. Chem. Commun*., **1977**, 768.

ylide, pristine fullerene was obtained. The catalytic version of the retro-cycloaddition, using $Cu(OTf)_2$ or the Wilkinson catalyst, allows highly efficient retro-cycloaddition reaction, independently of the substituents of the starting material. Furthermore, these conditions can be also successfully applied to bisadducts, higher fullerenes, or isoxazolinofullerenes.[58]

[4+2] Cycloadditions

The Diels-Alder reaction is one of the most versatile reactions of organic chemistry, and the most elegant method of creating six-membered rings because of its remarkable chemo- regio- and diastereoselectivity. Its application in fullerenes chemistry has led to a wide variety of products.[59] The conditions for cycloadduct formation strongly depend on the reactivity of the diene. Most [4+2] reactions with C_{60} are accomplished under thermal conditions. However, the main problem is that the resulting cycloadduct undergoes facile cycloreversion to the starting materials. In contrast, when the cycloaddition leads to stable products, this retro-Diels-Alder reaction doesn´t occur. An example is showed in Scheme 4 where *o*-quinodimethane reacts with C_{60} to form a very stable product due to the formation of an aromatic product that avoids the retro reaction.[60]

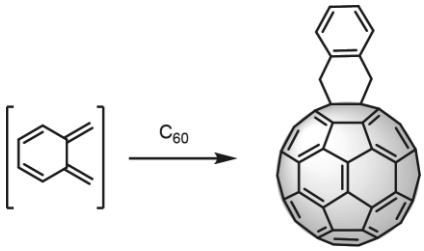

Scheme 5. [4+2] Cycloaddition reaction of *o*QDM to C_{60}.

58. N. Martín, M. Altable, S. Filippone, A. Martín-Domenech, R. Martínez-Álvarez, M. Suárez, M. E. Plonska-Brzezinska, O. Lukoyanova, L. Echegoyen, *J. Org. Chem*., **2007**, *72*, 3840.
59. a) N. Martín, J. L. Segura, F. Wudl, *New Concepts in Diels-Alder Cycloadditions to Fullerenes* in *Fullerenes: From Synthesis to Optoelectronic Properties*, Chapter 3, Eds. D. M. Guldi, N. Martín, Kluwer Academic Publishers, Dordrecht, Holland, **2002**.
60. J. L. Segura, N. Martín, *Chem. Rev*., **1999**, *99*, 3199.

[2+1] Cycloadditions

The [2+1] cycloaddition reactions allow synthesizing compounds wherein the fullerene sphere is fused to cyclic fragments of three links namely methanofullerenes.[61] The presence of two different kinds of bonds in C_{60} suggests that, in principle, two isomers of the methanofullerenes may be formed by such addition reactions, the [5,6]-open and [6,6]-closed isomers.

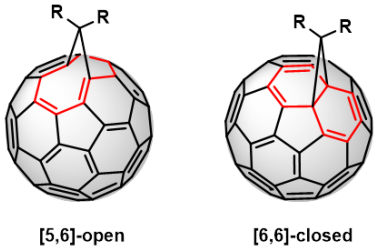

Figure 7. The two possible isomeric methanofullerenes.

The synthetic methods used to produce methanofullerenes may be conveniently divided into three categories. The most popular route is the thermal addition of diazocompounds,[62] the addition of free carbenes,[63] as well as cyclopropanation reactions which proceed by an addition/elimination mechanism, also known as Bingel reaction.[64]

61. F. Diederich, L. Isaacs, D. Philp, *Chem. Soc. Rev*., **1994**, 243.
62. a) T. Ohno, N. Martín, B. Knight, F. Wudl, T. Suzuki, H. Yu, *J. Org. Chem*., **1996**, *61*, 1306. b) M. H. Hall, H. Lu, P. B. Shevlin, *J. Am. Chem. Soc*., **2001**, *123*, 1349. c) A. B. Smith III, R. M. Strongin, L. Brard, G. T. Furst, W. J. Romanow, K. G. Owens, R. C. King, *J. Am. Chem. Soc*., **1993**, *115*, 5829. d) A. B. Smith III, R. M. Strongin, L. Brard, G. T. Furst, W. J. Romanow, K. G. Owens, R. J. Goldschmidt, R. C. King, *J. Am. Chem. Soc*., **1995**, *117*, 5492. e) L. Isaacs, A. Wehrsig, F. Diederich, *Helv. Chim. Acta*, **1993**, *76*, 1231. f) G. Schick, A. Hirsch, *Tetrahedron*, **1998**, *54*, 4283.
63. a) C. A. Merlic, H. D. Bendorf, *Tetrahedron Lett*., **1994**, *35*, 9529. b) T. S. Fabre, W. D. Treleaven, T. D. McCarley, C. L. Newton, R. M. Landry, M. C. Saraiva, R. M. Strongin, *J. Org. Chem*., **1998**, *63*, 3522. c) N. Dragoe, H. Shimotani, J. Wang, M. Iwaya, A. de Bettencourt-Días, A. Balch, K. Kitazawa, *J. Am. Chem. Soc*., **2001**, *123*, 1294. d) M. Yamada, T. Akasaka, S. Nagase, *Chem. Rev*., **2013**, *113*, 7209.
64. C. Bingel, *Chem. Ber*., **1993**, *126*, 1957.

The Addition of Diazocompounds to C_{60}

In 1991, Wudl and co-workers reported the synthesis of the first methanofullerene.[34a] C_{60} reacts with diphenyldiazomethane to give a [6,6]-ring bridged adduct. Subsequently, it was shown that this reaction tolerates the presence of a wide variety of substituents on the phenyl rings, implying its general applicability to the production of functionalized fullerene derivatives.[65]

The mechanism of diazo additions starts with the initial addition of the diazocompound as a 1,3-dipole to C_{60}. The reaction affords a pyrazoline which is thermally unstable under the experimental conditions and loses nitrogen rapidly to give [5,6]-open methanofullerenes, together with some [6,6]-closed isomer, under kinetic control. Thermal treatment of the isomeric mixture leads to the thermodynamically most stable [6,6]-closed methanofullerene.[66]

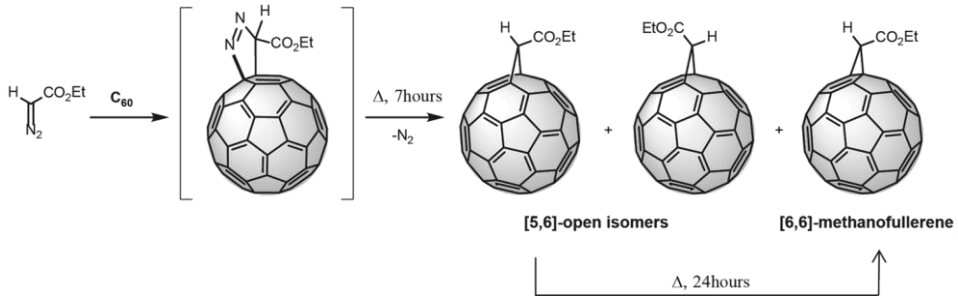

Scheme 6. Addition of alkyl diazoacetate to C_{60}.

65. a) F. Wudl, *Acc. Chem. Res*., **1992**, *25*, 157. b) S. Shi, K. C. Khemani, Q. Li, F. Wudl, *J. Am. Chem. Soc*., **1992**, *114*, 10656. c) M. Prato, A. Bianco, M. Maggini, G. Scorrano, C. Toniolo, F. Wudl, *J. Org. Chem*., **1993**, *58*, 5578. d) R. Sijbesma, G. Srdanov, F. Wudl, J. A. Castoro, C. Wilkins, S. H. Friedman, D. L. Decamp, G. L. Kenyon, *J. Am. Chem. Soc*., **1993**, *115*, 6510. e) T. Suzuki, Q. Li, K. C. Khemani, F. Wudl, O. Almarsson, *J. Am. Chem. Soc*., **1992**, *114*, 7300. f) M. Prato, V. Lucchini, M. Maggini, E. Stimpfl, G. Scorrano, M. Eiermann, T. Suzuki, F. Wudl, *J. Am. Chem. Soc*., **1993**, *115*, 8479. g) J. Osterodt, M. Nieger, P.-M. Windschief, I. Vogtle, *Chem. Ber*., **1993**, *126*, 2331. h) S. R. Wilson, Y. Wu, *J. Chem. Soc. Chem. Commun.*, **1993**, 784. i) M. Prato, T. Suzuki, F. Wudl, V. Lucchini, M. Maggini, *J. Am. Chem. Soc*., **1993**, *115*, 7876. j) J.-F. Nierengarten, Chapter 2 in *Fullerenes: From Synthesis to Optoelectronic Properties*, Eds. D. M. Guldi, N. Martín, Kluwer Academic Publishers, Dordrecht, Holland, **2002**.
66. R. F. Haldimann, F.-G. Klarner, F. Diederich, *Chem. Commun*., **1997**, 237.

Unsymmetrical diazocompounds give rise to two different [5,6]-open isomers. In these cases, the diastereomer with the bulkier group over the pentagon[67,68] predominates in the product mixture formed under kinetic control. This diastereoselectivity in the formation of the kinetic [5,6]-open isomers is a consequence of the minimization of the repulsive interactions between the substituents on the methylene unit and the N_2 moiety during the concerted process.

The Addition of Carbenes to C_{60}

Carbenes are well-known reactive intermediates that enable new carbon−carbon bond formation.[69] The reaction of C_{60} with carbenes is less complicated since it seems to insert exclusively in a [5,6]-bond of C_{60} in one step. Diazocompounds are useful carbene transfer reagents to fullerenes, so in a reaction with diazocompounds two possible mechanisms are postulated.

In the following scheme is shown the treatment of tosylhydrazones by Bamford-Stevens reaction[70] to generate *in situ* diazocompounds. From the diazocompound two possible mechanisms are formulated to justify the reaction product: 1,3-dipolar cycloaddition on a [6,6] bond of C_{60} to form a pyrazoline which is thermally unstable and loses nitrogen rapidly to give the thermodynamically most stable product, the [6,6]-closed methanofullerene, or extrusion of nitrogen followed by [2+1] cycloaddition reaction of the resulting carbene in a [5,6] bond of C_{60} to form the product of kinetic control, the [5,6]-open fulleroid. Conversion of the [5,6]-open fulleroid to the [6,6]-isomer was accomplished by heating as well as by photoexcitation.[71]

67. A. Skiebe, A. Hirsch, *J. Chem. Soc. Chem. Commun*., **1994**, 335.
68. J. Osterodt, A. Zett, F. Vögtle, *Tetrahedron*, **1996**, *52*, 4949.
69. G. Bertrand, *Carbene Chemistry: From Fleeting Intermediates to Powerful Reagents*, Ed. Marcel Dekker, New York, **2002**.
70. W. R. Bamford, T. S. Stevens, *J. Chem. Soc*., **1952**, 4735.
71. R. A. J. Janssen, J. C. Hummelen, F. Wudl, *J. Am. Chem. Soc*., **1995**, 117, 544.

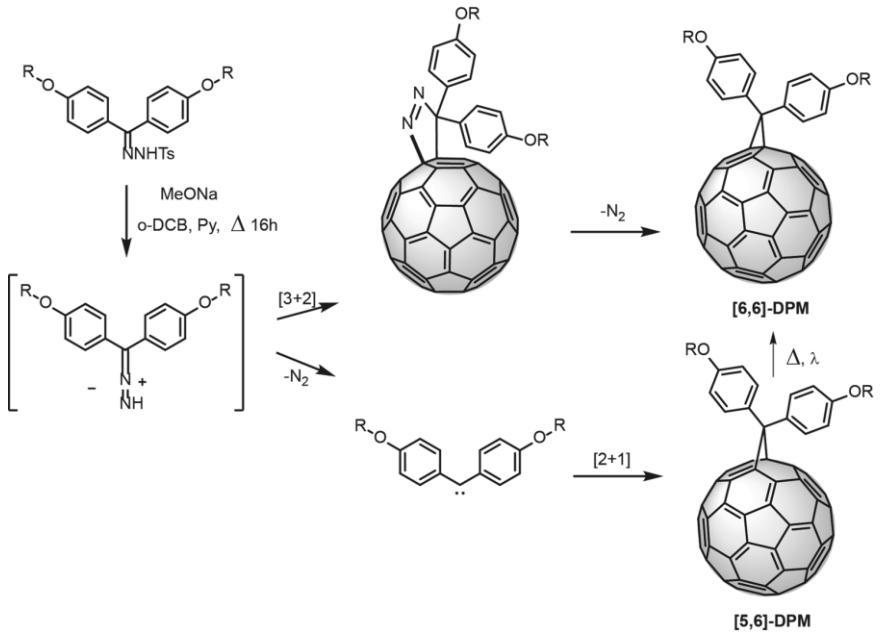

Scheme 7. Cyclopropanation by 1,3-dipolar cycloaddition to form [6,6]-diphenylmethanofullerenes (DPMs) or by insertion of a carbene to obtain the [5,6]-fulleroid.

Bingel Reaction to C_{60}

Bingel demonstrated that C_{60} reacts with several stabilized α-halocarbanions to give methanofullerenes.[64] This reaction is formulated as an addition of the stabilized α-halocarbanion to C_{60}, followed by intramolecular displacement of halide by the anionic center generated on the fullerene sphere. The reaction is fast, clean, and gives only [6,6]-closed methanofullerenes. The direct treatment of C_{60} with malonates in the presence of CBr_4 and DBU leads to an efficient conversion to methanofullerenes in good yields.

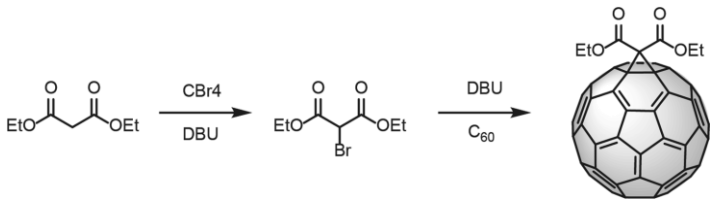

Scheme 8. Addition of α-bromomalonate to C_{60}.

No doubt, Bingel cyclopropanation is among the most successful reactions in fullerenes chemistry and a wide variety of derivatives have been prepared for applications both in materials science[72] as well as in bio-medicine, particularly involving hexakis-cycloadducts.[73]

72. a) W. Yan, S. M. Seifermann, P. Pierrat, S. Bräse, *Org. Biomol. Chem*., **2015**, *13*, 25. b) T. M. Figueira-Duarte, J. Clifford, V. Amendola, A. Gegout, J. Olivier, F. Cardinal, M. Meneghetti, N. Armaroli, J. F. Nierengarten, *Chem. Commun.*, **2006**, 2054.
73. A. Muñoz, D. Sigwalt, B. M. Illescas, J. Luczkowiak, L. Rodríguez-Pérez, I. Nierengarten, M. Holler, J. Remy, K. Buffet, S. P. Vincent, J. Rojo, R. Delgado, J. Nierengarten, N. Martín, *Nat. Chem.*, **2016**, *8*, 50.

2.3. Higher Fullerenes

The most important difference from the chemistry of C_{60} is due to the less symmetrical cages of the higher fullerenes, which exhibit a larger variety of bonds with different reactivity. Consequently, even for the monoadduct formation, many isomers can be expected.

2.3.1. Site-selectivity

Unlike C_{60}, higher fullerenes contain carbons with different degrees of pyramidalization corresponding to different degrees of the local curvature of the sphere. The reactivity of double bonds in higher fullerenes depends on the curvature of the sphere,[74] on the size of the fullerene and the relative position of the pentagonal and hexagonal rings on the fullerene surface. [6,6]-Bonds are more reactive as larger is the number of pentagons around them due to the highest degree of pyramidalization.

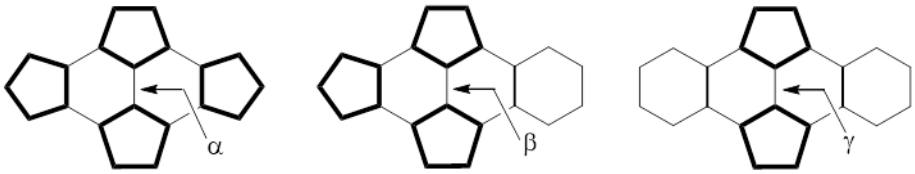

Figure 8. Different reactivity of the double bonds in higher fullerenes.

The most abundant and available higher fullerene, [70]fullerene, has to face different levels of selectivity since different double bonds are present as a result of the loosing of the spherical symmetry (Figure 9). Additions to C_{70} are driven by the release of strain of the attacked double bond. Thus, additions preferably take place at sites with the highest degree of pyramidalization.[74a,75] α Bond, [C(8)−C(25)] according to IUPAC nomenclature,[76] is the most reactive due to its greater local curvature, followed by β [C(7)−C(22)] and γ [C(1)−C(2)]. Additions only rarely occur at the δ site, located in the equatorial region, the less curved bonds and consequently the less reactive. For a greater

74. a) J. M. Hawkins, A. Meyer, *Science*, **1993**, *260*, 1918. b) R. C. Haddon, G. E. Scuseria, R. E. Smalley, *Chem Phys Lett.*, **1997**, *38*, 168. c) J. M. Hawkins, A. Meyer, M. A. Solow, *J. Am. Chem. Soc*., **1993**, *115*, 7499.
75. a) R. C. Haddon, *Science*, **1993**, *261*, 1545.
76. F. Cozzi, W. H. Powell, C. Thilgen, *Pure Appl. Chem*., **2005**, *77*, 843.

clarity, we proposed to designate these isomers (α, β, γ, and δ) as siteisomers and this selectivity as siteselectivity, following the particular nomenclature applied to systems where a functional group is repeated.[77,78]

Therefore, the mono-functionalization of C_{70} face a problem of siteselectivity and always produces a mixture of at least three isomers, since the dipole can be added in any of the three different double bonds, α, β, γ.

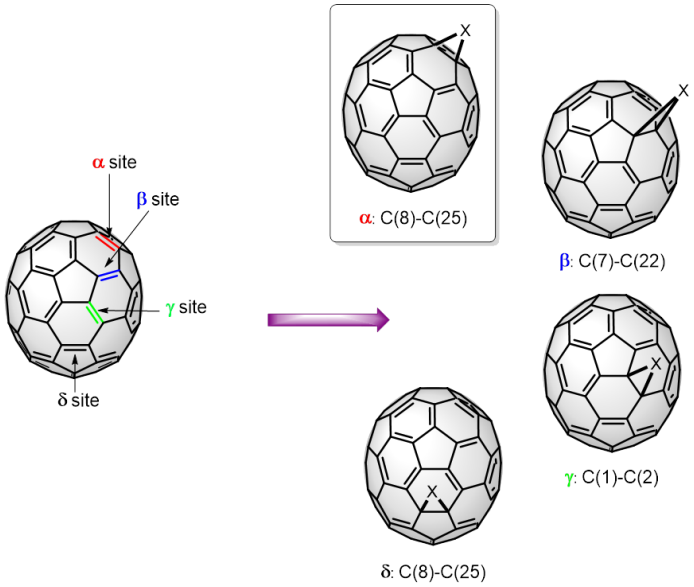

Figure 9. Possible addition sites on C_{70}.

Siteisomers identification can be done according to their UV-vis spectrum because each siteisomer α, β and γ always present the same characteristic spectrum, regardless of the type of chemical modification. Figure 10 shows the characteristic UV-vis of α-siteisomer and β-siteisomer.

77. I. Fleming, *Molecular Orbitals and Organic Chemical Reactions*, Wiley: Chichester, U.K., **2010**.
78. E. E. Maroto, A. de Cózar, S. Filippone, A. Martín-Domenech, M. Suárez, F. P. Cossío, N. Martín, *Angew. Chem. Int. Ed.*, **2011**, *50*, 6060.

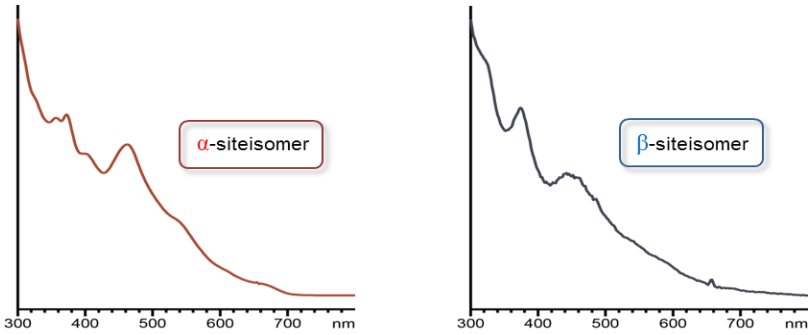

Figure 10. UV-vis spectra of α-siteisomer (left) and β-siteisomer (right).

2.3.2. Regioselectivity

If the dipole used in the functionalization of C_{70} is not symmetrical, the mixture of products obtained is much higher. Considering the two possible orientations of the dipole to attack each type of double bond, two possible regioisomers may be, in turn, formed for each siteisomer. Therefore, to the initial problem of siteselectivity, we must add the one of regioselectivity.

An illustrative example of this situation is showed in the Scheme 9. The cycloaddition of diazomethane to C_{70} leads to a mixture of products consisting of two regioisomers resulting from the addition to α bond (**4**, **5**) and a third derivative from the addition to β bond (**6**). The problem of the wide distribution of products obtained in the reactions with C_{70} has limited its study and its possible applications.

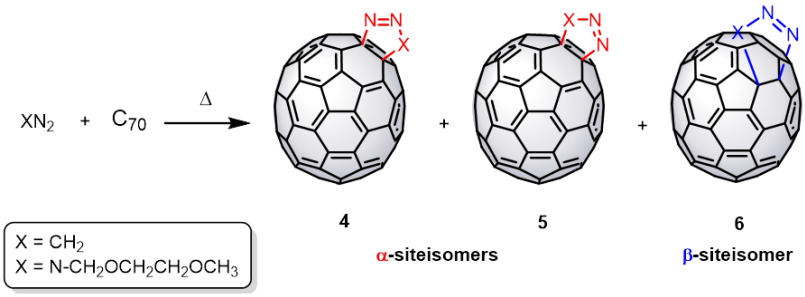

Scheme 9. Cycloaddition reaction of diazomethane as 1,3-dipole to C_{70}.

The use of higher fullerenes as building blocks for molecular materials is a promising and almost unexplored area. A photovoltaic cell built with a methano[70]fullerene shows better efficiency than one built with [60]PCBM, the most widely used fullerene derivative as electron acceptor component. The synthesis of [70]PCBM was performed in an analogous procedure to that described earlier for [60]PCBM. However, 1,3-dipolar cycloaddition to C_{70} leads to a mixture of three regioisomers.[79] The major isomer is the chiral α-siteisomer (**7**), and the two minor isomers are the achiral β-siteisomers (**8**, **9**).

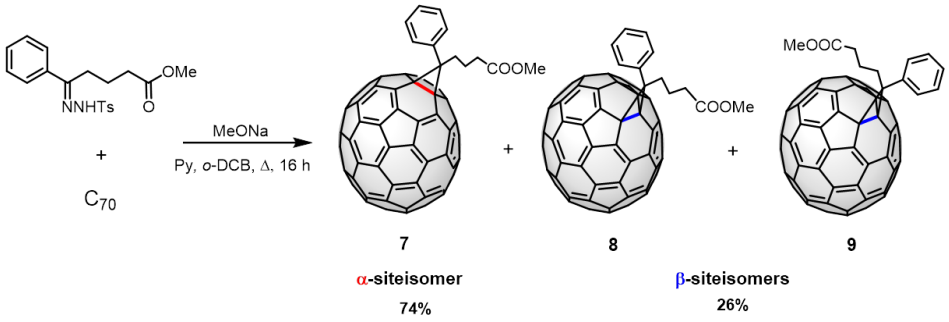

Scheme 10. Synthesis of [70]PCBM.

The chemistry of the higher fullerenes is less developed than the chemistry of C_{60} because the preparation of isomerically pure higher fullerenes is limited. The different site-isomers resulting in a reaction with C_{70} could be isolable only by tedious, highly expensive and time-consuming HPLC techniques. Controlling the site-selectivity on [70]fullerene is a challenge because only a few synthetic methods lead to isomeric pure C_{70} derivatives.[80]

79. M. Wienk, J. M. Kroon, W. J. H. Verhees, J. Krol, J. C. Hummelen, P. Van Haal, R. A. J. Janssen, *Angew. Chem. Int. Ed*., **2003**, *42*, 3371.
80. a) M. R. Cerón, M. Izquierdo, Y. Pi, S. L. Atehortúa, L. Echegoyen, *Chem. Eur. J*., **2015**, *21*, 7881. b) M. R. Cerón, M. Izquierdo, A. Aghabali, A. J. Valdez, K. B. Ghiassi, M. M. Olmstead, A. L. Balch, F. Wudl, L. Echegoyen, *J. Am. Chem. Soc*., **2015**, *137*, 7502. c) R. Tao, T. Umeyama, T. Higashino, T. Koganezawa, H. Imahori, *ACS Appl. Mater. Interfaces*, **2015**, *7*, 16676. d) M. R. Cerón, M. Izquierdo, A. Aghabali, S. P. Vogel, M. M. Olmstead, A. L. Balch, L. Echegoyen, *Carbon*, **2016**, *105*, 394.

2.4. Chiral Fullerenes

The chirality of fullerenes[81,82] can stem from an asymmetric arrangement of carbon atoms to afford chiral cages. Since the isolation of D_2-C_{76} (the first chiral fullerene) from fullerene soot extract,[83] a variety of such inherently chiral fullerenes have been reported.[81]

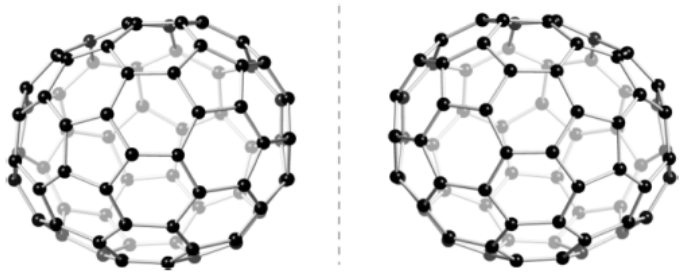

Figure 11. C_{76} structure (example of inherently chiral fullerenes).

Fullerene chirality is not limited only to the carbon skeleton (inherent chirality), but also can be induced by functionalization. Depending on the origin of their chirality, chiral fullerene derivatives can be classified as follows:[82]

1) Derivatives of achiral parent fullerenes in which the derivatization creates a chiral functionalization pattern on the fullerene skeleton, independent of the addends being identical or different, they have an *inherently chiral functionalization pattern*.
2) Derivatives of achiral parent fullerenes in which a chiral functionalization pattern is due exclusively to non-identities among addends, they have a *non-inherently chiral functionalization pattern*.
3) Derivatives of achiral parent fullerenes in which the addition of chiral residues does not create a chiral addition pattern on the fullerene surface, they have their chiral elements located exclusively in the addends.

81. C. Thilgen, I. Gosse, F. Diederich, *Top. Stereochem.*, **2003**, *23*, 1.
82. C. Thilgen, F. Diederich, *Chem. Rev*., **2006,** *106*, 5049.
83. R. Ettl, I. Chao, F. Diederich, R. L. Whetten, *Nature*, **1991**, *353*, 149.

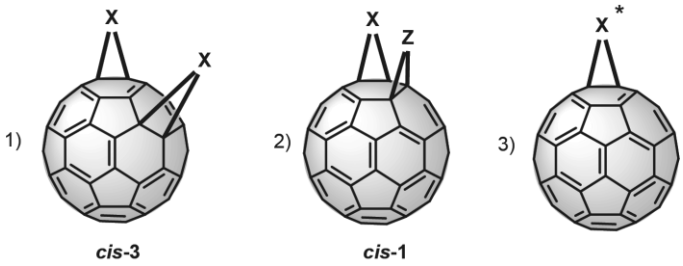

Figure 12. Representative examples of different ways to induce chirality in the [60]fullerene.

The addition patterns of [60]fullerene, namely, *cis*-3, *trans*-3, and *trans*-2, result in chiral products when the addends are identical and exhibit C_{2v} symmetry. Bisadducts (*cis*-1, *cis*-2, and *trans*-4) do not present inherently chiral addition patterns, but they can be chiral when the addends are not identical.[81]

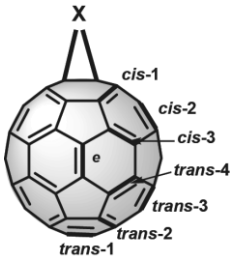

Figure 13. Relative positions of [6,6]-bonds in C_{60} adducts.

The control of some fundamental chemical aspects such as chirality is an issue of paramount importance that has not been properly covered to date. Chirality is a fundamental concept in chemistry and life with important scientific, technological and economic impact in modern industry. Furthermore, how chirality modifies the electronic properties of the carbon-based nanostructures is still an open question.

In particular, chiral fullerene derivatives have been shown to be important motifs in materials science[84] and medicinal chemistry,[85] where the biological response may depend on the used enantiomer.[86]

Moreover, fullerenes chirality represents a field of growing importance since the control of the absolute configuration can be a key factor for some fullerenes applications. Thus, as a representative example, chirality has demonstrated to be critical in creating supramolecular architectures of donor-acceptor dyads where photoconductive enantiomerically pure nanofibers exhibit much higher ambipolar charge-carrier mobility [$\sim 10^{-1}$ $cm^2/(Vs)$] than that measured for the spherical assembly formed from racemic dyads.[87]

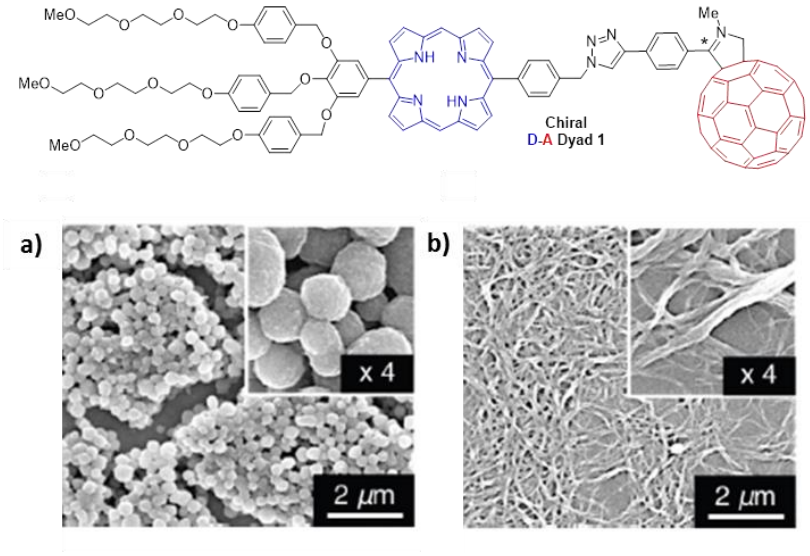

Figure 14. SEM micrographs of (a) assembled (±)-**10** showing uniformly sized spheres and (b) assembled enantiopure (+)-**10** displaying bundles of very long nanofibers.

84. T. Nishimura, K. Tsuchiya, S. Ohsawa, K. Maeda, E. Yashima, Y. Nakamura, J. Nishimura, *J. Am. Chem. Soc*., **2004**, *126*, 11711.
85. Z. Zhu, D. I. Schuster, M. E. Tuckerman, *Biochemistry*, **2003**, *42*, 1326.
86. S. H. Friedman, P. S. Ganapathi, Y. Rubin, G. L. Kenyon, *J. Med. Chem*., **1998**, *41*, 2424.
87. Y. Hizume, K. Tashiro, R. Charvet, Y. Yamamoto, A. Saeki, S. Seki, T. Aida, *J. Am. Chem. Soc*., **2010**, *132*, 6628.

Despite the impact of fullerenes in fields such as molecular electronics or nanoscience,[88] where their find their most important and promising applications, the synthesis of enantiomerically pure fullerene derivatives in an efficient, controlled and straightforward manner, has been very limited so far. Actually, only relatively few examples based on the use of chiral starting materials[89] or on expensive and highly-time consuming HPLC separations[90] have been reported.

Most of the enantioselective methods are based on chiral activation of the electron-deficient olefin. In this regard, the non-ligand character of fullerene double bonds might be the reason which has impeded using many of the available chiral protocols grounded on the activation of electron-deficient olefins. In the last decade, the catalytic asymmetric version of 1,3-dipolar cycloaddition of azomethine ylides to alkenes catalyzed by metals has emerged as an atom economical and powerful reaction for the synthesis of optically active pyrrolidines.[91,92] The structure of the azomethine ylide, allows the formation of the pyrrolidine ring contained in many biologically active compounds[93] with up to four stereogenic centers.

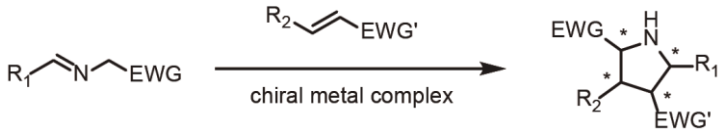

Scheme 11. Synthesis of enantiomerically pure pyrrolidines by asymmetric cycloaddition of azomethine ylides.

88. Y. Wang, J. Xu, Y. Wang, H. Chen, *Chem. Soc. Rev*., **2013**, *42*, 2930.
89. B. Illescas, N. Martín, J. Poater, M. Solà, G. P. Aguado, R. M. Ortuño, *J. Org. Chem*., **2005**, *70*, 6929. b) A. Bianco, M. Maggini, G. Scorrano, C. Toniolo, G. Marconi, C. Villani, M. Prato, *J. Am. Chem. Soc*., **1996**, *118*, 4072. c) J.-F. Nierengarten, V. Gramlich, F. Cardullo, F. Diederich, *Angew. Chem. Int. Ed*., **1996**, *35*, 2101.
90. F. Djojo, A. Hirsch, *Chem. Eur. J*., **1998**, *4*, 344.
91. a) C. Nájera, J. M. Sansano, *Angew. Chem. Int. Ed*., **2005**, *44*, 6272. b) J. Adrio, J. C. Carretero, *Chem. Commun*., **2011**, *47*, 6784. c) S. Cabrera, R. Gómez Arrayas, J. C. Carretero, *J. Am. Chem. Soc*., **2005**, *127*, 16394.
92. a) A. S. Gothelf, K. V. Gothelf, R. G. Hazell, K. A. Jørgensen, *Angew. Chem. Int. Ed*., **2002**, *41*, 4236. b) Y. Oderaotoshi, W. Cheng, S. Fujitomi, Y. Kasano, S. Minakata, M. Komatsu, *Org. Lett*., **2003**, *5*, 5043.
93. a) D. J. Denhart, D. A. Griffith, C. H. Heathcock, *J. Org. Chem*., **1998**, *63*, 9616. b) P. R. Sebahar, R. M. Williams, *J. Am. Chem. Soc*., **2000**, *122*, 5666.

In particular, the 1,3-dipolar cycloaddition of azomethine ylides formed by thermal treatment from aldehydes and aminoacids[36,38] or from iminoesters[94] onto C_{60} affords pyrrolidino[3,4:1,2][60]fullerenes, which are probably the most widely used fullerene derivatives due to their versatility, stability, and the availability of the starting materials. In addition, these heterocyclic-fused compounds constitute valuable building blocks to form fulleropeptides.[95]

In this context, the introduction of asymmetric metal catalysis by our group for the synthesis of pyrrolidinofullerenes, by reaction of 1,3-dipolar azomethine ylide and fullerene, with control of the absolute configuration of the created stereogenic centers, has been a first and significant breakthrough.

2.4.1. Chiral Functionalization of Fullerenes

2.4.1.1. Metal-Catalyzed Asymmetric [3+2] Cycloadditions onto [60]Fullerene

In the reaction with 1,3-dipoles, such as α-iminoesters,[96,97,98] or azlactones[99] catalyzed by metals, C_{60} acts as the dipolarophile giving rise to N-containing five-membered ring structures with a total stereocontrol of the new stereocenters.

α-Iminoesters as 1,3-dipoles: enantiomeric synthesis of fulleropyrrolidines

Under thermal conditions α-iminoester reacts in the presence of [60]fullerene leading to a mixture of two isomers, *cis* and *trans*.

94. S.-H. Wu, W.-Q. Sun, D.-W. Zhang, L.-H. Shu, H.-M. Wu, J.-F. Xu, X.-F. Lao, *J. Chem. Soc. Perkin Trans*., **1998**, *1*, 1733.
95. D. Pantarotto, A. Bianco, F. Pellarini, A. Tossi, A. Giangaspero, I. Zelezetsky, J.-P. Briand, M. Prato, *J. Am. Chem. Soc*., **2002**, *124*, 12543.
96. S. Filippone, E. E. Maroto, A. Martín-Domenech, M. Suárez, N. Martín, *Nat. Chem*., **2009**, *1*, 578.
97. E. E. Maroto, S. Filippone, A. Martín-Domenech, M. Suárez, N. Martín, *J. Am. Chem. Soc*., **2012**, *134*, 12936.
98. E. E. Maroto, S. Filippone, M. Suárez, R. Martínez-Álvarez, A. de Cózar, F. P. Cossío, N. Martín, *J. Am. Chem. Soc*., **2014**, *136*, 705.
99. J. Marco-Martínez, S. Reboredo, M. Izquierdo, V. Marcos, J. L. López, S. Filippone, N. Martín, *J. Am. Chem. Soc*., **2014**, *136*, 2897.

In order to control the stereochemistry of the products in terms of diastereo- and enantioselectivity, a deeper study was required.

Thus, screening of different metal–ligand complexes revealed the feasibility of the metal-mediated azomethine ylide cycloaddition onto the [60]fullerene sphere and, even in catalytic amounts, the reactions take place quickly at room temperature leading to the final fulleropyrrolidines in high conversions and excellent diastereo- and enantiomeric excesses.

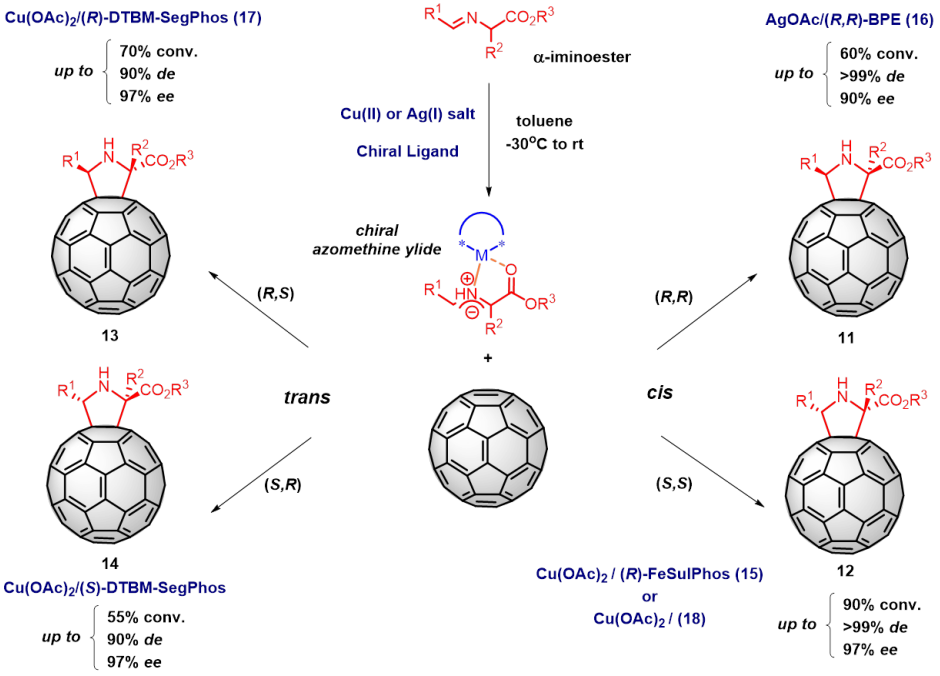

Scheme 12. Stereodivergent asymmetric 1,3-dipolar cycloaddition of N-metalated azomethine ylides onto C_{60}.

As shown in Scheme 12, depending on the metal and chiral ligand employed, a stereodivergent synthesis of fulleropyrrolidines can be achieved. Thus, for instance, when $Cu(OAc)_2$/(*R*)-FeSulPhos (**15**) or phosphoramidite (**18**) catalytic pairs are used, (*S*,*S*)-*cis* **12** is obtained with a high enantioselectivity (*ee* = 97%), in contrast to the system formed by AgOAc/(*R*,*R*)-BPE (**16**), which affords the opposite enantiomer, (*R*,*R*)-*cis* **11** (*ee* = 90%).

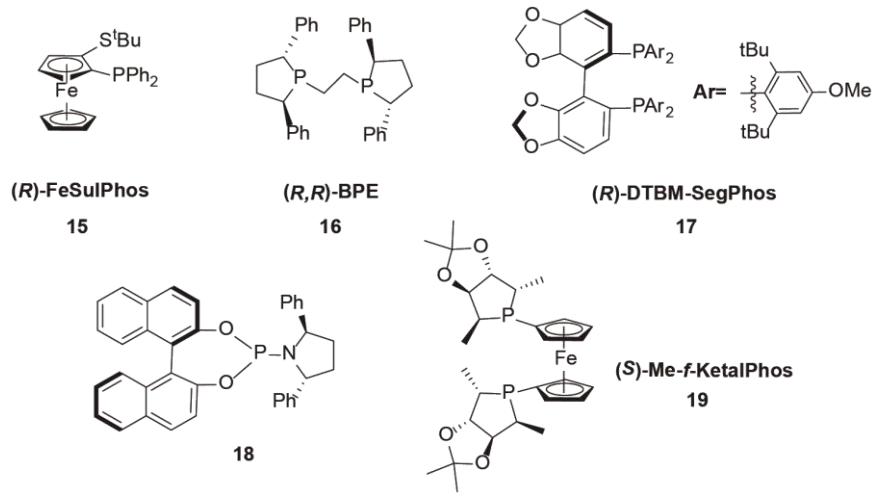

Figure 15. Chiral phosphines used in the preparation of fulleropyrrolidines.

On the other hand, *trans* enantiomers can also be obtained using commercially available (*R*)- or (*S*)-DTBM-SegPhos as the ligand and $Cu(OTf)_2$ as metal source, leading to (*R*,*S*)-*trans* **13** (*ee* = 97%), or (*S*,*R*)-*trans* **14**, (*ee* = 97%), respectively. In these cases an additional base (Et_3N) is necessary for the optimal outcome of the process, since the triflate counterion is not able to promote the formation of the azomethine ylide.

Azlactones as 1,3-dipoles: enantiomeric synthesis of fulleropyrrolines

After the aforementioned results, following the same strategy used before with α-iminoesters, our research group turned the attention onto azlactones **20** (Scheme 13), which are known to efficiently react as 1,3-dipoles with alkenes under Lewis acidic conditions.

These N-containing heterocyclic systems are extensively found in nature as biosynthetic intermediates and as part of pheromones, alkaloids, steroids, and chlorophylls.[100] However, the only stereoselective examples reported so far involve the silver mediated reaction and the enantioselective gold catalyzed

100. a) R. A. Mosey, J. S. Fisk, J. J. Tepe, *Tetrahedron: Asymmetry*, **2008**, *19*, 2755. b) N. M. Hewlett, C. D. Hupp, J. J. Tepe, *Synthesis*, **2009**, *17*, 2825.

synthesis, developed by the research groups of Tepe[101] and Toste,[102] respectively.

Chiral metal complexes that previously gave better results failed in the cycloaddition of azlactones. However, both Ag(I) and Cu(I) proved to be suitable metals for this transformation. Azlactones behave as monodentate ligands when coordinate to a metal and showed preference for less coordinating non-basic counterions as a result of a tighter interaction between the metal and the monodentate oxazolone. Indeed, the use of SbF_6^- as counterion of the complex Ag(I)/(*R*,*R*)-BPE (**16**) along with Et_3N as a base, afforded the pyrroline (*S*)-**22** with 87% *ee*. When the pair Cu(I)/(*R*)-FeSulPhos (**15**) was employed but using triflate, instead of acetate, and Et_3N as base, the opposite enantiomer (*R*)**-21** was obtained in 96% *ee*.

Using other chiral phosphine such as (*S*)-Me-f-KetalPhos (**19**) in combination with Cu(I)triflate-benzene complex led to higher enantioselectivity and opposite to the previous Cu(I) system. These results represented the first example of enantioselective cycloaddition of münchnones catalyzed by a copper salt.

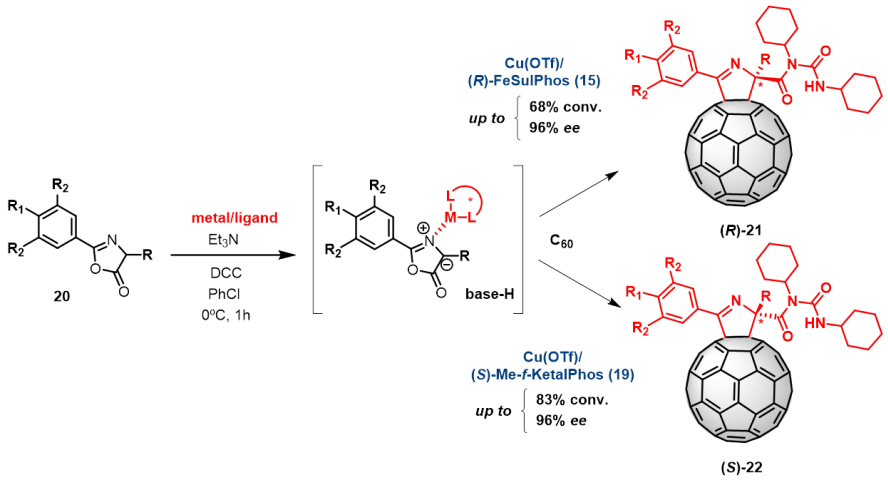

Scheme 13. Metal-catalyzed enantioselective [3+2] cycloaddition of azlactones onto C_{60}.

101. S. Peddibhotla, J. J. Tepe, *J. Am. Chem. Soc.*, **2004**, *126*, 12776.
102. a) A. D. Melhado, M. Luparia, F. D. Toste, *J. Am. Chem. Soc.*, **2007**, *129*, 12638. b) A. D. Melhado, G. W. Amarante, Z. J. Wang, M. Luparia, F. D. Toste, *J. Am. Chem. Soc.*, **2011**, *133*, 3517.

In general, metal-based chiral catalysts gave rise to the desired pyrrolinofullerene derivatives with moderate to good conversions and high enantiomeric excesses.

2.4.1.2. Metal-Catalyzed Asymmetric [3+2] Cycloadditions onto [70]Fullerene

The scope of this methodology was also investigated on the C_{70}, the most abundant and available higher fullerene. As mentioned above (2.3.1. Site-selectivity), [70]fullerene presents four different levels of selectivity since different double bonds are present as a result of the loss of the spherical symmetry. Thus, they preferentially take place at the most strained and reactive polar zone, α double bond followed by the β and, to a lesser extent, γ sites. This scenario is significantly more complex than that for C_{60}, and its control represents a real challenge.

The chiral complexes described for C_{60} were effective in the cycloaddition of non-symmetric azomethine ylides onto C_{70}. For all the tested α-imino esters, the enantiomeric excesses were excellent, and could be inverted by changing the metal chiral complex. The reaction occurred with very high site selectivity, affording almost exclusively the α-site-isomer. Good levels of regioselectivity were also achieved and the regioisomer with the alkoxycarboxyl group on the polar zone is preferentially formed **23**, regardless of the catalytic system used (Scheme 14).[78]

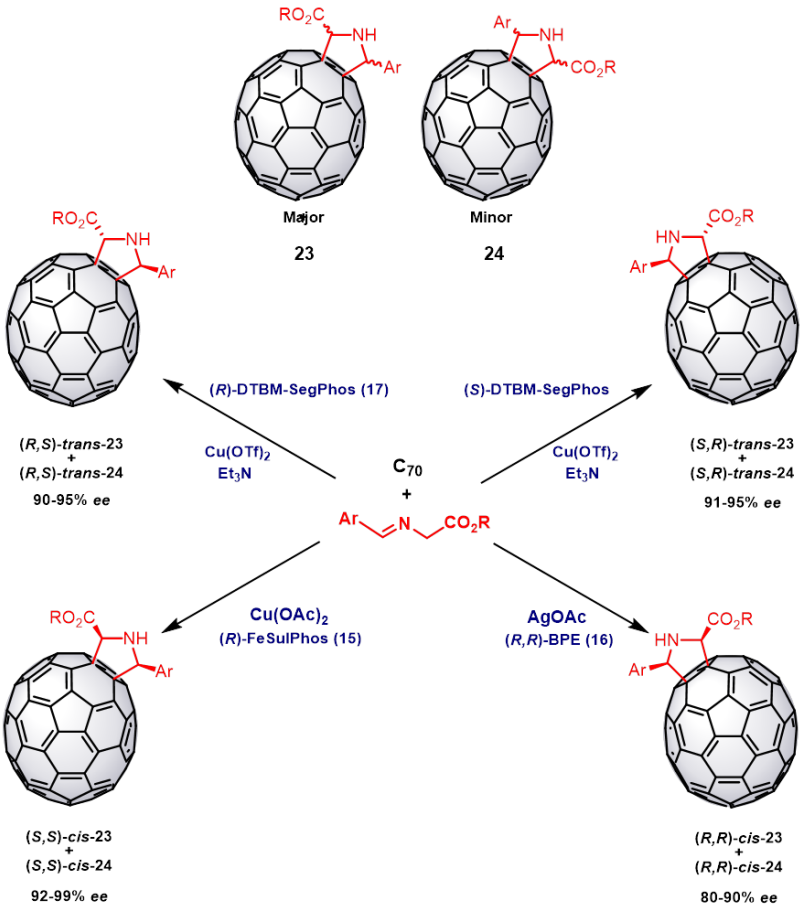

Scheme 14. Stereodivergent asymmetric 1,3-dipolar cycloaddition of N-metalated azomethine ylides onto C_{70}.

In the presence of Cu(II)acetate and (*R*)-FeSulPhos (**15**) the pyrrolidino[70]fullerene (*S*,*S*)-*cis* **23** was obtained with good regioselectivity (up to 80%) and excellent enantioselectivity (92-99%). The opposite enantiomer (*R*,*R*)-*cis* **23** was achieved with Ag(I)/(*R*,*R*)-BPE (**16**) affording slightly lower enantioselectivities (80-90%). The use of copper(II) triflate with (*R*)- or (*S*)-DTBM-SegPhos in the presence of Et_3N at room temperature yielded *trans* isomers with excellent enantioselectivities and good to excellent regio- and diastereoselectivities.

2.4.2. Asymmetric Organocatalysis in [3+2] Cycloaddition Reactions on Fullerenes

The concept of "organocatalysis" has grown quite dramatically in the last two decades.[103] Some advantages namely the robustness of the catalysts, their low price and the obvious less toxicity, are known so far.

Despite the different activation modes described in the literature, none of them is capable of activating fullerenes due to their non-coordinating nature. Among all the organocatalytic compounds, nucleophilic phosphines were evaluated as covalent organocatalysts[104] for fullerenes due to their commercial availability and high versatility.

Kroto and coworkers[105] reported the activation of allenoates by a nucleophilic attack of the phosphine to the central sp-hybridized carbon atom being able to react with electron-deficient double bonds.

The enantioselectivity of the process was studied by our research group. Several phosphines were evaluated according to their nucleophilicity in the reaction of ethyl 2,3-pentadienoate **25** with C_{60} (Scheme 15). The ferrocenyl-based phosphine (*S*,*S*)-f-Binaphane **26** was selected as the chiral organocatalyst and was able to perform the reaction in a very good conversion (48%) and excellent enantioselectivities, 91:9 enantiomeric ratio.

103. a) B. List, *Chem. Rev*., **2007**, *107*, 5413. b) D. W. C. MacMillan, *Nature*, **2008**, *455*, 304. c) B. Bertelsen, K. A. Jørgensen, *Chem. Soc. Rev*., **2009**, *38*, 2178. d) E. N. Jacobsen, D. W. C. MacMillan, *Proc. Natl. Acad. Sci. USA*, **2010**, *107*, 20618. e) B. List, *Asymmetric Organocatalysis* in *Topics in Current Chemistry*, Springer-Verlag: Berlin Heidelberg, **2010**.
104. J. Marco-Martínez, V. Marcos, S. Reboredo, S. Filippone, N. Martín, *Angew. Chem. Int. Ed*., **2013**, *52*, 5115.
105. B. F. O. Donovan, P. B. Hitchcock, M. F. Meidine, H. W. Kroto, R. Taylor, D. R. M. Walton, *Chem. Commun*., **1997**, 81.

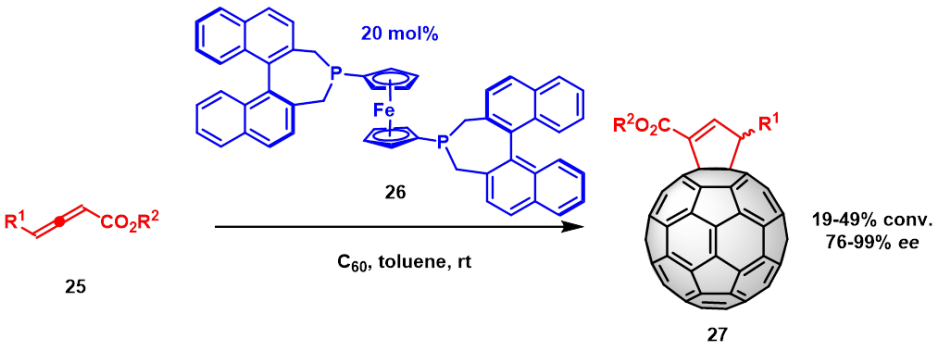

Scheme 15. (*S*,*S*)-f-Binaphane-catalyzed [3+2] cycloaddition of allenoates to C_{60}.

Going one step further in the use of organocatalytic methods for the preparation of chiral fullerene derivatives, our group studied a different type of 1,3-dipole, the azlactones, which afforded excellent results in its metallic version (section 2.4.1.1).[99] Chiral N-heterocyclic carbenes that have been widely employed as ligands in metal catalysis and more recently in organocatalysis[106] due to their ability of behaving as Brønsted base catalysts allowed the formation of the adducts, not only in good conversion but also in very interesting enantioselectivities.

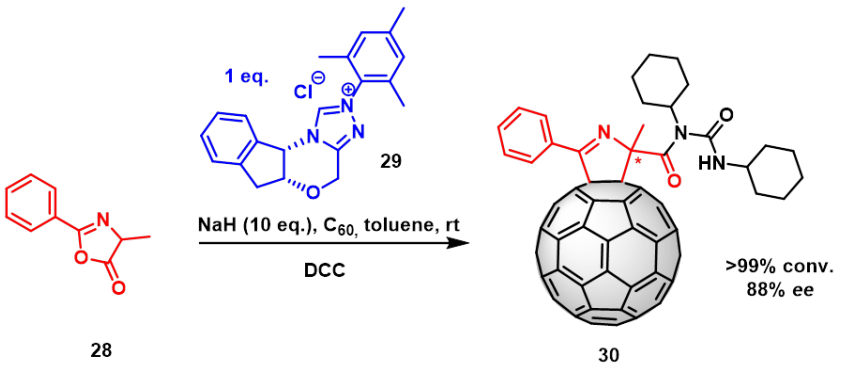

Scheme 16. Organocatalytic enantioselective [3+2] cycloaddition of azlactones onto C_{60}.

106. a) D. Enders, O. Niemeier, A. Henseler, *Chem. Rev.*, **2007**, *107*, 5606. b) X. Bugaut, F. Glorius, *Chem. Soc. Rev.*, **2012**, *41*, 3511. c) S. J. Ryan, L. Candish, D. W. Lupton, *Chem. Soc. Rev.*, **2013**, *42*, 4906.

The reaction between the azlactone **28**, C_{60}, NaH and the catalyst **29** in anhydrous toluene, gave rise to an enantioselective cycloaddition in excellent conversion (>99%, 88% *ee*), being even possible obtaining the opposite enantiomer by the use of the commercially available NHC opposite enantiomer (Scheme 16).

2.5. Fullerene-Transition Metal Hybrids

Although fullerene chemistry may be thought to be fully established, there are a wide variety of reactions to be explored, especially those involving the use of transition metals.

The combination of fullerene cages with transition-metal complexes,[107] which possess functional properties such as electron-donating and catalytic activity, can enhance and tune the properties of the resulting fullerene-containing compounds. These hybrid compounds have potential for application in various fields, depending on the nature of the transition metal and the way in which the fullerene and the transition metal are connected.

There are numerous ways in which fullerene cages combine with transition metals:

a) Coordination complexes by addition of the metal directly attached to one or more of the fullerene double bonds (Figure 17a). Examples of these complexes with numerous metals have been described: platinum,[108] palladium,[109] rhodium,[110] iridium,[111] molybdenum,[112] osmium,[113] ruthenium,[114] iron[115] or tungsten.[116]

107. A. L. Balch, M. Olmstead, *Chem. Rev*., **1998**, *98*, 2123.
108. a) P. J. Fagan, J. C. Calabrese, B. Malone, *Science*, **1991**, *252*, 1160. b) L.-C. Song, G.-F. Wang, P.-C. Liu, Q.-M. Hu, *Organometallics*, **2003**, *22*, 4593. c) L.-C. Song, G.-A. Yu, F.-H. Su, Q.-M. Hu, *Organometallics*, **2004**, *23*, 4192.
109. a) H. Nagashima, A. Nakaota, Y. Saito, M. Kato, T. Kawanishi, K. Itoh, *J. Chem. Soc. Chem. Commun.*, **1992**, 377. b) L.-C. Song, G.-A. Yu, H.-T. Wang, F.-H. Su, Q.-M. Hu, Y.-L. Song, Y.-C. Gao, *Eur. J. Inorg. Chem.*, **2004**, 866. c) L.-C. Song, F.-H. Su, Q.-M. Hu, E. Grigiotti, P. Zanello, *Eur. J. Inorg. Chem.*, **2006**, 422.
110. a) A. L. Balch, J. W. Lee, B. C. Noll, M. Olmstead, *Inorg. Chem.*, **1993**, *32*, 55. b) A. V. Usatov, K. N. Kudin, E. V. Voronstov, L. E. Vinogradova, Y. N. Novikov, *J. Organomet. Chem.*, **1996**, *522*, 147.

b) Systems in which the metal center is coordinated to a metal binding moiety attached to the fullerene cage through the formation of covalent bonds.[117]

c) Cocrystallates, host−guest inclusion complexes, and fulleride salts in which pristine fullerene cages and metal species are bound by noncovalent interactions such as van der Waals or electrostatic forces.[118]

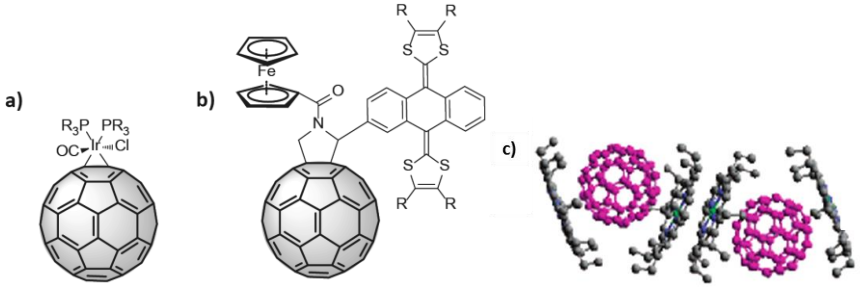

111. a) A. L. Balch, V. J. Catalano, J. W. Lee, *Inorg. Chem.*, **1991**, *30*, 3980. b) A. V. Usatov, E. V. Martynova, F. M. Dolgushin, A. S. Peregudov, M. Y. Antipin, Y. N. Novikov, *Eur. J. Inorg. Chem.*, **2002**, 2565. c) A. L. Balch, V. J. Catalano, J. W. Lee, M. Olmstead, S. R. Parkin, *J. Am. Chem. Soc.*, **1991**, *113*, 8953. d) A. L. Balch, A. S. Ginwalla, B. C. Noll, M. M. Olmstead, *J. Am. Chem. Soc.*, **1994**, *116*, 2227.
112. D. M. Thompson, M. Jones, M. C. Baird, *Eur. J. Inorg. Chem.*, **2003**, 175.
113. H. Song, K. Lee, J. T. Park, M.-G. Choi, *Organometallics*, **1998**, *17*, 4477.
114. a) K. Lee, H.-F. Hsu, J. R. Shapley, *Organometallics*, **1997**, *16*, 3876. b) D. M. Guldi, G. M. A. Rahman, R. Marczak, Y. Matsuo, M. Yamanaka, E. Nakamura, *J. Am. Chem. Soc.*, **2006**, *128*, 9420.
115. M. Sawamura, Y. Kuninobu, M. Toganoh, Y. Matsuo, M. Yamanaka, E. Nakamura, *J. Am. Chem. Soc.*, **2002**, *124*, 9354.
116. L.-C. Song, J.-T. Liu, Q.-M. Hu, L.-H. Weng, *Organometallics*, **2000**, *19*, 1643.
117. a) M. Maggini, A. Karlsson, G. Scorrano, G. Sandonà, G. Farnia, M. Prato, *J. Chem. Soc. Chem. Commun.*, **1994**, 589. b) M. Iyoda, F. Sultana, S. Sasaki, H. Butenschön, *Tetrahedron Lett.*, **1995**, *36*, 579. c) D. Guldi, M. Maggini, G. Scorrano, M. Prato, *J. Am. Chem. Soc.*, **1997**, *119*, 974. d) B. Illescas, N. Martín, *J. Org. Chem.*, **2000**, *65*, 5728.
118. a) J. D. Crane, P. B. Hitchcok, H. W. Kroto, R. Taylor, D. R. M. Walton, *J. Chem. Soc., Chem. Commun.*, **1992**, 1764. b) J. D. Crane, P. B. Hitchcok, *J. Chem. Soc., Dalton Trans.*, **1993**, 2537. c) M. M. Olmstead, D. A. Costa, K. Maitra, B. C. Noll, S. L. Phillips, P. M. Van Calcar, A. L. Balch, *J. Am. Chem. Soc.*, **1999**, *121*, 7090. d) P. D. W. Boyd, C. A. Reed, *Acc. Chem. Res.*, **2005**, *38*, 235.

Figure 16. Addition of a metal complex to the double bond of [60]fullerene (a) addition of metal complex ligands by covalent bonding (b) and [60]fullerene-metalloporphyrin cocrystallates(c).

A variety of important organic reactions, involving transition metal catalysts, have never been explored in fullerenes. An example where the transition metal plays an important role is the Pauson-Khand reaction on fullerenes developed in our research group.[119]

By intramolecular cycloaddition [2+2+1] with the double bond of the [60]fullerene, an alkyne and carbon monoxide, catalyzed by transition metals, led to cyclopentenones fused on the fullerene surface as shown in Scheme 17.[120] This process, which is not favored with electron-deficient olefins, takes place in the C_{60} thanks to the curvature of the double bonds, which makes them more reactive.

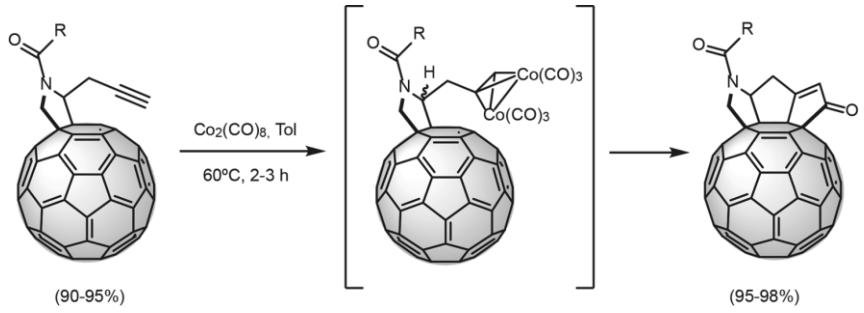

Scheme 17. Pauson-Khand reaction catalyzed by octacarbonyldicobalt on C_{60}.

Another reaction used to functionalize the C_{60} using metal catalysts is the cycloaddition of alkyl- or aryl- diazocompounds catalyzed by Pd(II) complexes. The functionalization is produced on the [5,6]-bond of the C_{60} with

119. N. Martín, M. Altable, S. Filippone, A. Martín-Domenech, *Chem. Commun*., **2004**, 1338.
120. a) N. Martín, M. Altable, S. Filippone, A. Martín-Domenech, *Chem. Commun*., **2004**, 1338. b) N. Martín, M. Altable, S. Filippone, A. Martín-Domenech, A. Poater, M. Solá, *Chem. Eur. J*., **2005**, *11*, 2716.

high selectivity (Scheme 18).[121] This sets a precedent for future works that allow the effective synthesis of substituted [5,6]-fulleroids.

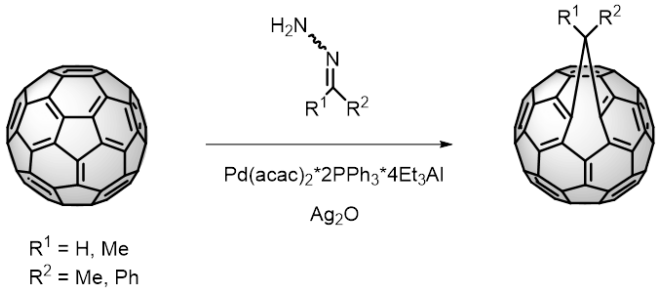

Scheme 18. Catalytic cycloaddition of diazocompounds to C_{60} in the presence of palladium.

2.5.1. Applications of Metal-Fullerene in Catalysis

The manifold of properties and structural features of fullerenes suggest a new promising field combining organic and coordination chemistry playing an important role in catalysis.

2.5.1.1. [60]Fullerene as Ligand for Homogeneous Catalysts

The catalytic properties of different metal-fullerene complexes have been studied. Sulman *et al.*[122] reported a new catalyst, $(\eta^2\text{-}C_{60})Pd(PPh_3)_2$, catalytically active in the hydrogenation of a triple bond of 3,7-dimethyl-octa-6-ene-1-in-3-ol (dehydrolinalool, DHL) to 3,7-dimethyl-octa-1,6-diene-2-ol (linalool, LN) with a selectivity of 99.5%. This hydrogenation is one of the stages of industrial production of fragrances and vitamins A and E.

Claridge *et al.*[123] developed an efficient catalyst $(\eta^2\text{-}C_{60})RhH(CO)(PPh_3)_2$ in olefin hydroformylation to aldehydes, intermediates in the synthesis of plasticizers and detergents, an important industrial process. The catalytic activity is somewhat lower than the previous used catalyst $RhH(CO)(PPh_3)_3$,

121. A. R. Tuktarov, V. V. Korolev, U. M. Dzhemilev, *Russian J. Org Chem.*, **2010**, *46*, 588.
122. E. Sulman, V. Matveeva, N. Semagina, I. Yanov, V. Bashilov, V. Sokolov, *J. Mol. Cat. A: Chemical*, **1999**, *146*, 257.
123. J. B. Claridge, R. E. Douthwaite, M. L. Green, R. M. Lago, S. C. Tsang, A. P. E. York, *J. Mol. Catal.*, **1994**, *89*, 113.

however, the presence of C_{60} noticeably enhances thermal stability. Therefore, the process could be carried out at higher temperatures increasing productivity.

2.5.1.2. Catalytic Reactions Involving [60]Fullerene

Transfer hydrogenation of C_{60}

The influence of C_{60} on the dehydrogenation of hydroaromatic compounds has been revealed by Malhotra *et al.*[124]. At elevated temperatures, fullerenes become strong dehydrogenating agents with respect to hydrocarbons.[13a] Treatment of C_{60} in a sealed glass tube at 350ºC under an inert atmosphere with a melt of 9,10-dihydroanthracene, which serves as a source of hydrogen,[125,126] leads to the hydrides $C_{60}H_{18}$ or $C_{60}H_{36}$ with high selectivity.[127] In the presence of C_{60}, the phenanthrene **32**: dihydrophenanthrene **31** ratio is 33, while in its absence, it is 1.3.[128] Heating of the corresponding hydrides in an inert gas leads to their quantitative dehydrogenation to pristine C_{60}. Thus, C_{60} behaves as a catalyst in this reaction.

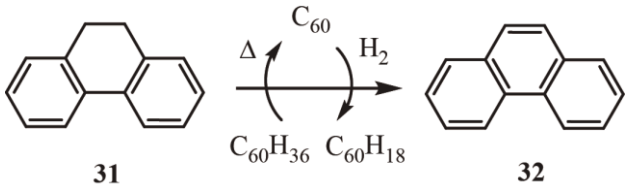

Scheme 19. Dehydrogenation of dihydrophenanthrene by using C_{60} as catalyst.

124. R. Malhotra, D. F. McMillen, D. S. Tse, D. C. Lorents, R. S. Ruoff, D. M. Keegan, *Energ. Fuel*, **1993**, *7*, 685.
125. C. Rüchardt, M. Gerst, J. Ebenhoch, H-D. Beckhaus, E. E. B. Campbell, R. Tellgmann, H. Schwarz, T. Weiske, S. Pitter, *Angew. Chem. Int. Ed.*, **1993**, *32*, 584.
126. J. Nossal, R. K. Saini, A. K. Sadana, H. F. Bettinger, L. B. Alemany, G. E. Scuseria W. E. Billups, M. Saunders, A. Khong, R. Weisemann, *J. Am. Chem. Soc*., **2001**, *123*, 8482.
127. C. Rüchardt, M. Gerst, J. Ebenhoch, H.-D. Beckhaus, E. E. B. Campbell, R. Tellgman, H. Schwarz, T. Weiske, S. Pitter, *Angew. Chem. Int. Ed*., **1993**, *32*, 584.
128. P. Chen, X. Wu, J. Lin, K. L. Tan, *Science*, **1999**, *285*, 91.

These results indicate the involvement of C_{60} in the capture of hydrogen atoms from the hydroaromatic compounds and the subsequent hydrogen transfer.

In 2009 Li and Xu reported that [60]fullerene could act as a non-metal catalyst for hydrogenation of aromatic nitrocompounds. These findings could revolutionize catalysis, because fullerenes are environmentally friendly compounds. The hydrogenation was achieved on this catalyst with high yield and selectivity under 1 atmospheric pressure of H_2 and light irradiation at room temperature or under dark conditions and elevated temperature and pressure.[129]

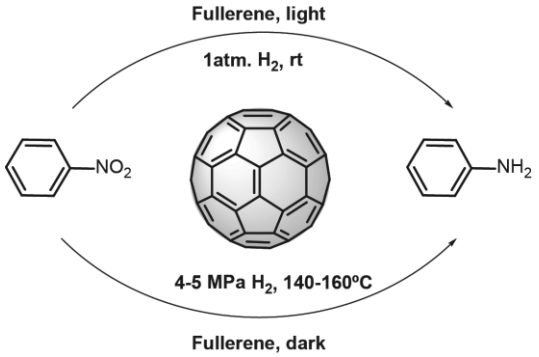

Scheme 20. Aromatic nitrocompound hydrogenation by using C_{60} as catalyst.

However, few years later, it was demonstrated that C_{60}^- is not a non-metal catalyst. To produce the active catalyst, C_{60} was treated with nickel and it was the true catalytic species. C_{60}^- prepared in the absence of Ni resulted to be inactive for hydrogenation.

The above examples show that fullerene-containing catalysts can be active and selective in different reactions. The use of fullerene represents an opportunity for creating new catalytic systems which, however, has not been properly addressed so far.

129. L. Baojun X. Zheng, *J. Am. Chem. Soc.*, **2009**, *131*, 16380.

2.6. Endohedral Fullerenes

Endohedral fullerenes are defined as carbon cages encapsulating different atoms, clusters or small molecules in their inner space. This type of fullerenes has attracted much attention due to its unique composition and exceptional properties that could be of interest for different fields such as biomedicine, molecular electronics, photovoltaics or materials science.[130]

The properties of endohedral fullerenes can be easily modified depending upon the species entrapped and the fullerene cages. Since the detection of endohedral fullerenes following the discovery of C_{60}, many species such as metals, noble gases, clusters, atoms or molecules, have been encapsulated in the empty fullerene cage. In this sense, endohedral fullerenes are classified in two principal categories:

- Metallofullerenes, which are those that contain elemental metals.[131] In this family are included: classical metallofullerenes, $M@C_{2n}$ or $M_2@C_{2n}$, with $60 \leq 2n \leq 88$,[132] metallic carbides, $M_2C_2@C_{2n}$ and $M_3C_2@C_{2n}$, where $68 \leq 2n \leq 92$,[133] metallic nitrides, $M_3N@C_{2n}$, with $68 \leq 2n \leq 96$[134] and more recently, metallic oxides, $M_4O_2@C_{80}$[135]. These fullerenes are typically produced by laser-vaporization or arc discharge techniques of graphite rods containing metals.[6c]

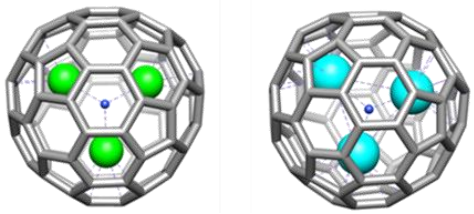

Figure 17. Molecular structures of $Sc_3N@C_{80}$ and $Gd_3N@C_{80}$.

130. a) T. Akasaka, F. Wudl, S. Nagase, *Chemistry of Nanocarbons*, Wiley-Blackwell, London, **2010**. b) X. Lu, T. Akasaka, S. Nagase, *Chem. Comm.*, **2011**, *47*, 5942.
131. M. Yamada, T. Akasaka, S. Nagase, *Acc. Chem. Res*., **2010**, *43*, 92.
132. X. Lu, T. Akasaka, S. Nagase, *Chem. Commun*., **2012**, 47, 5942.
133. A. Rodríguez-Fortea, A. L. Balch, J. M. Poblet, *Chem. Soc. Rev*., **2011**, *40*, 3551.
134. L. Dunsch, S. Yang, *Small*, **2007**, *3*, 1298.
135. S. Stevenson, M. A. Mackey, M. A. Stuart, J. P. Phillips, M. L. Easterling, C. J. Chancellor, M. M. Olmstead, A. L. Balch, *J. Am. Chem. Soc*., **2008**, *130*, 11844.

Because of the large variety of endohedral metallofullerenes, only some of the most relevant examples will be briefly described. Since the isolation and characterization of the first endohedral fullerene La@C_{82},[136] many other classical M@C_{2n} (M = Sc, Y, La, Ce, Gd, etc.) have been obtained, with a C_{2v}-C_{82} most abundant cage.[132] In all these fullerene cages filled with a single metal, the metal is not in the center of the cage, but tends to coordinate with the cage carbons, being situated under a hexagonal ring along the C2 axis (Figure x). From the 24 non-equivalent carbon atoms of different nature that can be identified, the carbons close to the La atom are more reactive than the others because of the interaction with the metal. Even more, the three electrons that are transferred from La to the cage are mainly located on these carbon atoms. As a result, the distribution of charge density is highly anisotropic over the surface, with electrophiles and nucleophiles selectively attacking the two different regions.[137]

In the case of the endohedral fullerenes containing two metals, the $M_2@I_h$-C_{80} (M = La, Ce, etc) cage is typically obtained.[132] The geometrical features analysis reveals only two kinds of carbon atoms, resulting in only two kind of bonds corresponding to [5,6] and [6,6] junctions. Each La atom can transfer 3 electrons to reach a total of 6, however both atoms are rotating with no preference location in $La_2@I_h$-C_{80} and the charge is homogenously distributed along the cage. In this case, the high symmetry is the responsible of the high regioselectivity on this cage and make it ideal for chemical modifications.

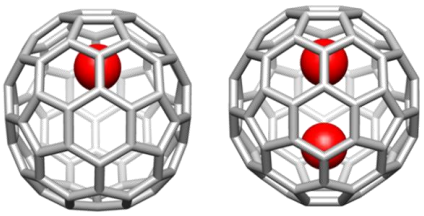

Figure 18. Molecular structures of La@C_{82} and $La_2@C_{80}$.

136. Y. Chai, T. Guo, C. Jin, R. E. Haufler, L. P. F. Chibante, J. Fure, L. Wang, J. M. Alford, R. E. Smalley, *J. Phys. Chem*., **1991**, *95*, 7564.
137. L. Feng, T. Tsuchiya, T. Wakahara, T. Nakahodo, Q. Piao, Y. Maeda, T. Akasaka, T. Kato, K. Yoza, E. Horn, N. Mizorogi, S. Nagase, *J. Am. Chem. Soc*., **2006**, *128*, 5990.

- Fullerenes encapsulating small molecules.

Controlling the size of the carbon cage or the product distribution by using arc discharge is not possible. "Molecular surgery" emerged as an alternative and suitable methodology to synthesize endohedral fullerenes in a controlled manner, and paved the way toward atoms or small molecules encapsulation. Some of the molecules trapped in C_{60} open cages are $H_2@C_{60}$,[138] $He@C_{60}$,[139] and $H_2O@C_{60}$[140] (Figure 19).

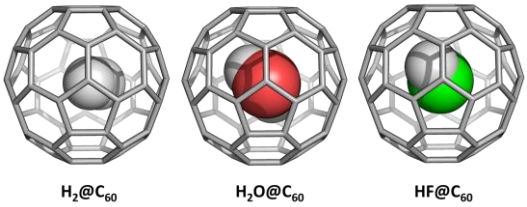

Figure 19. Endohedral [60]fullerenes bearing a neutral molecule in the inner cavity synthesized by molecular surgery.

The molecular surgery of C_{60} to create endohedral fullerenes, consists in a series of steps which involve, hole opening in the cage by organic reactions, hole enlargement to get a suitable size that allows the insertion of the desired molecule, insertion of the atom or molecule and finally close the hole to reproduce the fullerene cage, avoiding the loss of the encapsulated species. This idea was first proposed by Rubin, however, Komatsu and Murata were the first ones to get it.[141]

138. a) Y. Murata, M. Murata, K. Komatsu, *J. Am. Chem. Soc*., **2003**, *125*, 7152. b) K. Komatsu, M. Murata, Y. Murata, *Science*, **2005**, *307*, 238.
139. Y. Morinaka, F. Tanabe, M. Murata, Y. Murata, K. Komatsu, *Chem. Commun*., **2010**, *46*, 4532.
140. K. Kurotobi, Y. Murata, *Science*, **2011**, *333*, 613.
141. a) Y. Rubin, *Chem. Eur. J*., **1997**, *3*, 1009. b) G. Schick, T. Jarrosson, Y. Rubin, *Angew. Chem. Int. Ed*., **1999**, *38*, 2360.

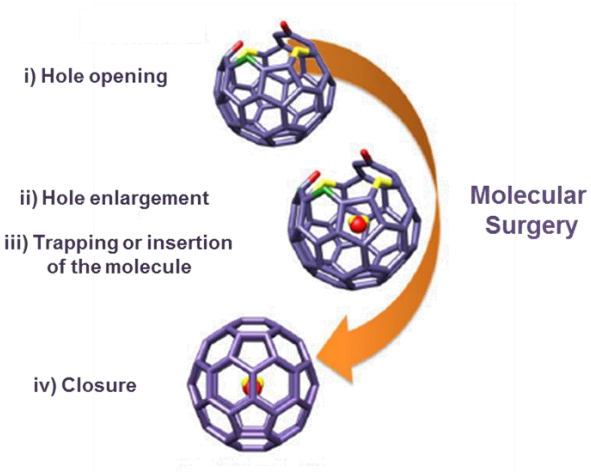

Figure 20. Molecular surgery procedure.

It is known that the encapsulated molecules in endofullerenes can affect the exohedral reactivity of the fullerenes carbon cage.[142] However, because of the inert character of the encapsulated H_2, no remarkable influence in the outer cage chemical reactivity has been found, in contrast to findings on many endohedral metallofullerenes.[143]

It was expected that more polar molecules, such as H_2O, may exhibit a different character. In this sense, a deep study on the $H_2O@C_{60}$ molecule, demonstrated the interaction of polar molecules inside fullerenes, showing the existence of a hydrogen bonding assistance of the trapped water molecule.[144]

Therefore, inner molecules can play an important role in the control of the selective reactivity of the cage in certain reactions. Recently, Krachmalnicoff *et*

142. a) M. R. Cerón, M. Izquierdo, M. Garcia-Borràs, S. S. Lee, S. Stevenson, S. Osuna, L. Echegoyen, *J. Am. Chem. Soc*., **2015**, *137*, 11775. b) M. Yamada, T. Wakahara, T. Nakahodo, T. Tsuchiya, Y. Maeda, T. Akasaka, K. Yoza, E. Horn, N. Mizorogi, S. Nagase, *J. Am. Chem. Soc*., **2006**, *128*, 1402. c) M. Yamada, M. Okamura, S. Sato, C. I. Someya, N. Mizorogi, T. Tsuchiya, T. Akasaka, T. Kato, S. Nagase, *Chem. Eur. J*., **2009**, *15*, 10533. d) M. Izquierdo, M. R. Cerón, M. M. Olmstead, A. L. Balch, L. Echegoyen, *Angew. Chem. Int. Ed*., **2013**, *52*, 11826.
143. E. E. Maroto, M. Izquierdo, M. Murata, S. Filippone, K. Komatsu, Y.Murata, N. Martín, *Chem. Commun*., **2014**, *50*, 740.
144. E. E. Maroto, J. Mateos, M. Garcia-Borràs, S. Osuna, S. Filippone, M. A. Herranz, Y. Murata, M. Solà, N. Martín, *J. Am. Chem. Soc*., **2015**, *137*, 1190.

al., have successfully isolated the HF molecule inside C_{60} fullerene, thus forming the new endohedral HF@C_{60} molecule.[145] The first exohedral functionalization on the novel HF@C_{60}, using an efficient methodology to obtain enantiomerically enriched fulleropyrrolidines, and its chemical behaviour will be discussed in following sections.

2.7. Fullerenes for Photovoltaic Devices

Energy is currently the most important problem facing mankind. The ever increasing demand of energy consumption, and the huge amounts of carbon dioxide emissions, which cause global warming and degradation of the planet, urgently need a new era based on non-contaminating renewable energies. In this regard, the Sun, represents the most powerful source of energy available in our solar system and, therefore, its use for providing energy to our planet is among the most important challenges nowadays in science. Actually, the energy received from Sun, calculated as 120.000 TW (5% ultraviolet, 43% visible and 52% infrared), surpasses that consumed on the planet over a year by several thousand times.[146] In the last years, the need to develop inexpensive renewable energy sources stimulates scientific research for efficient, low-cost photovoltaic devices.

Silicon-based devices have been the responsible in bringing solar cell technology to the consumer market. Silicon is one of the most abundant semiconducting material in our planet but in turn, it is difficult to extract and manipulate. Besides, fabrication processes are complex and involve a number of steps that make solar panels expensive. Moreover, silicon solar cells are rigid and cannot be industrially fabricated in large sizes due to the limitation of the silicon wafer processing technology. These disadvantages of silicon PVs are some of the reasons that have led many researchers to explore alternative materials for solar energy harvesting. Since the first silicon-based device prepared by Chapin in 1954 exhibiting an efficiency around 6%,[147] different semiconducting materials (inorganic, organic, molecular, polymeric, hybrids,

145. A. Krachmalnicoff, R. Bounds, S. Mamone, S. Alom, M. Concistrè, B. Meier, K. Kouřil, M. E. Light, M. R. Johnson, S. Rols, A. J. Horsewill, A. Shugai, U. Nagel, T. Rõõm, M. Carravetta, M. H. Levitt, R. J. Whitby, *Nat. Chem*., **2016**, *8*, 953.
146. N. Armaroli, V. Balzani, *Angew. Chem. Int. Ed.*, **2007**, *46*, 52.
147. D. M. Chapin, C. S. Fuller, G. L. Pearson, *J. Appl. Chem*., **1954**, *25*, 676.

quantum dots, etc.) have been used for transforming sun light into electrical energy. Among them, organic materials are promising due to key advantages, such as the possibility of processing directly from solution, thus affording lighter, cheaper and flexible all-organic PV devices. A key factor contributing to the low price of emerging photovoltaics is the ability to produce the modules as large rolls of thin film via high-speed processes.

Fullerenes and their derivatives, especially the so-called PCBM, are currently considered to be the ideal acceptors for organic solar cells for several reasons. Fullerenes possess important electronic properties like small reorganization energy, high electron affinity, ability to transport charge and stability. These fundamental properties, coupled with the ability of soluble fullerene derivatives to pack effectively in crystalline structures suitable to charge transport,[148] have made fullerenes the most important acceptor materials for organic solar cells.[149]

For synthetic chemists the challenge is the design and synthesis of new fullerene derivatives with better absorption values that can compete with efficient PV materials such as silicon or the most recent perovskites.

2.7.1. Photovoltaic Process

Transformation of solar energy into electricity occurs through a series of key stages which basically involves: [150]

1. **Sun ligh absorption and exciton formation**. Absorption of a photon leading to the formation of an excited state, by transferring an electron to a higher energy orbital, that is, electron-hole pair (exciton). It is important that the material absorb as much as possible in the UV-vis and IR to maximize the solar spectrum.

148. M. T. Rispens, A. Meetsma, R. Rittberger, C. J. Brabec, N. S. Sariciftci, J. C. Hummelen, *Chem. Commun*., **2003**, 2116.
149. a) J. L. Delgado, P.-A. Bouit, S. Filippone, M. A. Herranz, N. Martín, *Chem. Commun*., **2010**, *46*, 4853. b) G. Dennler, M. C. Scharber, C. J. Brabec, *Adv. Mater*., **2009**, *21*, 1323. c) B. Kippelen, J.-J. Brédas, *Energy Environ. Sci*., **2009**, *2*, 251. d) B. C. Thompson, J. M. J. Fréchet, *Angew. Chem. Int. Ed*., **2008**, *47*, 58.
150. a) G. Yu, J. Gao, J. C. Hummelen, F. Wudl, A. J. Heeger, *Science*, **1995**, *270*, 1789. b) S. Gunes, H. Neugebauer, S. Sariciftci Niyazi, *Chem Rev*., **2007**, *107*, 1324.

2. **Exciton migration to the donor-acceptor interface**. It is necessary the use of materials with different electronic properties. One must have electron donor character, polymer, and the other one an acceptor character, fullerene derivative.
3. **Exciton dissociation into charges (electrons and holes)**. It needs to reach the donor–acceptor interface to dissociate into free charges.
4. **Transport of the free charges**. The created charges need to be transported to the appropriate electrodes. The holes are transported through the polymer donor and the electrons through the electron acceptor material, fullerene derivative. The charge carriers need a driving force to reach the electrodes. It is provided by the energy difference between the highest occupied molecular (HOMO) level of the donor and the lowest unoccupied molecular orbital (LUMO) level of the acceptor.

All these steps are not totally understood at present and many research groups are currently dedicated to study essential aspects in the search for better energy transformation efficiencies.[151] The transport of the generated free charges toward the electrodes represents another important issue. Since charge carrier mobility is strongly dependent on the molecular organization of the material, in order to achieve better efficiencies, a good control on the morphology of the donor–acceptor materials is necessary. Furthermore, an efficient charge carrier mobility is essential to prevent charge recombination processes which result in lower energy conversion efficiencies.

In summary, an appropriate choice of the donor and acceptor materials is critical to ensure a good match between them in terms of electronic and morphological properties, which eventually determine the effective photocurrent and performance of the PV device. Therefore, the rational design of new materials able to improve some specific demands within the PV device is critical for the successful development of competitive solar cells.

151. a) L.-M. Chen, Z. Hong, G. Li, Y. Yang, *Adv. Mater*., **2009**, *21*, 1434. b) M. T. Dang, L. Hirsch, G. Wantz, J. D. Wuest, *Chem. Rev*., **2013**, *113*, 3734.

2.7.2. Organic Photovoltaic Device Architectures

The general structure used for organic solar cells is fabricated in sandwich geometry (Figure 18). The active layer is sandwiched between two contacts: an indium-tin-oxide (ITO) transparent electrode coated with a hole transport layer poly(ethylene-dioxythiophene) doped with polystyrenesulfonic acid, (PEDOT:PSS), and an aluminum top electrode acting as anode and cathode respectively. Upon irradiation with light, the molecules of the active layer are excited. This excited state is disabled by a process of electron transfer between the donor and acceptor, resulting in a state with charge separation. These charges migrate to the corresponding electrodes due to the electric field generated as a consequence of the redox potentials of the electrodes. This movement of charges finally generates electrical power.

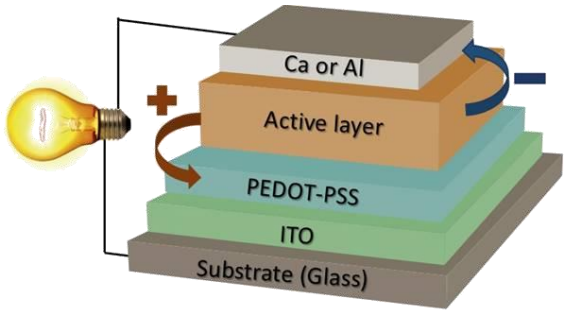

Figure 21. Sandwich structure for an organic solar cell.

a) Bilayer devices

A bilayer heterojunction is obtained by joining two different semiconductors, p-type and n-type. These devices consist of four layers sequentially stacked on top of each other: one electron donor layer (p-type), one electron acceptor layer (n-type), and the two electrodes.

In this arrangement, only a very thin layer of the interface is photovoltaic active, and the rest of the donor and acceptor layer act as useless light absorbing filter. The main limitation to the efficiency of bilayer heterojunction devices is due to the short exciton diffusion length, around 10-20 nm. Excitons generated at a distance longer than about 10 nm from the donor/acceptor interface cannot reach it and, therefore, recombine and are lost. To overcome this problem bulk heterojunction (BHJ) solar cells were designed.

b) Bulk heterojunction devices (BHJ)

Bulk heterojunction plastic solar cells consisting of a semiconducting electron donor π-conjugated polymer and a fullerene as the acceptor moiety are currently the most promising devices for practical applications. The active layer is formed by a blend of a bicontinuous network of a small bandgap polymer and a soluble fullerene that act as an electron donor and acceptor (D/A) pair intimately intermixed.[152]

The BHJ concept involves the self-assembly of nanoscale heterojunctions by spontaneous phase separation of the donor and the acceptor material. As a result of this self-assembly, charge-separating heterojunctions are formed throughout the bulk of the material. It exhibits a donor-acceptor phase separation in a 10-20 nm length scale. In such a nanoscale interpenetrating network, each interface is within a distance lower than the exciton diffusion length from the absorbing site. Thus, most of the formed excitons reach the interface resulting in holes and separated electrons that travel to the respective device electrodes (Figure 22). The interfacial area between the donor and acceptor phases has heavily increased, resulting in improved efficiency solar cells.[152]

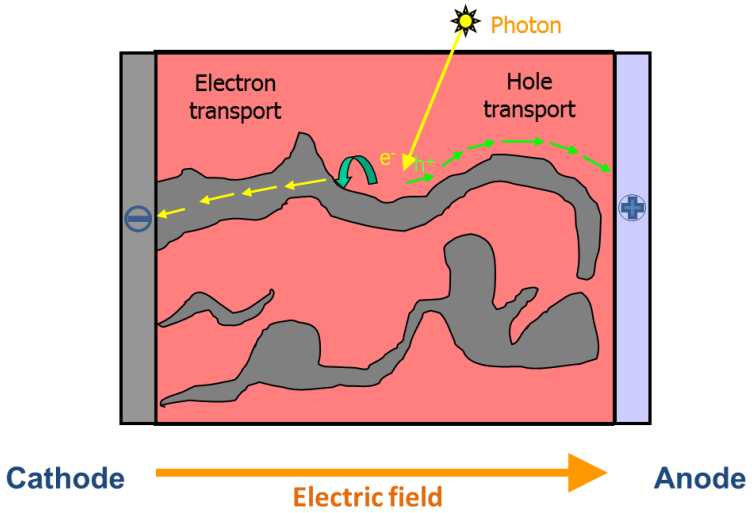

Figure 22. Schematic device structure for polymer/fullerene bulk heterojunction solar cell (BHJ).

152. H. Hoppe, N. S. Sariciftci, *J. Mater. Chem*., **2004**, *19*, 1924.

Morphologhy Control in the Bulk-Heterojunction Active Layer

The performance of organic bulk heterojunction solar cells is strongly dependent on the donor/acceptor morphology. Generation and transport of free charge carriers throughout the active layer depends on size, composition and crystallinity of the separated domains.

Controlling the nanomorphology of the phase separation in an interpenetrating network (BHJ) has increased significantly the power conversion efficiency of solar cells.[153] Hence, a nanoscale interpenetrating network with crystalline order of both constituents seems a desirable architecture for the active layer of organic photovoltaic devices.

Depending on the processing conditions, such as solvent choice, overall concentration of the blend components, deposition technique (spin coating, CVD, etc.), as well as thermal annealing, the active layer can exhibit a morphology which varies between an extremely finely dispersed mixture of donor and acceptor to a coarse phase-separated film.

It is clear that the number of factors affecting the morphology of the active layer is immense and specific to the polymer–fullerene pair used. Much effort is needed to fine tuning the morphology in the BHJ blend to achieve a high power conversion efficiency (PCE).

2.7.3. Parameters of Solar Cells Devices

To compare the performance of different solar cells, it must be defining standard conditions for measurements. An important factor to consider is the type of light used to irradiate the device. Two types of radiation, monochromatic light and light AM 1.5 (polychromatic light directly related to the solar spectrum) are typically used.

As with other optoelectronic devices, the performance of a solar cell is extracted from current-voltage curves (*J*-V), both in the dark and under irradiation (Figure 23).

153. S. E. Shaheen, C. J. Brabec, N. S. Sariciftci, F. Padinger, T. Fromherz, J. C. Hummelen, *Appl. Phys. Lett*., **2001**, *78*, 841.

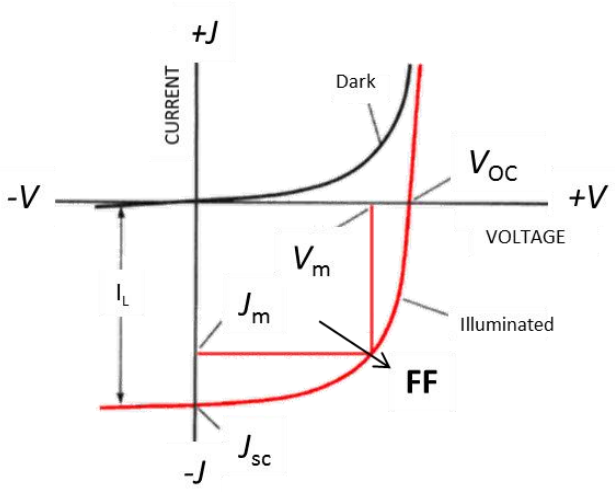

Figure 23. Current-voltage (*J*-*V*) curves of an organic solar cell.

The photovoltaic power conversion efficiency of a solar cell is determined by the following formula:

$$\eta = \frac{\text{Voc} \times \text{Jsc}}{\text{Pin}} \times FF \times m$$

Equation 1

where

-Voc is the open circuit voltage, is defined as the voltage at which the current is zero, *J*=0.

-*J*sc is the short circuit current, is obtained when the potential is zero and the electrodes are connected.

-Pin, is the power of the incident radiation per cm^2.

-m is a factor that corrects the spectral deviation of solar simulator.

-FF is the fill factor and is defined as:

$$FF = \frac{\text{Pmax}}{\text{Voc} \times \text{Jsc}}$$

Equation 2

Pmax is the maximum power value, which is obtained when the product *J* x V is maximum.

In organic solar cells, the open circuit voltage (Voc) is found to be linearly dependent on the highest occupied molecular orbital HOMO level of the donor and lowest unoccupied molecular orbital LUMO level of the acceptor. Therefore, increasing the energy difference between the HOMO and the LUMO, the value of Voc is improved. Fullerene derivatives with high values of reduction potentials lead to high values of Voc and, therefore, to increase the efficiency of the device.

$$V_{oc} \propto E_{LUMO\,A} - E_{HOMO\,D}$$

Equation 3

Brabec *et al*. clearly showed a linear correlation of the first reduction potential (LUMO level) of the fullerenes and the observed open circuit potential (Figure 21). [154]

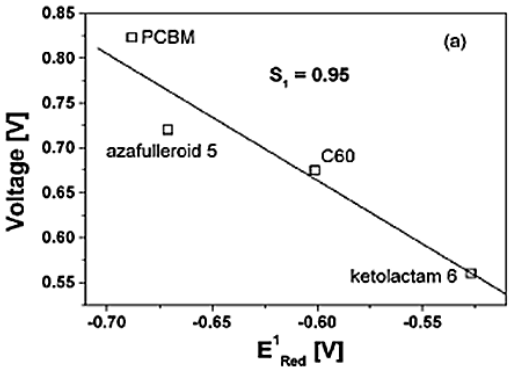

154. C. J. Brabec, A. Cravino, D. Meissner, N. S. Sariciftci, T. Fromherz, M. T. Rispens, L. Sánchez , J. C. Hummelen, *Adv. Funct. Mater*., **2001**, *11*, 374.

Figure 24. *V*oc of different bulk heterojunction solar cells plotted versus the reduction potential/LUMO of the fullerene derivative used in each individual device.

In the graph is reflected an inverse correlation between acceptor strength and the Voc value. Some key issues such as those requirements to increase the efficiency of preparations devices are specified in the following points:

1) The energy difference between the HOMO and the LUMO (band gap) in polymeric materials (p-type) should be relatively low (1.2-1.9 eV), in order to absorb as much photons as possible from solar radiation. An energy jump of 1.1 eV is able to absorb 77% of solar radiation. However, most semiconductor polymers present a band gap higher than 2 eV, limiting absorption to 30%.

2) In a study by Koster *et al*. in 2006, it was found that cell efficiency increases proportionally to the approach of the LUMO levels of the donor and acceptor.[155]

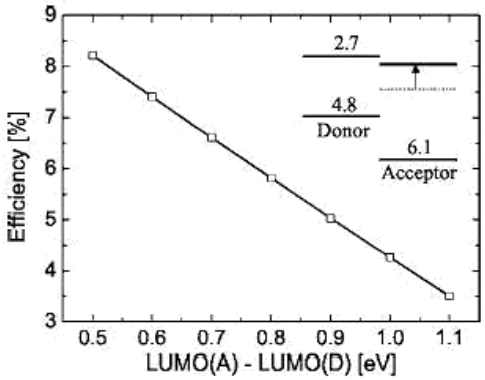

Figure 25. Graph of the difference in LUMO levels between the donor and the acceptor plotted versus the cell efficiency.

3) Both materials must provide good mobility for the holes transport through the polymer and electrons through the fullerenes. Finally, both materials must

155. L. J. A. Koster, V. D. Mihailetchi, P. W. M. Blom, *Appl. Phys. Lett*., **2006**, *88*, 052104.

have adequate solubility in organic solvents for effective preparation of the device.

2.7.4. Fullerenes for BHJ Photovoltaics

A variety of chemically modified fullerenes were initially synthesized for blending with semiconducting polymers to prepare photovoltaic devices. The best known and most widely used fullerene derivative as acceptor for PV devices is [6,6]-phenyl-C_{61} butyric acid methyl ester (PCBM),[156] firstly prepared by Hummelen and Wudl in 1995.[157] Since its first reported application in solar cells,[158] it has been by far the most widely used fullerene, being considered as a benchmark material for testing new devices.

One of the best combination polymer/fullerene used is poly-3-hexylthiophene (P3HT) as electron donor and PCBM as electron acceptor, getting values of external quantum efficiency (EQE) around 75%, and conversion efficiency of 5%.[159] The high efficiency of these devices is proposed to be due to a microcrystalline lamellar stacking in the solid state packing.[160]

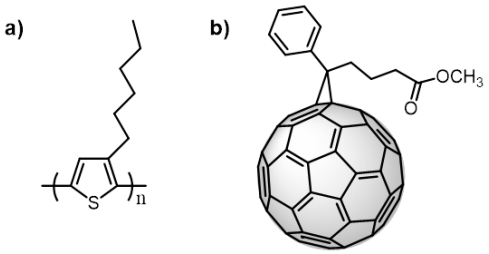

Figure 26. (a) Polymer P3HT and (b) $PC_{61}BM$, the most used fullerene derivative in organic photovoltaic devices.

156. a) F. Zhang, W. Mammo, L. M. Andresson, S. Admassie, M. R. Andresson, O. Inganäs, *Adv. Mater*., **2006**, *18*, 2169. b) O. Inganäs, F. Zhang, M. R. Andersson, *Acc. Chem. Res*., **2009**, *42*, 1731.
157. J. C. Hummelen, B. W. Knight, F. LePeq, F. Wudl, J. Yao, C. L. Wilkins, *J. Org. Chem*., **1995**, *60*, 532.
158. G. Yu, J. Gao, J. C. Hummelen, F. Wudl, A. J. Heeger, *Science*, **1995**, *270*, 1789.
159. a) F. Padinger, R. S. Rittberger, N. S. Sariciftci, *Adv. Funct. Mater*., **2003**, *13*, 85. b) P. Schilinsky, C. Waldauf, C. J. Brabec, *Appl. Phys. Lett*., **2002**, *81*, 3885.
160. T. J. Prosa, M. J. Winokur, M. M. Moulton, P. Smith, A. J. Heeger, *Macromolecules*, **1992**, *25*, 4364.

Although the PCBM is the acceptor with the best performance at the moment, a variety of other fullerene derivatives have been synthesized in order to improve the device efficiency or to achieve a better understanding on the dependence of the cell parameters from the structure of the acceptor.

Among the different modified fullerenes synthesized so far, diphenylmethanofullerene (DPM)[161] prepared by our research group is another successful type of methanofullerene endowed with two alkyl chains of twelve carbon atoms (DPM-12) to drastically improve the solubility of the acceptor in the blend and reaching efficiencies in the range of 3%. Although the LUMO energy level for DPM-12 is the same as that for [60]PCBM, an increase for the Voc of 100 mV for DPM-12 over PCBM has been observed.[162] This is justified based on their different crystallinity in the mixture with the polymer.

Devices based on dihydronaphthylfullerene benzyl alcohol benzoic ester synthesized by Fréchet *et al*. reported one of the highest power conversion efficiencies (up to 4.5%) for a non PCBM based polymer–fullerene solar cell.[163]

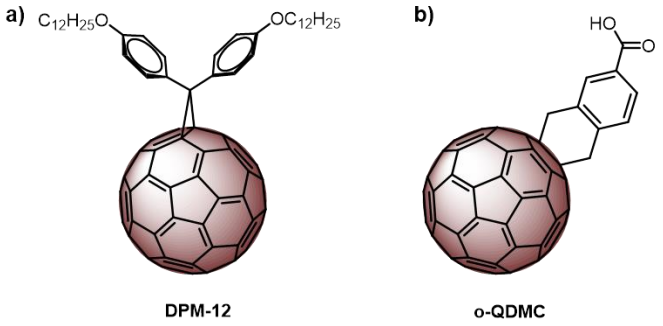

Figure 27. Fullerene derivatives, (a) DPM-12 and (b) *o*-QDMC used as electron acceptor components for organic photovoltaic devices.

161. D. Fernández, A. Viterisi, J. W. Ryan, F. Gispert-Guirado, S. Vidal, S. Filippone, N. Martín, E. Palomares, *Nanoscale*, **2014**, *6*, 5871.
162. a) I. Riedel, E. von Hauff, J. Parisi, N. Martín, F. Giacalone, V. Diakonov, *Adv. Funct. Mater*., **2005**, *15*, 1979. b) A. Sánchez-Díaz, M. Izquierdo, S. Filippone, N. Martín, E. Palomares, *Adv. Funct. Mater*., **2010**, *20*, 2695.
163. S. Backer, K. Sivula, D. F. Kavulak, J. M. J. Fréchet, *Chem. Mater*., **2007**, *19*, 2927.

Replacing the C_{60} moiety of [60]PCBM by C_{70} fullerene derivative makes the HOMO-LUMO transitions slightly more allowed and increases the light absorption/harvesting.[164] $PC_{71}BM$[79] is considered a suitable candidate for more efficient solar devices. In fact, the highest verified efficiency determined so far in a BHJ solar cell, with an internal quantum efficiency approaching 100% has been reported for [70]PCBM.[165] Other larger fullerenes such as, for instance, [84]PCBM, have been prepared as a mixture of isomers showing low solubility and significantly lower conversion efficiencies.[166]

The highest efficiency value reported for a BHJ solar cell has been published in 2016 by the group of He Yan from the Hong Kong University of Science and Technology. The fabricated organic solar cells showed a record efficiency of 11.5%. Actually, the same group has surpass their own record by introducing a non-halogenated hydrocarbon-based processing system that yields cells with power conversion efficiencies of up to 11.7%.[167]

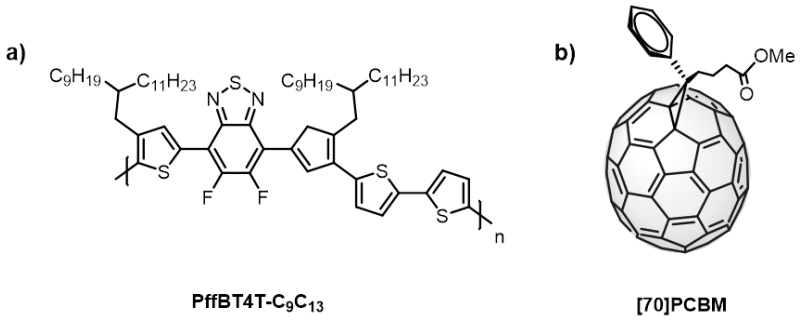

Figure 28. Chemical structures of the (a) semiconducting polymer and (b) fullerene derivative [70]PCBM, which blended in the right conditions, afforded the highest record efficiency in BHJ solar cells.

164. J. W. Arbogast, C. S. Foote, *J. Am. Chem. Soc*., **1991**, *113*, 886.
165. S. H. Park, A. Roy, S. Beaupré, S. Cho, N. Coates, J. S. Moon, D. Moses, M. Leclerc, K. Lee, A. J. Heeger, *Nat. Photonics*, **2009**, *3*, 297.
166. F. B. Kooistra, V. D. Mihailetchi, L. M. Popescu, D. Kronholm, P. W. M. Blom, J. C. Hummelen, *Chem. Mater*., **2006**, *18*, 3068.
167. J. Zhao, Y. Li, G. Yang, K. Jiang, H. Lin, H. Ade, W. Ma, H. Yan, *Nat. Energy*, **2016**, *1*, 15027.

Although some of the fullerene derivatives prepared so far exhibit good performance in PV devices, the synthesis of new fullerene derivatives with stronger visible absorption and higher LUMO energy levels than PCBM is currently a challenge for all those chemists engaged in the chemical modification of fullerenes for PV applications.

2.7.5. Fullerenes for Perovskite Solar Cells

In the last few years, the photovoltaic field has experienced a dramatic enhance due to the development of perovskite-based solar cells (PSCs). They have shown an unprecedented speed of evolution and outperform established organic and hybrid materials just after only a few years of investigation. A perovskite solar cell is a type of solar cell which includes a perovskite structured compound, commonly a hybrid organic-inorganic lead or tin halide-based material, as the light harvesting active layer. Perovskite structure is anything that has the generic form ABX_3. In the case of perovskite solar cells, the most efficient devices so far have been produced with the following combination of materials:

A = an organic cation, methylammonium $(CH_3NH_3)^+$

B = a big inorganic cation, usually Pb^{2+}

X_3= a slightly smaller halogen anion, usually chloride Cl^- or iodide I^-

Solar cell efficiencies of devices using these materials have increased from 3.8% in 2009[168] to 22.1% in early 2016, the fastest advancing solar technology to date.[169] It is important to note that some carbon nanoforms are currently being used in the perovskites-based device fabrication as electron transporting materials.[170] Although non-fullerene electron acceptors have recently been

168. A. Kojima, K. Teshima, Y. Shirai, T. Miyasaka, *J. Am. Chem. Soc*., **2009**, *131*, 6050.
169. N. J. Jeon, J. H. Noh, W. S. Yang, Y. C. Kim, S. Ryu, J. Seo, S. I. Seok, *Nature*, **2015**, *517*, 476.
170. K. Wojciechowski, T. Leijtens, S. Siprova, C. Schlueter, M. T. Hçrantner, J. T.-W. Wang, C.-Z. Li, A. K. Y. Jen, T.-L. Lee, H. J. Snaith, *J. Phys. Chem. Lett*., **2015**, *6*, 2399.

reported,[171] $PC_{71}BM$ is the widely used electron acceptor because of its lower reorganization energy and appropriate molecular orbital energy, compatible with almost all the currently available electron donors applicable in efficient organic/polymer solar cells and perovskite solar cells.[172]

Ng, Lee *et al*.,[173] showed that perovskite solar cells built with $CH_3NH_3PbI_{3-x}Cl_x$ perovskite/[60]fullerene are more similar to a n-n junction than a p-n junction, which is typical for OPVs. The authors demonstrated that the perovskite/[60]fullerene interface does not provide enough driving force for the charge dissociation process. This device is efficient due to the instant charge dissociation which efficiently produces free carriers in the perovskite film.

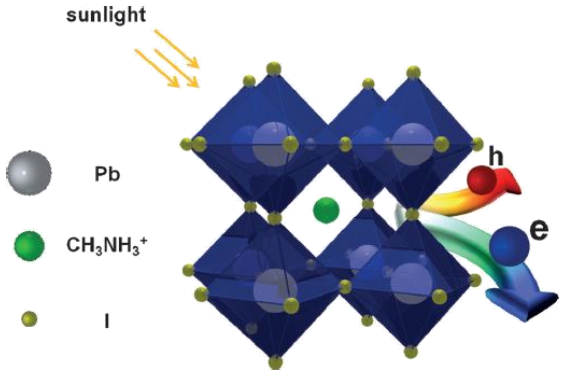

Figure 29. Schematic illustration that shows the effective free charge generation.

The absorption of incident photons results in the almost instantaneous generation of free charges. This is one of the main advantages of perovskite solar cells. In contrast, in organic solar cells, significant losses in energy occur through exciton migration, exciton dissociation, and charge transport and

171. a) C. L. Chochos, N. Tagmatarchis, V. G. Gregoriou, *RSC Adv*., **2013**, *3*, 7160. b) Y.-J. Hwang, B. A. E. Courtright, A. S. Ferreira, S. H. Tolbert, S. A. Jenekhe, *Adv. Mater*., **2015**, *27*, 4578.
172. J. Y. Jeng, Y. F. Chiang, M. H. Lee, S. R. Peng, T. F. Guo, P. Chen, T. C. Wen, *Adv. Mater*., **2013**, *25*, 3727. b) O. Malinkiewicz, A. Yella, Y. H. Lee, G. M. Espallargas, M. Grätzel, M. K. Nazeeruddin, H. J. Bolink, *Nat. Photon*., **2014**, *8*, 128.
173. a) M.-F. Lo, Z.-Q. Guan, T.-W. Ng, C.-Y. Chan, C.-S. Lee, *Adv. Funct. Mater*., **2015**, *25*, 1213.

collection. Nevertheless, perovskites-based devices have important drawbacks, being the most important that concerned with their stability under ambient conditions.

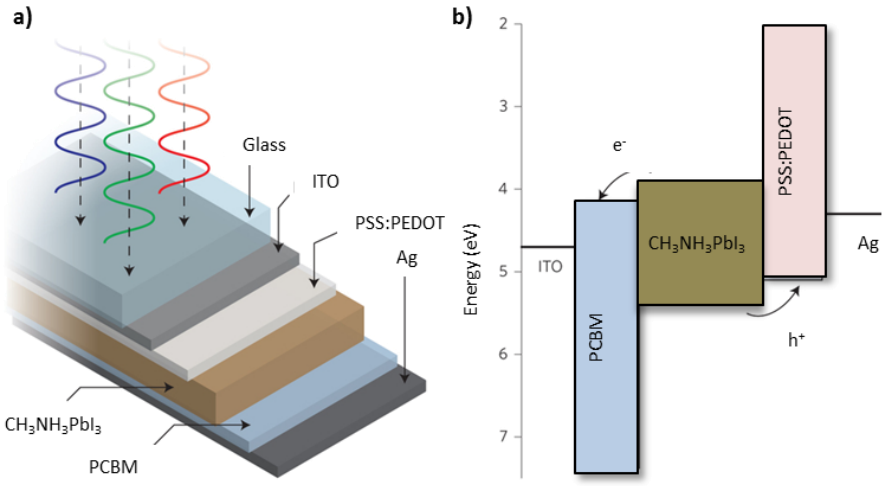

Figure 30. Perovskite solar cells employing $CH_3NH_3PbI_3$ as the light absorber, PCBM as the electron acceptor/conductor, and poly(3,4-ethylenedioxythiophene):polystyrenesulfonate (PEDOT:PSS) as the hole conductor.

Strong optical absorption is the key to the outstanding performance of these perovskite cells, reducing both the required thickness and the challenges in collecting photogenerated carriers. With the potential of achieving even higher efficiencies and the very low production costs, perovskite solar cells have become commercially attractive, with start-up companies already promising modules on the market by 2017.

OBJECTIVES

3. OBJECTIVES

The main objective in this thesis is the development of new fullerene derivatives with chemical and electronic properties of interest for answering fundamental questions as well as to search for practical applications in organic chemistry and organic photovoltaics.

3.1. Synthesis of Chiral Fullerene Hybrids for Catalysis

3.1.1. Synthesis of Chiral Fullerene Hybrids

The aim in this topic is the design and synthesis of new chiral fullerene hybrids endowed with different metals, such as iridium, rhodium or ruthenium, which are active in hydrogenation reactions. Therefore, we have undertaken the design and synthesis of unprecedented stereogenic at metal fullerene hybrids with a high stability toward racemization or epimerization processes.

Despite chiral fullerene derivatives have been prepared by enantioselective metal and organocatalytic functionalization of fullerenes, their chirality stems from new formed asymmetric carbon centers. In this regard, due to the pivotal importance of the metal in a variety of chemical transformations, metal centered chirality would be highly beneficial for different purposes.

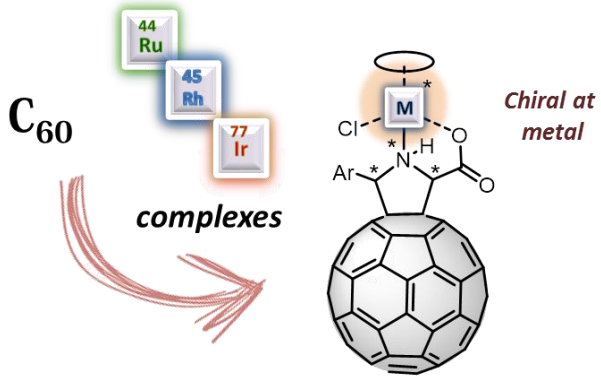

Figure 31. Enantioselective synthesis of fullerene-metal hybrids (M = Ir, Rh, or Ru).

3.1.2. Catalytic Activity of Fullerene Hybrids

Once synthesized the fullerene-metal hybrids, we wondered about the effectiveness of these hybrids in hydrogen transfer reactions, namely fundamental reactions such as ketones hydrogenation and *N*-alkylation by the so-called hydrogen borrowing mechanism and, finally, about the ability to transfer chiral information in the ketones hydrogenation.

Furthermore, we wondered if [60]fullerene itself could act as a carbon-based molecular co-catalyst with a synergic activity in hydrogen transfer processes.

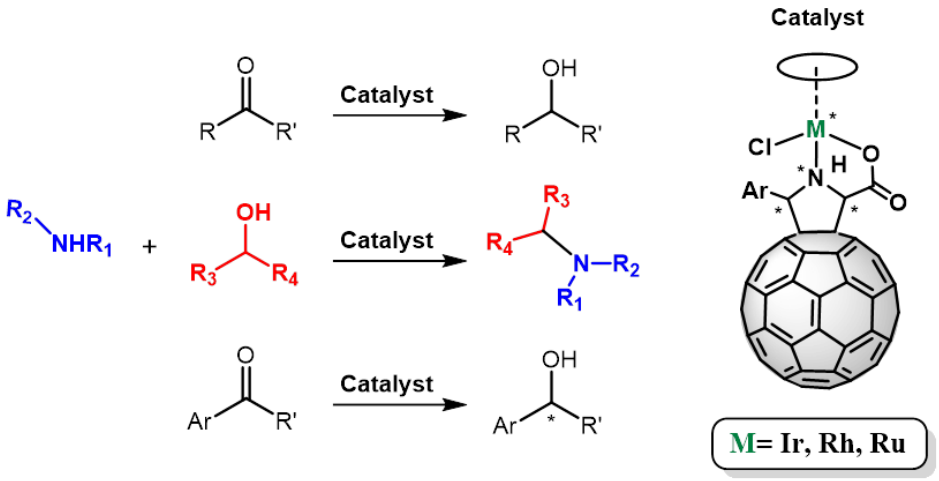

Scheme 21. Reactions catalyzed by metal-containing fullerene hybrids.

3.2. Selectivity in Higher Fullerenes for OPV

The use of higher fullerenes has to face different levels of selectivity since different double bonds are present as a result of their lower degree of symmetry. In consequence, complex mixtures of products are obtained, preventing the appropriate exploration of their properties and applications. Therefore, the availability of an efficient methodology that affords isomeric purity on C_{70} is essential.

We have addressed this challenge from two different perspectives focusing in fullerenes for photovoltaic applications, as it is shown in the following paragraphs.

3.2.1. Selective Synthesis of [5,6]Fulleroids

Most of the known reactions carried out on fullerenes obtain a closed [6,6]-derivative as the major product. The objective is to reverse the reactivity of the fullerene for selectively obtaining the open and more unstable [5,6]-derivative as the main product, thus allowing to study its properties, since not much is known about these compounds due to the lack of an effective synthetic methodology. To consolidate this strategy, fullerene derivatives based on different diazocompounds have been synthesized.

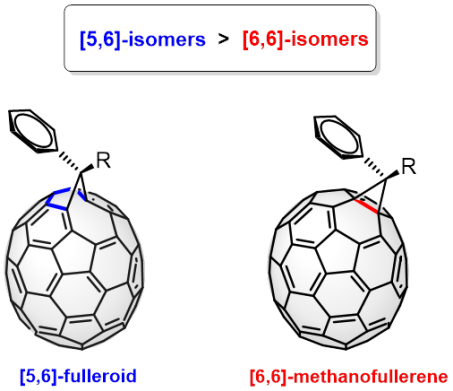

Figure 32. Chemical structures of [5,6]-fulleroid and [6,6]-methanofullerene.

3.2.2. Selective Synthesis of [70]Methanofullerenes for OPV

Our aim is to develop a new methodology controlling the site-selectivity on [70]fullerene. The isomeric purity of the involved electroactive materials in the bulk heterojunction may be crucial to enhance a suitable molecular organization, thus increasing the power conversion efficiency, in the photovoltaic device.

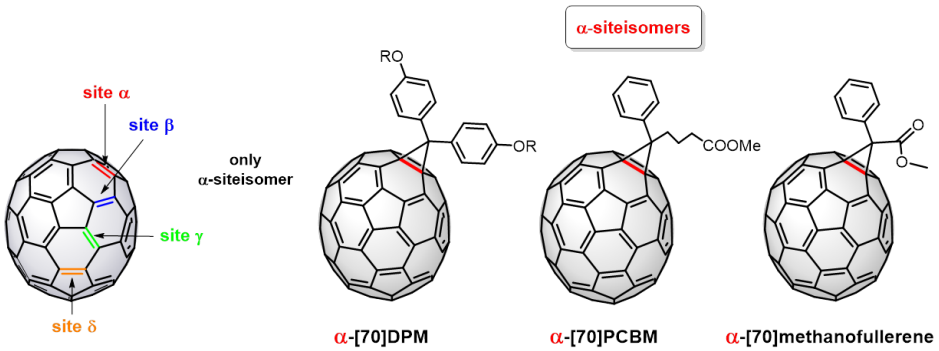

Figure 33. Chemical structures of α-[70]DPM, α-[70]methanofullerene and α-[70]PCBM, the most employed fullerene derivatives as electron acceptor component in BHJ solar cells.

3.3. Chemical Reactivity on Endohedral Fullerenes

Endohedral fullerenes are a singular scenario to test stereoselective methods and explore the contribution of the entrapped species. In this sense, the proposed goal is to explore the reactivity of the novel HF@C_{60} molecule. Therefore, we propose to carry out the synthesis of enantiomerically enriched HF@C_{60} pyrrolidines, using the methodology involving a 1,3-dipolar cycloadditions of *N*-metalated azomethine ylides.

To understand the effect of the inner molecule inside the cage, we propose to study the *cis-trans* isomerization process in pristine C_{60}, and in two different endohedral molecules, $H_2O@C_{60}$ and HF@C_{60}.

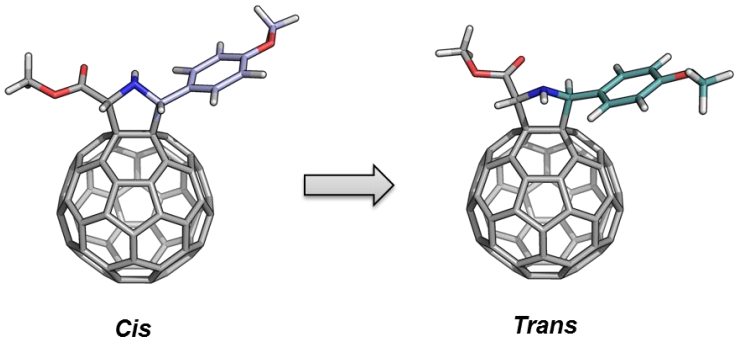

Figure 34. *Cis-trans* isomerization process in HF@C_{60}-pyrrolidine.

RESULTS AND DISCUSSION

4. RESULTS AND DISCUSSION

4.1. Synthesis of Chiral Fullerene/Metal Hybrids

As discussed in the background, chirality is a fundamental concept in chemistry. In particular, chirality in fullerenes has recently proved to play a critical role for some fullerene properties.[87]

The use of asymmetric metal- and organo-catalysis in fullerenes chemistry has provided an easy access to optically active fullerene derivatives with a total control on the absolute configuration of the created stereogenic centers.[96]

To date, interest in fullerene–transition metal complexes has been renewed in the search for new applications and synergies arising from their complementary properties. Despite many metal–fullerene hybrids have been reported to date, only a few are optically active.[104] Moreover, in all the examples, the chiral information stems from the use of chiral ligands.[174]

Considering the versatility and enormous potential of asymmetric catalysis developed on the fullerene system, the new challenge is the synthesis of chiral metal complexes, specifically, with a metal-centered chirality. This is an important issue due to its relevance in enantioselective metal-mediated processes. However, a control of the metal-centered chirality is not a trivial question because of the configurational lability of the metals, which often undergo a rapid ligand exchange.[175]

Therefore, we propose the enantioselective synthesis of [60]fullerene hybrids endowed with a stable stereogenic metal center that present a high activity in transfer hydrogenation reactions and whose configuration can be defined by the appropriate choice of the chiral catalyst.

174. a) V. V. Bashilov, P. V. Petrovskii, V. L. Sokolov, F. M. Dotgushin, A. L. Yanovsky, Y. T. Struchkov, *Russ. Chem. Bull*., **1996**, *45*, 1207. b) V. I. Sokolov, V. V. Bashilov, F. M. Dolgushin, N. V. Abramova, K. K. Babievsky, A. G. Ginzburg, P. V. Petrovskii, *Tetrahedron Lett*., **2009**, *50*, 5347. c) V. V. Bashilov, P. V. Petrovskii, V. I. Sokolov, *Russ. Chem. Bull*., **1993**, *42*, 392.
175. a) E. B. Bauer, *Chem. Soc. Rev*., **2012**, *41*, 3153. b) C. Tian, L. Gong, E. Meggers, *Chem. Commun*., **2016**, *52*, 4207. c) C. Ganter, *Chem. Soc. Rev*., **2003**, *32*, 130. d) H. Brunner, *Angew. Chem. Int. Ed*., **1999**, *38*, 1194.

4.1.1. Synthesis of Iridium Complexes

The syntheses of the chiral metal-fullerene hybrids was inspired on the preparation of half-sandwich complexes with aminocarboxylate ligands,[176] taking advantage of the full control previously achieved in the stereodivergent synthesis of pyrrolidino[60]fullerenes.[96]

Thus, the α-iminoester **31** bearing a *tert*-butyl ester moiety, was chosen for the cycloaddition reaction onto C_{60} since allows a further functionalization (Scheme 22). The α-iminoester was obtained using the general procedure described in the literature.[177]

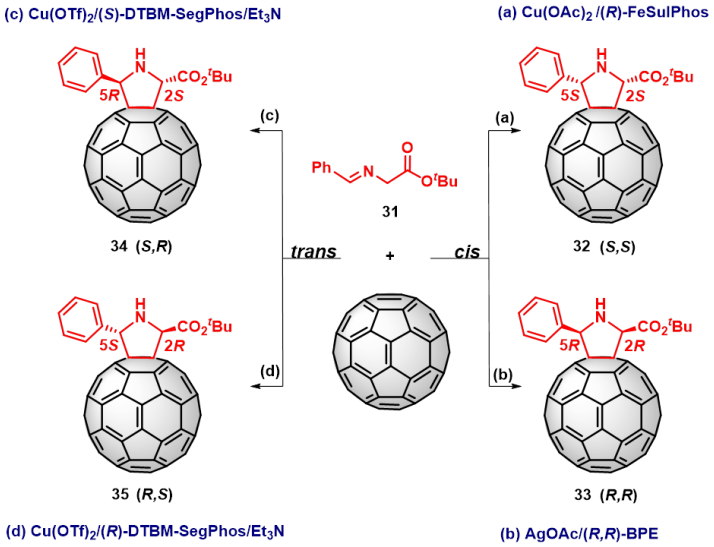

Scheme 22. Synthesis of *cis*- and *trans*-pyrrolidino[60]fullerene.

As it is shown in the Scheme x, selecting the appropriate chiral metal catalyst, the four possible stereoisomeric pyrrolidino[60]fullerenes can be achieved. A solution of α-iminoester **31** and the corresponding catalytic pair (metal-ligand) in dry toluene was stirred for 30 min at room temperature. Later, C_{60} and triethylamine (for *trans* isomers) were added. The mixture was stirred at 25°C for 2 h. in the case of *trans* isomers and cooled to -15ºC for 2 h. for *cis* isomers.

176. D. Carmona, M. P. Lamata, F. Viguri, E. San José, A. Mendoza, F. J. Lahoz, P. García-Orduña, R. Atencio, L. A. Oro, *J. Organomet. Chem.*, **2012**, *717*, 152.
177. A. López-Pérez, J. Adrio, J. C. Carretero, *Angew. Chem. Int. Ed.*, **2009**, *48*, 340.

Longer reaction times favor isomerization processes and formation of bisadducts. For instance, the catalytic pair $Cu(OAc)_2$/(*R*)-FeSulPhos, afforded the pyrrolidine (*S,S*)-*cis* **32** with excellent *ee* (99%), in contrast to the system formed by AgOAc/(*R,R*)-BPE, that led to the opposite enantiomer (*R,R*)-*cis* **33** in 96% *ee*. The absolute configuration was assigned by analogy with other related systems and confirmed by CD.[96] In the same way, *trans* enantiomers were obtained by using (*R*)- or (*S*)-DTBM-SegPhos and $Cu(OTf)_2$, leading to (*S,R*)-*trans* **34** and (*R,S*)-*trans* **35**, with 70% *ee* and 84% *ee*, respectively. The optical purity of compounds **32-35** was determined by HPLC using a chiral column, *Pirkle Covalent (R,R) Whelk-02*.

Compounds **32-35** were isolated and characterized by standard spectroscopic techniques. In the ^{1}H-NMR spectrum of the *trans* isomers **34**, **35**, the signals corresponding to the methylene protons of the pyrrolidine ring appear as singlets at 6.49 and 5.68 ppm. In contrast, the proton signals of the *cis* isomers **32**, **33**, appear as doublets and are observed more closely, at 5.84 and 5.55 ppm, as it has always been observed in related compounds.[178]

All compounds show the typical UV–vis profile of [60]fullerene monoadducts. The 430 nm band is considered as the fingerprint for all saturated C–C bonds between two hexagons of the C_{60} sphere, regardless of the nature of the substituents involved.

The circular dichroism analysis was employed to confirm the absolute configuration of the formed pyrrolidines by using the sector rule reported.[179] The *cis*-pyrrolidine **32** formed by the catalytic pair Cu(II)/(*R*)-FeSulPhos showed a positive Cotton effect in the circular dichroism spectrum, (blue line, Figure 35b) which is consistent with a stereochemistry (*S,S*)-*cis*. The *cis*-pyrrolidine **33** obtained by the catalytic system Ag(I)/(*RR*)-BPE presented a negative Cotton effect (red line, Figure 35b) corresponding with a stereochemistry (*R,R*)-*cis*.[91c]

178. S. H. Wu, W. Q. Sun, D. W. Zhang, L. H. Shu, H. M. Wu, J. F. Xu, X. F. Lao, *J. Chem. Soc. Perkin Trans*, **1998**, *1*, 1733.
179. E. E. Maroto, M. Izquierdo, S. Reboredo, J. Marco-Martínez, S. Filippone, N. Martín, *Acc. Chem. Res.*, **2014**, *47*, 2660.

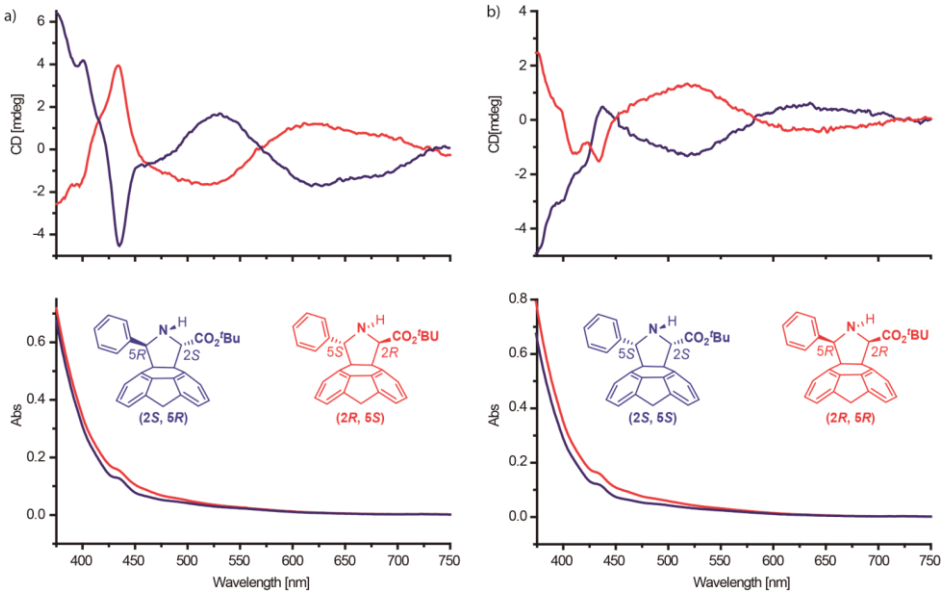

Figure 35. Circular dichroism and UV-vis spectra of *trans*-fulleropyrrolidines (a) and *cis*-fulleropyrrolidines (b) (concentration, $1x10^{-6}$M in dichloromethane).

On the other hand, *trans*-pyrrolidine **34** obtained by the catalytic pair Cu(II)/(*S*)-DTBM-SegPhos exhibited a negative Cotton effect in the circular dichroism spectrum, (blue line, Figure 35a) which is consistent with a stereochemistry (*S*,*R*)-*trans*. Conversely, *trans*-pyrrolidine **35** formed by the pair Cu(II)/(*R*)-DTBM-SegPhos showed a positive Cotton effect (red line, Figure 35a) corresponds to a stereochemistry (*R*,*S*)-*trans*. The circular dichroism recorded for these compounds clearly shows the presence of enantiomeric fullerene pairs, in which one spectrum appears as the mirror image of the other.

The sector rule consists in applying a plane tangent to the sphere of C_{60} in the single bond [6,6] where the addition took place, and which is later divided into four sectors, as shown in Figure 36. Subsequently, each sector is assigned with a positive or negative sign alternately. The fulleropyrrolidines that show a positive Cotton effect in their spectrum of circular dichroism present the highest number of atoms located in the upper right quadrant or lower left, which are those that have the positive sign.

Comparing the CD spectra of *cis*- and *trans*-fulleropyrrolidines, as expected from the empirical sector rule, the *trans* diastereomers **34, 35** give rise to a higher signal at 430 nm when compared to the *cis* diastereomers **32, 33**. This experimental finding is the result of the additive effect of the pyrrolidine substituents that lay in opposite sectors but with the same sign (Figure 36).

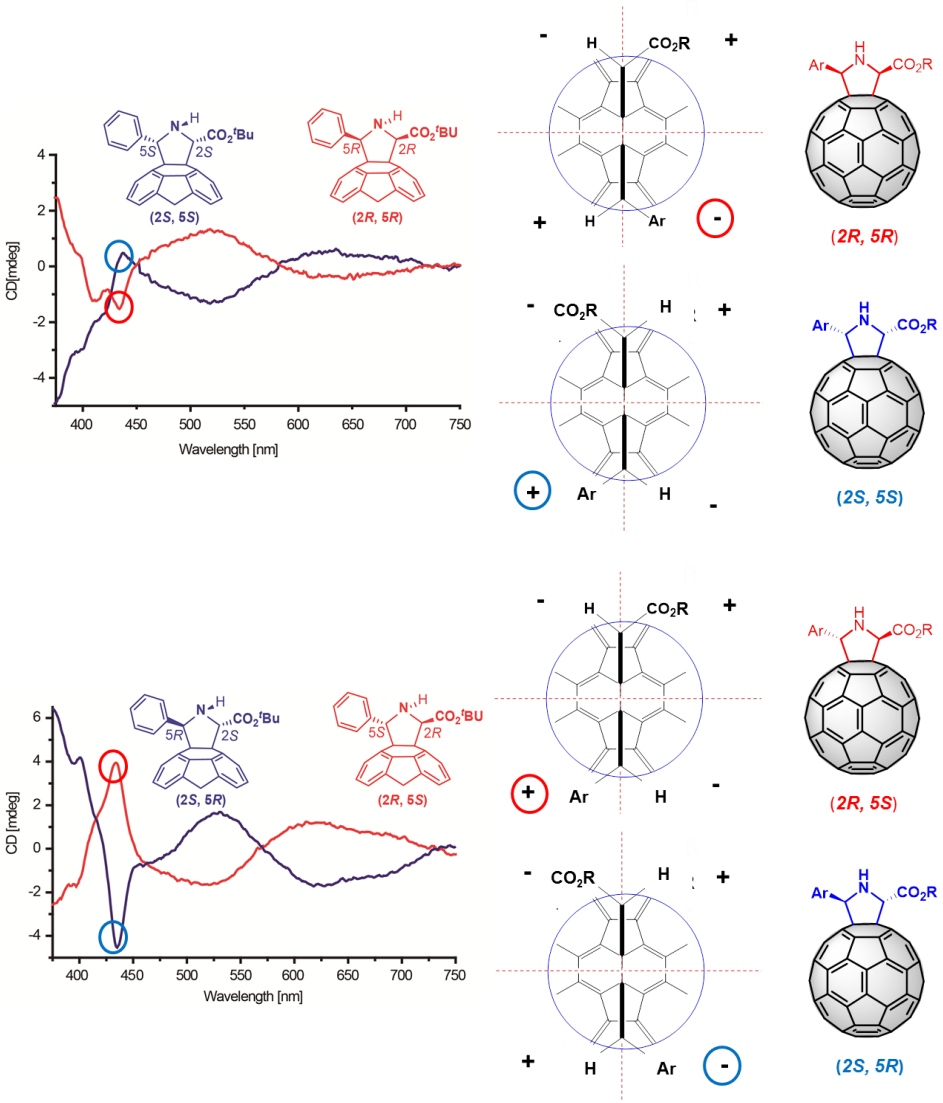

Figure 36. Circular dichroism and sector rule for the assignment of the absolute configuration of chiral *cis*-fulleropyrrolidines (top) and *trans*-fulleropyrrolidines (bottom).

For the synthesis of the chiral fullerene/metal hybrids, a ^{t}Bu-α-iminoester endowed with a labile ester moiety **31**, was selected for its further hydrolysis and successive complexation. Thus, optically pure fulleropyrrolidine (*S*,*S*)-*cis* **32**, was treated with pentamethylcyclopentadienyl iridium dichloride dimer, $[Cp^{*}IrCl_2]_2$, in "one pot" procedure after the ester hydrolysis with a mixture TFA/DCM (1:4). After two hours of stirring at room temperature, the iridium half-sandwich fullerene hybrid **36** was afforded in 77% yield (Scheme 23). As expected, we also obtained the fullerene hybrids with the opposite *R* configuration at the iridium metal atom by using optically pure fulleropyrrolidine (*R*,*R*)-*cis* **33** and following the procedure previously described, hydrolysis of the ester group and subsequent complexation. The formed complex **37** was obtained in 65% yield maintaining the configuration determined by the C-2 atom without any loss of enantiomeric excess.

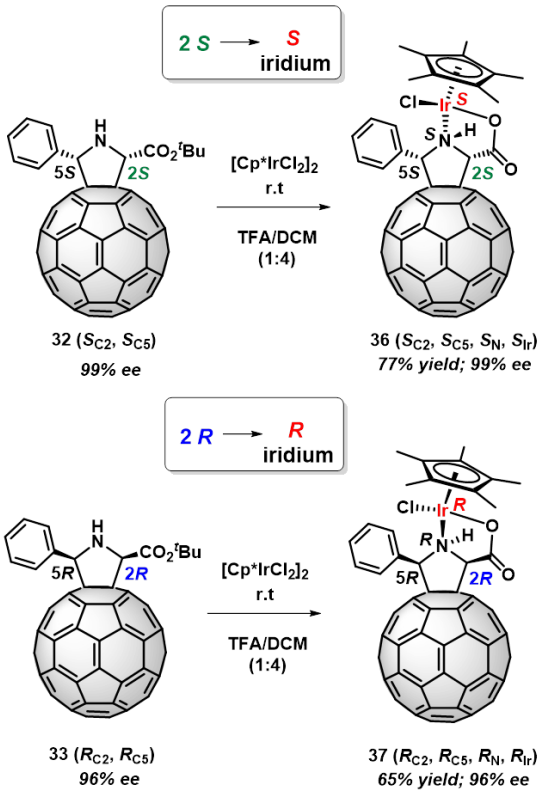

Scheme 23. Synthesis of iridium half-sandwich [60]fullerene complexes from *cis*-pyrrolidino[60]fullerene isomers.

As a result of the coordination of the pyrrolidino[60]fullerene carboxylate moiety, two additional stereogenic centers were formed, the pyrrolidine nitrogen atom and the iridium atom. Despite the iridium center can adopt two different configurations, only one product was formed. In contrast to related complexes based on a prolinate ligand, no evidence of diastereomeric mixture or epimerization process at the metal center has been found.

The ^{1}H NMR spectrum of chiral fullerene hybrids **36**, **37** showed the signals of a single isomer. Due to the coordination of the pyrrolidine with the iridium atom, the configuration of the nitrogen is fixed and the NH is coupled with the two protons of the pyrrolidine appearing as a triplet at 6.88 ppm (J = 13.1 Hz). Thus, the methylene protons of the pyrrolidine ring at *cis* position, appeared as doublets at 6.12 ppm (J = 13.1 Hz, C5H-pyrrolidine), and 5.69 ppm (J = 13.1 Hz, C2H-pyrrolidine) respectively.

Analogously to other related systems,[176] the N-H bond remains in a *cis* disposition with respect to the C2-H pyrrolidine bond, probably to avoid an unfavorable *trans* disposition between the two fused five membered rings.

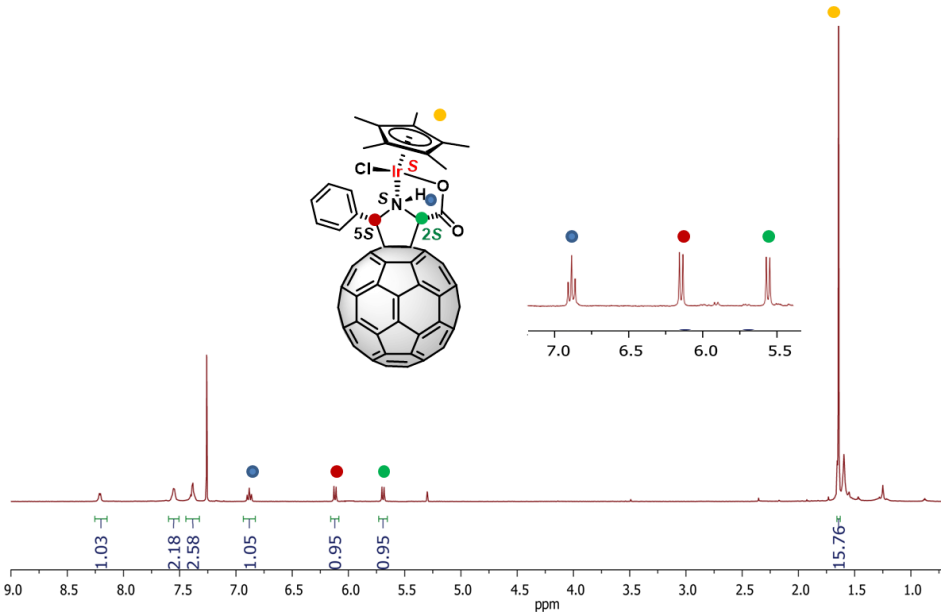

Figure 37. ^{1}H NMR (700 MHz, 298K, $CDCl_3$) of chiral fullerene hybrids **36** and **37**.

The no evidence of diastereomeric mixture at the metal center can be explained by the diastereospecific addition of the metal fragment where its configuration is determined by the chirality of the C-2 of the pyrrolidine ring, without any loss of optical purity. Therefore, the configuration of the two new stereogenic centers is just like C-2 carbon atom.

To prove the formation of a single isomer, variable temperature ^{1}H-NMR experiments were performed with chiral compound **36** in a range of temperature from -30ºC to 90ºC.

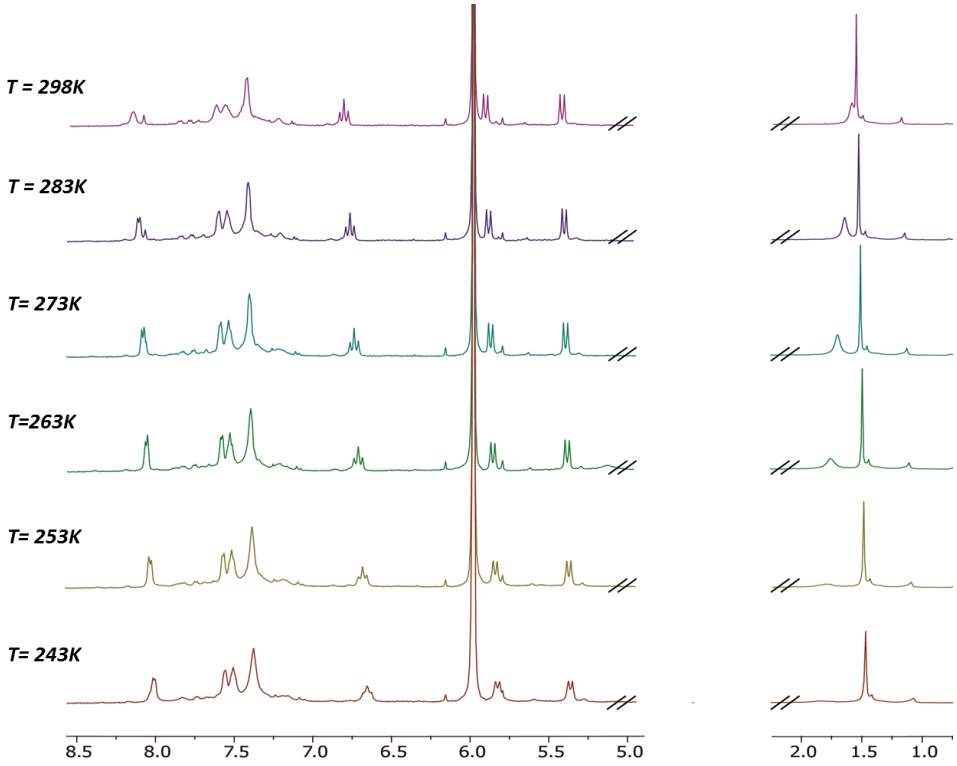

Figure 38. ^{1}H NMR (700 MHz, $C_2D_2Cl_4$) of compound **36** in a range of temperature from 243K to 298K.

As we can see in figure 38, the decrease of temperature does not produce a splitting of the signals, they remain intact with the temperature, showing the high stability of the stereoisomer and confirming that the metal center does not undergo any epimerization process.

In an effort to determine the stereochemistry of the metal center, NOE experiments with *cis* stereoisomer **36** were performed.

In the NMR experiment, when the Cp^* moiety was irradiated, it was observed Noe effect with the methylene proton at C-5 carbon atom of the pyrrolidine ring and also with the *ortho* aromatic protons (Figure 39). In the same way, when the methylene proton at C5 carbon atom was irradiated, they showed Noe effect with the Cp^* moiety.

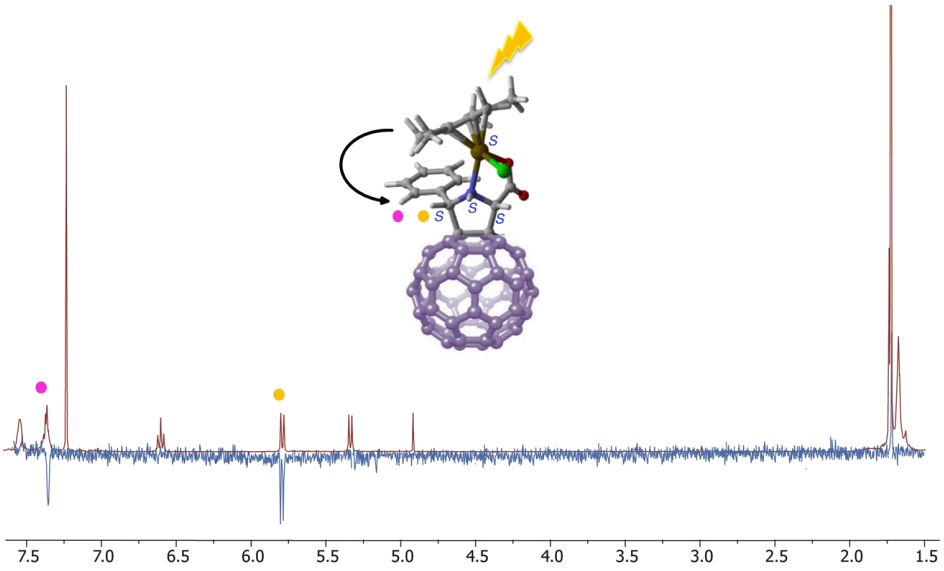

Figure 39. NOE experiment for *cis* stereoisomer **36**.

For the epimers with configuration (S_{C2}, S_{C5}, S_N), the calculated distances between the hydrogen atoms of the methyl group of the Cp^* moiety and the C5-H are 2.9 Å, for the epimer with *S* configuration at metal, and 3.6 Å for the epimer with *R* configuration. This difference is not enough to discriminate the two epimers, however, the calculated distances between the hydrogen atoms of the Cp^* moiety and the *ortho* aromatic protons of the phenyl substituent at C-5 carbon atom are 2.8 Å, in the case that the absolute configuration at metal is *S*, and 5.0 Å when the absolute configuration is *R* (Figure 40).

Thus, the presence of NOE effect between the Cp^* moiety and the *ortho* aromatic protons leads to assign *S* configuration at iridium metal.

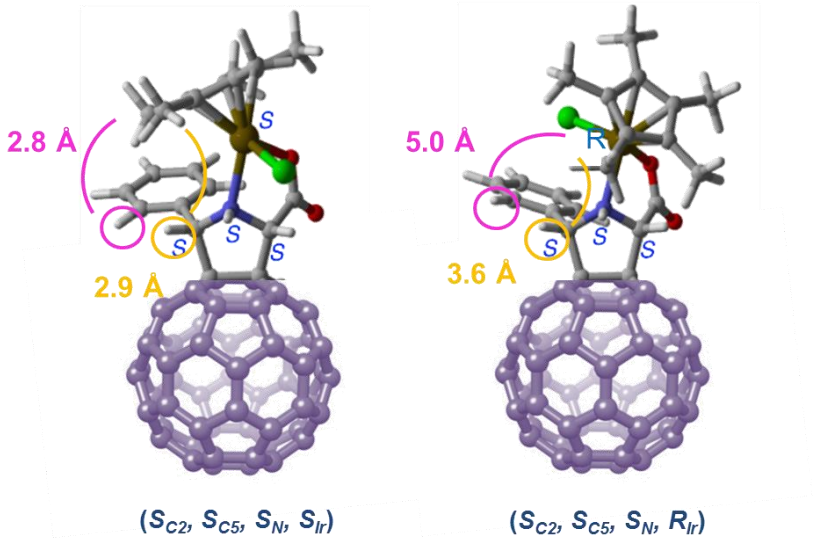

Figure 40. Calculated distances of the two possible stereoisomers at metal for *cis* iridium hybrid.

Density Functional Theory (DFT) calculations at the dispersion corrected RI-BP86-D3/def2-SVP level were carried out to understand the configurational stability of the metal center and the observed stereochemistry. The two possible stereoisomers at metal for *cis* iridium hybrid, namely **36** (S_{C2}, S_{C5}, S_N, S_{Ir}) and its transition metal epimer **36-epi** (S_{C2}, S_{C5}, S_N, R_{Ir}) were studied.

Calculations indicate that the formed isomer **36** (S_{C2}, S_{C5}, S_N, S_{Ir}) is 8.7 kcal/mol more stable than (S_{C2}, S_{C5}, S_N, R_{Ir}) (Figure 41). This result is in accordance with the observed diastereoselectivity and with the aforementioned lack of epimerization at the transition metal center.

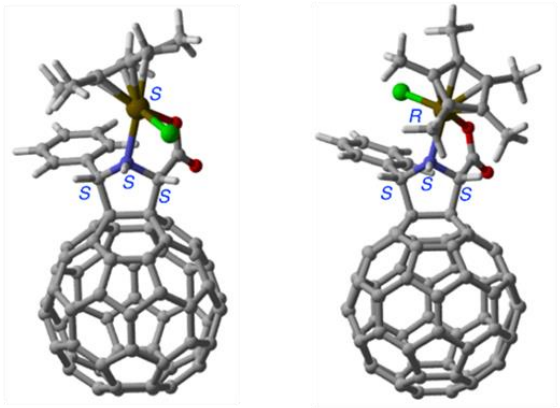

36
(S_{C2}, S_{C5}, S_N, S_{Ir})
E_{rel} = 0.0 kcal/mol

36-epi
(S_{C2}, S_{C5}, S_N, R_{Ir})
E_{rel} = 8.7 kcal/mol

Figure 41. Optimized geometries of the two possible stereoisomers at metal for *cis* iridium hybrid.

Two principal reasons are responsible for the much higher stability of **36** (S_{C2}, S_{C5}, S_N, S_{Ir}). The less stable isomer is affected by a strong repulsive interaction between the lone-pair (LP) of the chloride ligand and the π-electrons of the adjacent phenyl ring, which is not present in the chiral hybrid **36** (S_{C2}, S_{C5}, S_N, S_{Ir}). Indeed, the calculated Cl···π-centroid distances of 3.35 Å is shorter than the sum of van der Waals radii of the involved atoms (Cl = 1.75 Å, phenyl group = 1.7 Å).

On the other hand, there is a stabilizing CH–π interaction between the hydrogen atoms of two methyl groups of the Cp^* ligand and the adjacent phenyl substituent on the pyrrolidine C-5 carbon atom, in the most stable isomer **36** (S_{C2}, S_{C5}, S_N, S_{Ir}). This positive interaction has been widely described as "β phenyl effect" because of the aryl substitution at the beta position of the metal.[180]

180. H. Brunner, *Angew. Chem. Int. Ed*., **1983**, *22*, 897.

The computed CH···π-centroid distance of 2.54 Å nicely fits in the typical range reported for this type of non-covalent interaction.[181] This stabilizing interaction can be easily visualized by means of the NCIPLOT method.[182] As clearly shown in Figure 42, there is a non-covalent attractive interaction (green surface) between the methyl groups of the Cp^* moiety and the adjacent phenyl ring.

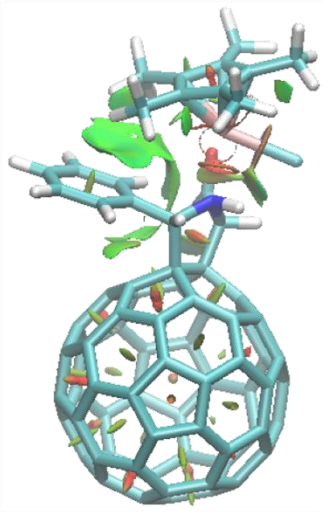

Figure 42. Representation of non-covalent attractive interactions in compound **36** (S_{C2}, S_{C5}, S_N, S_{Ir}).

The combination of the repulsive interaction LP (Cl)–π and attractive CH–π interaction is responsible for the energy differences between the considered stereoisomers. Therefore, after all the studies carried out, we can safely attribute the configuration (S_{C2}, S_{C5}, S_N, S_{Ir}) to compound **36** and (R_{C2}, R_{C5}, R_N, R_{Ir}) for the iridium chiral hybrid **37**.

181. M. Nishio, M. Hirota, Y. Umezawa, *The CH/π Interaction: Evidence, Nature, and Consequences*, Wiley, **1998**.
182. E. R. Johnson, S. Keinan, P. Mori-Sánchez, J. Contreras-García, A. J. Cohen, W. Yang, *J. Am. Chem. Soc*., **2010**, *132*, 6498.

The optical purity of compounds **36** and **37** was analyzed by HPLC using a chiral column *ChiralPack IA*. The products showed the same enantiomeric excess as the starting [60]fulleropyrrolidines, (*S*,*S*)-*cis* **32** (99% *ee*) and (*R*,*R*)-*cis* **33** (96% *ee*). $t_R(S_{C2}, S_{C5}, S_N, S_{Ir})$ = 7.2 min, $t_R(R_{C2}, R_{C5}, R_N, R_{Ir})$ = 35.3 min.

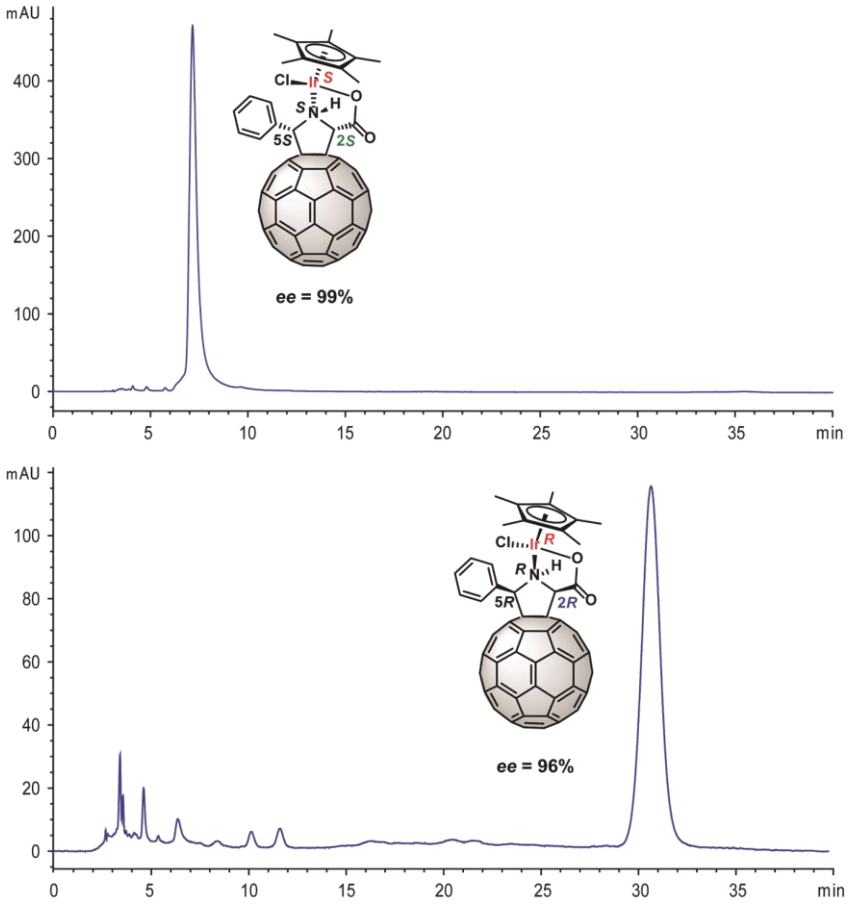

Figure 43. HPLC profiles of chiral iridium fullerene hybrids **36** (top) and **37** (bottom). HPLC column: *ChiralPack IA* (4.6 x 250mm; dichloromethane/isopropyl alcohol (98:2); 1 ml/min; 320 nm; 25ºC).

Because of the importance of the aryl group at C-5 to fix the stereochemistry of the iridium atom in the *cis* pyrrolidino[60]fullerenes, we wondered about the diastereoselectivity in the *trans* isomers where the C-5 carbon atom inverts its configuration and the aryl group is placed far away from the metal atom.

Thus, each *trans* isomers (*S*,*R*)-*trans* **34** and (*R*,*S*)-*trans* **35**, obtained by using Cu(II)/(*S*)-DTBM-SegPhos and Cu(II)/(*R*)-DTBM-SegPhos respectively, after the ester hydrolysis with a mixture TFA/DCM (1:4), were treated with $[Cp^*IrCl_2]_2$ affording an individual stereoisomer **38** and **39** respectively (Scheme 24).

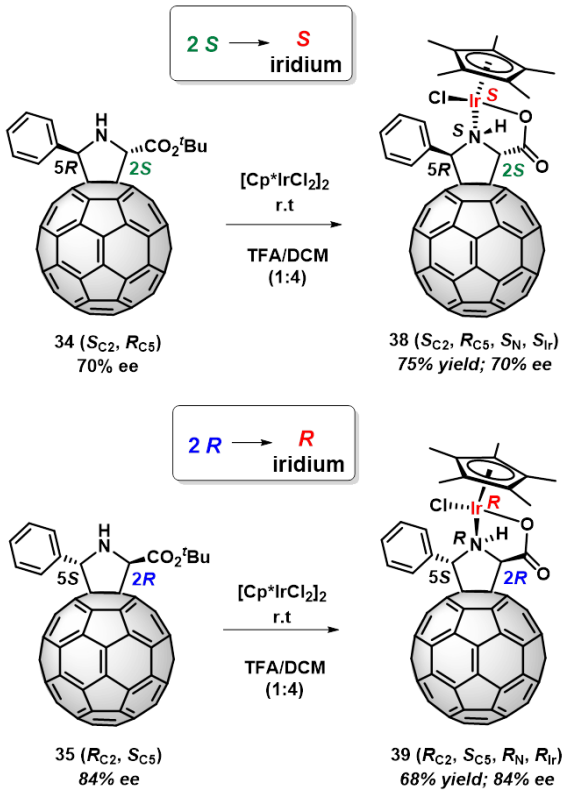

Scheme 24. Synthesis of iridium half-sandwich [60]fullerene complexes from *trans*-pyrrolidino[60]fullerene isomers.

While the two chiral carbon atoms at the pyrrolidine ring (C2 and C5) and the asymmetric nitrogen atom remains unchanged, the iridium metal atom

maintains the same configuration as the C-2 pyrrolidine carbon. The configurational change of C-5 does not modify the iridium configuration which is determined by the C-2 carbon atom.

Once the products were purified and characterized by spectroscopic techniques, the ^{1}H NMR analysis revealed the presence of only one isomer. To prove it, variable temperature experiments were performed with compound **38** at temperatures from -30ºC to 90ºC.

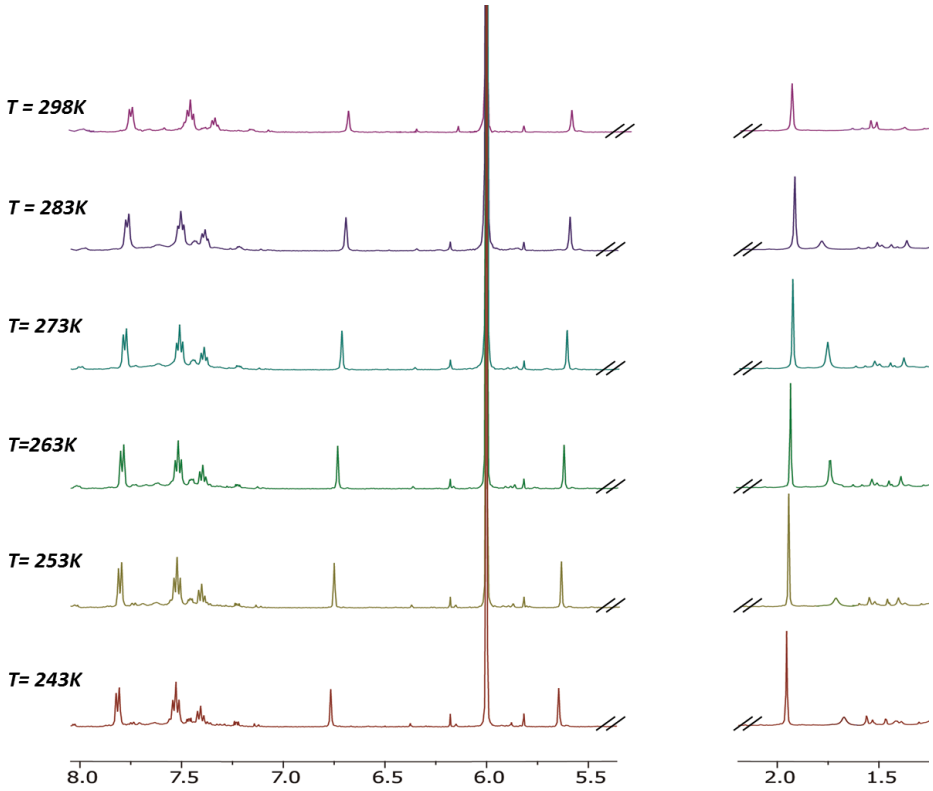

Figure 44. ^{1}H NMR (700 MHz, $C_2D_2Cl_4$) of compound **38** (S_{C2}, R_{C5}, S_N, S_{Ir}) in a range of temperature from 243K to 298K.

The experiments ranging from 0°C to 90°C and from 0°C to -30°C in tetrachloroethane, did not show any change in the signals of the ^{1}H NMR spectrum, showing the high stability of the stereogenic metal center. Actually, none of the four stereoisomers undergo any epimerization process.

The optical purity of compounds **38** and **39** was analyzed by HPLC, using a chiral column *ChiralPack IA*. The enantiomeric excess was the same that the starting [60]fulleropyrrolidines, (*S*,*R*)-*trans* **34** (70% *ee*) and (*R*,*S*)-*trans* **35** (84% *ee*). $t_R(S_{C2}, R_{C5}, S_N, S_{Ir})$ = 3.9 min, $t_R(R_{C2}, S_{C5}, R_N, R_{Ir})$ = 5.6 min.

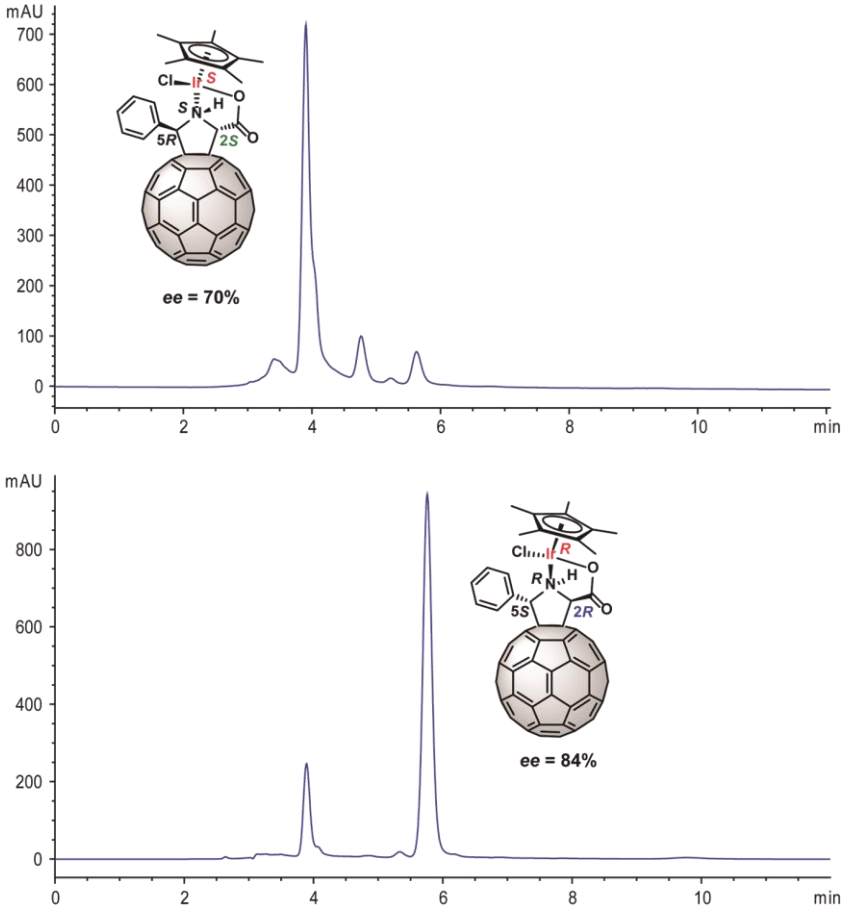

Figure 45. HPLC profiles of chiral iridium fullerene hybrids **38** (top) and **39** (bottom). HPLC column: *ChiralPack IA* (4.6 x 250mm; dichloromethane/isopropyl alcohol (98:2); 1 ml/min; 320 nm; 25ºC).

To confirm the optical activity of the four stereoisomers, **36** (S_{C2}, S_{C5}, S_N, S_{Ir}), **37** (R_{C2}, R_{C5}, R_N, R_{Ir}), **38** (S_{C2}, R_{C5}, S_N, S_{Ir}) and **39** (R_{C2}, S_{C5}, R_N, R_{Ir}), the circular dichroism spectra were recorded.

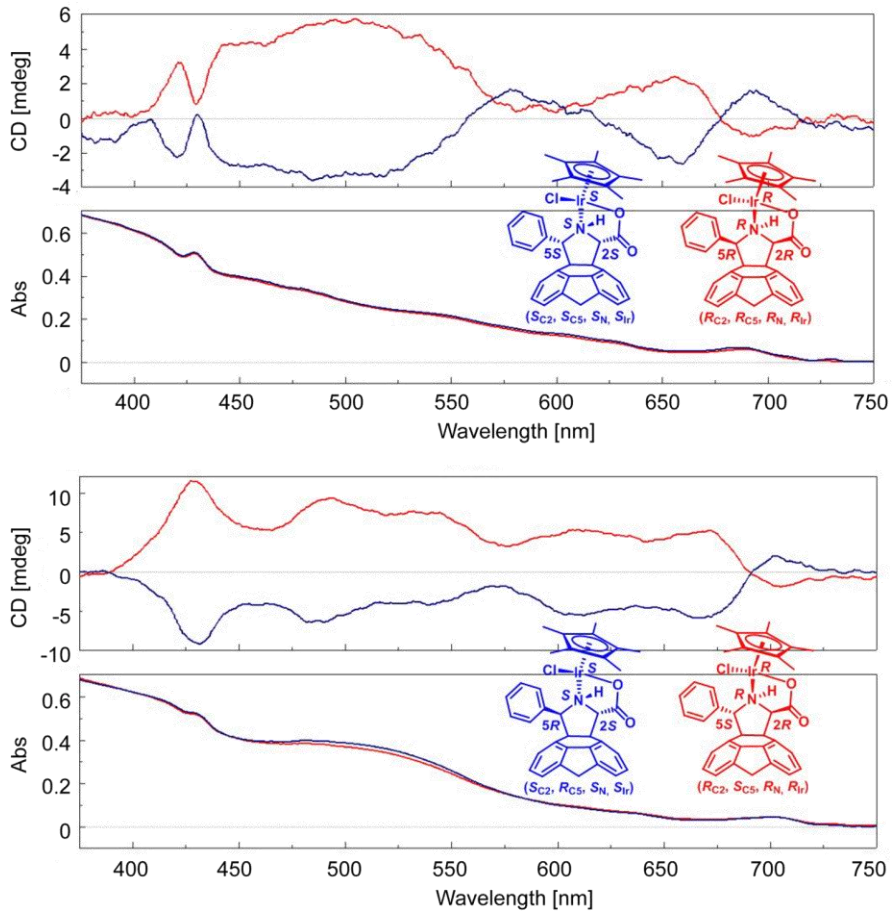

Figure 46. Circular dichroism and UV-vis spectra for the enantiomers **36**, **37** (top) and **38**, **39** (bottom) (concentration, $1x10^{-6}$M in dichloromethane).

Comparing the CD spectra of fullerene derivatives, with or without metal (Figures 35 and 46), it was observed that compounds **32** (*S*,*S*) and **36** (S_{C2}, S_{C5}, S_N, S_{Ir}), present the same sign and the same Cotton effect at 430 nm (blue lines). In the same way, compounds **33** (*R*,*R*) and **37** (R_{C2}, R_{C5}, R_N, R_{Ir}) show a negative Cotton effect (red lines).

On the other hand, the circular dichroism of the chiral hybrids and the *trans*-[60]fulleropyrrolidines are consistent. Compounds **34** (*S*,*R*) and **38** (S_{C2}, R_{C5}, S_N, S_{Ir}), present a negative Cotton effect at 430 nm (blue lines), while

compounds **35** (*R*,*S*) and **39** (R_{C2}, S_{C5}, R_N, R_{Ir}) show a positive Cotton effect (red lines).

In the UV-vis spectra of the hybrids, an additional weak shoulder at 480 nm for *cis* stereoisomers and a broad peak for *trans* stereoisomers was observed. These peaks correspond to a broad peak in their respective CD spectra. The aforementioned peaks could be assigned to the presence of the metals in these complexes. However, the lack of a significant number of examples does not allow inferring these signals as a typical signature for these compounds.

4.1.2. Synthesis of Rhodium Complexes

In order to extend the scope of the synthetic methodology to other metals, we carried out the synthesis of rhodium-fullerene hybrids.

The previously synthesized optically pure [60]fulleropyrrolidines, *cis* diastereomers **32** and **33**, were treated with pentamethylcyclopentadienyl rhodium(III) chloride dimer $[Cp^*RhCl_2]_2$, in "one pot" procedure after the ester hydrolysis with a mixture TFA/DCM (1:4). After two hours of stirring at room temperature, the rhodium fullerene hybrids **40** and **41** were obtained in 48% and 77% yields, respectively.

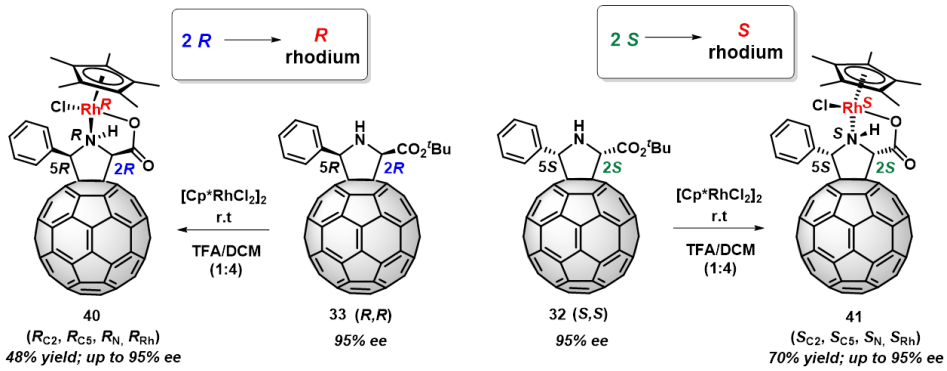

Scheme 25. Synthesis of rhodium half-sandwich [60]fullerene complexes from *cis*-pyrrolidino[60]fullerene isomers.

Chiral fullerene hybrids were characterized using standard spectroscopic techniques. The ^{1}H NMR spectrum of compounds **40** and **41** showed the presence of a single isomer. The aromatic protons appeared at 8.27-7.30 ppm, the N-H presented a *cis* disposition with respect to the C2-H and was exhibited as a triplet at 6.08 ppm. Therefore, the methylene protons of the pyrrolidine ring were showed as doublets at 6.23 and 5.87 ppm. The characteristic signal of the Cp^* moiety appeared as a singlet at 1.67 ppm (Figure 47).

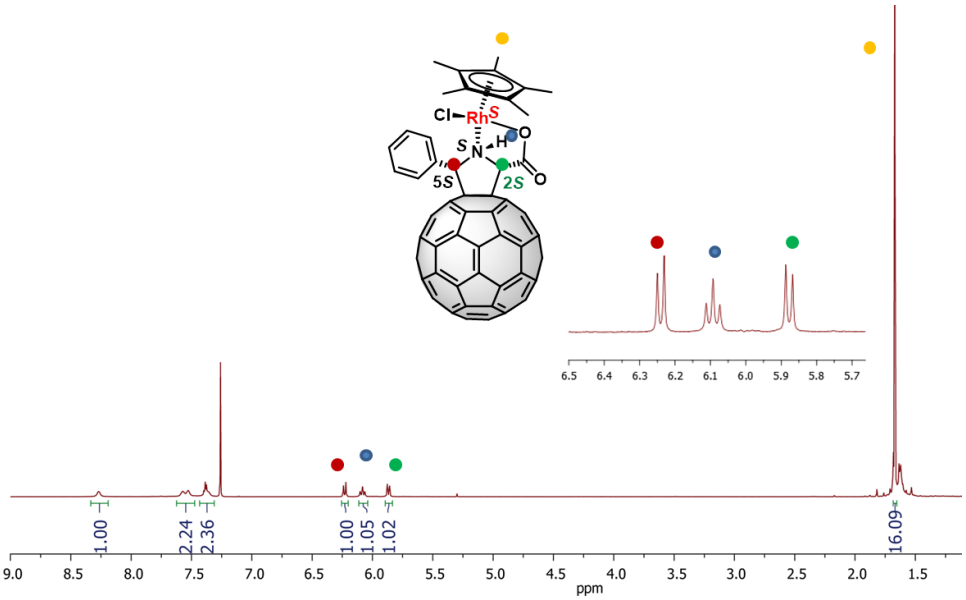

Figure 47. ^{1}H NMR (700 MHz, 298K, $CDCl_3$) of chiral fullerene hybrids **40** and **41**.

The optical purity of compounds **40**, **41** was determined by HPLC using a chiral column, *ChiralPack IA*, showing high values of enantiomeric excesses. $t_R(S_{C2}, S_{C5}, S_N, S_{Rh})$ = 7.7 min, $t_R(R_{C2}, R_{C5}, R_N, R_{Rh})$ = 39.6 min.

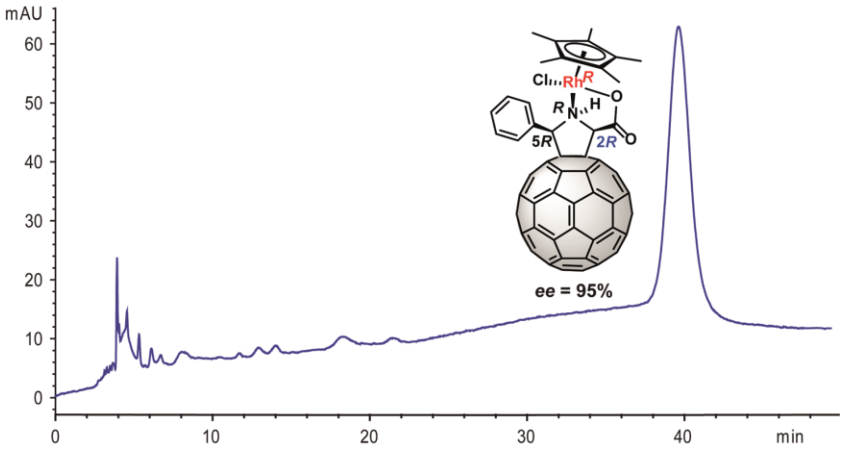

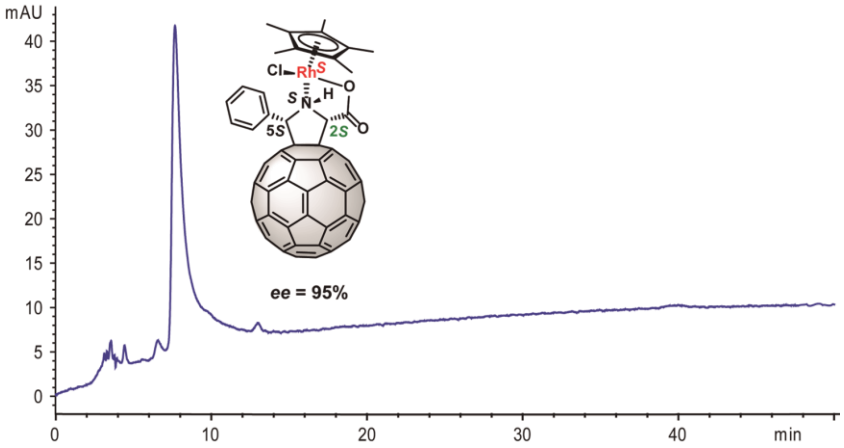

Figure 48. HPLC profiles of chiral rhodium fullerene hybrids **40** (top) and **41** (bottom). HPLC column: *ChiralPack IA* (4.6 x 250mm; dichloromethane/isopropyl alcohol (96:4); 1 ml/min; 320 nm; 25ºC).

To confirm the absolute configuration of the chiral hybrids, the CD was recorded. Compound **40** formed from the pyrrolidine **33** *cis*-(*R*,*R*), obtained by the catalytic pair Ag(I)/(*R*)-BPE, presented a positive Cotton effect in the circular dichroism spectrum (red line). On the other hand, the pyrrolidine **32** *cis*-(*S*,*S*), obtained from the catalytic system Cu(II)/(*R*)-Fesulphos, led to the chiral hybrid **41** that showed a negative Cotton effect (blue line). Thus, the chiral fullerene metal hybrid presented the same trend as the starting [60]fulleropyrrolidines (Figures 35, 49).

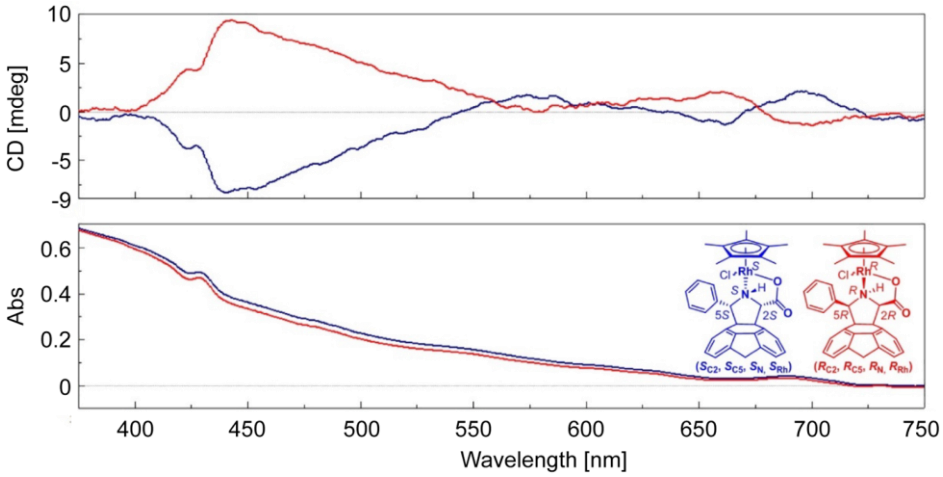

Figure 49. Circular dichroism and UV-vis spectra for the *cis* enantiomers **40** and **41** (concentration, $1x10^{-6}$M in dichloromethane).

Based on the extensive study carried out with chiral iridium fullerene derivatives and the results obtained, we can attribute the configuration (R_{C2}, R_{C5}, R_N, R_{Rh}) to compound **40** and (S_{C2}, S_{C5}, S_N, S_{Rh}) for the rhodium chiral hybrid **41**.

4.1.3. Synthesis of Ruthenium Complexes

Finally, the aforementioned synthetic methodology was also applied to other transition metal, to obtain ruthenium-fullerene complexes.

The optically pure *cis* pyrrolidines **32** (99% *ee*) and **33** (99% *ee*), were treated with dichloro(*p*-cymene) ruthenium(II) dimer $[(p\text{-cymene})RuCl_2]_2$, in "one pot" procedure after the ester hydrolysis with a mixture TFA/DCM (1:4). After two hours of stirring at room temperature, the ruthenium fullerene hybrids **42** and **43** were obtained in 83% and 80% yield respectively.

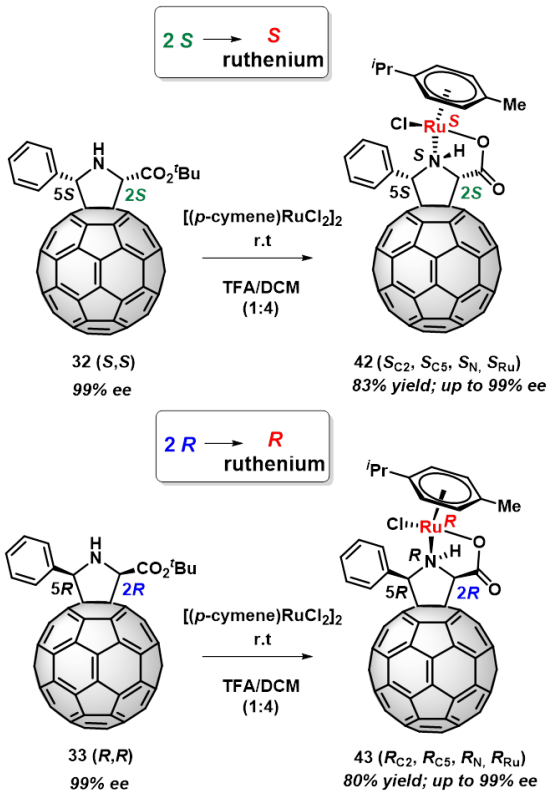

Scheme 26. Synthesis of ruthenium half-sandwich [60]fullerene complexes from *cis*-pyrrolidino[60]fullerene isomers.

In the ^{1}H NMR spectrum of compounds **42** and **43** only was observed a single product. The signals of the aromatic protons appeared at 7.97-7.47 ppm, the signal of the N-H as a triplet at 5.77 ppm and the methylene protons of the pyrrolidine ring as doublets at 6.26 and 5.65 ppm. The signals of the *p*-cymene group were shown in a range from 5.74 to 1.23 ppm (Figure 50).

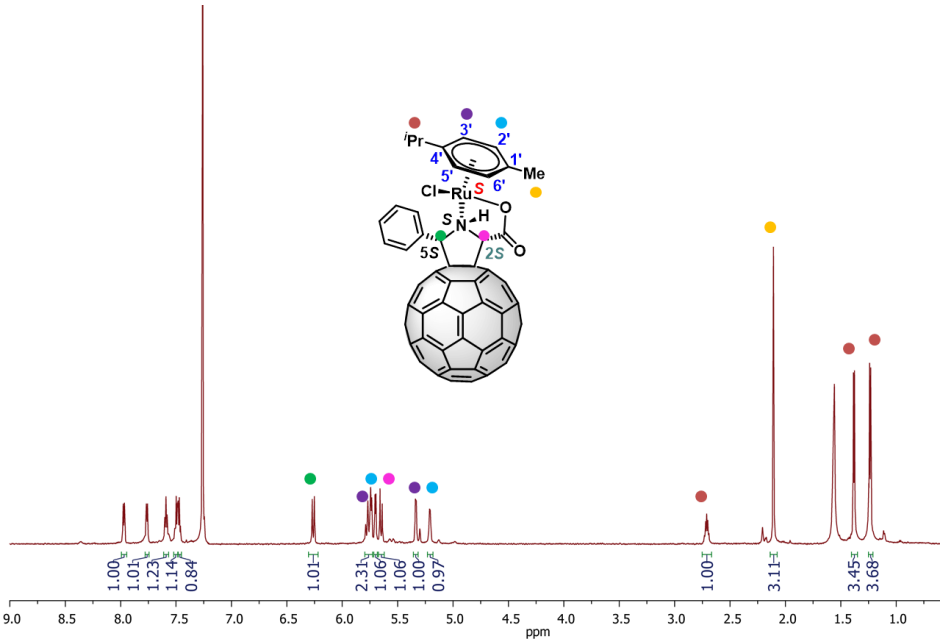

Figure 50. ^{1}H NMR (700 MHz, 298K, $CDCl_3$) of compounds **42** and **43**.

The optical purity of compounds **42** and **43** was analyzed by HPLC, using a chiral column *ChiralPack IA*. The enantiomeric excess of the products was the same that the starting [60]fulleropyrrolidines, **32** (*S*,*S*)-*cis* (99% *ee*) and **33** (*R*,*R*)-*cis* (99% *ee*). $t_R(S_{C2}, S_{C5}, S_N, S_{Ru})$ = 8.9 min, $t_R(R_{C2}, R_{C5}, R_N, R_{Ru})$ = 61.3 min.

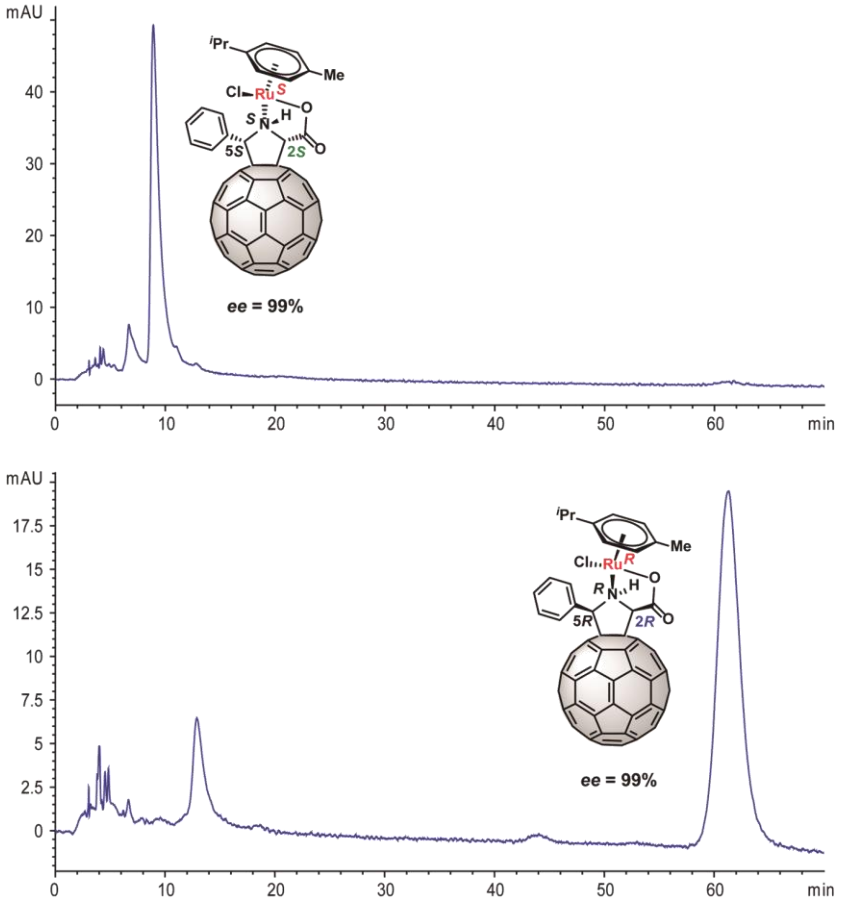

Figure 51. HPLC profiles of chiral ruthenium fullerene hybrids **42** (top) and **43** (bottom). HPLC column: *ChiralPack IA* (4.6 x 250mm; dichloromethane/isopropyl alcohol (98:2); 1 ml/min; 320 nm; 25ºC).

The stereochemistry of the hybrids was confirmed by circular dichroism. The chiral hybrid **42** presented a negative Cotton effect in the circular dichroism spectrum (blue line) as well as the starting [60]fulleropyrrolidine **32** *cis*-(*S*,*S*). In contrast, the chiral hybrid **43** showed a positive Cotton effect (red line) as its starting pyrrolidine **33** *cis*-(*R*,*R*) (Figures 35, 52).

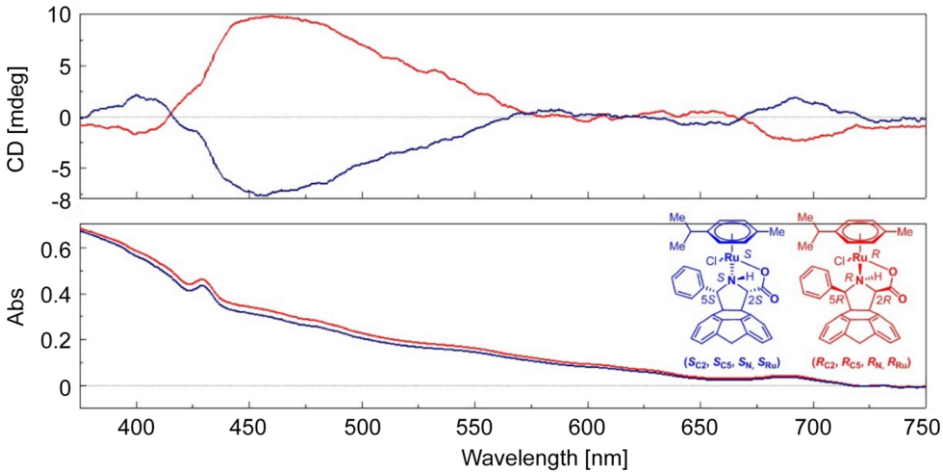

Figure 52. Circular dichroism and UV-vis spectra for the *cis* enantiomers **42** and **43** (concentration, $1x10^{-6}$M in dichloromethane).

To complete the synthesis of the four stereoisomers, optically pure *trans* isomers **34** (*S*,*R*)-*trans* (74% *ee*) and **35** (*R*,*S*)-*trans* (80% *ee*), were treated with [(*p*-cymene)$RuCl_2]_2$, after the ester hydrolysis with a mixture TFA/DCM (1:4). Compounds **44** and **45** were obtained as a single product in 62% and 45% yields, respectively (Scheme 27).

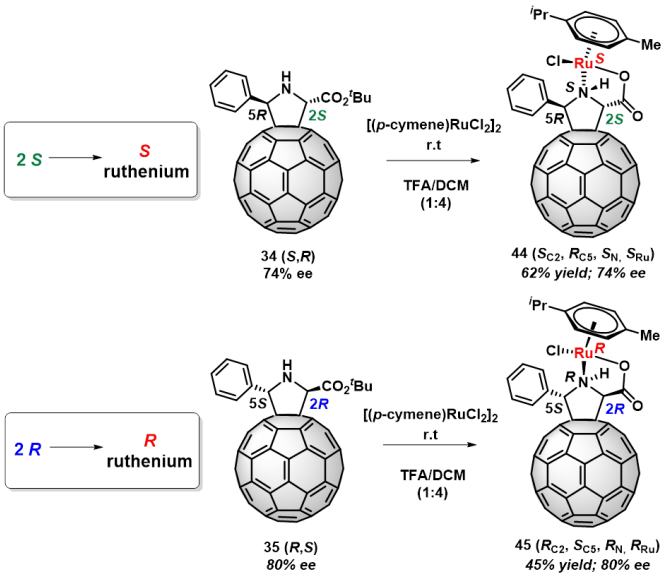

Scheme 27. Synthesis of ruthenium half-sandwich [60]fullerene complexes from *trans*-pyrrolidino[60]fullerene isomers.

The products were purified and characterized by standard spectroscopic techniques. The ^{1}H NMR spectrum of compounds **44** and **45** shows the signals of the aromatic protons appearing at 7.95-7.64 ppm, the signal of the N-H as a doublet of doublets at 5.95 ppm and the methylene protons of the pyrrolidine ring at *trans* position as doublets at 6.03 and 5.84 ppm. The signals of the *p*-cymene group appear in the range of 5.49-1.37 ppm.

To determine the stereochemistry of the metal center, NOE experiments with *cis* and *trans* stereoisomers were carried out.

In the *cis* isomer **42**, when the pyrrolidine proton C5-H at 6.26 ppm was irradiated, it was observed NOE effect with the methylene proton at C-2 carbon atom (5.65 ppm) of the pyrrolidine ring, with the *ortho* aromatic protons (7.76 ppm) and also with the aromatic proton of the cymene group (5.74 ppm), as expected (Figure 53). These effects do not allow determining the configuration at metal since for both epimers the calculated distances between the aforementioned protons are similar.

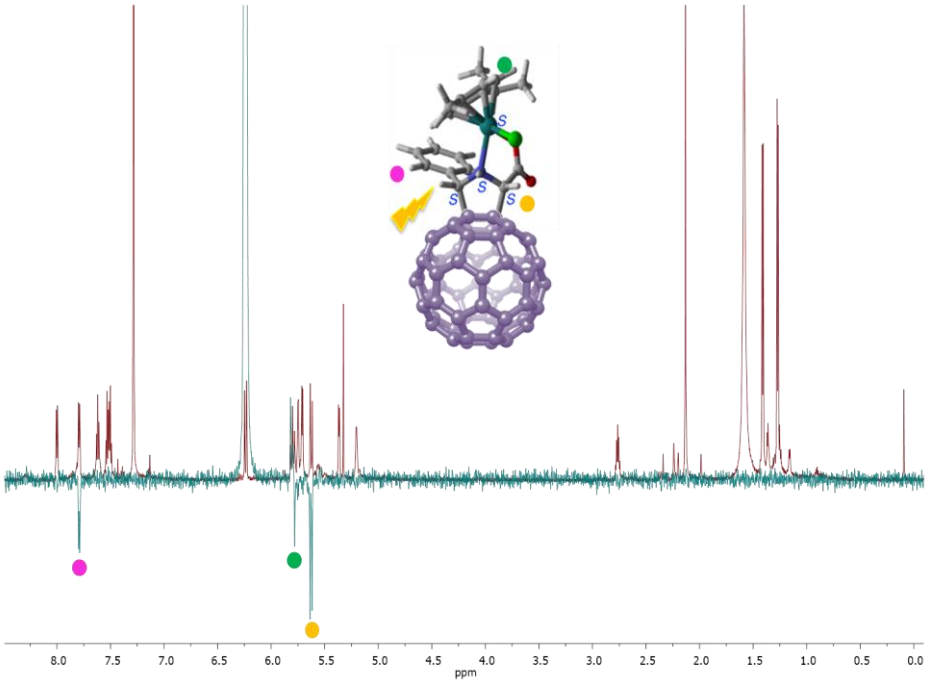

Figure 53. NOE experiment for compound **42** *cis*-(S_{C2}, S_{C5}, S_N, S_{Ru}).

However, the lack of NOE effect between the methyl group of the isopropyl and the methylene proton at C-5 tends towards the assignment of an *S* configuration at metal since for this epimer the distance between the methyl group of the isopropyl and the methylene proton at C-5 is 6.70 Å *vs* 2.60 Å of the epimer with *R* configuration at metal.

Conversely, despite that the same groups (C5-H and methyl group of the isopropyl) feature a NOE effect in the *trans* isomer **44**, the definitive assignment of the absolute configuration at metal has been based on theoretical calculations.

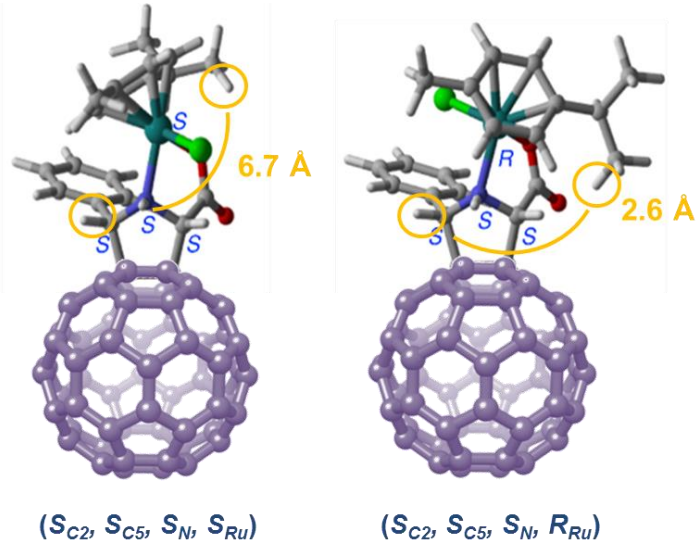

Figure 54. Calculated distances of the two possible stereoisomers at metal for *cis* ruthenium hybrid.

To corroborate the absolute configuration of the metal center, the two possible stereoisomers at metal for *cis* ruthenium hybrid, **42** (S_{C2}, S_{C5}, S_N, S_{Ru}) and its transition metal epimer **42-epi** (S_{C2}, S_{C5}, S_N, R_{Ru}), were studied by DFT calculations at the dispersion corrected RI-BP86-D3/def2-SVP level. In this case, the formed isomer **42** (S_{C2}, S_{C5}, S_N, S_{Ru}) was calculated to be 14.5 kcal/mol more stable than (S_{C2}, S_{C5}, S_N, R_{Ru}) (Figure 55), in accordance with the observed diastereoselectivity.

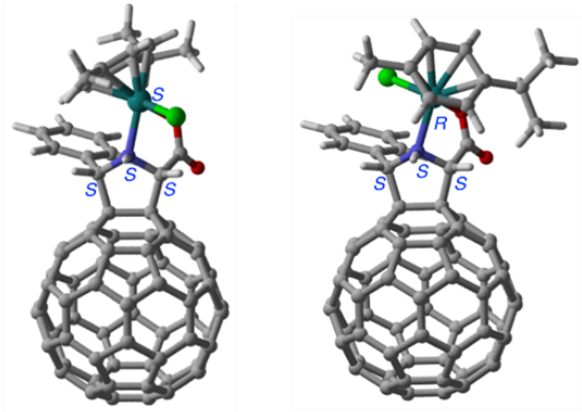

42
(S_{C2}, S_{C5}, S_N, S_{Ru})
E_{rel} = 0.0 kcal/mol

42-epi
(S_{C2}, S_{C5}, S_N, R_{Ru})
E_{rel} = 14.5 kcal/mol

Figure 55. Optimized geometries of the two possible stereoisomers at metal for *cis* ruthenium hybrid.

The highest stability of **42** (S_{C2}, S_{C5}, S_N, S_{Ru}) is justified due to a stabilizing CH–π interaction between the methyl group of the *p*-cymene group and the phenyl ring substituent at C5 carbon atom. On the other hand, the less stable isomer is affected by a strong repulsive interaction between the lone-pair of the chloride ligand and the π-electrons of the phenyl ring. Indeed, the calculated Cl···π-centroid distance of 3.38 Å for **42-epi** (S_{C2}, S_{C5}, S_N, R_{Ru}), is shorter than the sum of van der Waals radii of the involved atoms (Cl = 1.75 Å, phenyl group = 1.7 Å). Therefore, we can confirm the configuration (S_{C2}, S_{C5}, S_N, S_{Ru}) to compound **42** and (R_{C2}, R_{C5}, R_N, R_{Ru}) to compound **43.** The ruthenium metal atom maintains the same configuration as the C-2 pyrrolidine carbon, the configurational change of C-5 does not modify the ruthenium configuration.

The optical purity of compounds **44** and **45** was analyzed by HPLC, using a chiral column *ChiralPack IA*. The enantiomeric excess was the same that the starting [60]fulleropyrrolidines, **34** (*S*,*R*)-*trans* (74% *ee*) and **35** (*R*,*S*)-*trans* (80% *ee*).t_R*(*S_{C2}, R_{C5}, S_N, S_{Ru}*)* = 10.9 min, t_R*(*R_{C2}, S_{C5}, R_N, R_{Ru}*)* = 6.6 min.

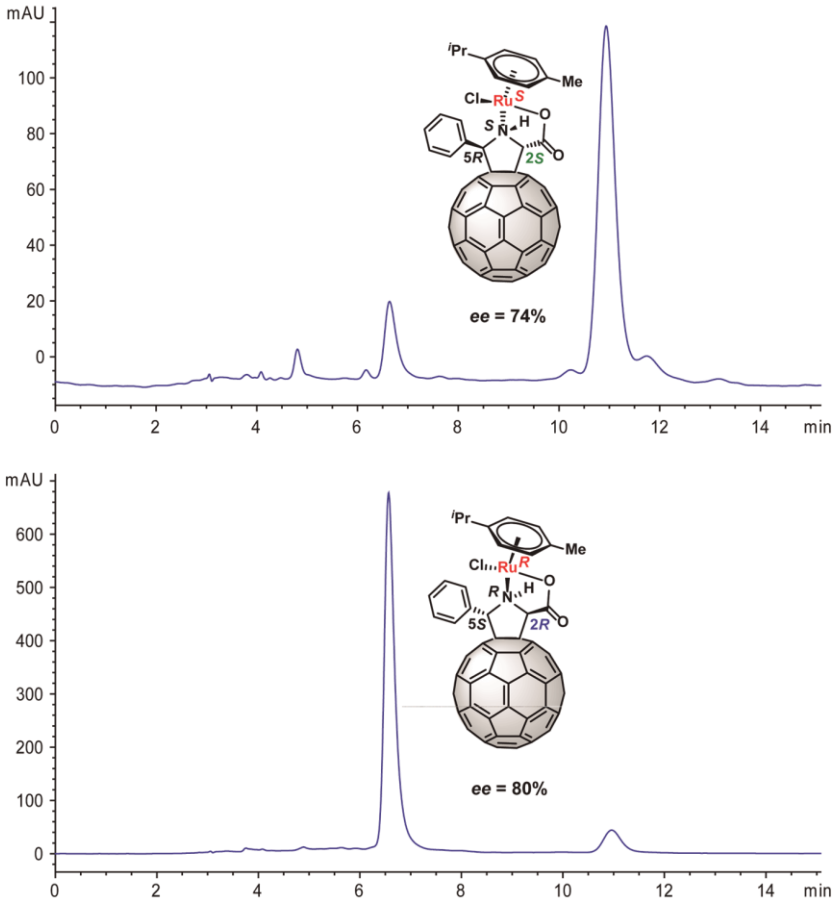

Figure 56. HPLC profiles of chiral ruthenium fullerene hybrids **44** (top) and **45** (bottom). HPLC column: *ChiralPack IA* (4.6 x 250mm; dichloromethane/isopropyl alcohol (98:2); 1 ml/min; 320 nm; 25ºC).

4.2. Catalytic Activity of Chiral Fullerene/Metal Hybrids

4.2.1. Hydrogen Transfer Reactions

Hydrogen transfer is an alternative hydrogenation process that avoids the use of potentially explosive and difficult to handle gaseous H_2. In this process, hydrogen formed from dehydrogenation of a donor molecule (typically an alcohol that is used as solvent or in a large excess) is added to a hydrogen acceptor molecule. In this regard, transition metal-catalyzed hydrogen transfer reactions are undergoing a growing interest since they fulfill the needs for safe, clean and atom economy processes.[183,184]

Recently, the use of a non-molecular carbon based material has proved its efficiency in hydrogen transfer reactions.[185] In this regard, we wondered if [60]fullerene could act as a carbon-based molecular co-catalyst with a synergic activity in hydrogen transfer processes. Despite the rich chemistry developed "onto fullerenes", the chemistry carried out "with fullerenes" has been almost neglected.

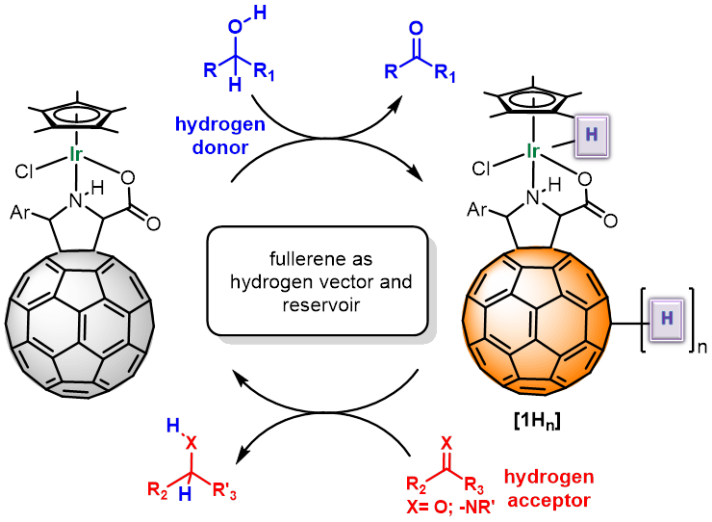

Figure 57. Iridium-fullerene hybrid catalyzed hydrogen transfer reactions.

183. a) L. A. Oro, C. Claver, *Iridium Complexes in Organic Synthesis*, Wiley, **2009**. b) O. Saidi, J. M. J. Williams, P. G. Andersson, *Iridium Catalysis*, **2011**.
184. M. Kitamura, R. Noyori, *Ruthenium in Organic Synthesis*, Wiley-VCH Verlag GmbH & Co. KGaA, **2005**.
185. H. Yang, X. Cui, X. Dai, Y. Deng, F. Shi, *Nat. Commun.*, **2015**, *6*, 6478.

Thus, we carried out a preliminary study of the previously prepared metal-fullerene hybrids, where C_{60} is endowed with metals such as Ir, Rh or Ru that present a high activity in transfer hydrogenation reactions, with the aim to evaluate the efficiency of these new catalysts, the easy isolation of the products from the catalyst and the ability of the latter to be reused maintaining efficiency and enantioselectivity. In the following sections, the outstanding catalytic behaviour exhibited by the newly synthesized hybrid catalysts on different fundamental reactions will be discussed.

As a first approximation, we tested the catalytic activity of metal-fullerene racemic mixture of *cis* adduct, synthesized analogously to the methodology previously described for the synthesis of enantiomerically pure hybrids but using the catalytic system Ag(OAc)/dppe instead of a chiral ligand.

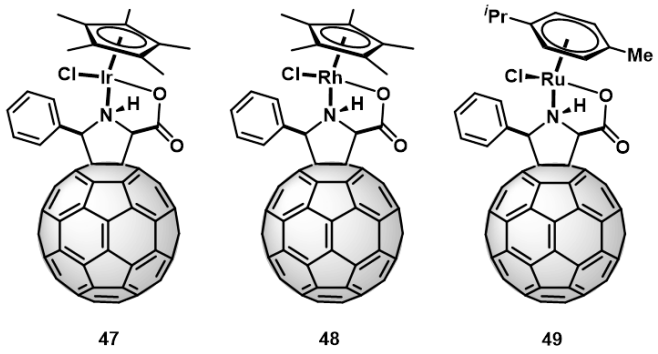

47 48 49

Figure 58. Racemic mixtures of *cis*-metal fullerene hybrids.

Initially, we studied the reduction of acetophenone in the presence of 2-propanol as hydrogen donor and solvent. As a first step, we carried out the reaction using iridium dimer $[Cp^*IrCl_2]_2$ as benchmark. Thus, 0.5 mol% of iridium was dissolved in 2-propanol (2 mL) along with 40 mg of acetophenone and the mixture was heated at 90ºC. The acetophenone reduction was afforded with a 65% yield after 18h (Table 1, entry 1).

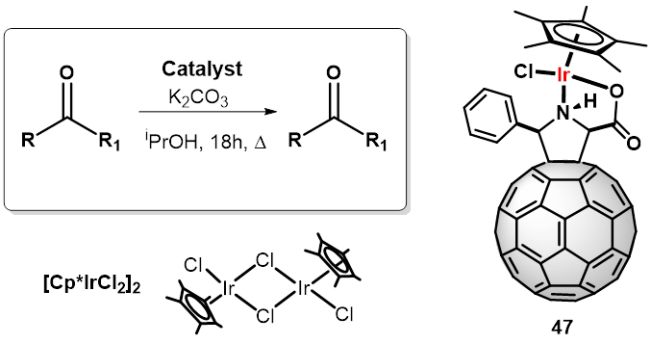

Scheme 28. Ketones reduction by transfer hydrogenation from 2-propanol.

For our delight, iridium-fulleropyrrolidine **47** gives rise to a quantitative reduction of acetophenone after 18 hours with only 0.5% of catalyst loading (Table 1, entry 2). The efficiency of the reduction was determined by ^{1}H NMR spectroscopy.

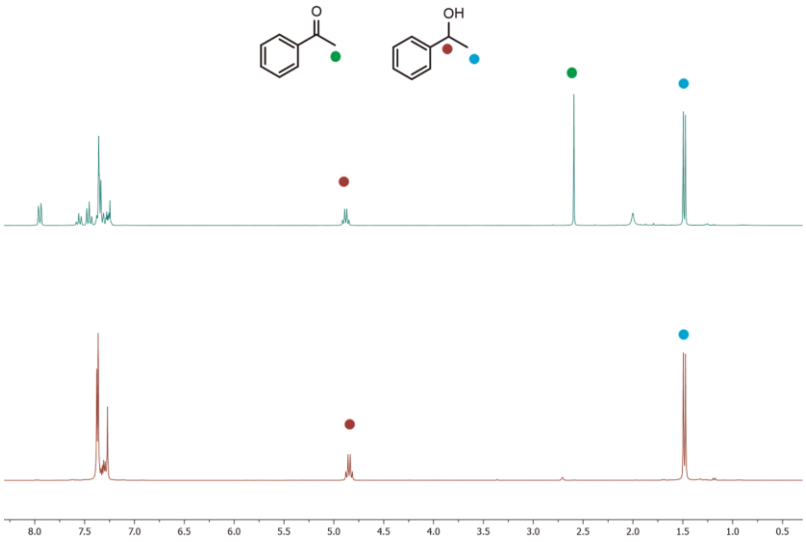

Figure 59. ^{1}H NMR (300 MHz, 298K, $CDCl_3$) spectra from the reaction crude (without any purification) of hydrogenation of acetophenone catalyzed by iridium dimer (top) and iridium-fullerene hybrid **47** (bottom) (Table 1, entries 1 and 2).

The NMR spectrum of the acetophenone reduction catalyzed by iridium dimer complex (entry 1) showed the aromatic signals of the acetophenone and the methyl group as a singlet at 2.52 ppm along with the signals of the alcohol (top). In contrast, when the reaction was catalyzed by iridium hybrid **47** (Table 1, entry 2), the acetophenone was totally consumed (> 99%) and in the spectrum only the signals of 1-phenylethanol, a multiplet at 4.85 ppm and a doublet at 1.49 ppm (bottom) were observed.

The use of minor amounts of catalyst led to 66% of conversion after 18 hours (Table 1, entry 3). Finally, metal fullerene hybrids **48** and **49** did not display the same efficiency and afforded the corresponding alcohol in 76% and 17% yield respectively (Table 1, entries 4, 5). Thus, we focused on iridium complexes, which are the ones that give better results.

Table 1. Ketones hydrogenation by transfer hydrogenation from 2-propanol.

Entry	**Catalyst (mol% Ir)**	**Yield (%)**
1	**$[Cp^*IrCl_2]_2$** (0.5)	65
2	**47** (0.5)	>99
3	**47** (0.1)	66
4	**48** (0.5)	76
5	**49** (0.5)	17

These hybrid catalysts present another important advantage. The iridium fullerene hybrid is mostly insoluble in isopropanol at room temperature and therefore, after filtration or centrifugation, the catalyst could be removed from the solution and recovered for a further use, keeping the product pure without any further purification but solvent elimination.

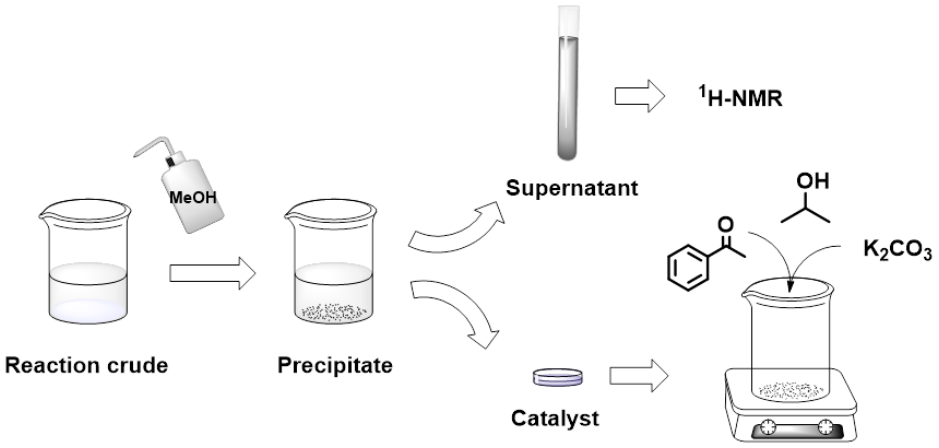

Figure 60. Methodology to recover the catalyst from the reaction medium.

Subsequently, the recovery capacity of the catalyst once used and the number of cycles that could be reused without losing catalytic efficiency were evaluated. Reactions were performed in refluxing 2 mL of isopropanol by using 40 mg of acetophenone and K_2CO_3 in the same amount as the catalyst. Once carried out the reaction, the catalyst was precipitated at room temperature by adding methanol to the reaction mixture. The solution was centrifuged at 6000 rpm for 15 minutes (this procedure was repeated for three times) and after solvent evaporation, the product formed was fully characterized by spectroscopic techniques. The isolated catalyst was employed (recycled) in a new reaction without any further purification. It is important to note that the recovered catalyst should be used immediately (or stored under argon atmosphere) to prevent catalyst oxidation.

Table 2. Catalytic efficiency and recovery capacity of the catalyst.

Entry	Catalyst (mol% Ir)	Yield (%)
1	**47** (1.0)	>99
2	**47** (rc.)	>99
3	**47** (rc.)	>99
4	**47** (rc.)	>99
5	**47** (rc.)	>99
6	**47** (rc.)	15

rc: recycled

The results summarized in table 2 show that the recovered catalyst has successfully been reused for up to 5 times without observing any loss of catalytic efficiency. However, exposition to oxygen and or light has to be carefully avoided since it is the main cause of decreasing efficiency (entry 6).

As result of the very poor solubility of fullerene cages in polar solvents, they merge the advantages of the molecular homogeneous catalyst (defined structures and stereochemical configurations) with those of heterogeneous catalysts (products are readily isolated and the catalyst recovered by mechanical means and reused).

After the excellent results obtained in the reduction of acetophenone catalyzed by metal fullerene hybrids, we evaluated the reduction of different ketones by transfer hydrogenation to extend the scope of the reaction. Reactions were performed in the same conditions, refluxing 2 mL of 2-propanol by using 40 mg of ketone and K_2CO_3 in the same amount as the catalyst.

Table 3. Reduction of different ketones.

Entry	Catalyst (mol% Ir)	R-; R'-	Yield (%)
1	**47** (0.5)	-$(CH_2)_5$-	>99
2	**47** (0.5)	Cyclohexyl-; -H	>99
3	**47** (0.5)	*n*Bu-; -H	>99

Iridium fullerene hybrid catalyst **47** was also able to efficiently reduce other ketones as cyclohexanone, cyclohexanecarboxaldehyde and even aldehydes such as pentanal (Table 3, entries 1-3). In all the cases the reduction was quantitative (> 99%).

These results reveal a strong increase of the catalytic efficiency in the reduction of different ketones by transfer hydrogenation with respect to the iridium dimer complex, being among the most efficient iridium-based catalysts. This high efficiency is the result of a synergic effect of the metal and the hydrogen borrowing ability of C_{60} carbon cage. It is known that fullerenes reversibly add hydrogen, giving rise to fullerene hydrides[40] which has been envisaged as an interesting method for the storage of hydrogen.

In order to prove the role of fullerene moiety and the reversibility of the C_{60}-H bonds formation onto the carbon cage, we performed the same experiment that with the ketones. The use of iridium dimer complex $[Cp^*IrCl_2]_2$, in the presence of pristine [60]fullerene as hydrogen acceptor, in 2-propylalcohol at 90ºC for 16h, gave rise to the formation of $C_{60}H_2$ in a 5-10% yield, thus proving the ability of the fullerene cage to add hydrogen during the reaction (Scheme x).

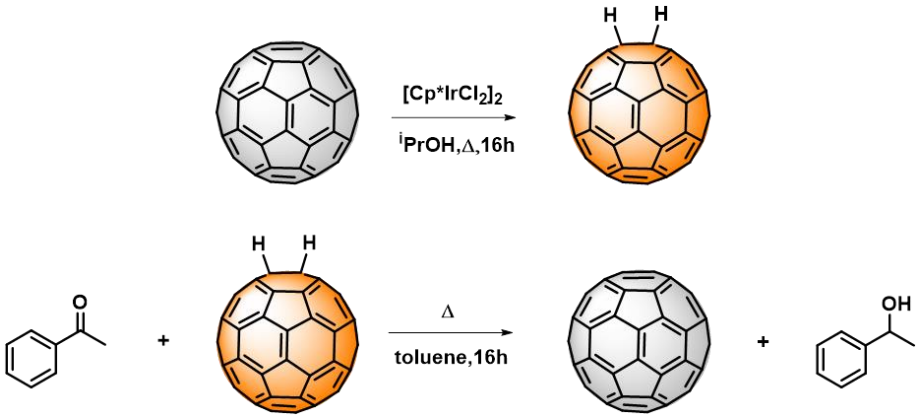

Scheme 29. Hydrogenation process carried out by [60]fullerene.

The reaction of fullerene hydrides with acetophenone in refluxing toluene for one night afforded the corresponding phenylethanol in 66% (Scheme x). These experimental findings, the isolation of fullerene hydrides such as $C_{60}H_2$, or $C_{60}H_4$ and their further ability to release these hydrogen atoms to reduce an unsaturated functionality such as, a ketone, reveal the ability of [60]fullerene to act as a hydrogen carrier.

The HPLC analysis of the fraction of fullerene hydrides revealed a higher peak corresponding to $C_{60}H_2$ and a small peak corresponding to C_{60}, in a ratio 92/8. On the other hand, after the hydrogenation process carried out by the hydrogenated fullerenes, the peak corresponding to $C_{60}H_2$ decreases due to the release of the hydrogens, increasing the signal of the C_{60} in a final ratio 40/60 (Figure 61).

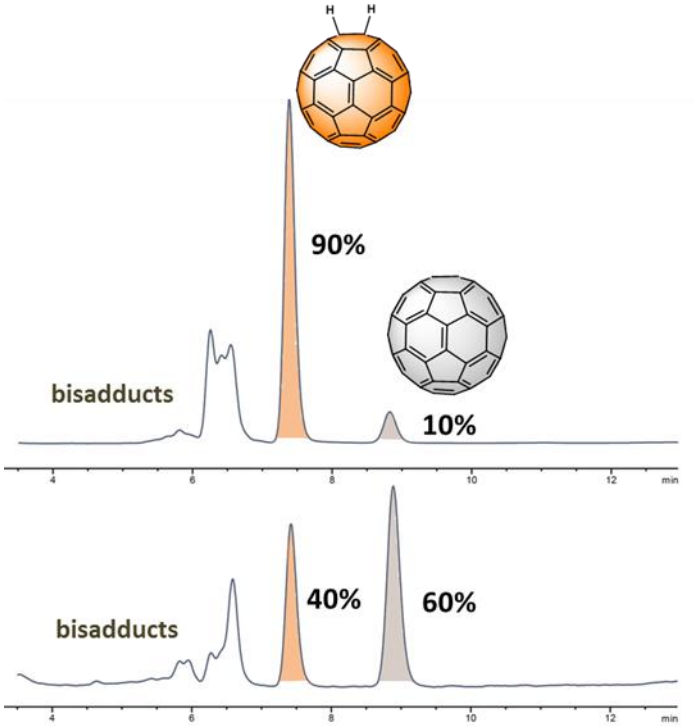

Figure 61. HPLC profile of fullerene hydrides ($C_{60}H_2$) before (top) and after (bottom) the reaction with acetophenone. HPLC column: Buckyprep Waters (4.6 x 250mm; toluene/acetonitrile (90:10); 1 ml/min; 320 nm; 25ºC).

To the best of our knowledge, the employment of fullerenes as active species in a catalytic process is unprecedented. Moreover, the high efficiencies achieved in these transfer hydrogenation reactions reveal fullerenes as appealing candidates for a variety of still unexplored catalytic processes.

4.2.2. *N*-alkylation of Amines by Hydrogen Autotransfer Process

Based on the aforementioned results, we wondered if these hybrid catalysts could be useful in hydrogen auto-transfer processes where hydrogen donor and acceptor stem from the same source as it occurs in the *N*-alkylation of amines with alcohols (Scheme 30).[186]

We have chosen the *N*-alkylation of aniline with *p*-methoxybenzyl alcohol as reaction model to study the efficiency of the new hybrid catalyst and the effect of the fullerene cage in the process.

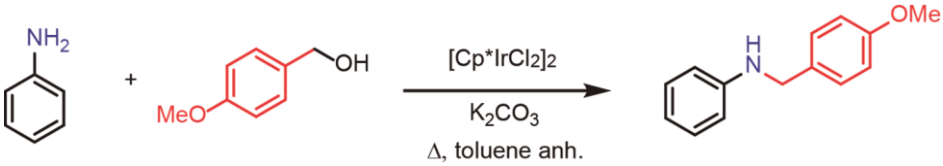

Scheme 30. Amine *N*-alkylation by hydrogen borrowing.

On the basis of the optimization of the reaction conditions, we carried out the reaction using equimolar amounts of aniline and benzyl alcohol in toluene (0.3 mL) in the presence of $[Cp^*IrCl_2]_2$ as catalyst (2.5 mol% Ir) and K_2CO_3 as base (2.5 mol%) at 110ºC for 17 h. The most relevant results are summarized in table 4. The mono-alkylated *N*-*p*-methoxybenzylaniline was formed in 67% yield and no formation of di-alkylated product was observed (entry 1). When the reaction was carried out without a base, *N*-*p*-methoxybenzylaniline was formed in 50% yield (entry 2). In order to study the efficiency of other iridium complexes, we synthesized an iridium prolinate **50**, following the procedure described in the literature.[187] This derivative afforded the alkylated product in 50% yield using 2% of catalytic loading, after 24 h (entry 3). Notably, the use of the iridium-fullerene hybrid **47** promotes an increase of the catalytic efficiency, obtaining the product in an excellent yield 98% with 2.5% of catalyst (entry 4). The absence of a base causes a significant decrease in the yield 86% (entry 5). The use of tetrachloroethane as solvent resulted in lower

186. a) M. H. S. A. Hamid, P. A. Slatford, J. M. J. Williams, *Adv. Synth. Catal.*, **2007**, *349*, 1555. b) G. Guillena, D. J. Ramón, M. Yus, *Chem. Rev.*, **2010**, *110*, 1611. c) G. E. Dobereiner, R. H. Crabtree, *Chem. Rev.*, **2010**, *110*, 681.
187. A. Wetzel, S. Wöckel, M. Schelwies, M. K. Brinks, F. Rominger, P. Hofmann, M. Limbach, *Org. Lett.*, **2013**, *15*, 266.

yield 22% (entry 6). We also examined the reaction using the *p*-methoxybenzyl alcohol as solvent, however the yield was very poor 22% (entry 7). The reduction reaction was completed with 1.25% of catalyst (entry 8) and the use of minor catalytic load (0.5%) afforded the product in 66% yield (entry 9).

These results clearly show that the catalytic performance of the hybrid catalyst **47** is higher than the iridium complexes ($[Cp^*IrCl_2]_2$ and iridium prolinate **50** due to the combination of metal-fullerene which result in a higher hydrogen uploading.

Table 4. Optimization of reaction conditions in amine *N*-alkylation by hydrogen borrowing.

Entry	Catalyst (mol% Ir)	Volume (mL)	Base	Solvent	Yield (%)
1	**$[Cp^*IrCl_2]_2$** (2.5)	0.3	K_2CO_3	Toluene	67
2	**$[Cp^*IrCl_2]_2$** (2.5)	0.3	-	Toluene	50
3	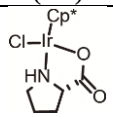 **50** (2.0)	0.3	K_2CO_3	Toluene	50
4	**47** (2.5)	0.5	K_2CO_3	Toluene	99
5	**47** (2.5)	0.5	-	Toluene	86
6	**47** (2.5)	0.5	K_2CO_3	TCE	48
7	**47** (2.5)	-	K_2CO_3	Alcohol	22
8	**47** (1.25)	0.5	K_2CO_3	Toluene	>99
9	**47** (0.5)	0.5	K_2CO_3	Toluene	66

The ^{1}H NMR spectrum of the reaction crude catalyzed by iridium hybrid **47** (entry 4), showed the signals of *N*-*p*-methoxybenzylaniline. The aromatic signals at 7.25-6.50 ppm, a singlet corresponding to the methylene at 4.15 ppm and a singlet for the methoxy group at 3.65 ppm (bottom). In the case of the reaction catalyzed by iridium prolinate **50** complex (entry 3) a mixture of the

starting products along with the signals of the mono alkylated product was observed (top).

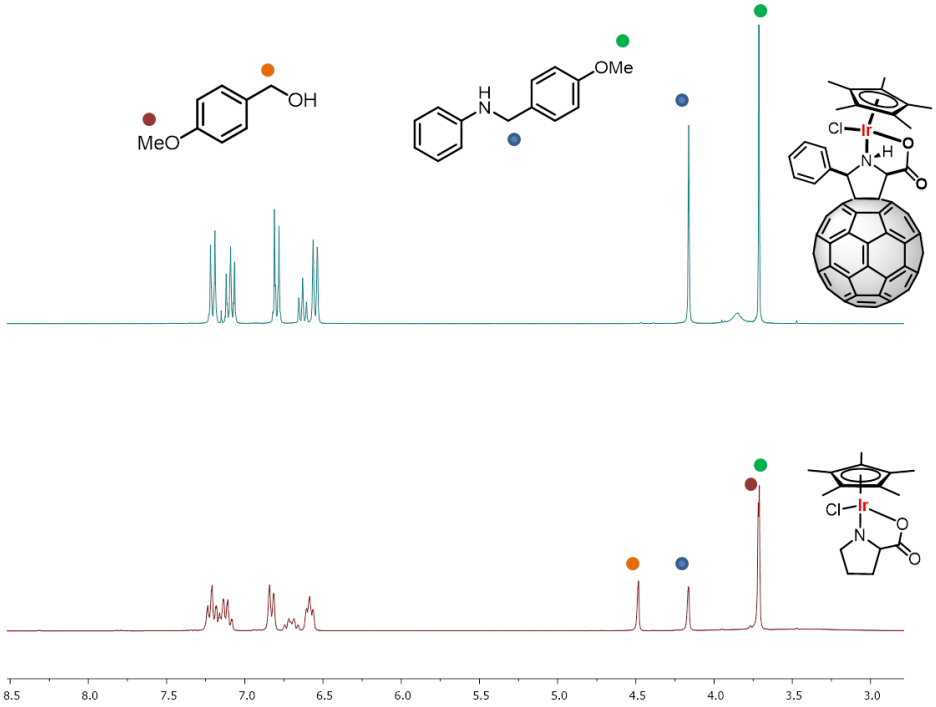

Figure 62. ^{1}H NMR (300 MHz, 298K, $CDCl_3$) spectra from the reaction crude (without any purification) of *N*-alkylation by hydrogen autotransfer process catalyzed by iridium-fullerene hybrid **47** (top) and iridium prolinate **50** (bottom) (Table 4, entries 3 and 4).

We propose that the initial stage of the reaction is the oxidation of the alcohol to a carbonyl intermediate accompanied by the generation of a transient iridium hydride. Then, the carbonyl intermediate reacts with the amine to afford an imine with formation of water. Transfer hydrogenation of the imine with the iridium hydride give an alkylated amine as product (Scheme 31).

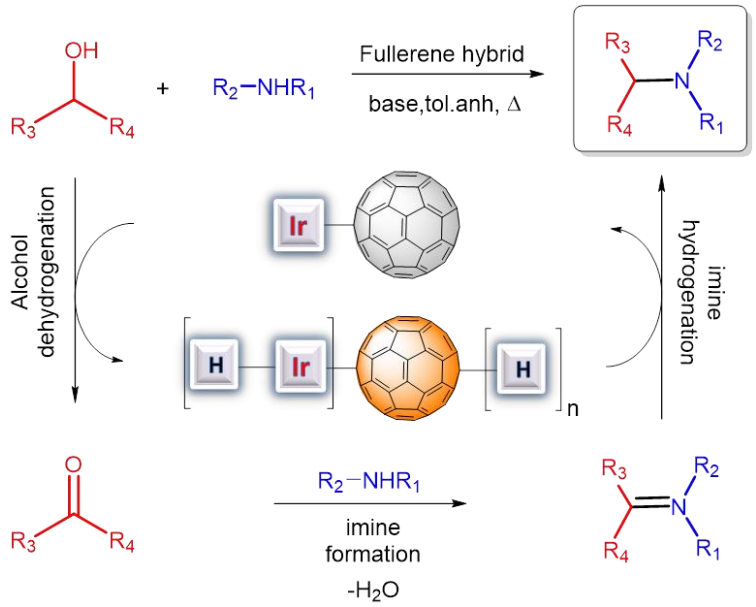

Scheme 31. Amine *N*-alkylation by hydrogen borrowing.

The scope of this catalyst has also been extended to other substrates such as aliphatic alcohols, other primary amines and secondary alcohols. Although primary alcohols easily react to produce the corresponding amines, secondary alcohols proved to be less reactive. As a general rule, the efficiency and yields obtained depend on the facility of formation of the intermediate imine.

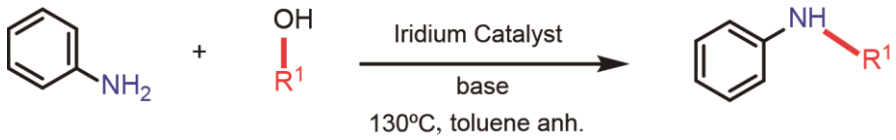

Scheme 32. Amine *N*-alkylation by hydrogen borrowing.

The reactions were carried out with 1 equivalent of the amine, 1.2 equivalents of the alcohol and the same equivalents of base as that of the catalyst in refluxing toluene for 17h. The results are summarized in Table 5. Our racemic hybrid catalyst **47** (1.25%) successfully carried out the alkylation of aniline with aliphatic alcohols such as cyclohexanol, 2-octanol and 3-hexanol, in the presence of $MgSO_4$ as dehydrating agent, with yields that depend on the

stability of the corresponding imines, 99%, 91% and 40%, respectively (entries 1, 2 and 3). Alkylation of *N*-methylaniline with *p*-methoxybenzyl alcohol catalyzed by $[Cp^*IrCl_2]_2$ complex (4%), afforded dialkylated aniline in 65% (entry 4) while iridium-fullerene hybrid displayed a better efficiency 86% (entry 5). A similar behaviour was observed in the *N*-alkylation of piperidine that occurs with only 6% yield when $[Cp^*IrCl_2]_2$ complex was used and in 32% yield with fullerene-iridium catalyst (entries 6, 7). Finally, benzylamine was alkylated by cyclohexanol with excellent yield 99% (entry 8). When Rh or Ru fullerene derivatives were used, the reactions occurred with a remarkably lower yield in comparison to the related iridium fullerene derivatives.

Table 5. Amine *N*-alkylation by hydrogen borrowing.

Entry	Catalyst (mol%)	Amine	Alcohol	Product	Yield (%)
1[a]	**47** (1.25)			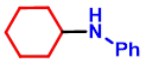	99
2[a]	**47** (1.25)		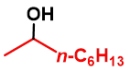	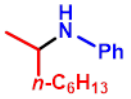	91
3[a]	**47** (1.25)		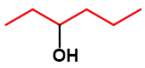	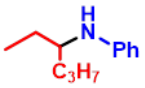	40
4[b]	$[Cp^*IrCl_2]_2$ (4.0)	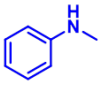	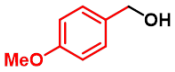	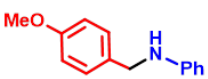	65
5	**47** (4.0)	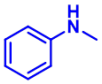	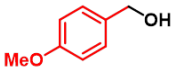	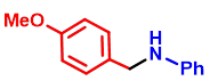	86
6[a]	$[Cp^*IrCl_2]_2$ (2.0)		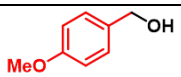	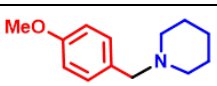	6
7[a]	**47** (2.0)		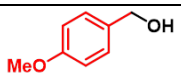	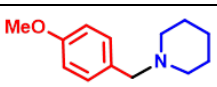	32
8	**47** (1.25)	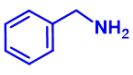		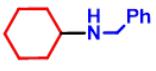	99

[a] $MgSO_4$ was used. [b] Data reported in the literature.

4.2.3. Hydrogen and Chirality Transfer in Ketones Reduction

Asymmetric transfer hydrogenation of ketones with chiral catalysts is one of the most powerful tools to obtain chiral alcohols. Thus, the metal-fullerene hybrids have been tested for hydrogen and chirality transfer in ketones reduction. As reaction model to study the ability of these new catalysts, we have chosen as ketones, 2-acetylnaphthalene and 2-bromoacetyl pyrene, due to the easy and fast monitoring of the reaction by HPLC.

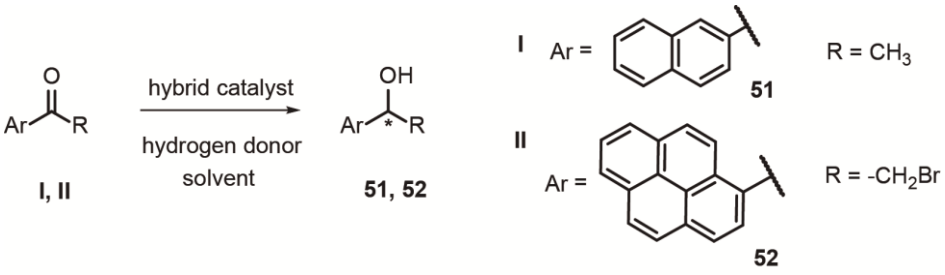

Scheme 33. Enantioselective hydrogen transfer reaction in ketones reduction.

In this regard, although isopropanol proved to be a good hydrogen donor, the high temperature required for the reaction was not suitable for obtaining high enantiomeric excesses. Therefore, we propose to use sodium formate as hydrogen donor for the reduction of 2-acetylnaphthalene and 2-bromoacetyl pyrene at room temperature, with the aim to ensure the catalytic action of the chiral metal center under milder experimental conditions.

On the optimization of the experimental conditions, a screening of solvents and reagents was carried out using the enantioenriched fullerene hybrids prepared by the aforementioned enantioselective methodology, without any further purification. A mixture of 2-acetylnaphthalene (7 mg, 0.06 mmol), HCOONa (20 mg, 0.3 mmol) and the catalyst (5%) was stirred at room temperature for 20h. The most relevant results are summarized in table 6.

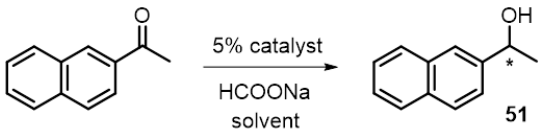

Table 6. Effect of the solvent in asymmetric transfer hydrogenation.

Entry	Catalyst (mol%; optical purity)	Additive	Solvent	Yield (%)	*ee*[a] (%)
1	**36** (5%; *ee* 92%)	-	THF	16	8
2	**36** (5%; *ee* 92%)	water	Toluene	2	-
3	**36** (5%; *ee* 92%)	water	DCM	35	22
4	**36** (5%; *ee* 92%)	water	ACN	40	14
5	**36** (5%; *ee* 92%)	water	DMF	45	6
6	**36** (5%; *ee* 92%)	water	THF	46	28

[a] *ee* values and yields were determined by HPLC.

The addition of water as an additive (three drops), significantly promotes the reaction (entry 1). In the literature was reported that the asymmetric transfer hydrogenation of aromatic ketones was significantly accelerated when the reaction was carried out in water with sodium formate as hydrogen donor.[188] However, the role of the water in these reactions has not been clearly defined. When the reaction was carried out using toluene as solvent, practically, no formation of the product was observed (entry 2). The use of polar solvents notably increases the yield of the reaction (entries 4, 5). The highest enantiomeric excess and yield was achieved by using THF as solvent (entry 6).

188. a) X. G. Li, X. F. Wu, W. P. Chen, F. Hancock, F. King, J. L. Xiao, *Org. Lett*., **2004**, *6*, 3321. b) X. F. Wu, X. G. Li, F. King, J. L. Xiao, *Angew. Chem*., **2005**, *117*, 3473, *Angew. Chem. Int. Ed*., **2005**, *44*, 3407. c) X. F. Wu, D. Vinci, T. Ikariya, J. L. Xiao, *Chem. Commun*., **2005**, 4447. d) X. H. Li, J. Blacker, I. Houson, X. F. Wu, J. L. Xiao, *Synlett*, **2006**, 1155. e) X. F. Wu, J. K. Liu, X. H. Li, A. ZanottiGerosa, F. Hancock, D. Vinci, J. W. Ruan, J. L. Xiao, *Angew. Chem. Int. Ed*., **2006**, *45*, 6718. f) X. F. Wu, J. K. Liu, D. D. Tommaso, J. A. Iggo, C. R. A. Catlow, J. Bacsa, J. L. Xiao, *Chem. Eur. J*., **2008**, *14*, 7699.

After these results, we studied the reaction in the presence of different silver salts. A mixture of 2-acetonaphthone (7 mg, 0.06 mmol), HCOONa (20 mg, 0.3 mmol) and the catalyst (5%) in 0.14 mL of THF, in the presence of three drops of water, was stirred at room temperature for 20h. In table 7, the most relevant results are summarized.

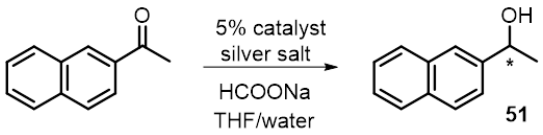

Table 7. Effect of the silver salts in asymmetric transfer hydrogenation.

Entry	Catalyst (mol%; optical purity)	Additive	Yield (%)	*ee*[a] (%)
1	**36** (5%; *ee* 92%)	CH_3COOAg	39	10
2	**36** (5%; *ee* 92%)	$AgNO_3$	23	6
3	**36** (5%; *ee* 92%)	Ag_2CO_3	10	2
4	**36** (5%; *ee* 92%)	$AgPF_6$	39	10
5	**36** (5%; *ee* 92%)	$AgSbF_6$	32	6
6	**36** (5%; *ee* 92%)	AgF	51	22
7	**40** (5%; *ee* 90%)	CH_3COOAg	46	40
8	**40** (5%; *ee* 90%)	$AgNO_3$	42	38
9	**40** (5%; *ee* 90%)	Ag_2CO_3	32	40
10	**40** (5%; *ee* 90%)	$AgPF_6$	42	40
11	**40** (5%; *ee* 90%)	$AgSbF_6$	41	40
12	**40** (5%; *ee* 90%)	AgF	84	41

[a] *ee* values and yields were determined by HPLC.

As we can see in the table, rhodium catalyst **40** proved to be more efficient in asymmetric transfer hydrogenation than iridium catalyst. The iridium catalyst **36** led to the alcohol with lower conversions and enantiomeric excesses (entries

1-5). The addition of a spatula tip of silver fluoride remarkably enhanced the yield and the enantiomeric excess (entry 6). When the reaction was carried out using rhodium catalyst **40**, in the presence of the different silver salts, the results obtained were very similar. After 20 hours, the final product was obtained with a moderate conversion and enantiomeric excess (entries 7-11). However, the addition of silver fluoride notably increases the yield to 84% (entry 12).

Finally, once the reaction conditions were optimized, a mixture of 2-acetylnaphthalene (7 mg, 0.06 mmol) or 2-bromoacetyl pyrene (3 mg, 0.009 mmol), HCOONa (20 mg, 0.3 mmol) and the catalyst (5% or 10%) in 0.14 mL of THF, in the presence of three drops of water and silver fluoride, was stirred at room temperature for 20h. Table 8 presents the most relevant results.

Table 8. Asymmetric transfer hydrogenation.

Entry	Ketone	Additive	Catalyst (mol%; optical purity)	Temp (ºC)	Yield (%)	*ee*[a] (product)
1	I	AgF	**36** (5%; *ee* 92%)	rt	51	22 (*S*)-**51**
2	I	AgF	**41** (5%; *ee* 90%)	rt	84	42 (*S*)-**51**
3	I	-	**41** (5%; *ee* 90%)	rt	53	42 (*S*)-**51**
4	I	-	**40** (5%; *ee* 90%)	rt	51	42 (*R*)-**51**
5	I	AgF	**42** (5%; *ee* 92%)	rt	-	-
6	II	AgF	**36** (10%; *ee* 92%)	rt	85	60 (**52**, 2nd)[b]
7	II	AgF	**40** (10%; *ee* 90%)	rt	100	70 (**52**, 1st)[b]
8	II	AgF	**42** (10%; *ee* 92%)	rt	-	-
9	II	AgF	**40** (10%; *ee* 90%)	0	53	76 (**52**, 1st)[b]
10	II	AgF	**40** (10%; *ee* 90%)	-15	39	84 (**52**, 1st)[b]
11	II	AgF	**41** (10%; *ee* 90%)	-15	40	90 (**52**, 2nd)[b]

[a] *ee* values and yields were determined by HPLC. [b] 1st or 2nd refers to the elution order of the products in the chiral column.

All the catalysts employed, but the ruthenium-based hybrids, were able to carry out the transfer of hydrogen from sodium formate with yields that depended on the amount of catalyst, on the temperature, and on the presence of an additive as silver fluoride. Thus, the use of 5% of **36** (S_{C2}, S_{C5}, S_N, S_{Ir}) in a 92% of *ee*, afforded (*S*)-α-methyl-2-naphthalenemethanol **51** in moderate yield and poor enantioselectivity (entry 1). Rhodium catalyst proved to be more efficient and enantioselective, obtaining the alcohol in 84% yield and with 42% *ee* (entry 2). We also examined the reaction in the absence of silver fluoride, obtaining worst yields. Similarly, the opposite enantiomer (*R*)-α-methyl-2-naphthalenemethanol **51** was obtained with 5% of **40** (R_{C2}, R_{C5}, R_N, R_{Rh}) (entry 4). The use of **40** (R_{C2}, R_{C5}, R_N, R_{Rh}) or **41** (S_{C2}, S_{C5}, S_N, S_{Rh}) led to the same values of enantioselectivity (entries 3, 4). Ruthenium hybrid **42** (S_{C2}, S_{C5}, S_N, S_{Ru}) was not able to carry out the reaction (entry 5).

Higher enantioselectivities were observed in the reduction of 2-bromoacetylpyrene with a higher steric demand where 10% of catalyst was employed to increase the yield of the corresponding alcohol **52** (entries 6-11). Thus, **36** (S_{C2}, S_{C5}, S_N, S_{Ir}) increased its enantioselectivity to 60% (entry 6). While ruthenium hybrid **42** (S_{C2}, S_{C5}, S_N, S_{Ru}) was again ineffective (entry 8), catalyst **40** (R_{C2}, R_{C5}, R_N, R_{Rh}) used in 90% of optical purity, gives rise to a quantitative reduction with 85/15 enantiomeric ratio (entry 7).

Higher enantiomeric excesses were obtained with the same catalyst at lower temperature but with lower yields (entry 9). Thus, by using **41** (S_{C2}, S_{C5}, S_N, S_{Rh}) at -15ºC, an almost complete enantioselectivity, 90% *ee* (considering that the catalyst was in 92% *ee*) was obtained (entry 11). The use of silver fluoride as an additive, afforded to higher yields and allowed to decrease the temperature to obtain slightly higher enantiomeric excess. Finally, we confirmed that both enantiomers could be obtained by changing chirality of the catalysts (entries 10, 11).

The optical purity of compounds **51** and **52** was analyzed by HPLC, using a chiral column *ChiralPack IA*.

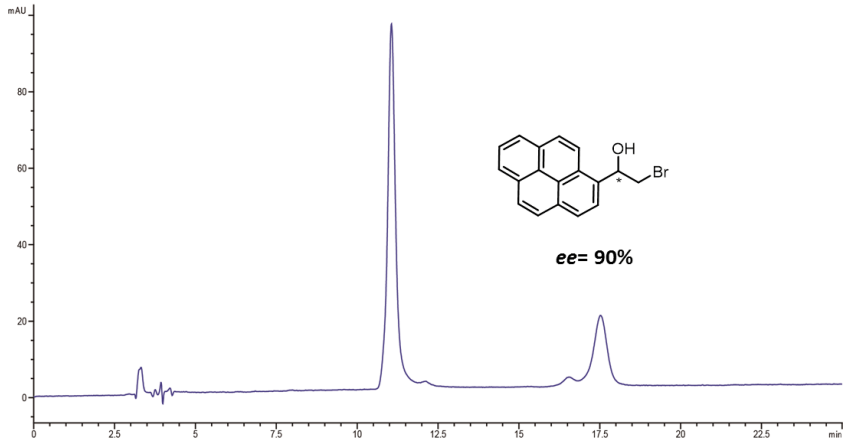

Figure 63. HPLC profile of the reaction crude catalyzed by rhodium catalyst **41**. HPLC column: *IA* (4.6 x 250mm; Hexane/isopropyl alcohol (95:5); 1 ml/min; 280 nm; 25ºC) (table 8, entry 11).

Despite there is much room for the catalyst improvement, these preliminary results demonstrate that these fullerene hybrids are able to efficiently transfer hydrogen with chirality induction.

4.3. Selectivity in Higher Fullerenes

In contrast to highly symmetric [60]fullerene, higher fullerenes present a lower symmetry which leads to a complex chemistry.[81] Reactions onto C_{70} lead to a mixture of different site- and regioisomers limiting the appropriate exploration of their properties as well as their potential applications in organic electronics and materials science. The availability of an efficient synthetic methodology to limit a broad distribution of products constitutes a chemical challenge and an essential issue for further applications.

Therefore, we decided to develop synthetic tools for a precise control in the molecular construction with the aim of directing the reactivity in these complex systems. In the case of the addition of diazocompounds to higher fullerenes, we have to face different levels of selectivity.

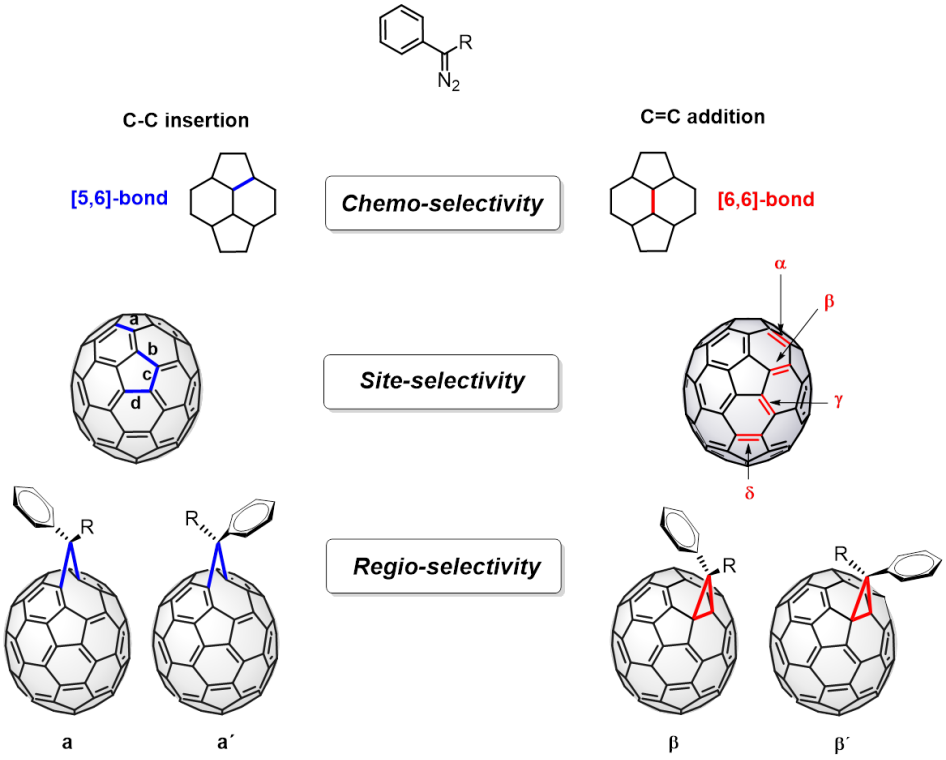

Figure 64. Different levels of selectivity in [70]fullerene.

Firstly, it can be differentiated two types of bonds, [5,6]-bond, at the junction of a hexagon and a pentagon and [6,6]-bond, at the junctions of two hexagons. We face with a problem of chemo-selectivity, which according to IUPAC is defined as the preferential reaction of a chemical reagent with one of two or more different functional groups. Unlike C_{60} in which all the single and double bonds are equivalent, the lower symmetry of C_{70} increases the number of possible isomeric monoadducts to eight, when a symmetrical addend is involved, namely a, b, c and d ([5,6]-bonds) and α, β, γ and δ ([6,6]-bonds).[189] Finally, considering that in the addition of unsymmetrically substituted diazocompounds, two stereoisomers can be obtained for each addition site, according to the orientation of the adduct, the number of non optical isomers increases to 12.

In the search for new methods to achieve selectivity on C_{70}, we describe an approach for selectively obtaining the [5,6]-derivative as the principal product of the reaction.

4.3.1. Chemoselectivity [5,6] *vs* [6,6]

In contrast to methanofullerenes ([6,6] derivatives), fulleroids ([5,6] derivatives) are usually unstable and difficult to isolate. Although the most common method to synthesize fulleroids is the addition of diazocompounds to fullerenes, they are usually formed in low yield together with the [6,6]-methanofullerene derivative as the main product.[190] The mechanism of cycloaddition of diazocompounds to fullerenes has been described by two routes: i) thermolysis of diazocompounds to form carbenes that cycloadd on the [5,6] bonds[65e] and ii) 1,3-dipolar cycloaddition of the diazocompound to give rise to a fulleropyrazoline, followed by extrusion of N_2 to achieve [5,6]-open fulleroids.[191] Thermal treatment or light irradiation transform the

189. a) A. B. III Smith, R. M. Strongin, L. Brard, G. T. Furst, W. J. Romanow, K. G. Owens, R. J. Goldschmidt, *J. Chem. Soc., Chem. Comm.*, **1994**, 2187. b) A. F. Kiely, R. C. Haddon, M. S. Meier, J. P. Selegue, C. Pratt Brock, B. O. Patrick, G. W. Wang, Y. Chen, *J. Am. Chem. Soc.*, **1999**, *121*, 7971. c) T. Sternfeld, C. Thilgen, R. E. Hoffman, M. R. Colorado Heras, F. Diederich, F. Wudl, L. T. Scott, J. Mack, M. Rabinovitz, *J. Am. Chem. Soc.*, **2002**, *124*, 5734.
190. C. Hadad, Z. Syrgiannis, A. Bonasera, M. Prato, *Eur. J. Org. Chem.*, **2015**, *7*, 1423.
191. H. Kitamura, K. Kokubo, T. Oshima, *Org. Lett.*, **2007**, *9*, 4045.

kinetically favorable product [5,6]-open fulleroid, to the thermodynamically favored product [6,6]-closed methanofullerene.[62c]

The lack of an efficient methodology to obtain [5,6]-derivatives is responsible for the scarce studies carried out on these compounds whose properties remain almost unexplored.

4.3.1.1. Chemoselective Synthesis of [5,6]fulleroids on [70]PCBM

Diazocompound **56** was prepared from commercially available 4-benzoylbutyric acid **53**, by a well stablished procedure shown in Scheme 34.[157] Precursor **54** was synthesized by reacting **53** with oxalyl chloride in refluxing methanol for 24 hours. Further treatment with *p*-toluenesulfonylhydrazine leads to hydrazine **55**. Decomposition of tosylhydrazone **55** allows the *in situ* generation of the diazocompound **56** without the requirement of its purification prior to the addition to C_{70}.

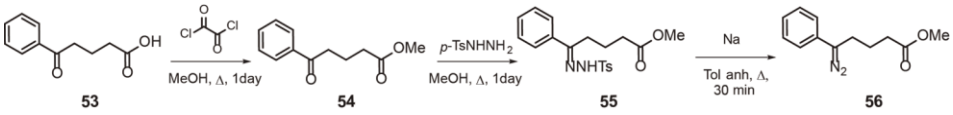

Scheme 34. Synthesis of diazocompound **56**.

A solution of **56** and C_{70} in toluene was stirred at room temperature for 2 minutes in the dark, leading to the corresponding [5,6]fulleroids in 86% yield (based on recovered C_{70}) in a ratio fulleroid/methanofullerene 99:1 (Scheme 35). The control of light is a critical factor, since the [5,6] isomer gives rise to the formation of the [6,6] isomer by the action of light.[71] Therefore, the almost exclusive formation of [5,6] isomers (99%) is a great success, given the difficulty of working under conditions of complete absence of light.

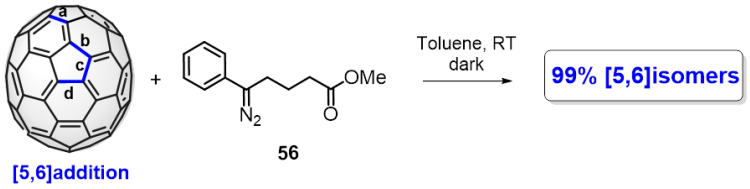

Scheme 35. Chemoselective synthesis of [70]PCBM fulleroids.

Analysis of the reaction crude by HPLC revealed that the addition was almost completely [5,6] chemoselective and was crucial to determine the number of different [5,6] fulleroids obtained in the reaction. The HPLC chromatogram showed three different peaks with analogous UV-vis absorption and identical to that of pristine C_{70}, thus confirming their fulleroid nature.

In this regard, it is important to note that fulleroids and their respective pristine fullerenes share the same π-homo-conjugation since any of the double bonds of the fullerene sphere has been saturated.

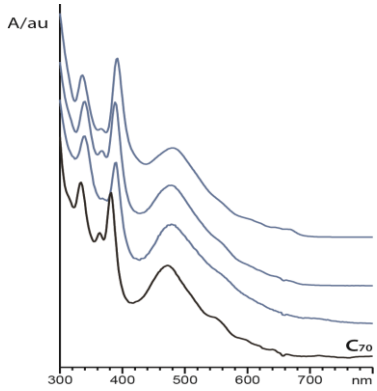

Figure 65. UV-vis spectra of fulleroids fraction and C_{70} in toluene at room temperature.

Considering that the addition of alkyl-aryl-diazocompounds to C_{70} preferentially forms the fulleroid in which the aryl group is over the pentagon ring,[67,157] the three peaks observed in the HPLC profile, should correspond to three isomers attached to three different [5,6] bonds.

The assignment of each isomer to their corresponding peak was based on the relative yield (area) showed in the HPLC chromatogram. We considered that the main product of the reaction corresponds to fulleroid-a, followed by fulleroid-b and fulleroid-c as the minor product. It was also observed one small peak (1%) corresponding to a [6,6]-methanofullerene, in accordance with the ratio fulleroid/methanofullerene 99:1.

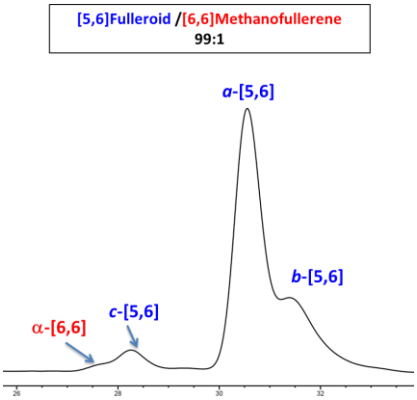

Figure 66. HPLC profile of reaction crude that reveals the formation of [5,6] fulleroids in 99%. HPLC column: 5PYE (4.6 x 250mm; toluene/hexane/acetonitrile (60:36:4); 0.5 ml/min; 320 nm; 25ºC).

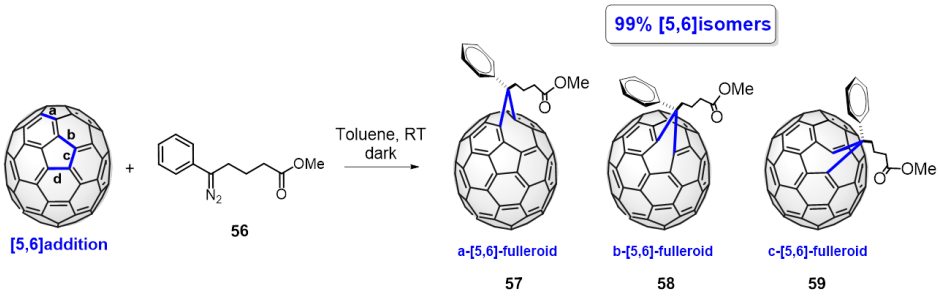

Scheme 36. Chemoselective synthesis of [70]PCBM fulleroids.

In the ^{1}H-NMR spectrum of the fulleroids fraction are mainly observed the signals of fulleroid-a **57**, which is the one that is in greater proportion. The presence of three different -OCH_3 resonances indicated that three isomers were present. The protons corresponding to the methyl ester group of the three fulleroids appeared well differentiated as singlets at 3.80, 3.70 and 3.64 ppm for fulleroid-c, fulleroid-b and fulleroid-a, respectively. This assignment was

done in accordance with the intensity of the signals and by analogy with other related systems.[192]

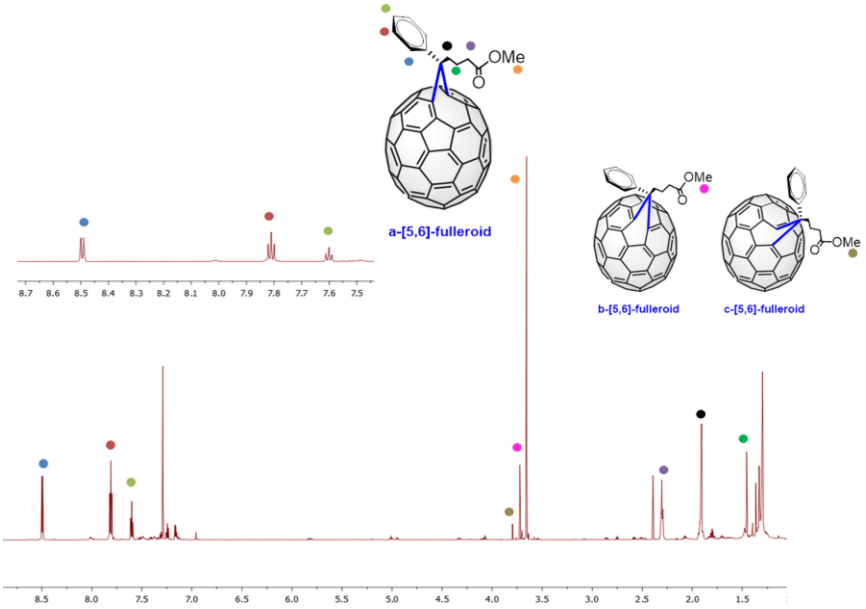

Figure 67. ^{1}H NMR (700 MHz, 298 K, $CDCl_3$) of fulleroids fraction containing compounds **57**-**59**.

The site-selectivity for the addition of diazocompound **56** to a [5,6]-bond of C_{70} (a > b > c > d), revealed a similar trend as for the addition to a [6,6] double bond (α > β > γ > δ), being the addition driven by the release of strain. The assignment of the peaks has been confirmed with the isomerization process from the [5,6]-open isomers to the respective [6,6]-closed methanofullerenes (see below).

It is well-known that fulleroids isomerize to methanofullerenes through a di-π-methane rearrangement by the action of light or heat.[71] Thus, three different [6,6]-closed siteisomers should be formed after the isomerization process. When the fulleroids fraction was irradiated at 360nm in a photoreactor for 4

192. M. S. Meier, M. Poplawska, A. L. Compton, J. P. Shaw, J. P. Selegue, T. F. Guarr, *J. Am. Chem. Soc.*, **1994**, *116*, 7044.

hours at room temperature, the isomerization from fulleroids **57-59** to the corresponding methanofullerenes was quantitative.

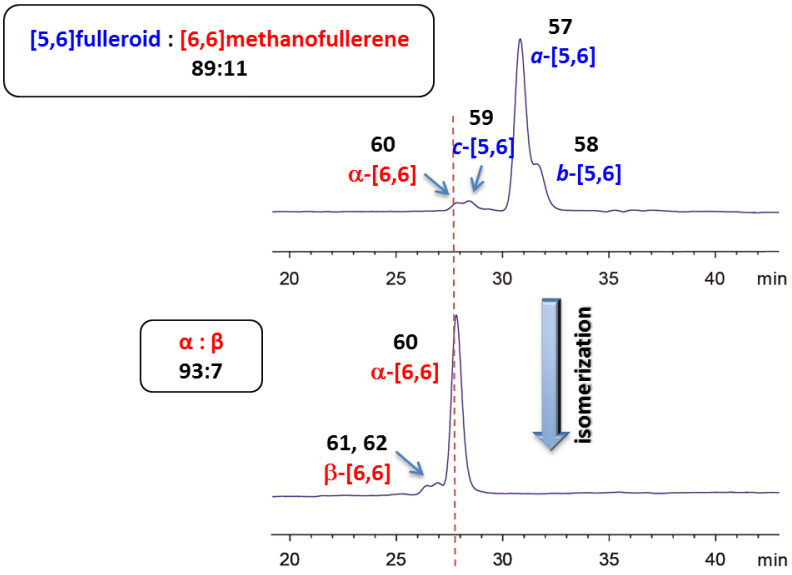

Figure 68. HPLC profiles of fulleroids fraction (**57-59**) after the reaction of diazocompound and C_{70} in the dark (top) and after irradiation at 360nm (bottom). HPLC column: 5PYE (4.6 x 250mm; toluene/hexane/acetonitrile (60:36:4); 0.5 ml/min; 320 nm; 25ºC).

Despite three different [5,6]-open isomers (a, b and c) were obtained in the reaction, after irradiation only two [6,6]-methanofullerenes were observed in a ratio 93:7 (α:β). The UV-vis confirmed that compound **60** corresponds to α-siteisomer while **61** and **62** are β-siteisomers composed by two stereoisomers depending on the orientation of the adduct.

An explanation that justify why three [5,6] bonds are isomerized to only two [6,6] bonds can be found in the regioespecific di-π-methane isomerization tendency of each fulleroid. Fulleroid-a **57** can only be transformed into α-siteisomer, however fulleroid-b **58** can be isomerized both to α-siteisomer and β-siteisomer, although probably most of the isomerization will progress toward the α-siteisomer **60** since is the most reactive. Finally, fulleroid-c **59** is the only one able to isomerize to the γ-bond. However, γ-bonds are poorly reactive.

Therefore, the isomerization should occur only towards the β-siteisomer (Scheme 37).

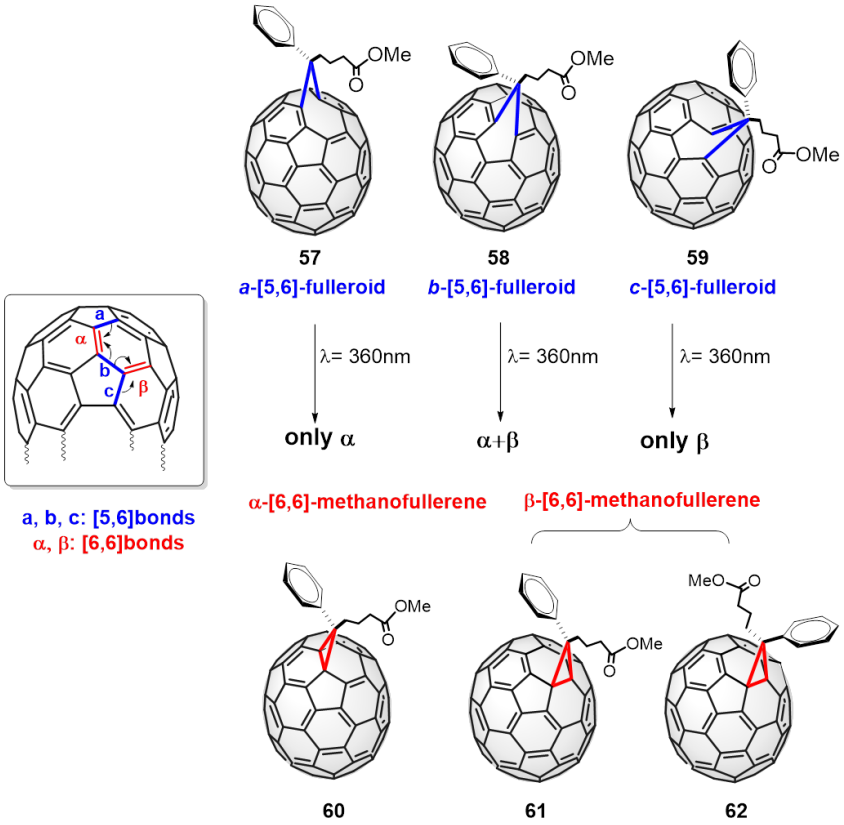

Scheme 37. Isomerization routes from [5,6]-bonds to [6,6]-bonds, α and β-methanofullerenes.

To corroborate these assumptions, the fulleroid regioisomer separation (**57-59**) was performed by HPLC using a semipreparative column, 5PYE (10 x 250mm; toluene/hexane/acetonitrile (60:36:4); 1 ml/min; 320 nm; 25ºC). Each fraction corresponding to an individual isomer was irradiated at λ = 360nm for 4 hours at room temperature. Fulleroid-a was exclusively isomerized to α-siteisomer **60**. Fulleroid-b was isomerized to methanofullerene **60** in 85% and to β-siteisomers **61**, **62** in 15%. Finally fulleroid-c was only isomerized to β-siteisomers. Any attemps to separate β-siteisomers **61** and **62** were failed. Thus, we were not able to shed light in the stereochemical outcome.

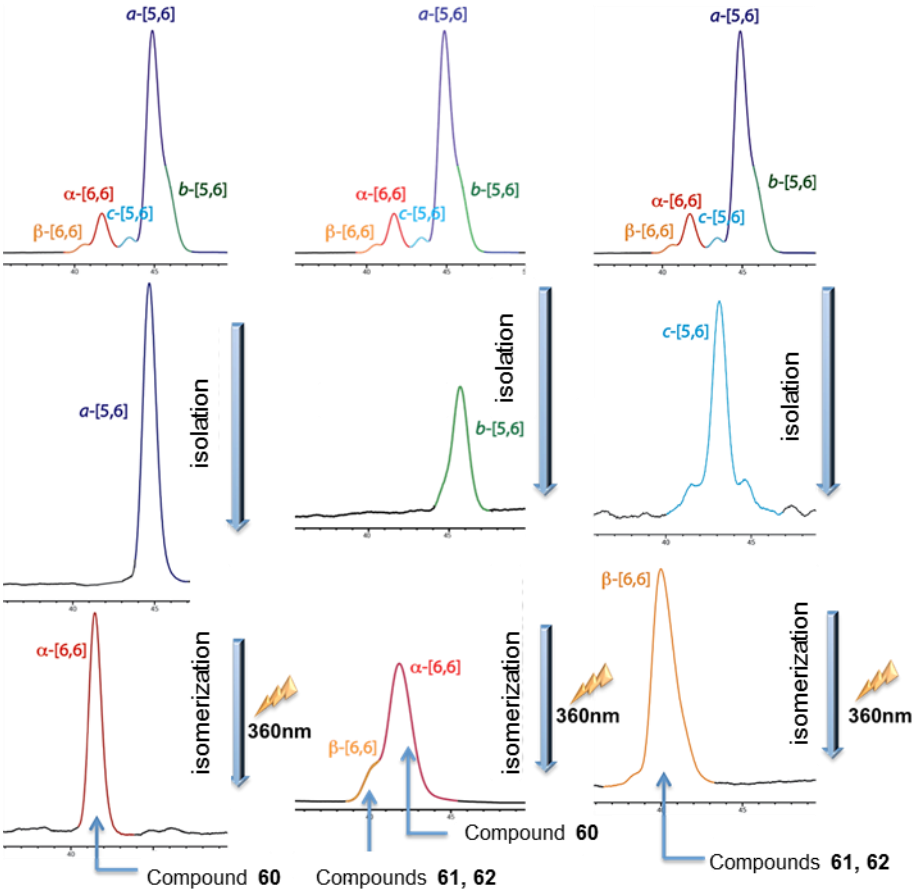

Figure 69. HPLC profiles of the products before and after the isomerization. HPLC column 5PYE semipreparative (10 x 250mm; toluene/hexane/acetonitrile (60:36:4); 1 ml/min; 320nm; 25ºC).

Therefore, we can confirm the siteselectivity of the aforementioned C-C single bond insertion. Thus, among the eight possible isomers (a, b, c, d), the site-isomer fulleroid-a **57**, is formed predominantly. To extend the scope of the reaction and explore the tendency of diaryl-diazocompounds towards the formation of fulleroids on C_{70}, we have synthesized a diaryl-methano bridged fulleroid, namely [5,6]-[70]DPM with an electron-donating substituent in the *para* position of the phenyl group.

4.3.1.2. Chemoselective Synthesis of [5,6]fulleroids on [70]DPM

Diaryldiazocompound **66** was prepared in three synthetic steps from *p*-substituted benzophenone **63**. Alkylation with the corresponding halogenated derivative, reaction with hydrazine and subsequent oxidation with manganese dioxide, led to the final diazocompound **66**.

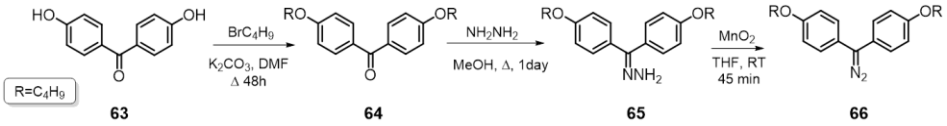

Scheme 38. Synthesis of diazocompound **66**.

A solution of 1 equivalent of **66** and C_{70} in toluene was stirred at room temperature for 2 min in the dark (Scheme 39). The reaction crude was purified by silica-gel column chromatography using CS_2/hexane as eluent to recover the unreacted C_{70}, and CS_2 to collect the fraction of monoadducts, (fulleroids/methanofullerenes) in a ratio 89:11, in 72% yield (based on recovered C_{70}).

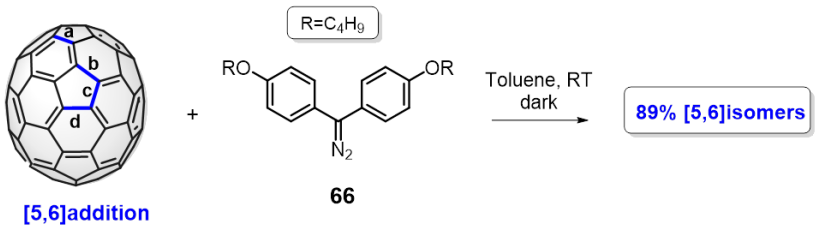

Scheme 39. Synthesis of [70]DPM fulleroids.

The HPLC analysis of the fraction of monoadducts revealed three different peaks corresponding to [5,6]-fulleroids with analogous UV-vis absorption and identical to that of pristine C_{70}, and two small peaks corresponding to [6,6]-methanofullerenes, in accordance with their respective UV-vis spectra.

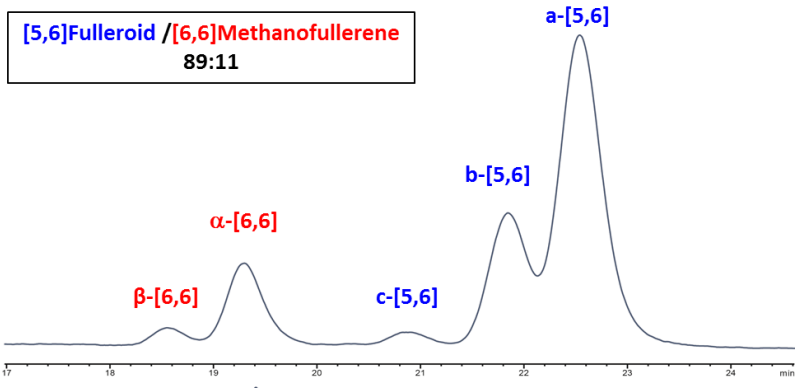

Figure 70. HPLC profile of [70]DPM-fulleroids (89%) together with [6,6]-methanofullerenes. HPLC column: Buckyprep waters (4.6 x 250mm; toluene/hexane/acetonitrile (60:36:4); 0.5 ml/min; 320 nm; 25ºC).

The chemoselectivity, as resulted from the experimental ratio fulleroid/methanofullerene was 89:11, that is lower than in the case of $PC_{71}BM$, since the tendency towards the formation of fulleroids is higher for diazoalkanes than for alkyl-aryl-diazocompounds, being diaryl-diazocompounds those with lower tendency of all of them.[193] However, this ratio is higher when compared with other examples using diaryl-diazocompounds. The reason is probably due to the presence of an electron-donating group in the *para* position of the phenyl group, which favors the formation of [5,6]-open-derivatives.[194]

By analogy with the $PC_{71}BM$ case, we assigned the principal peak to fulleroid-a **67**, followed by fulleroid-b **68** and fulleroid-c **69**.

193. T. Oshima, H. Kitamura, T. Higashi, K. Kokubo, N. J. Seike, *J. Org. Chem*., **2006**, *71*, 2995.
194. M. Izquierdo, M. R. Cerón, M. M. Olmstead, A. L. Balch, L. Echegoyen, *Angew. Chem. Int. Ed*., **2013**, *52*, 11826.

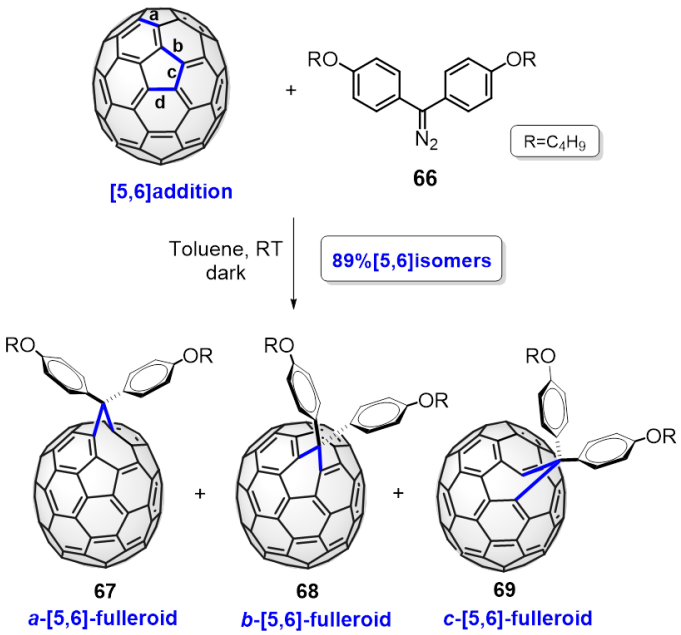

Scheme 40. Synthesis of [70]DPM fulleroids.

The fraction containing fulleroids (**67**-**69**) and methanofullerenes (**70**, **71)** was also analyzed by spectroscopic techniques. In the ^{1}H-NMR spectrum, the major signals correspond to fulleroid-a **67** the principal product of the reaction, followed by fulleroid-b **68** and methanofullerenes. Unfortunately, the yield of compound **69** was too low to assign the signals with accuracy (Figure 71).

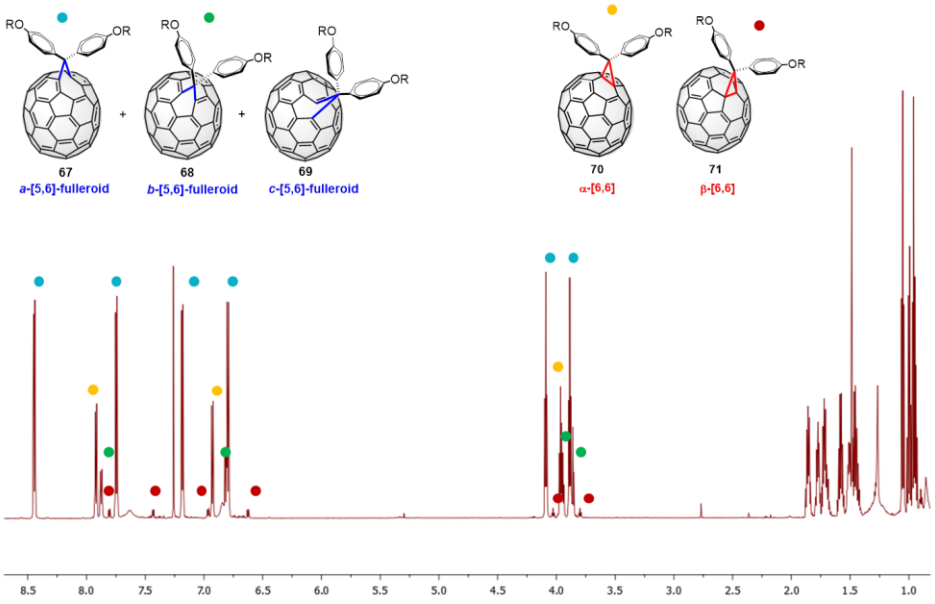

Figure 71. ^{1}H NMR (700MHz, 298K, $CDCl_3$) of the fraction of monoadducts containing fulleroids (**67**-**69**) and methanofullerenes (**70**, **71**).

The siteselectivity of the reaction was confirmed with the isomerization process from the [5,6]-open isomers (**67**-**69**) to the corresponding [6,6]-closed derivatives (**70**, **71**). The irradiation at λ = 360nm at room temperature led to the isomers in a quantitative manner. The [6,6]-methanofullerenes were formed by a mixture of two siteisomers in a ratio 88:12 (α:β), observing only one β-siteisomer since the addend is symmetrical (Figure 71).

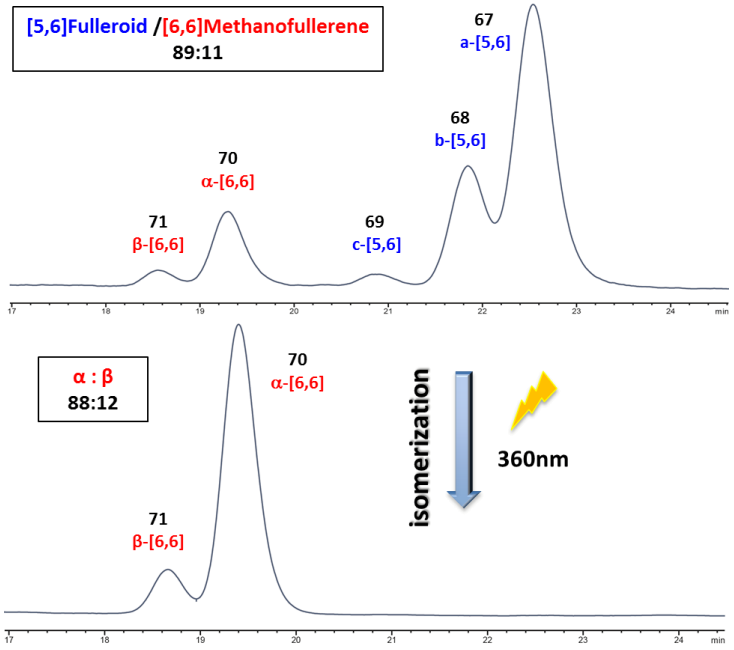

Figure 72. HPLC profile of [70]DPM-fulleroids (**67**-**69**) after the reaction of **66** and C_{70} in the dark (top), and after the irradiation at 360nm (bottom). HPLC column: Buckyprep waters (4.6 x 250mm; toluene/hexane/acetonitrile (60:36:4); 0.5 ml/min; 320 nm; 25ºC).

4.3.2. Siteselective Synthesis of [6,6] [70]Methanofullerenes

Once determined the conditions for the selective synthesis of [5,6]-open isomers, we dedicated our efforts to switch the chemo-selectivity toward the formation of the [6,6]-closed isomers in [70]fullerene.

The synthetic pathway for obtaining [6,6]-methanofullerenes, such as the well-known [70]PCBM, consists on the Bamford-Stevens reaction, previously reported by Hummelen *et al.*[157] This reaction involves the *in situ* generation of a diazocompound by thermolysis of tosylhydrazone with metal alkali salts, which, in the presence of C_{70}, leads to a mixture of two site-isomers in a 75:25 (α:β) ratio.[79] Moreover, since very often fulleroids are present along with α and β site-isomers, a further boiling in *o*-DCB is necessary.

Since this procedure is carried out under drastic conditions, strong bases and high temperatures (refluxing *o*-DCB), is not considered a suitable method to reach isomeric purity. The purification of the siteisomers from the reaction crude is not possible by silica-gel column chromatography, and only by using time and solvent-consuming HPLC separation, it is possible to isolate the α-siteisomer from the β-siteisomers.

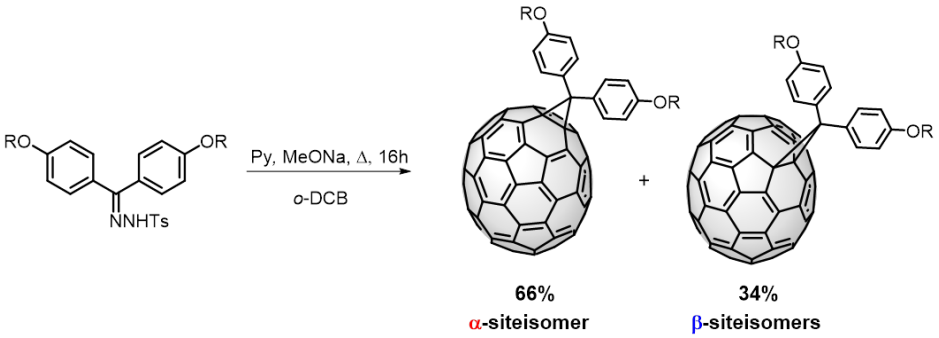

Scheme 41. Unselective thermal reaction of [70]DPM which leads to a mixture of two major isomers in a ratio 66:34 (α: β).

Controlling the siteselectivity on C_{70} is a challenge. The lack of a synthetic method able to discriminate between siteisomers, encouraged us to develop a new and unprecedented methodology based on light irradiation under mild conditions.

4.3.2.1. Siteselective Synthesis of α-[70]PCBM

As a first approach, we carried out the synthesis of pure α-[70]PCBM, the most used fullerene derivative as electron acceptor component in OPV, using soft conditions such as low temperature and light irradiation. The tosylhydrazone PCBM precursor **55** was transformed into the corresponding diazocompound **56**, following the same procedure previously described in the chemoselective synthesis of [5,6]-fulleroids (Scheme 34).

A solution of C_{70} and diazocompound **56** in dry toluene was irradiated at λ = 360nm at -78°C for 4 hours, affording compound **60** (α-siteisomer) as the main product of the reaction together with a small amount of compounds **61** and **62** (β-siteisomers) with high siteselectivity (96%).

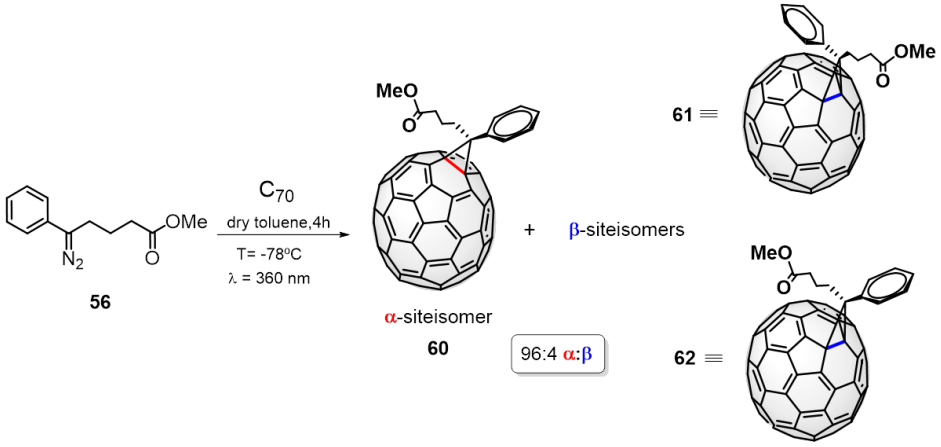

Scheme 42. Siteselective synthesis of α-[70]PCBM by photochemical irradiation under mild conditions.

As expected, β-siteisomer consists of two different diastereoisomers, depending on the orientation of the ester group on an equatorial **61** or polar **62** position in the fullerene cage.[78]

The siteselectivity of the reaction was determined by HPLC, 5PYE BuckyPrep column, resulting in a ratio 96:4 (α:β). t_R(β-siteisomer) = 31.5 min, t_R(α-siteisomer) = 33 min.

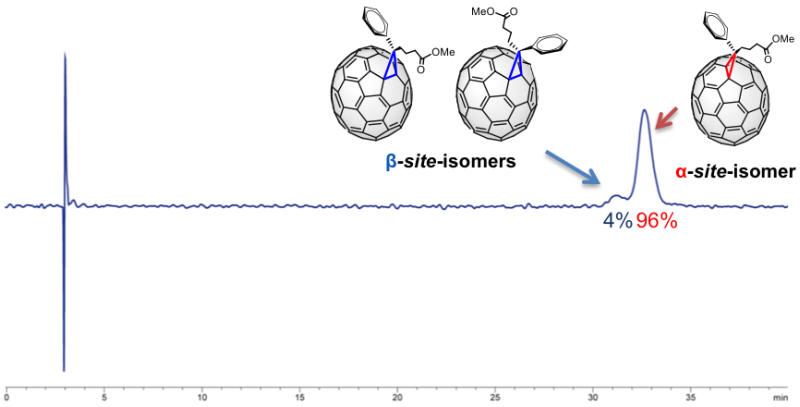

Figure 73. HPLC profile that reveals the formation of α-siteisomer in a ratio (96:4 α:β). HPLC column: 5PYE (4.6 x 250mm; toluene/acetonitrile (1:1); 1 ml/min; 320 nm; 25ºC).

The reaction mixture was characterized by standard spectroscopic techniques, NMR and UV-vis spectroscopy, revealing that the addition is almost completely [6,6] site-selective and confirming that the principal product of the reaction corresponds to α-siteisomer.

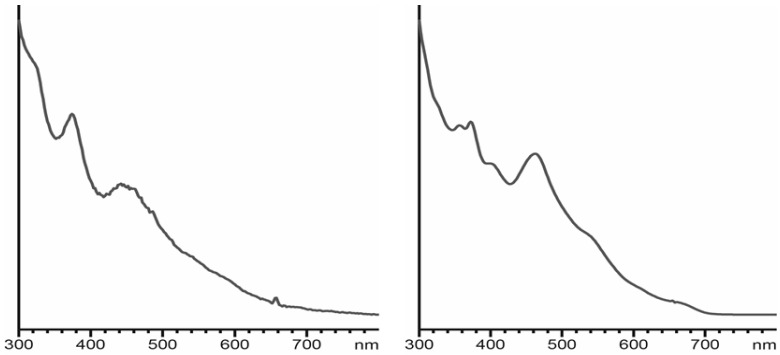

Figure 74. UV-vis spectra of α-siteisomer (right) (**60**) and β-siteisomers (left) (**61**, **62**) in toluene at room temperature.

4.3.2.2. Siteselective Synthesis of α-[70]DPM

To analyze the scope of this new methodology, the reaction was also carried out with diaryldiazocompounds. These compounds are highly reactive and have been shown to behave different to the alkylaryl-diazocompounds. From the 4,4'-dihydroxybenzophenones **63a,b** and the corresponding halogenated derivative, the 4,4'-alkyloxybenzophenones **64a,b** were synthesized. Reaction with hydrazine and subsequent oxidation with manganese dioxide, led to the diazocompounds **66a,b**. When diazocompound **66a,b** was irradiated at λ = 360nm at -20°C for 4 hours in the presence of C_{70} in dry toluene, the α-siteisomer **70** was exclusively formed (> 99%).

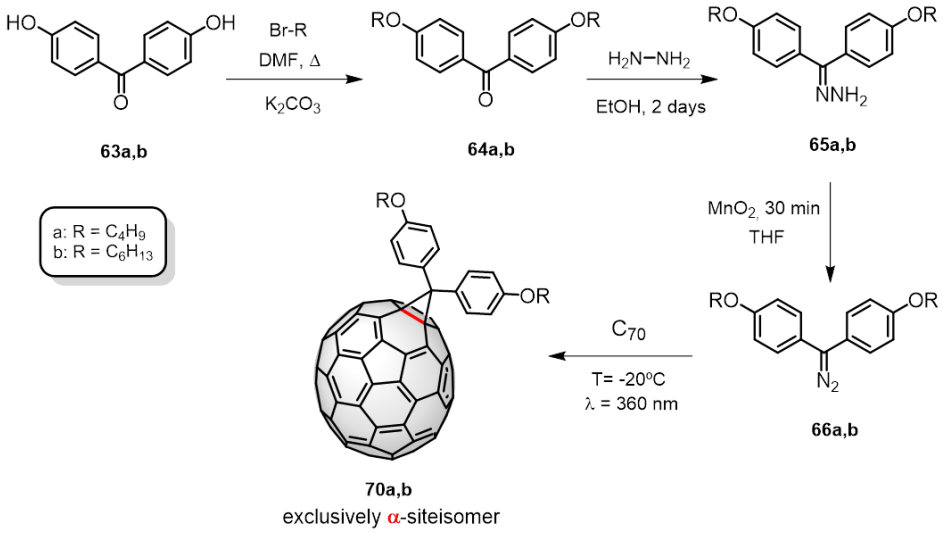

Scheme 43. Siteselective synthesis of α-[70]DPM by photochemical irradiation under mild conditions.

The corresponding β-siteisomers were not observed. These soft conditions were enough to reach an excellent siteselectivity, quantitative α-siteisomer. Diarylmethano[70]fullerenes ([70]DPMs) **70a,b** were also characterized by standard spectroscopic techniques.

The siteselectivity was determined by HPLC with a BuckyPrep column, showing the exclusive formation of α-siteisomer. t_R(α-[70]DPM4*)* = 5.75 min, t_R(α-[70]DPM6*)* = 5.35 min.

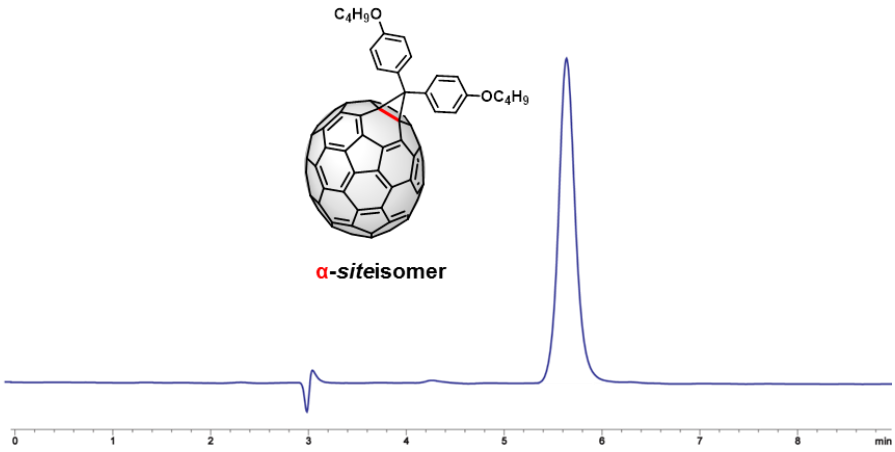

Figure 75. HPLC profile of α-[70]DPM-4. HPLC column: Buckyprep Waters (4.6 x 250mm; toluene/acetonitrile (90:10); 1 ml/min; 320 nm; 25ºC).

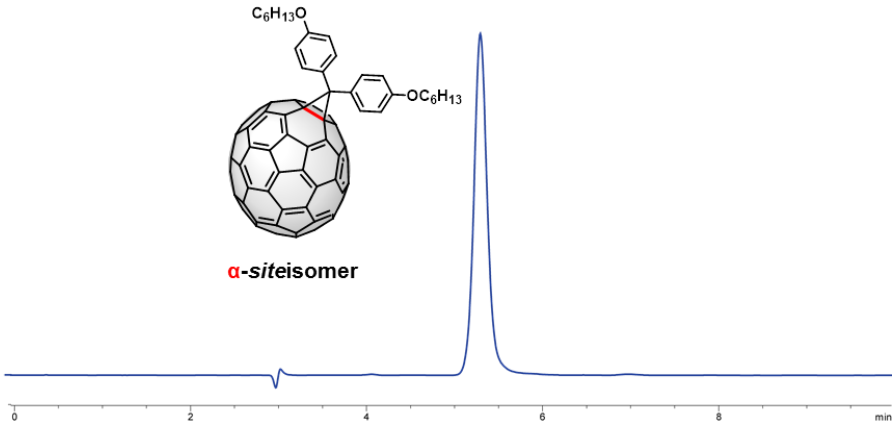

Figure 76. HPLC profile of α-[70]DPM-6. HPLC column: Buckyprep Waters (4.6 x 250mm; toluene/acetonitrile (90:10); 1 ml/min; 320 nm; 25ºC).

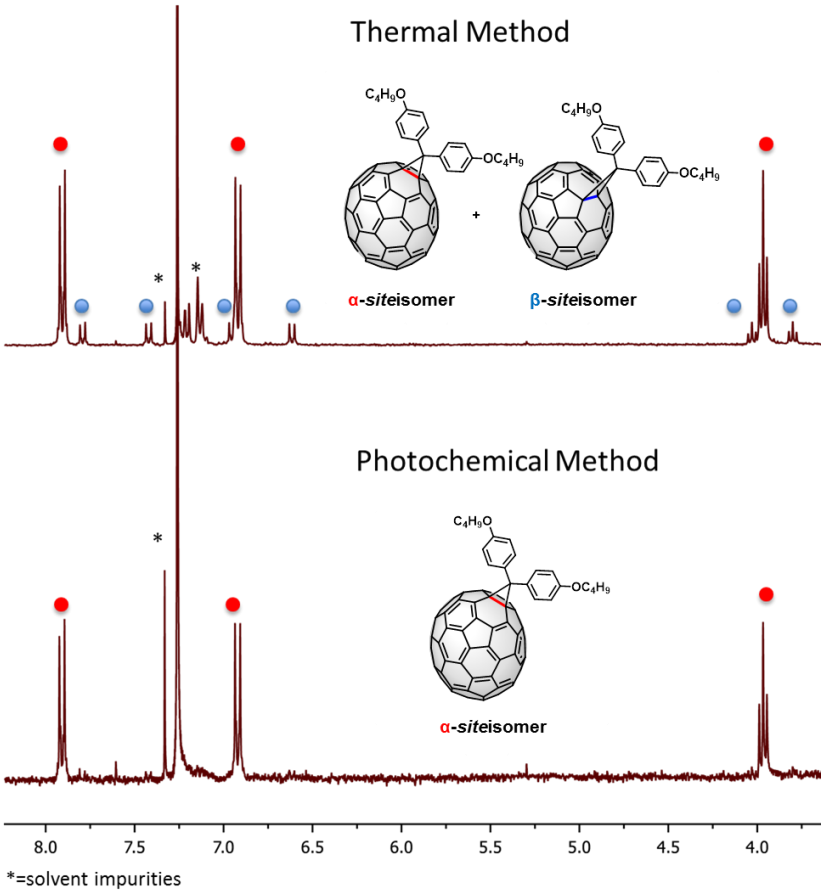

Figure 77. ^{1}H NMR (300MHz, 298K, $CDCl_3$) spectra of compounds α-siteisomer (red) and β-siteisomer (blue) obtained by the classic thermal treatment (top, ratio α:β, 75:25) and by the new photochemical method (bottom, quantitative α-siteisomer).

In figure 77 the ^{1}H NMR spectra of the compounds obtained by the classic thermal method and the new photochemical method are compared. As checked by HPLC, with this new synthetic methodology, α-siteisomer was exclusively formed. It should be noted that four aromatic signals corresponding to the phenyl group of β-siteisomer are observed since it is not a symmetric compound. In contrast, the α-siteisomer exhibits only one set of signals evidencing the plane of symmetry across the α-bond. The protons

corresponding to the methylene group directly attached to the oxygen of the aliphatic chain are observed like two triplets for β-siteisomer while α-siteisomer exhibits only one due to the different symmetry of both compounds.

The structure of pure α-[70]DPM-6 **70b**, was confirmed by single-crystal X-ray analysis. A suitable dark purple crystal of α-70DPM6 of approximate dimensions 0.040 mm x 0.200 mm x 0.220 mm was obtained by vapor diffusion from a solution of carbon disulfide placed in a large vial containing hexane. The structure was solved in the monoclinic $P2_1/c$ and the asymmetric unit contains a formula unit ($C_{95}H_{34}O_2$) as depicted in Figure 78a. There is a supramolecular C-H•••O interaction between neighbour molecules in the [001] direction that yields 1D chains (Figure 78b). On the other hand, a π-π interaction is also present between the bottom C6 rings in the C_{70} fullerene. These rings are completely parallel and located at a distance of 3.199 Å, with their centroids displaced from each other and separated 3.807 Å. Each pair of molecules displaying this interaction are related by an inversion center from the ones located in the middle of the b and c cell vectors (Figure 81). The crystal structure of compound **70b** has been deposited at the Cambridge Crystallographic Data Centre with code CCDC 1493981.

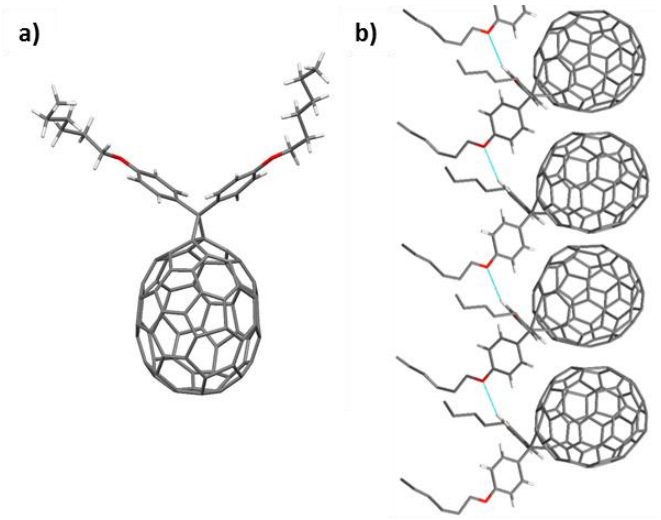

Figure 78. a) Molecular plot of compound **70b**. b) Detail of the supramolecular C-H•••O interaction between molecules in the [001] direction.

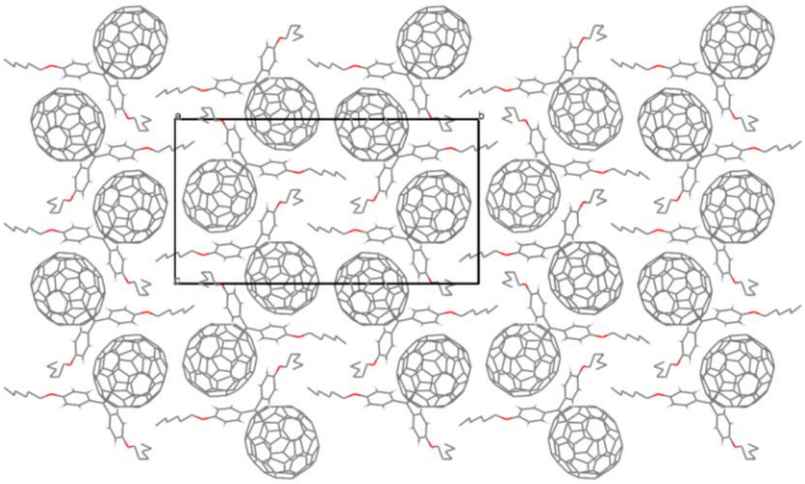

Figure 79. View of the packing of the molecules along the [100] direction.

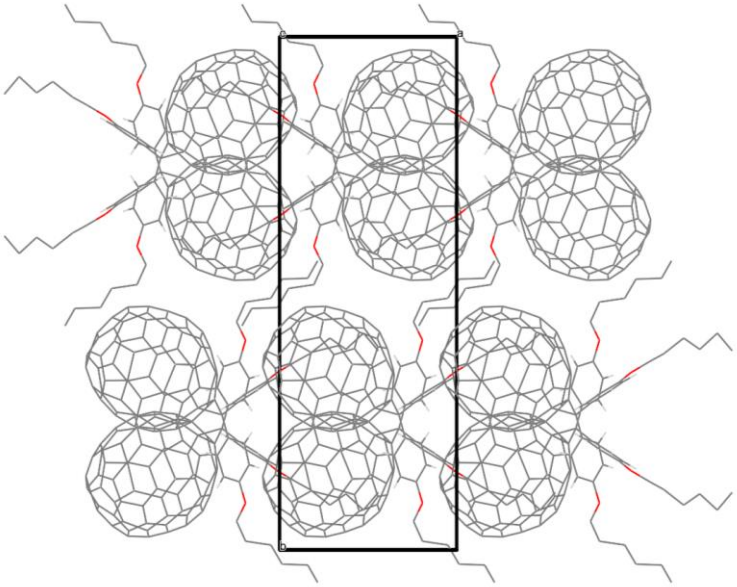

Figure 80. Representation of the crystal packing in the unit cell along the [001] direction.

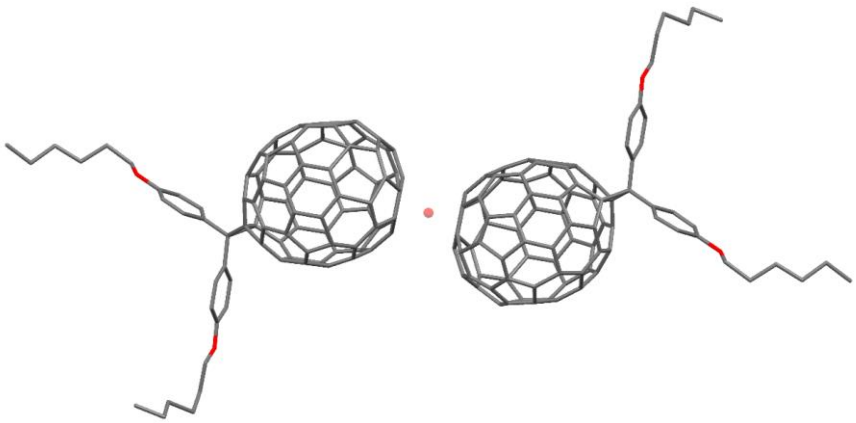

Figure 81. View of one of the pairs of molecules that display a π-π interaction between C6 rings with the inversion center depicted in translucent red. These inversion centers are the ones with coordinates 0, ½, 0 and 0, 0, ½; and their equivalents by translation.

4.3.2.3. Siteselective Synthesis of α-[70]Methanofullerene from Sulfonium Salts

In an effort to extend this selective addition to other addends, we selected another kind of precursors that also led to methanofullerenes, the α-bromo-derivative **72**, which has an analog structure to PCBM. Among the different synthetic approaches to get methanofullerenes, the reactions of stabilized sulfur ylides, efficiently afford only [6,6]-methanofullerenes.[195,196] Methyl α-Br-phenylacetate **72** reacted with dimethylsulfide and silver tetrafluoroborate to afford the sulfonium salt **73**. To a solution of C_{70} and **73** in *o*-DCB was added triethylamine and was stirred at room temperature for 2 hours, affording exclusively the α-siteisomer **74** in 70% yield.

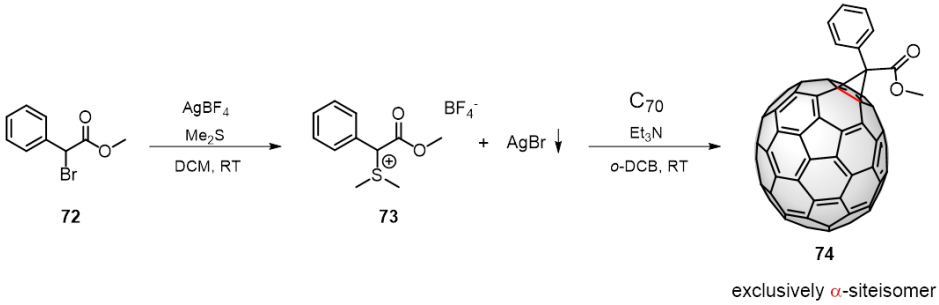

Scheme 44. Siteselective synthesis of α-[70]methanofullerene from sulfonium salt.

Compound **74** was isolated and characterized by standard spectroscopic techniques. The siteselectivity of the reaction was determined by HPLC. In figure 82 it is shown the HPLC profile where a unique peak is observed, that demonstrates the exclusive formation of the α-siteisomer. t_R(α-[70]methanofullerene) = 33.5 min.

195. T. Tada, Y. Ishida, K. Saigo, *J. Org. Chem*., **2006**, *71*, 1633.
196. T. Ito, T. Iwai, F. Matsumoto, K. Hida, K. Moriwaki, Y. Takao, T. Mizuno, T. Ohno, *Synlett*., **2013**, *24*, 1988.

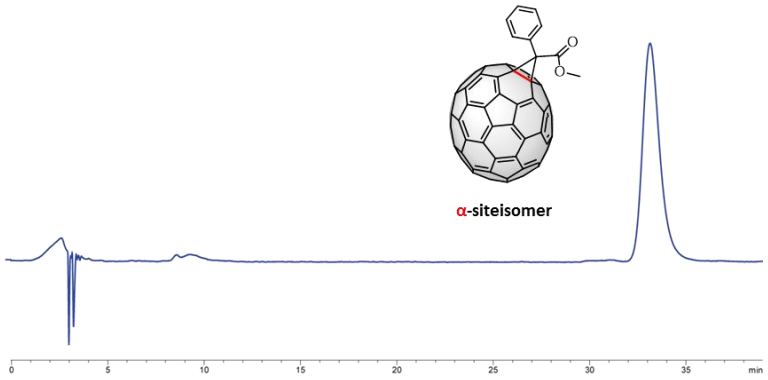

Figure 82. HPLC profile of α-[70]methanofullerene that reveals the exclusive formation of α-siteisomer. HPLC column: 5PYE (4.6 x 250mm; toluene/acetonitrile (1:1); 1 ml/min; 320 nm; 25ºC).

The ^{1}H-NMR spectrum showed the signals of the aromatic protons at 8.09 - 7.49 ppm and the signal of the methyl ester group as a singlet at 3.93 ppm (Figure 83).

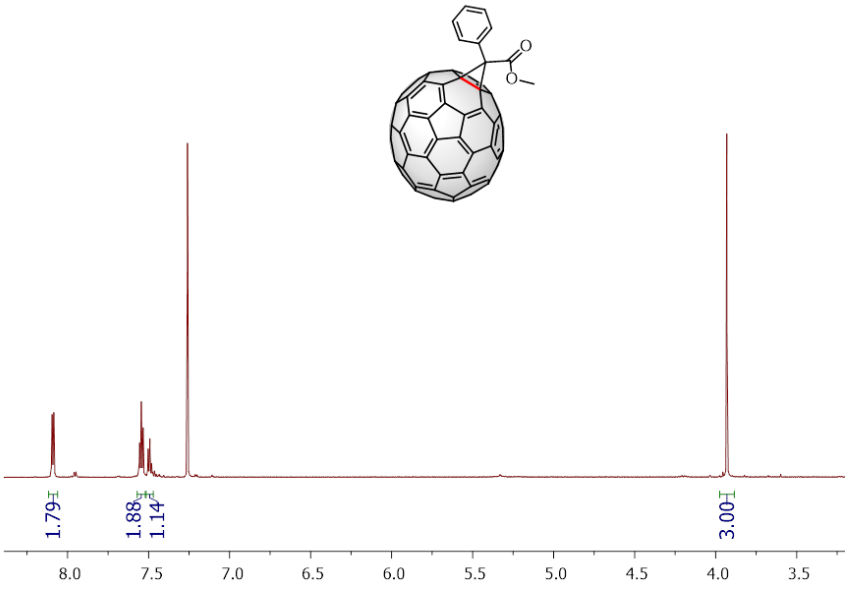

Figure 83. ^{1}H NMR (300MHz, 298K, $CDCl_3$) spectrum of α-siteisomer **74**.

4.3.2.4. Synthesis of Enriched β-[70]Methanofullerene

Since the α bond in [70]fullerene is the most reactive in all the reactions, β-siteisomers are obtained as minor products. For this reason, the reactivity and electrochemical properties of this β-siteisomer has been barely studied.

Thus, we focused our attention on develop an alternative methanofullerene synthesis by switching the siteselectivity toward the addition to the less reactive β double bond.

In regular Bingel conditions, a solution of [70]fullerene and methyl α-Br-phenylacetate **72** in toluene reacts with DBU and gives rise to compounds α-siteisomer **75** and β-siteisomers **76**, **77** in a ratio 75:25. However, we noticed that in the presence of a polar solvent (DMF) the ratio α:β can be turned to 38:62 (Scheme 45).

This exciting result where for the first time the β-siteisomer is obtained as the main product of the reaction, opens a wide opportunity to investigate a new reactivity on C_{70} and making a deep study of the less-known β-derivatives.

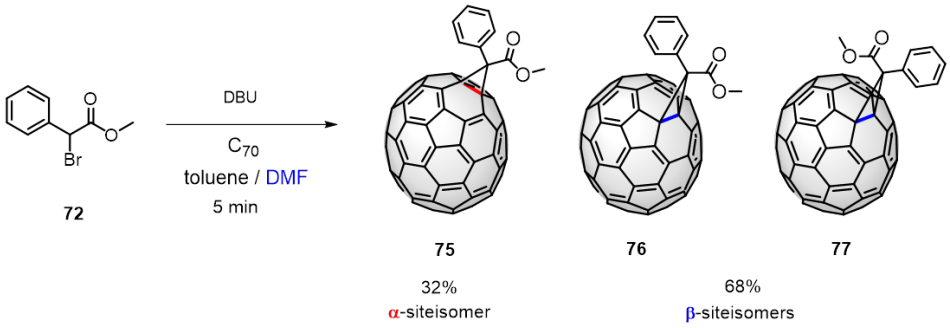

Scheme 45. Synthesis of enriched β-siteisomers.

The ^{1}H NMR spectrum of β-[70]methanofullerene demonstrates the presence of the two regioisomers formed, depending on the orientation of the methyl ester group to the pole (**77**) or the equatorial position (**76**), with two singlets corresponding to the methyl ester group at 3.60 and 3.95 ppm. By analogy with related systems, we assigned compound **77** to the signal of the methyl ester appearing at the lowest field.[192]

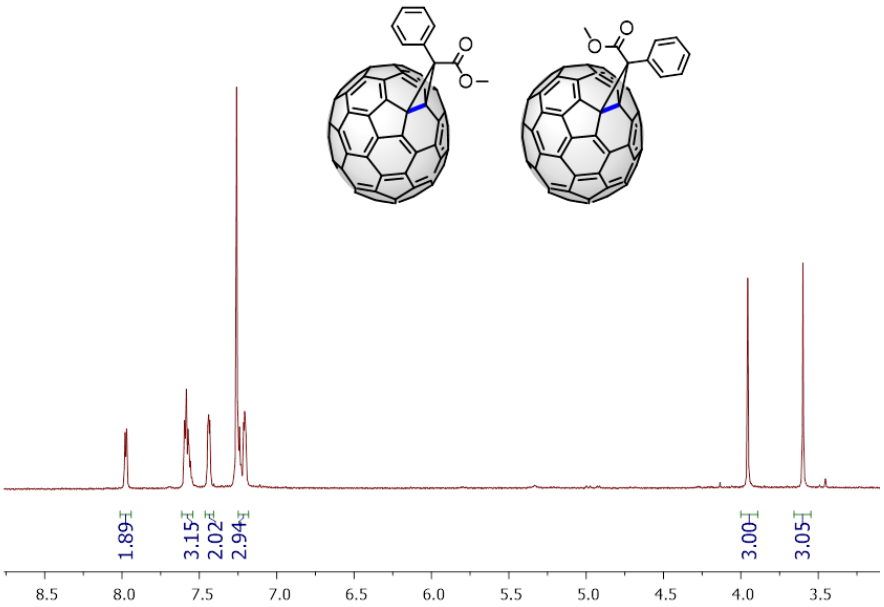

Figure 84. ^{1}H NMR (300MHz, 298K, $CDCl_3$) spectrum of β-siteisomers **76**, **77**.

Electrochemical characterization of fullerene derivatives

The electrochemical behavior of fulleroids and methanofullerenes, pure monoadducts α-siteisomer, β-siteisomers and the corresponding isomeric mixtures, was studied by cyclic voltammetry using *o*-DCB/MeCN (4:1) as solvent at room temperature and tetrabutylammonium hexafluorophosphate as the supporting electrolyte. The β-siteisomers were isolated from the mixture of isomers obtained by the traditional method by HPLC using a semipreparative column: 5PYE (10 x 250mm; toluene/acetonitrile (1:1); 4 ml/min; 320 nm; 25ºC).

It is well known that the saturation of a double bond of the carbon cage modifies the electrochemical behavior. Therefore, derivatization of the fullerene produces a cathodic shift (towards more negative values) about 80-100 mV per saturation for the first three reduction waves with respect to pristine $C_{70.}$ In contrast, in fulleroid derivatives the π-homoconjugation in the fullerene cage is not disturbed and the reduction potentials are not significantly modified. The isomeric mixture presents practically the same reduction potentials as each one of the isomers, α-siteisomer and β-siteisomer, since the functionalization position is independent of the reduction potential.

The cyclic voltammogram of both the [5,6] and [6,6] isomers of the [70]PCBM exhibits three well defined quasireversible reduction waves assigned to the first three reduction potentials and are shown in Figure 85. The reduction potential values for the pure compounds and their respective isomeric mixtures, are shown in Table 9. As expected, the reduction potentials of fulleroids are similar to that of pristine C_{70}. However, methanofullerenes show higher reduction potential values (Table 9).

Table 9. Reduction potential values of C_{70}, fulleroids **57-59**, **67-69**, α-siteisomers, β-siteisomers and the corresponding isomeric mixture (α+β), obtained by the classic method, in V *vs* Fc/Fc^{+} couple.

Compound	E^1_{red}/V	E^2_{red}/V	E^3_{red}/V
C_{70}	-1.02	-1.40	-1.82
[5,6]-70PCBM 57-59	-1.03	-1.37	-1.83
[5,6]-70DPM 67-69	-1.04	-1.40	-1.87
α-70PCBM 72	-1.13	-1.50	-1.90
β-70PCBM 73a,b	-1.15	-1.51	-1.95
α+β 70PCBM	-1.13	-1.52	-1.92
α-70DPM4 74a	-1.13	-1.49	-1.90
α+β 70DPM4	-1.12	-1.49	-1.91
α-70DPM6 74b	-1.13	-1.52	-1.93
α+β 70DPM6	-1.12	-1.49	-1.91
α-[70]methanofullerene 77	-1.10	-1.47	-1.86
β-[70]methanofullerene 78a,b	-1.07	-1.45	-1.87
α+β [70]methanofullerene	-1.07	-1.44	-1.85

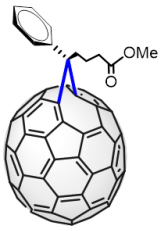

[5,6]-[70]PCBM
57-59

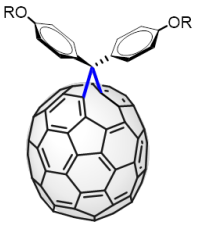

[5,6]-[70]DPM
67-69

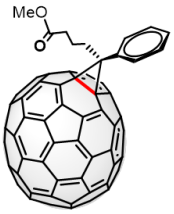

α-[70]PCBM
72

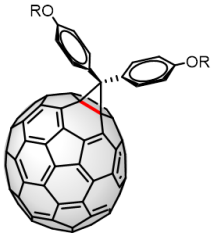

α-[70]DPM
74a,b

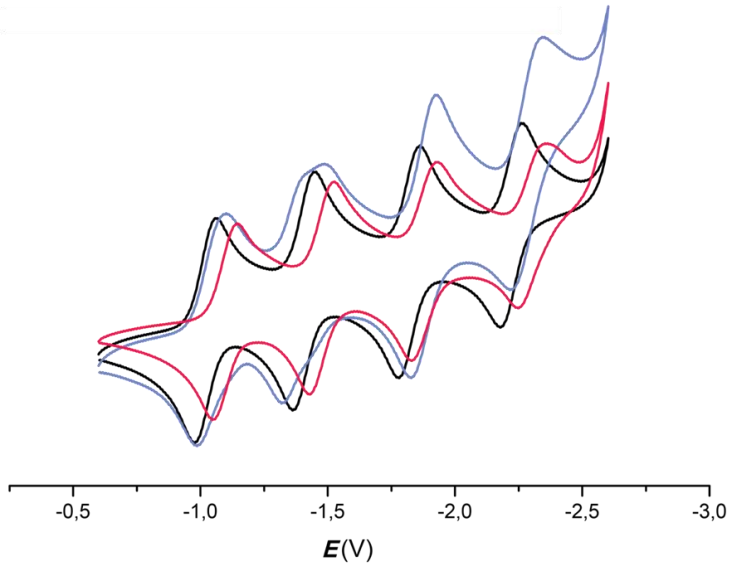

Figure 85. Cyclic voltammogram of C_{70} (black), fulleroids fraction **57-59** (blue) and methanofullerenes **60-62** (red) in *o*-DCB/ACN 4:1 using a GCE (glassy carbon electrode) as the working electrode, $Ag/AgNO_3$ as the reference electrode and $Bu_4N{\cdot}PF_6$ as the supporting electrolyte at 100 mVs^{-1}.

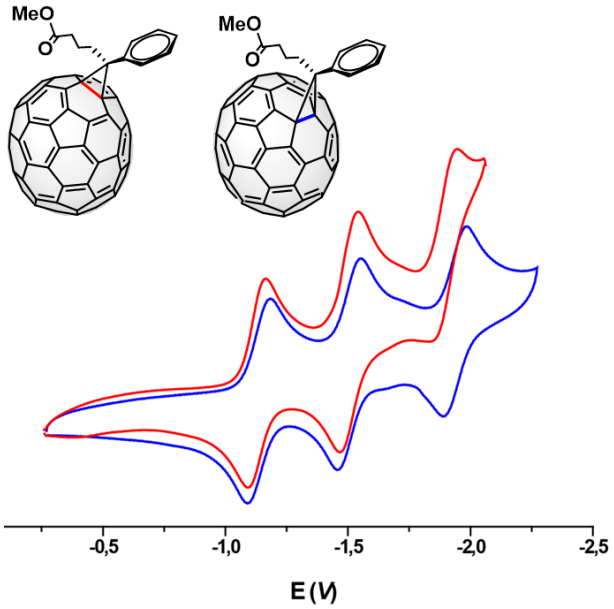

Figure 86. Cyclic voltammogram of α-siteisomer-[70]PCBM (red) and β-siteisomer-[70]PCBM (blue) in *o*-DCB/ACN 4:1 using a GCE (glassy carbon

electrode) as the working electrode, $Ag/AgNO_3$ as the reference electrode and $Bu_4N{\cdot}PF_6$ as the supporting electrolyte at 100 mVs^{-1}.

4.3.3. Organic Solar Cells Based on [70]PCBM

In the last years, many efforts have been made to improve the power conversion efficiency of organic photovoltaic devices. Higher fullerenes such as C_{70} display better light absorption in the visible region of the solar spectrum compared to the most abundant C_{60}, resulting in higher photocurrent values and, therefore, in higher power conversion efficiencies. For instance, the *Jsc* value of [70]PCBM is 50% higher when compared to its [60]PCBM analog.[149d,197]

On the other hand, there are several examples of fullerene bisadducts in which regioisomerically pure derivatives exhibited higher PCE values than the corresponding isomeric mixtures.[198] Thus, control on the isomeric purity of the involved materials may be crucial to enhance a suitable molecular organization of the photoactive layer in the device. Considering that the molecular arrangement of [70]fullerene derivatives in the active layer has a large impact on charge separation and charge-transporting properties, pure isomers of C_{70} would yield a more desirable donor–acceptor network toward highly efficient BHJ.

However, there are not many examples that illustrate the correlation between isomeric purity and device performance. One of the reasons is the lack of selective methods affording pure compounds in higher fullerenes. Thus, most of the OPV devices based on C_{70} are formed by a mixture of isomers in which the α- and β-siteisomers are the most abundant.[79] The isomeric effects of fullerene-based electron acceptors led to some contradiction on isomer-dependent photovoltaic performance. Some works concluded that a purified

197. D. Mühlbacher, M. Scharber, M. Morana, Z. Zhu, D. Waller, R. Gaudiana, C. Brabec, *Adv. Mater*., **2006**, *18*, 2884.
198. a) W. W. H. Wong, J. Subbiah, J. M. White, H. Seyler, B. Zhang, D. J. Jones, A. B. Holmes, *Chem. Mater*., **2014**, *26*, 1686. b) R. Tao, T. Umeyama, K. Kurotobi, H. Imahori, *ACS Appl. Mater. Interfaces*, **2014**, *6*, 17313.

isomer shows higher performance than isomeric mixtures,[199] whereas others display a different conclusion.[200]

As preliminary results, some organic devices were fabricated with two different fullerene samples, from pure α-[70]PCBM isomer **72** and the commercially available isomeric mixture [70]PCBM (Solenne), in order to determine how the purity of the organic sample affects the device efficiency. The polymer used for the blend was PffBT4T-2OD, one of the most successful polymers reaching solar energy conversion efficiencies as high as ~10% in polymer:fullerene bulk heterojunction solar cells.[201]

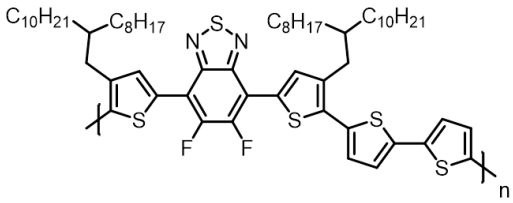

PffBT4T-2OD

Figure 87. Semiconducting polymer used as electron donor in the blend.

The average efficiency was calculated from three batches of devices from three different days. Comparing the pure α-siteisomer **72** with the mixture of siteisomers, no significant difference in the photovoltaic parameters was observed. Thus, the studied systems showed a remarkable *Voc* as well as *Jsc* values, with PCEs of 6.45 % for the commercial sample (Solenne) and 6.63 % for the pure α-[70]PCBM site-isomer. The two sets of comparison are given in Table 10.

199. a) X. Meng, G. Zhao, Q. Xu, Z. a. Tan, Z. Zhang, L. Jiang, C. Shu, C. Wang, Y. Li, *Adv. Funct. Mater*., **2014**, *24*, 158. b) W. W. Wong, J. Subbiah, J. M. White, H. Seyler, B. Zhang, D. J. Jones, A. B. Holmes, *Chem. Mater*., **2014**, *26*, 1686.
200. F. Zhao, X. Meng, Y. Feng, Z. Jin, Q. Zhou, H. Li, L. Jiang, J. Wang, Y. Li, C. Wang, *J. Mater. Chem. A*, **2015**, *3*, 14991.
201. Y. H. Liu, J. B. Zhao, Z. K. Li, C. Mu, W. Ma, H. W. Hu, K. Jiang, H. R. Lin, H. Ade, H. Yan, *Nat. Commun*., **2014**, *5*, 5293.

Table 10. Average PCE% reached in a polymer:fullerene BHJ solar cell using pure α-[70]PCBM isomer and commercially available isomeric mixture.

Active layer	V_{oc}(V)	J_{sc}(mAcm^{-2})	FF(%)	PCE(%)
PffBT4T-2OD/pure α-[70]PCBM	0.78	14.83	0.57	6.63
PffBT4T-2OD/Solenne [70]PCBM	0.76	14.62	0.57	6.45

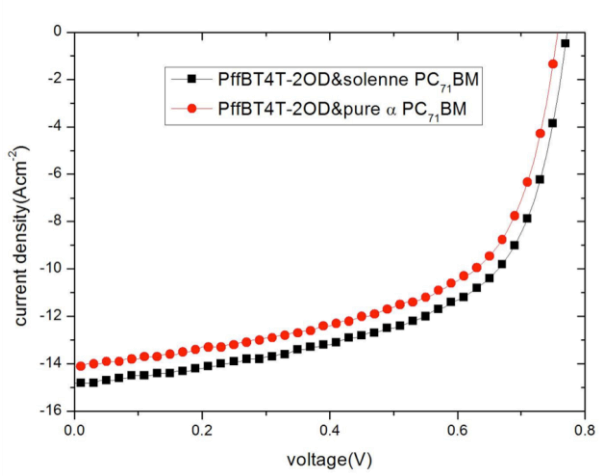

Figure 88. *J-V* graphs for pure α-[70]PCBM (red) and Solenne isomeric mixture (black).

Although more studies mostly involving aspects of the materials used such as morphology, crystallinity, isomeric ratio in the blend and the polymer/fullerene ratio, as well as other fabrication device conditions are needed, the conclusion at this stage is based on the above experimental evidences, the use of pure α-siteisomer does not produce a significant benefit on the device performance. The efficacy of this approach, based on the use of pure isomers for improving

the performance of the device, has been demonstrated in a recent work,[202] in which the use of pure isomers of different [70]fullerene monoadducts, separated all of them by HPLC, achieved greater efficiencies.

4.3.4. Organic Solar Cells Based on [70]Methanofullerenes

With isomeric structure and similar electron properties, individual isomer of fullerene derivatives (α-siteisomer and β-siteisomer), have been thought to show comparable photovoltaic performance to each other. However, a recent work, revealed a significant difference of power conversion efficiency (PCE = 0.38, 3.7 and 9.37%) for the perovskite solar cells with each of the purified α-, β1- or β2-$PC_{71}BM$ isomers as electron acceptor.[203]

As preliminary results, some organic devices were fabricated from pure α-[70]methanofullerene, pure β-[70]methanofullerene and the isomeric mixture (α+β), in order to determine how the different pure isomers affects the device efficiency. This new set of fullerene derivatives were tested using as electroactive material a mixture of the corresponding fullerene and PTB7 as electron donor polymer, in a ratio (1:2) PTB7:fullerene.

Table 11. Average PCE% reached in a polymer:fullerene BHJ solar cell using pure α-[70]methanofullerene, pure β-[70]methanofullerene and the isomeric mixture.

Active layer	V_{oc}(V)	J_{sc}(mAcm^{-2})	FF(%)	PCE(%)
PTB7/pure α-[70]methanofullerene	0.74±0.01	20.77±0.65	0.48±0.03	7.30±0.72
PTB7/pure β-[70]methanofullerene	0.59±0.04	6.64±0.55	0.26±0.02	1.02±0.12
PTB7/(α+β) [70]methanofullerene	0.62±0.06	7.93±0.73	0.26±0.01	1.31±0.23

202. T. Umeyama, T. Miyata, A. C. Jakowetz, S. Shibata, K. Kurotobi, T. Higashino, T. Koganezawa, M. Tsujimoto, S. Gélinas, W. Matsuda, S. Seki, R. H. Friend, H. Imahori, *Chem. Sci.*, **2016**, *8*, 181.
203. S. Dai, X. Zhang, W. Chen, X. Li, Z. Tan, C. Li, L. Deng, X. Zhan, M. Lin, Z. Xing, T. Wen, R. Ho, S. Xie, R. Huanga, L. Zhenga, *J. Mater. Chem. A*, **2016**, *4*, 18776.

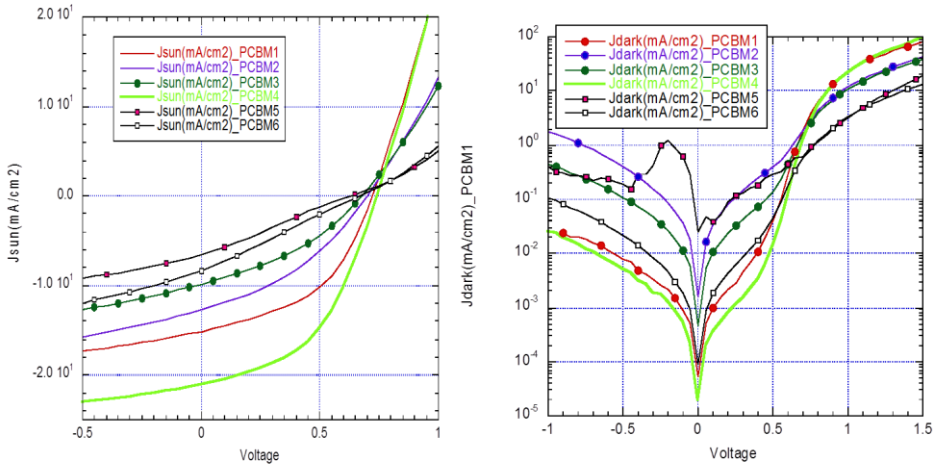

Figure 89. *J-V* graphs for pure α-[70]methanofullerene (red), β-[70]methanofullerene (blue) and isomeric mixture (black).

These are preliminary results and more experiments involving different aspects of the materials used, such as the morphology and crystallinity, are needed to understand the differences found between solar cells made with the different isomers. The conclusion at this stage is based on the experimental evidences. The use of pure α-siteisomer or β-siteisomer does not produce a significant benefit on the device performance.

4.4. Chemical Reactivity on Endohedral Fullerenes

Endohedral fullerenes are a family of novel compounds whose properties differ substantially from those exhibited by empty fullerenes due to the metals, metal complexes or small molecules encapsulated inside them.[6a] This type of fullerenes are generally less reactive, and although their chemistry is in constant development, it is still difficult to predict their reactivity.

Because of their size, diatomic guest molecules are ideal candidates to be encapsulated inside C_{60}. Hydrogen fluoride (HF) is frequently used in a variety of organic synthetic protocols and has been extensively studied.[204] HF molecules create hydrogen bonds between them forming aggregates; therefore, the study of isolated HF molecules is complicated. Recently, Krachmalnicoff *et al*., have reported the new endohedral HF@C_{60} molecule.[145] A single HF molecule trapped in a fullerene cage provides the opportunity to analyze its singular properties in an interaction free situation as well as in a well-defined environment.

Dolgonos *et al*. reported a computational study of several diatomic molecules encapsulated into C_{60}.[205] They surmised that the dipole moment of the polar guest molecules trapped inside C_{60} is decreased after the encapsulation, and specifically, the HF molecule exhibits the lowest interaction energy with the C_{60} compared with other polar molecules investigated.

We report the first exohedral functionalization on the novel HF@C_{60} to obtain new enantiomerically enriched HF@C_{60} pyrrolidines. The synthesis was carried out using the reported methodology involving a 1,3-dipolar cycloaddition of *N*-metalated azomethine ylide.[96] In order to determine the difference in the chemical reactivity between empty C_{60} and HF@C_{60}, the reaction was performed with a mixture of both fullerenes in a ratio 12:88 (C_{60}:HF@C_{60}), thus ensuring the same experimental conditions.

The mixture of fullerenes reacted with α-iminoester **78**. In the presence of the corresponding metal salt/chiral ligand pair, the four enantiomers for the C_{60} and HF@C_{60}, were obtained in good enantiomeric excesses (Scheme 46).

204. D. Feller, K. A. Peterson, *Theochem.*, **1997**, *400*, 69.
205. G. A. Dolgonos, G. H. Peslherbe, *Phys. Chem. Chem. Phys*., **2014**, *16*, 26294.

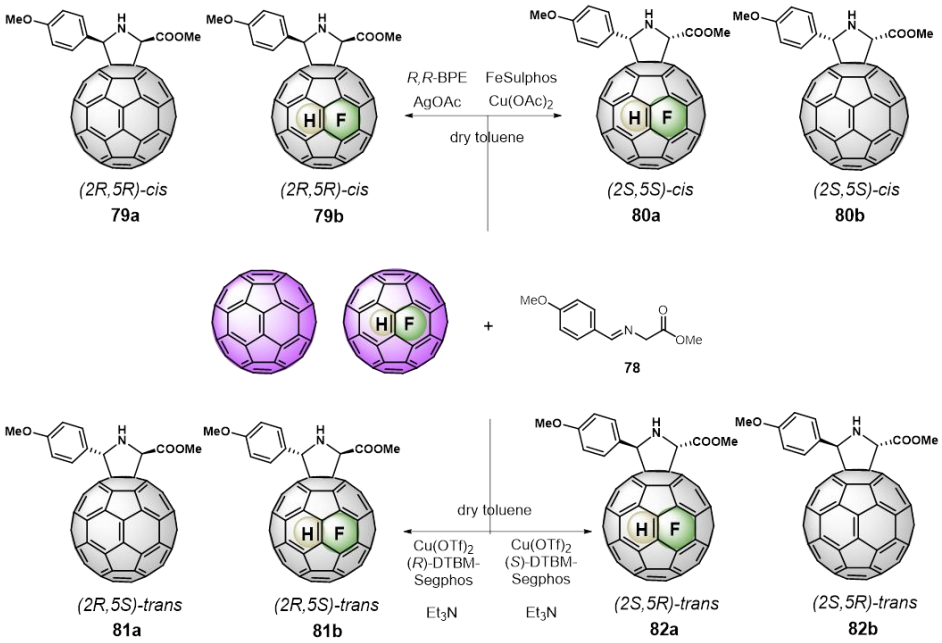

Scheme 46. Synthesis of enantiomerically pure *cis*- and *trans*- HF@C_{60}-pyrrolidines.

The catalytic pair AgOAc/(*R*,*R*)-BPE, afforded the pyrrolidine (*R*,*R*)-*cis* **79b** with 90% *ee*, in contrast to the system formed by $Cu(OAc)_2$/(*R*)-FeSulPhos, that led to the opposite enantiomer (*S*,*S*)-*cis* **80b** in 93% *ee*. In the same way, *trans* enantiomers were obtained by using (*R*)- or (*S*)-DTBM-SegPhos and $Cu(OTf)_2$, leading to (*R*,*S*)-*trans* **81b** and (*S*,*R*)-*trans* **82b** with 75% *ee* and 84% *ee*, respectively. The optical purity of the compounds was determined by HPLC using a chiral column, *Pirkle Covalent (R,R) Whelk-02* for *cis* enantiomers and *ChiralPack IC* for *trans* enantiomers.

The four new enantiomers *cis*- and *trans*- endohedral [60]fulleropyrrolidines. were fully characterized by NMR spectroscopy and mass spectrometry. The signal for the inner proton of pristine HF@C_{60} in the ^{1}H-NMR spectrum appears as a doublet at -2.65 ppm (J = 505.6 Hz). However, if the carbon cage is functionalized that signal is shifted to -5.81 ppm (J = 505.8 Hz) for *cis* and to -5.88 ppm (J = 506.0 Hz) for *trans*.

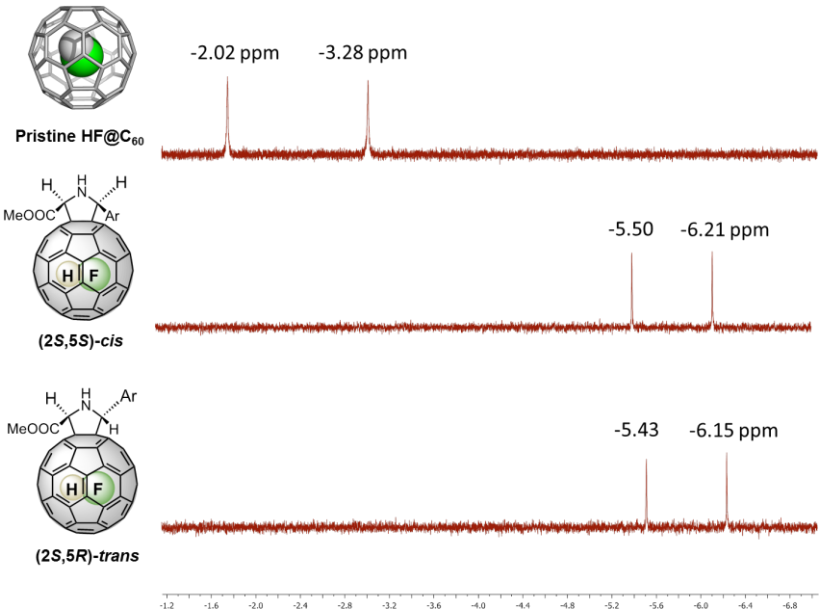

Figure 90. ^{1}H-NMR (400MHz, $CDCl_3$, 298K) spectrum of pristine HF@C_{60} and ^{1}H-NMR (700MHz, $CDCl_3$, 298K) spectra of compounds *cis*- and *trans*-endohedral [60]fulleropyrrolidines (-1.2 to -7 ppm).

Despite the polarity of the HF molecule, we did not observe significant differences in terms of reactivity on the carbon cage of the HF@C_{60} compared with the empty C_{60}. Indeed, the ratio of the pristine cages before and after reacting remained unaltered, as well as the ratio of pyrrolidine-C_{60} and pyrrolidine-HF@C_{60}. These experimental data, corroborated by theoretical calculations (see below), contradict a priori the expected higher reactivity for the HF@C_{60} considering the polarity of the HF molecule.

In order to get a better understanding of the HF behavior inside the carbon cage, we studied the isomerization process from the optically pure (*2S,5S*)-*cis* **80b** to the (*2S,5R*)-*trans* **82b**, that involves the exohedral [60]fullerene functionalization.

This process can be accounted by a stepwise mechanism with a configuration inversion at the pyrrolidine C5 carbon atom while the configuration at C2 is maintained without losing enantiomeric excess. This enantiospecificity is coherent with the formation of a zwitterionic intermediate by heterolytic pyrrolidine ring opening between the C5 and the cage that gives rise to a stable benzylic cation and a negative charge on the cage.

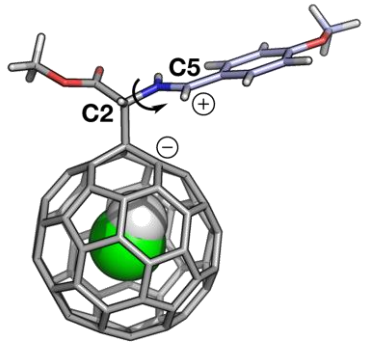

Figure 91. Zwitterionic intermediate formed by a carbanion on the C_{60} cage and a benzylic cation on the former pyrrolidine ring.

The carbanion of the zwitterionic intermediate can interact with the inner species and determine its stability. The negative charge in the carbon atom of the [60]fullerene cage is stabilized by the H atom of the inner HF molecule, thus making the process faster. In a second step, the N-C2 bond of the intermediate rotates and is bonded back to the fullerene cage.

For a better understanding of the effect of the molecule inside C_{60} cage, a comparative study between pristine C_{60}, $H_2O@C_{60}$, and $HF@C_{60}$ on the isomerization process, is also discussed. Thus, we can explore the influence of the hydrogen bonding, generated by the carbanion on the fullerene sphere and the hydrogen of the inner molecule (H_2O and HF).

The synthesis of analogous pyrrolidinofullerenes on an endohedral $H_2O@C_{60}$ molecule was proposed. Under the same conditions employed for the $HF@C_{60}$-pyrrolidines, the $H_2O@C_{60}$-pyrrolidines were obtained in an enantioespecific manner.

The synthesis was carried out with a mixture of fullerenes (C_{60}:$H_2O@C_{60}$) in a ratio (25:75), thus ensuring the same experimental conditions. The mixture reacted with α-iminoester **78.** In the presence of the corresponding metal salt/chiral ligand pair, the two enantiomers for the C_{60} and $HF@C_{60}$, required for the isomerization process were obtained in good enantiomeric excesses (Scheme 47).

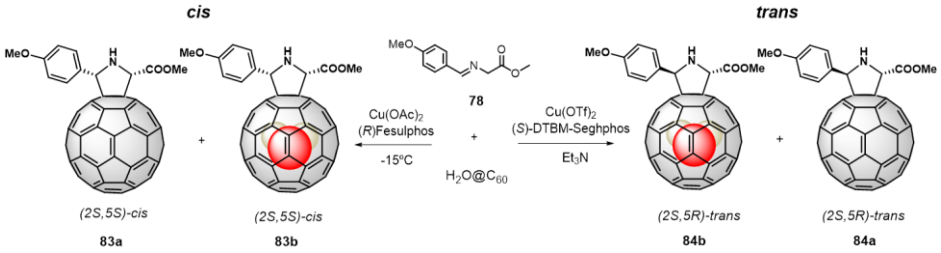

Scheme 47. Synthesis of enantiomerically pure *cis*- and *trans*- $H_2O@C_{60}$-pyrrolidines.

The catalytic pair $Cu(OAc)_2$/(*R*)-FeSulPhos, afforded the pyrrolidine (*S*,*S*)-*cis* **83b** with 93% *ee*. In the same way, *trans* enantiomer (*S*,*R*) **84b** was obtained by using (*S*)-DTBM-SegPhos and $Cu(OTf)_2$, with 76% *ee*. The optical purity of the compounds was determined by HPLC using a chiral column, *Pirkle Covalent (R,R) Whelk-02*.

Once the synthesis and characterization was accomplished, the *cis*/*trans* isomerization was studied. The selected system used for the experiment was the enantiomer (2*S*,5*S*)-*cis*-fulleropyrrolidine for all the cases with a *cis*/*trans* ratio of 98/2 for **80b** ($HF@C_{60}$) and **83b** ($H_2O@C_{60}$) and 96/4 for empty C_{60} **80a**. In order to avoid competitive cycles of retro-cyloaddition/cycloaddition reactions, moderate temperatures have been used. The experiments were performed in a mixture chlorobenzene/acetonitrile 1:1 as solvent, at three different temperatures (25ºC, 30ºC, and 40ºC).

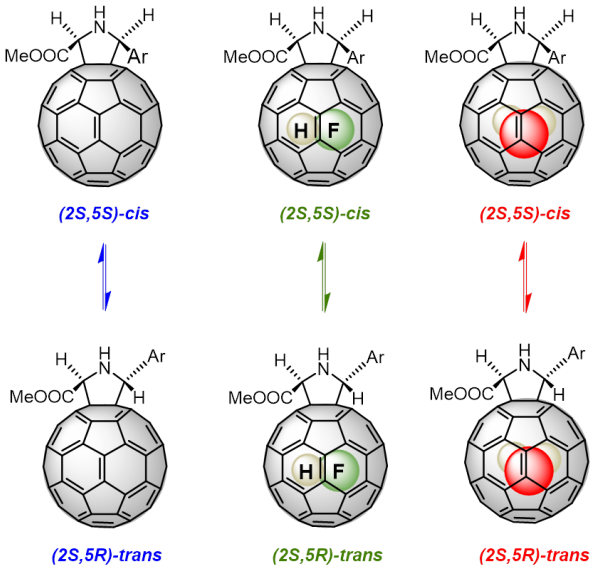

Figure 92. Isomerization process from the optically pure (2*S*,5*S*)-*cis*-pyrrolidino[60]fullerene to the (2*S*,5*R*)-*trans*-pyrrolidino[60]fullerene.

The reactions were monitored by HPLC until the equilibrium stages were reached (Figure 92). Integration of the peak areas was used to determine the relative amount of the isomers at any time during the isomerization. These equilibrium stages and the time needed to reach them were different for each system and are summarized in Table 12.

At 25ºC, the equilibrium stage *cis*/*trans* was 77/23 while at 30ºC and 40ºC, the ratio *cis*/*trans* changed significantly toward 59/41 and 55/45, respectively. In all cases, the enantiomeric excesses of the *trans* derivatives remained unaltered demonstrating the enantiospecificity of the isomerization process.

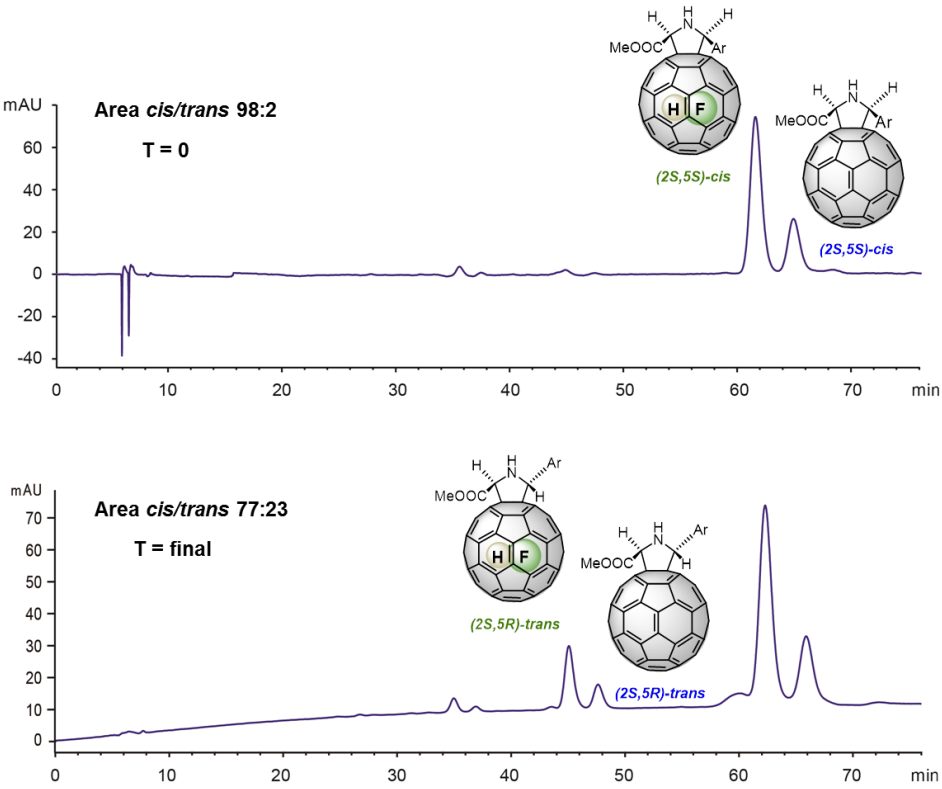

Figure 93. HPLC profile of compound **80b** (sample is composed by **80b**:**80a** 88:12) before the isomerization reaction, t=0 (top) and after the isomerization reaction, t=final (bottom) at room temperature. Conditions: Buckyprep Waters (4.6 x 250mm; toluene/hexane/acetonitrile (20:70:10); 0.5 ml/min; 320 nm; 25ºC).

Table 12. Isomerization reaction rates of (2*S*,5*S*)-*cis* **80a**, (2*S*,5*S*)-*cis* **80b** and (2*S*,5*S*)-*cis* **83b** in chlorobenzene:acetonitrile 1:1 at 25°C, 30ºC, and 40ºC.

Compound	T (ºC)	*cis*/*trans*[a]	*K* (h^{-1})
80a	25	77/23	$-5.29x10^{-3} \pm 1.90x10^{-4}$
80b	25	77/23	$-9.03x10^{-3} \pm 3.92x10^{-4}$
83b	25	77/23	$-10.95x10^{-3} \pm 1.08x10^{-3}$
80a	30	59/41	$-8.50x10^{-3} \pm 2.88x10^{-4}$
80b	30	59/41	$-10.26x10^{-3} \pm 4.01x10^{-4}$
83b	30	59/41	$-12.90x10^{-3} \pm 5.99x10^{-4}$
80a	40	55/45	$-11.80x10^{-3} \pm 6.34x10^{-4}$
80b	40	55/45	$-12.10x10^{-3} \pm 5.54x10^{-4}$
83b	40	55/45	$-13.99x10^{-3} \pm 6.40x10^{-4}$

[a] Ratio *cis*/*trans* at equilibrium stage.

Comparing the experimental findings of the three systems, the two endohedral fullerenes have the highest isomerization rates $K_{H2O@C60} > K_{HF@C60} > K_{C60}$. This confirms that the encapsulated molecule plays an important role in the zwitterionic intermediate stability. In view of the aforementioned results, the H-bonding assistance is stronger for the $H_2O@C_{60}$ system according to the kinetic constants. These experimental results are in agreement with that predicted by theoretical calculations (see below).

The proposed mechanism for the isomerization follows a first-order rate law. However, competing reactions such as the previously reported retro-cycloaddition and the racemization process are also involved. This process could be outlined according to the following scheme:

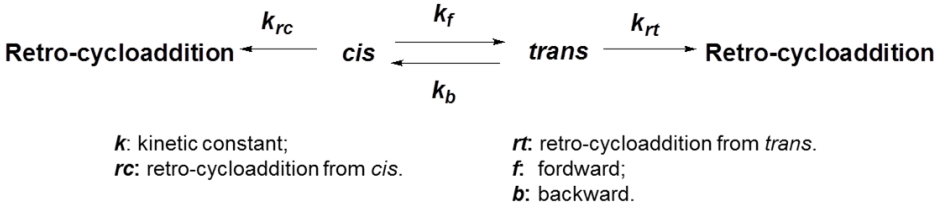

Scheme 48. Representation of the reactions involved in the isomerization process.

If we ignore the retro-cycloaddition reaction contribution, the reaction rate would remain:

$$v = -\frac{d[cis]}{dt} = k_f[cis] - k_b[trans] \qquad \textbf{Equation 4}$$

$$\ln\frac{(x-x_e)}{(x_0-x_e)} = -(k_f+k_b)t \qquad \textbf{Equation 5}$$

$$K = k_f + k_b \qquad \textbf{Equation 6}$$

Where x, x_e, and x_o are the concentrations of *cis* adduct at the time t, at equilibrium, and at the starting point, respectively, and k_f and k_b are the rate constants for the forward and backward *cis-trans* isomerization.

In Figure 94 we represent the experimental data corresponding to the isomerization process of compounds **80a**, **80b** and **83b** at 25ºC, 30ºC and 40ºC, following equation 5, to afford the kinetic constant for each process. It is important to note that all the experiments follow the same trend, a first-order rate law. To simplify the graphics, $A = \frac{(x-x_e)}{(x_0-x_e)}$

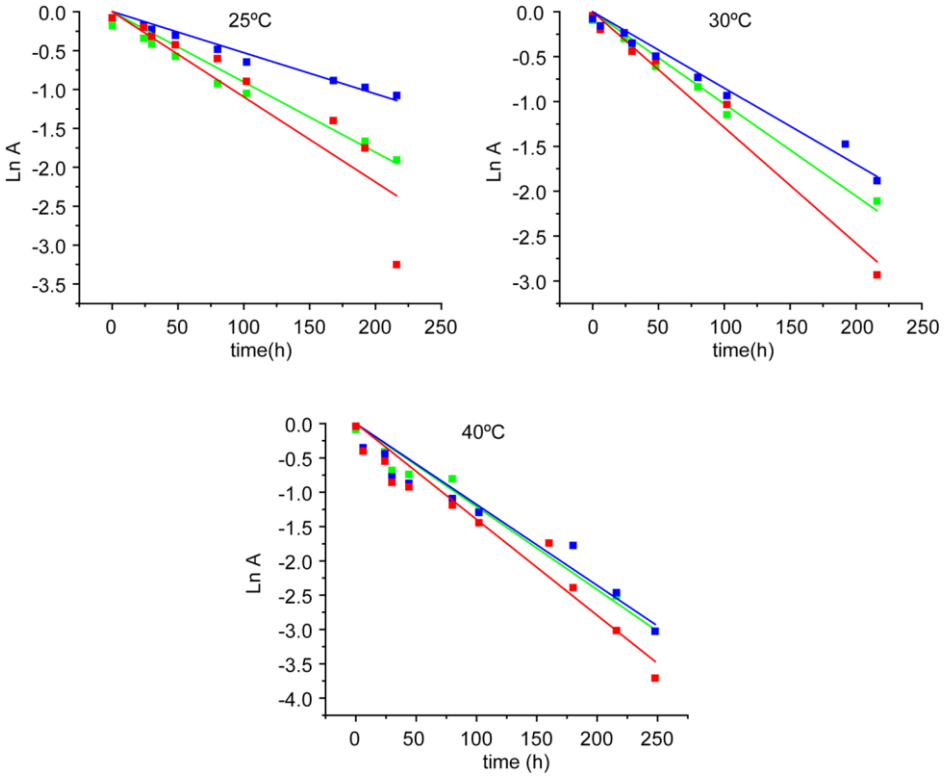

Figure 94. Plotting data of the *cis-trans* isomerization process of empty C_{60} **80a** (blue), HF@C_{60} **80b** (green) and H_2O@C_{60} **83b** (red) at 25°C, 30ºC and 40ºC.

Density Functional Theory calculations at the M06-2X/6-311++G(d,p)//OLYP/TZP level of theory were carried out to understand the *cis-trans* isomerization in the HF@C_{60} chiral fulleropyrrolidine. The computed reaction path for the *cis-trans* isomerization and the retro-cycloaddition process for the three systems, C_{60}, H_2O@C_{60}, and HF@C_{60}, are shown in Figure 95.

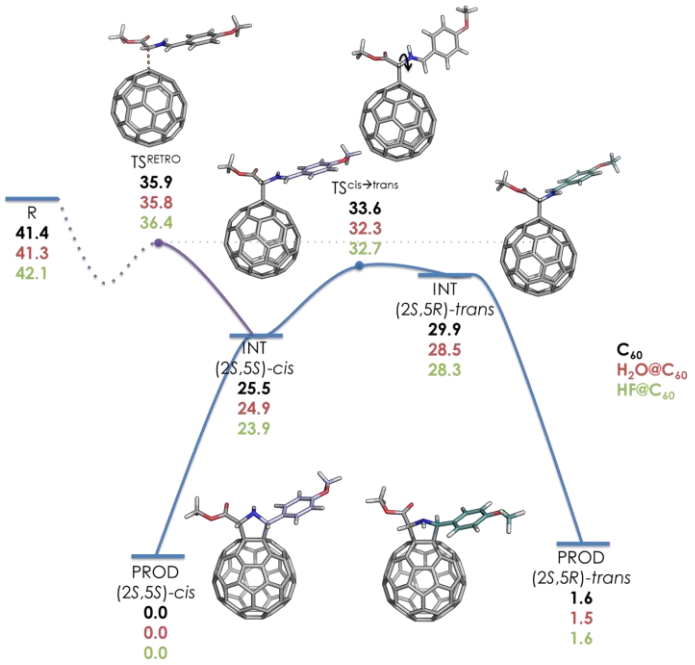

Figure 95. Electronic energies (kcal/mol) for the *cis-trans* isomerization in **80a** (black values), **83b** (red values) and **80b** (green values). The retro-Prato process is also included (in purple).

In agreement with experimental observations, PROD-(2*S*,5*S*)-*cis* is more stable by 1.6 kcal/mol than PROD-(2*S*,5*R*)-*trans*. The *cis-trans* isomerization occurs through a stepwise mechanism with the formation of zwitterionic intermediates referred as INT-(2*S*,5*S*)-*cis* and INT-(2*S*,5*R*)-*trans* (Figure 95). The heterolytic dissociation of the C–C bond to form the zwitterionic intermediate is much easier at C5 (with an energy barrier less than 1 kcal/mol) than at C2 position because of the electron withdrawing character of the carboxylic group.[206] This result is in concordance with the experimental observation that the C2 configuration is preserved along the whole isomerization process.

206. S. Aroua, M. Garcia-Borràs, S. Osuna, Y. Yamakoshi, *Chem. Eur. J.*, **2014**, *20*, 14032.

Zwitterionic intermediates are about 1.5 kcal/mol more stable in HF@C_{60} than in the C_{60}. The reason is the formation of an interaction between the H of the HF molecule and the negatively charged C atom on the fullerene cage. The distance between the H atom of HF and C5 in the zwitterionic intermediate is 2.6 Å. The H–F distance in *cis* and *trans* intermediates is 0.931 Å, somewhat elongated as compared to that of HF@C_{60}, 0.929 Å. Therefore, this H···C interaction in the zwitterionic intermediate can be classified as a weak hydrogen bond.

From the zwitterionic INT-(2*S*,5*S*)-*cis*, the system can evolve through two different pathways: i) *cis*-*trans* isomerization to produce INT-(2*S*,5*R*)-*trans* or ii) retro-Prato reaction to recover the initial reactants. The retro-Prato reaction has a barrier that is about 3.7 kcal/mol higher than the *cis*-*trans* isomerization process. This difference between the activation barrier for the retro-Prato and isomerization process is substantially larger in the case of HF, as compared to free C_{60} and $H_2O@C_{60}$ (ca. 2.3 and 3.5 kcal/mol, respectively). Therefore, especially in the case of C_{60}, the retro-Prato can compete with the isomerization process at high temperatures.

It is important to note that the presence of the inner HF molecule does not affect the final relative stability of the *cis* and *trans* products. However, it has an important effect on the retro-reaction pathway and, especially, it has a significant influence on the energy barrier of the *cis*-*trans* isomerization process. The activation barrier is considerably lower in HF@C_{60} (32.7 kcal/mol) as compared to the empty C_{60} (33.6 kcal/mol). This difference is in agreement with the improved stereochemical outcome observed experimentally for the HF@C_{60} chiral fulleropyrrolidine.

The encapsulated HF molecule assists the isomerization process by stabilizing the formed fullerene anion, where the hydrogen atom of HF is directly pointing to the negatively charged carbon atom on fullerene surface. This distance is ca. 2.6 Å in INT-(2*S*,5*S*)-*cis*-**80b**, and slightly longer in $TS^{cis\text{-}trans}$ (ca. 2.7 Å) (Figure 96).

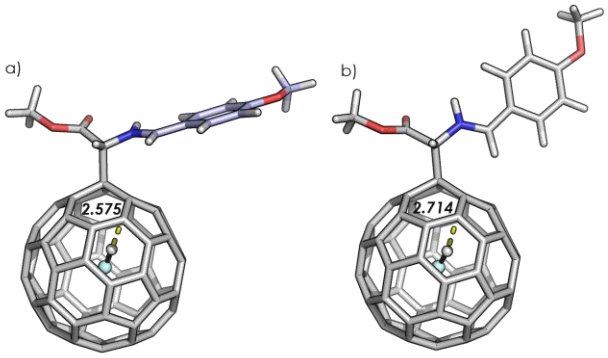

Figure 96. Optimized geometries of a) INT-(2*S*,5*S*)-*cis*-**80b** and b) $TS^{cis\text{-}trans}$ for HF@C_{60}.

The slightly smaller energy barrier (by 0.4 kcal/mol) for the *cis*-*trans* isomerization process in **83b** (32.3 kcal/mol) as compared to **80b** (by 33.7 kcal/mol) also concurs with the experimental rate constants (see Table 12).

EXPERIMENTAL SECTION

5. EXPERIMENTAL SECTION

5.1. General Methods

-***Thin layer chromatography:*** Reactions were monitored by thin-layer chromatography carried out on 0.2 mm TLC-aluminium sheets of silica gel (Merck, TLC Silica gel 60 F_{254}).

-***Purification of Reaction Mixtures****:* Flash column chromatographies were performed using silica gel (Merck, 230-400 mesh).

-***Infrared Spectroscopy***: FTIR spectra were carried out using ATR of the solid compounds. The instrument used was a Bruker TENSOR FTIR. The spectral range was 4000-550 cm^{-1}.

-***Nuclear Magnetic Resonance Spectroscopy:*** ^{1}H NMR and ^{13}C NMR spectra were recorded on a BRUKER DPV-300MHz, BRUKER AV-500MHz or BRUKER AVIII-700MHz using deuterated solvents as reference. Coupling constants (*J*) are reported in Hz and the chemical shifts (δ) in ppm relative to tetramethylsilane (δ=0) at room temperature. Spin multiplicities are reported as a singlet (s), broad singlet (br s), doublet (d), triplet (t) quartet (q) and multiplet (m).

-***Mass Spectrometry:*** Matrix-assisted laser desorption ionization (MALDI) mass spectrometry (MS) was performed on a BRUKER-REFLEX spectrometer using dithranol as matrix, or on a HP1100EMD with electrospray ionization (ESI).

-***Cyclic Voltammetry****:* Cyclic voltammograms were recorded with a potentiostat/galvanostat AUTOLAB PGSTAT30 equipped with GPES software for Windows version 4.9 in a conventional three-compartment cell by using a GCE (glassy carbon electrode) as the working electrode, $Ag/AgNO_3$ as the reference electrode, Bu_4NPF_6 as the supporting electrolyte, o-dichlorobenzene/acetonitrile as the solvent (4:1 v/v), and a scan rate of 100 mVs^{-1}.

-***HPLC***: *Agilent 1100 Series* and *Agilent 1260 Infinity*. The *ee* values were determined by Chiral HPLC. Columns *Pirkle Covalent* (*R,R*) *Whelk-02 10/100 FEC* (4.6 x 250 mm) and *ChiralPack IA* (4.6 x 250 mm) were used. The relative yield and the isolation of some products was carried out in HPLC,

columns: Buckyprep Waters (4.6 x 250 mm), 5PYE (4.6 x 250 mm) and 5PYE semipreparative (10 x 250 mm). All the HPLC chromatograms were monitored in a 320 nm spectrophotometer detector.

-***UV-vis***: UV-vis spectra were recorded with a Shimadzu Spectrophotometer UV-3600.

-***Circular Dichroism***: Measurements were carried out on a JASCO J-815 DC spectrometer.

-**Solvents**: The solvents used were purified and dried following the usual methods.[207]

-***Reagents***: Reagents for synthesis were mostly purchased from Sigma-Aldrich and Acros.

207. D. D. Perrin, I. F. Amariego, D. R. Perrin, *Purification of laboratory Chemicals*, Pergamon Press, Oxford, **1980**.

5.2. Synthesis of α-iminoester (*E*)-*N*-(benzyliden)*tert*-butyl glycinate (31)

α-iminoester **31** was synthesized following the procedure described in the literature which showed identical spectroscopic properties.[177]

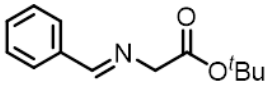

31

^{1}H NMR (300 MHz, 298 K, $CDCl_3$) δ: 8.23 (s, 1H), 7.80-7.68 (m, 2H), 7.45-7.30 (m, 3H), 4.29 (s, 2H), 1.47 (s, 9H).

5.3. General Procedure for the Synthesis of ^{t}Bu-pyrrolidino[3,4:1,2][60]fullerene esters

^{t}Bu-pyrrolidino[3,4:1,2][60]fullerene esters were prepared following a similar procedure to that previously described in our research group.[96]

A suspension of a mixture of metal salt (0.023 mmol, 0.1 eq.) and optically pure chiral ligand (0.023 mmol, 0.1 eq.) in anhydrous toluene (50 mL) was prepared. After 30 minutes of stirring at room temperature, α-iminoester **31** (50 mg, 0.228 mmol, 1 eq.) was added to the solution. Later, [60]fullerene (160 mg, 0.228 mmol, 1 eq.) and, only in case it be necessary, Et_3N (0.05 mmol, 0.2 eq.) were added. The purple mixture was stirred at room temperature for 2 hours for *trans* isomers, and cooled to -15°C for 2 hours for *cis* isomers. Longer reaction times favor isomerization processes and formation of bisadducts.

Finally, the solvent was evaporated under vacuum and the dark residue was purified by silica-gel column chromatography using CS_2 as eluent (recovering unreacted [60]fullerene). Then, mixtures of hexane/DCM (2:1 to 1:1) and DCM were employed to obtain the desired products. In all cases, dark brown solids were stable and stored as highly enantioenriched compounds, determined by HPLC analysis.

5.3.1. *cis*-(2*S*)-*terc*-butoxycarbonyl-(5*S*)-phenylpyrrolidino[3,4:1,2][60]fullerene (32) and *cis*-(2*R*)-*terc*-butoxycarbonyl-(5*R*)-phenylpyrrolidino[3,4:1,2][60]fullerene (33)

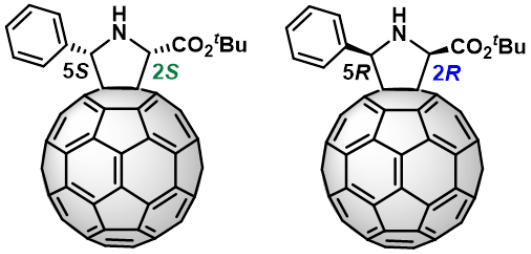

32 (S_{C2}, S_{C5}) 33 (R_{C2}, R_{C5})

The enantiopure products were obtained following the standard procedure as brown solids after flash chromatography in 40-50% isolated yield, using (*R*)-FeSulPhos as chiral ligand and $Cu(OAc)_2$ as metallic salt for compound **32** and (*R*,*R*)-BPE as chiral ligand and Ag(OAc) as metallic salt for compound **33**.

HPLC conditions: chiral column: *Pirkle Covalent* (*R*,*R*) *Whelk-02*; solvents: hexane/IPA (95:5); flow rate: 3.0 mL/min; λ= 320 nm; temperature: 25ºC. $t_R(R_{C2}, R_{C5})$ = 11.0 min, $t_R(S_{C2}, S_{C5})$ = 13.5 min.

^{1}H NMR (700 MHz, 298 K, $CDCl_3$) δ: 7.77 (d, *J* = 7.5 Hz, 2H, Ph), 7.45 (t, *J* = 7.5 Hz, 2H, Ph), 7.37 (t, *J* = 7.5 Hz, 1H, Ph), 5.84 (br s, 1H, C_5H-pyrrolidine), 5.55 (br s, 1H, C_2H-pyrrolidine), 4.04 (br s, 1H, NH), 1.51 (s, 9H, ^{t}Bu).

^{13}C NMR (175 MHz, 298 K, $CDCl_3$) δ: 168.51 (C=O), 153.16, 153.05, 152.39, 150.93, 147.17, 147.06, 146.93, 146.43, 146.32, 146.29, 146.24, 146.22, 146.06, 146.03, 145.93, 145.76, 145.66, 145.60, 145.49, 145.44, 145.36, 145.33, 145.27, 145.24, 145.15, 144.48, 144.43, 144.34, 144.25, 143.16, 143.00, 142.71, 142.64, 142.38, 142.34, 142.22, 142.12, 142.08, 142.04, 141.99, 141.70, 141.59, 139.98, 139.68, 139.66, 138.91, 137.13, 136.21, 136.16, 135.96, 135.41, 128.81 (CH-Ph), 128.72 (CH-Ph), 128.09 (CH-Ph), 83.77 (C-^{t}Bu), 79.68 (C_4sp^3-adduct), 76.01 (C_3sp^3-adduct), 75.89 (C_5H-pyrrolidine), 73.61 (C_2H-pyrrolidine), 28.24 (Me-^{t}Bu).

HRMS (ESI): $[M+H]^+$ m/z calculated for $C_{73}H_{18}NO_2$: 940.13321; found: 940.12899.

ATR-FTIR ν (C=O) = 1733 cm^{-1}.

5.3.2. *trans*-(2*S*)-*terc*-butoxycarbonyl-(5*R*)-phenylpyrrolidino[3,4:1,2][60]fullerene (34) and *trans*-(2*R*)-*terc*-butoxycarbonyl-(5*S*)-phenylpyrrolidino[3,4:1,2][60]fullerene (35)

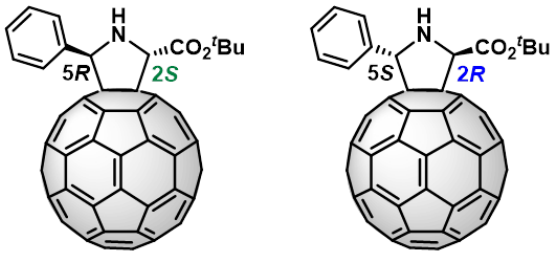

34 (S_{C2}, R_{C5}) 35 (R_{C2}, S_{C5})

The enantioenriched products were obtained following the standard procedure as brown solids after flash chromatography in 15-20% isolated yield, using (*S*)-DTBM-SegPhos as chiral ligand and $Cu(OTf)_2$ as metallic salt for compound **34** and (*R*)-DTBM-SegPhos and $Cu(OTf)_2$ for compound **35**.

HPLC conditions: chiral column: *Pirkle Covalent* (*R,R*) *Whelk-02*; solvents: hexane/IPA (95:5); flow rate: 3.0 mL/min; λ= 320 nm; temperature: 25ºC. t_R(S_{C2}, R_{C5}) = 5.5 min, t_R(R_{C2}, S_{C5}) = 6.7 min.

^{1}H NMR (700 MHz, 298 K, $CDCl_3$) δ: 7.87 (d, *J* = 7.5 Hz, 2H, Ph), 7.42 (t, *J* = 7.5 Hz, 2H, Ph), 7.34 (t, *J* = 7.5 Hz, 1H, Ph), 6.49 (s, 1H, C_5H-pyrrolidine), 5.68 (s, 1H, C_2H-pyrrolidine), 3.60-3.45 (br s, 1H, NH), 1.56 (s, 9H, ^{t}Bu).

^{13}C NMR (175 MHz, 298 K, $CDCl_3$) δ: 171.72, 156.44, 154.17, 153.22, 152.09, 147.40, 147.24, 146.82, 146.51, 146.41, 146.35, 146.26, 146.24, 146.21, 146.11, 145.96, 145.68, 145.56, 145.44, 145.36, 145.32, 145.30, 145.21, 144.90, 144.64, 144.54, 144.46, 144.29, 143.14, 143.08, 142.66, 142.60, 142.31, 142.26, 142.21, 142.16, 142.11, 142.09, 142.06, 141.87, 141.77, 141.57, 140.08, 139.96, 139.60, 139.50, 138.15, 136.42, 136.33, 135.59, 128.56 (CH-Ph), 128.51 (CH-Ph), 83.47 (C-^{t}Bu), 76.16 (C_4sp^3-adduct), 74.36 (C_5H-pyrrolidine), 73.46 (C_3sp^3-adduct), 71.18 (C_2H-pyrrolidine), 28.34 (Me-^{t}Bu).

HRMS (ESI+) $[M+H]^+$ m/z calculated for $C_{73}H_{18}NO_2$: 940.13321; found: 940.12899.

ATR-FTIR ν (C=O) = 1724 cm^{-1}.

5.4. General Procedure for the Synthesis of [(η^n-ring)M(Pyrrolidino[3,4:1,2][60]fullerene carboxylate)Cl]

A solution of the starting ^{t}Bu-pyrrolidino[3,4:1,2][60]fullerene ester (25 mg, 0.027 mmol, 1 eq.) and the corresponding metal dimer (Ir, Rh or Ru, 0.5 eq.) in a mixture of DCM/TFA (2.5 mL, 4:1) was stirred for 2 hours. Finally, the solvent was evaporated under vacuum and the dark residue was purified by silica-gel column chromatography in DCM and mixtures of DCM/MeOH (indicated in each case) to obtain the desired products. In all cases, dark brown solids were obtained and centrifuged in dry MeOH (3 x 2 mL, 15 min at 60 rpm) and dried under vacuum.

Optical purity of the isolated products was determined by HPLC analysis. The enantiomeric excess of the final hybrids is the same as that of the starting ^{t}Bu-pyrrolidino[3,4:1,2][60]fullerene esters employed for their synthesis.

5.4.1. *cis*-[Cp*Ir(Pyrrolidino[3,4:1,2][60]fullerene carboxylate)Cl] 36 (S_{C2}, S_{C5}, S_N, S_{Ir}) and 37 (R_{C2}, R_{C5}, R_N, R_{Ir})

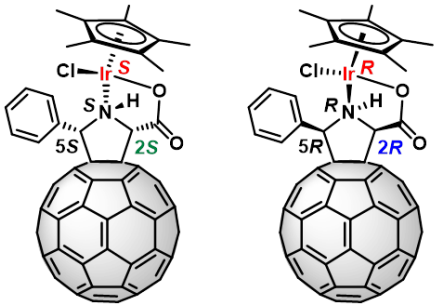

36 (S_{C2}, S_{C5}, S_N, S_{Ir}) 37 (R_{C2}, R_{C5}, R_N, R_{Ir})

The products were obtained following the standard procedure as brown solids after flash chromatography, eluent DCM and DCM/MeOH (50:1) in 77% and 65% isolated yields, respectively. The *ee* values were determined by HPLC.

HPLC conditions: chiral column: *ChiralPack IA*; solvents: DCM/IPA (98:2); flow rate: 1.0 mL/min; λ= 320 nm; temperature: 25ºC. t_R(S_{C2}, S_{C5}, S_N, S_{Ir}) = 7.2 min, t_R(R_{C2}, R_{C5}, R_N, R_{Ir}) = 35.3 min.

^{1}H NMR (700 MHz, 298 K, $CDCl_3$) δ: 8.21 (d, *J* = 7.5 Hz, 1H, Ph), 7.55 (m, 2H, Ph), 7.38 (m, 2H, Ph), 6.88 (t, *J* = 13.1 Hz, 1H, NH), 6.12 (d, *J* = 13.1 Hz,

1H, C_5H-pyrrolidine), 5.69 (d, *J* = 13.1 Hz, 1H, C_2H-pyrrolidine), 1.64 (s, 15H, Me-Cp*).

^{13}C NMR (175 MHz, 298 K, $CDCl_3$) δ: 171.01 (C=O), 151.49, 150.17, 149.96, 149.71, 148.33, 147.89, 147.34, 147.17, 146.54, 146.39, 146.33, 146.27, 146.18, 146.09, 145.92, 145.84, 145.80, 145.72, 145.62, 145.38, 145.34, 144.96, 144.75, 144.51, 144.22, 144.04, 143.02, 142.86, 142.81, 142.77, 142.72, 142.62, 142.45, 142.02, 141.98, 141.78, 141.75, 141.67, 141.60, 141.56, 140.02, 139.83, 139.61, 139.00, 136.51, 136.20, 135.64, 132.69 (C-Ph), 129.77 (CH-Ph), 129.31 (CH-Ph), 129.05 (CH-Ph), 128.75 (CH-Ph), 128.35 (CH-Ph), 85.35 (Cp*), 79.15 (C_4sp^3-adduct), 77.61 (C_5H-pyrrolidine), 77.18 (C_2H-pyrrolidine), 72.28 (C_3sp^3-adduct), 9.42 (Me-Cp*).

MS (MALDI$^+$) $[M\text{-}2H\text{-}Cl]^+$ m/z calculated for $C_{79}H_{21}NO_2Ir$: 1208.1; found: 1208.1. (MALDI$^-$) $[M\text{-}2H]^+$ m/z calculated for $C_{79}H_{21}ClNO_2Ir$: 1243.1; found: 1243.1.

ATR-FTIR ν (C=O) = 1662 cm^{-1}.

5.4.2. *trans*-[Cp*Ir(Pyrrolidino[3,4:1,2][60]fullerene carboxylate)Cl] 38 (S_{C2}, R_{C5}, S_N, S_{Ir}) and 39 (R_{C2}, S_{C5}, R_N, R_{Ir})

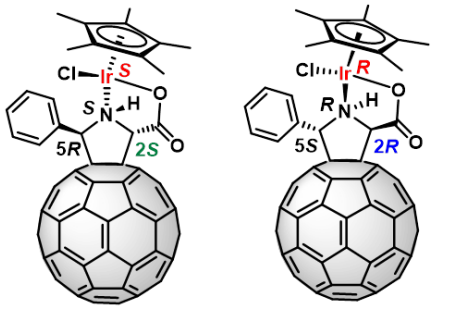

38 (S_{C2}, R_{C5}, S_N, S_{Ir}) 39 (R_{C2}, S_{C5}, R_N, R_{Ir})

The products were obtained following the standard procedure as brown solids (dark red in solution) after flash chromatography, eluent DCM and DCM/MeOH (50:1) in 75% and 68% isolated yields, respectively. The *ee* values were determined by HPLC.

HPLC conditions: chiral column: *ChiralPack IA*; solvents: DCM/IPA (98:2); flow rate: 1.0 mL/min; λ= 320 nm; temperature: 25ºC. t_R(S_{C2}, R_{C5}, S_N, S_{Ir}) = 5.6 min, t_R(R_{C2}, S_{C5}, R_N, R_{Ir}) = 3.9 min.

^{1}H NMR (700 MHz, 298 K, $CDCl_3$) δ: 7.85 (d, *J* = 7.5 Hz, 2H, Ph), 7.52 (t, *J* = 7.5 Hz, 2H, Ph), 7.41 (t, *J* = 7.5 Hz, 1H, Ph), 6.81 (s, 1H, C_5H-pyrrolidine), 5.74 (s, 1H, C_2H-pyrrolidine), 1.97 (s, 15H, Me-Cp*).

^{13}C NMR (175 MHz, 298 K, $CDCl_3$) δ: 183.68 (C=O), 157.93, 153.44, 152.39, 151.94, 148.01, 147.52, 147.33, 147.07, 146.35, 146.29, 146.19, 146.14, 146.00, 145.87, 145.82, 145.47, 145.41, 145.17, 145.08, 144.73, 144.44, 144.26, 144.10, 143.11, 142.99, 142.59, 142.51, 142.19, 142.04, 141.86, 141.75, 140.28, 140.13, 139.96, 139.77, 137.43, 136.19, 136.01, 134.19, 129.00 (CH-Ph), 127.94 (CH-Ph), 127.76 (CH-Ph), 85.17 (Cp*), 85.12 (C_5H-pyrrolidine), 80.32 (C_2H-pyrrolidine), 79.27 (C_4sp^3-adduct), 73.21 (C_3sp^3-adduct), 10.42 (Me-Cp*).

ATR-FTIR ν (C=O) = 1671 cm^{-1}.

5.4.3. *cis*-[Cp*Rh(Pyrrolidino[3,4:1,2][60]fullerene carboxylate)Cl] 40 (R_{C2}, R_{C5}, R_N, R_{Rh}) and 41 (S_{C2}, S_{C5}, S_N, S_{Rh})

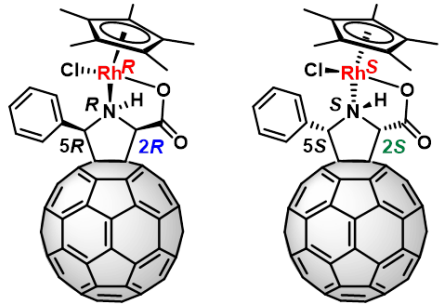

40 (R_{C2}, R_{C5}, R_N, R_{Rh}) 41 (S_{C2}, S_{C5}, S_N, S_{Rh})

The products were obtained following the standard procedure as brown solids after flash chromatography, eluent DCM and DCM/MeOH (50:1 to 20:1) in 70% and 48% isolated yields, respectively. The *ee* values were determined by HPLC.

HPLC conditions: chiral column: *ChiralPack IA*; solvents: DCM/IPA (96:4); flow rate: 1.0 mL/min; λ= 320 nm; temperature: 25ºC. t_R(S_{C2}, S_{C5}, S_N, S_{Rh}) = 7.7 min, t_R(R_{C2}, R_{C5}, R_N, R_{Rh}) = 39.6 min.

^{1}H NMR (700 MHz, 298 K, $CDCl_3$) δ: 8.27 (s, 1H, Ph), 7.60-7.50 (m, 2H, Ph), 7.42-7.30 (m, 2H, Ph), 6.23 (d, *J* = 13.4 Hz, 1H, C_5H-pyrrolidine), 6.08 (t, *J* = 13.4 Hz, 1H, NH), 5.87 (d, *J* = 13.4 Hz, 1H, C_2H-pyrrolidine), 1.67 (s, 15H, Me-Cp*).

^{13}C NMR (175 MHz, 298 K, $CDCl_3$) δ: 170.69 (C=O), 152.20, 150.63, 150.37, 150.11, 148.58, 148.23, 147.27, 147.15, 146.49, 146.41, 146.34, 146.29, 146.25, 146.14, 146.05, 145.88, 145.83, 145.59, 145.55, 145.34, 145.25, 145.10, 144.74, 144.47, 144.22, 144.06, 143.00, 142.84, 142.76, 142.69, 142.59, 142.37, 142.05, 142.01, 141.99, 141.85, 141.75, 141.60, 139.81, 139.60, 138.78, 136.62, 136.57, 136.12, 135.78, 133.14, 129.23 (CH-Ph), 94.13 (Cp*), 79.28 (C_4sp^3-adduct), 77.23 (C_2H-pyrrolidine), 76.18 (C_5H-pyrrolidine), 72.58 (C_3sp^3-adduct), 9.36 (Me-Cp*).

ATR-FTIR ν (C=O) = 1647 cm^{-1}.

5.4.4. *cis*-[(η^6-cymene)Ru (Pyrrolidino[3,4:1,2][60]fullerene carboxylate)Cl] 42 (S_{C2}, S_{C5}, S_N, S_{Ru}) and 43 (R_{C2}, R_{C5}, R_N, R_{Ru})

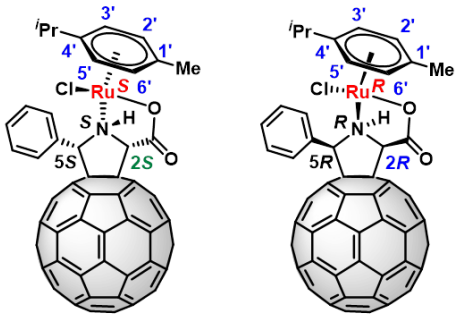

42 (S_{C2}, S_{C5}, S_N, S_{Ru}) 43 (R_{C2}, R_{C5}, R_N, R_{Ru})

The products were obtained following the standard procedure as brown solids after flash chromatography, eluent DCM and DCM/MeOH (50:1) in 83% and 80% isolated yields, respectively. The *ee* values were determined by HPLC.

HPLC conditions: chiral column: *ChiralPack IA*; solvents: DCM/IPA (98:2); flow rate: 1.0 mL/min; λ= 320 nm; temperature: 25ºC. t_R(*S*$_{C2}$, *S*$_{C5}$, *S*$_N$, *S*$_{Ru}$) = 8.9 min, t_R(*R*$_{C2}$, *R*$_{C5}$, *R*$_N$, *R*$_{Ru}$) = 61.3 min.

^{1}H NMR (700 MHz, 298 K, $CDCl_3$) δ: 7.97 (d, *J* = 7.5 Hz, 1H, Ph), 7.76 (d, *J* = 7.3 Hz, 1H, Ph), 7.59 (t, *J* = 7.5 Hz, 1H, Ph), 7.50 (t, *J* = 7.5 Hz, 1H, Ph), 7.47 (t, *J* = 7.5 Hz, 1H, Ph), 6.26 (d, *J* = 13.1 Hz, 1H, C_5H-pyrrolidine), 5.77 (t, *J* = 13.1 Hz, 1H, NH), 5.74 (d, *J* = 5.8 Hz, 1H, $C_{3'\text{-}5'}$Hcym), 5.70 (d, *J* = 5.8 Hz, 1H, $C_{2'\text{-}6'}$Hcym), 5.65 (d, *J* = 13.1 Hz, 1H, C_2H-pyrrolidine), 5.34 (d, *J* = 6.0 Hz, 1H, $C_{3'\text{-}5'}$Hcym), 5.21 (d, *J* = 5.0 Hz, 1H, $C_{2'\text{-}6'}$Hcym), 2.71 (ht, *J* = 7.0 Hz, 1H, CH ^{i}Pr-cym), 2.11 (s, 3H, Me-cym), 1.38 (d, *J* = 6.8 Hz, 3H, Me-^{i}Pr), 1.23 (d, *J* = 6.9 Hz, 3H, Me-^{i}Pr).

^{13}C NMR (175 MHz, 298 K, $CDCl_3$) δ: 170.22 (C=O), 151.43, 150.40, 149.75, 149.47, 148.22, 147.56, 147.37, 147.17, 146.55, 146.41, 146.26, 146.19, 146.10, 145.92, 145.78, 145.73, 145.65, 145.40, 145.36, 145.33, 145.29, 144.88, 144.74, 144.51, 144.21, 144.00, 143.03, 142.86, 142.81, 142.76, 142.72, 142.61, 142.53, 142.02, 141.95, 141.84, 141.73, 141.61, 141.48, 140.15, 139.96, 139.69, 139.14, 136.46, 136.22, 135.35, 132.97 (C-Ph), 129.83, 129.71 (CH-Ph), 129.31 (CH-Ph), 129.12 (CH-Ph), 129.06 (CH-Ph), 128.89 (CH-Ph), 128.25, 104.60 (^{i}Pr-Ccym), 94.43 (Me-Ccym), 82.84 ($C_{2'\text{-}6'}$Hcym), 80.94 ($C_{2'\text{-}6'}$Hcym), 80.31 (C_5H-pyrrolidine), 79.32 (C_4sp^3-adduct), 78.37 ($C_{3'\text{-}5'}$Hcym), 78.15 ($C_{3'\text{-}5'}$Hcym), 77.34 (C_2H-pyrrolidine), 71.79 (C_3sp^3-adduct), 31.24 (CH ^{i}Pr-cymene), 22.54 (Me-^{i}Pr), 22.38 (Me-^{i}Pr), 18.47 (Me-cymene).

HRMS (MALDI+) $[M+Na]^+$ m/z calculated for $C_{79}H_{22}ClNNaO_2Ru$: 1176.0293; found: 1176.0250.

ATR-FTIR ν (C=O) = 1657 cm^{-1}.

5.4.5. *trans*-[(η^6-cymene)Ru (Pyrrolidino[3,4:1,2][60]fullerene carboxylate)Cl] 44 (S_{C2}, R_{C5}, S_N, S_{Ru}) and 45 (R_{C2}, S_{C5}, R_N, R_{Ru})

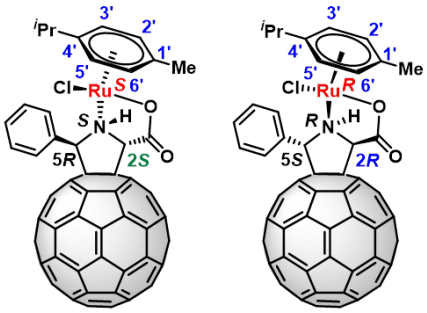

44 (S_{C2}, R_{C5}, S_N, S_{Ru}) 45 (R_{C2}, S_{C5}, R_N, R_{Ru})

The products were obtained following the standard procedure as brown solids after flash chromatography, eluent DCM and DCM/MeOH (50:1) in 62% and 45% isolated yields, respectively. The *ee* values were determined by HPLC.

HPLC conditions: chiral column: *ChiralPack IA*; solvents: DCM/IPA (98:2); flow rate: 1.0 mL/min; λ= 320 nm; temperature: 25ºC. t_R(S_{C2}, R_{C5}, S_N, S_{Ru}) = 10.9 min, t_R(R_{C2}, S_{C5}, R_N, R_{Ru}) = 6.6 min.

^{1}H NMR (700 MHz, 298 K, $CDCl_3$) δ: 7.95 (s, 2H, Ph), 7.68 (s, 2H, Ph), 7.64 (t, *J* = 7.3 Hz, 1H, Ph), 6.03 (d, *J* = 13.6 Hz, 1H, C_5H-pyrrolidine), 5.95 (dd, *J* = 13.6, 6.8 Hz, 1H, NH), 5.84 (d, *J* = 6.8 Hz, 1H, C_2H-pyrrolidine), 5.49 (d, *J* = 5.6 Hz, 1H, $C_{3'\text{-}5'}$Hcym), 5.30 (br s, 1H, $C_{2'\text{-}6'}$Hcym), 5.10 (br s, 1H, $C_{2'\text{-}6'}$Hcym), 4.87 (br s, 1H, $C_{3'\text{-}5'}$Hcym), 3.08 (t, *J* = 7.0 Hz, 1H, CH ^{i}Pr-cym), 2.34 (s, 3H, Me-cym), 1.38 (d, *J* = 7.0 Hz, 3H), 1.37 (d, *J* = 7.0 Hz, 3H).

^{13}C NMR (175 MHz, 298 K, $CDCl_3$) δ: 175.42 (C=O), 155.39, 154.31, 150.51, 149.82, 147.51, 147.27, 146.53, 146.49, 146.22, 146.10, 146.04, 145.97, 145.70, 145.66, 145.58, 145.47, 145.16, 145.10, 144.84, 144.78, 144.53, 144.22, 143.82, 143.37, 143.23, 143.06, 142.91, 142.77, 142.62, 142.49, 142.27, 142.10, 141.90, 141.86, 141.78, 141.65, 141.53, 140.15, 139.96, 139.50, 139.34, 137.31, 136.41, 135.32, 134.29, 133.48, 130.62 (CH-Ph), 129.65 (CH-Ph), 102.73 (HMBC, ^{i}Pr-Ccym), 96.21 (HMBC, Me-Ccym), 83.66 (HSQC, $C_{3'\text{-}5'}$Hcym), 82.97 (HSQC, $C_{2'\text{-}6'}$Hcym), 81.62 (C_5H-pyrrolidine), 79.66 ($C_{2'\text{-}6'}$Hcym), 78.27 (C_4sp^3-adduct), 77.50 ($C_{3'\text{-}5'}$Hcym), 74.77 (C_2H-pyrrolidine), 71.23 (C_3sp^3-adduct), 30.63 (CH ^{i}Pr-cymene), 22.79 (Me-^{i}Pr), 22.14 (Me-^{i}Pr), 18.37 (Me-cymene).

HRMS (MALDI+) $[M+Na]^+$ m/z calculated for $C_{79}H_{22}ClNNaO_2Ru$: 1176.0293; found: 1176.0291.

ATR-FTIR ν (C=O) = 1655 cm^{-1}.

5.5. General Procedure for the Synthesis of Racemic Mixture of *cis*-^{t}Bu-pyrrolidino[3,4:1,2][60]fullerene ester

A suspension of a mixture of Ag(OAc) as metallic salt (0.023 mmol, 0.1 eq.) and dppe as racemic ligand (0.023 mmol, 0.1 eq.) in dry toluene (50 mL) was prepared. After 30 minutes of stirring at room temperature, α-iminoester **31** (50 mg, 0.228 mmol, 1 eq.) was added to the solution. Later, [60]fullerene (160 mg, 0.228 mmol, 1 eq.) was added and the mixture was cooled to -15°C and stirred for 2 hours.

Finally, the solvent was evaporated under vacuum and the dark residue was purified by silica-gel column chromatography using CS_2 as eluent to recover unreacted [60]fullerene. Then, mixtures of hexane/DCM (2:1 to 1:1) and DCM were employed to obtain the product as a brown solid in 40% isolated yield.

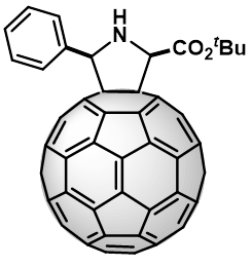

46

5.6. General Procedure for the Synthesis of Racemic Mixture of [(η^n-ring)M(Pyrrolidino[3,4:1,2][60]fullerene carboxylate)Cl]

A solution of the racemic mixture of ^{t}Bu-pyrrolidino[3,4:1,2][60]fullerene ester (25 mg, 0.027 mmol, 1 eq.) and the corresponding metal dimer (Ir, Rh or Ru, 0.5 eq.) in a mixture of DCM/TFA (2.5 mL, 4:1) was stirred for 2 hours. Finally, the solvent was evaporated under vacuum and the dark residue was purified by silica-gel column chromatography in DCM and mixtures of DCM/MeOH (indicated in each case) to obtain the final product. In all cases, dark brown solids were obtained and centrifuged in dry MeOH (3 x 2 mL, 15 min at 60 rpm) and dried under vacuum.

5.6.1. racemic mixture of *cis*-[Cp*Ir(Pyrrolidino[3,4:1,2][60]fullerene carboxylate)Cl] (47)

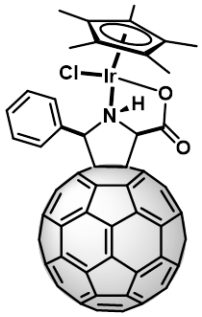

47

The product was obtained following the standard procedure as brown solid after flash chromatography, eluent DCM and DCM/MeOH (50:1) in 75% isolated yield.

5.6.2. racemic mixture of *cis*-[Cp*Rh(Pyrrolidino[3,4:1,2][60]fullerene carboxylate)Cl] (48)

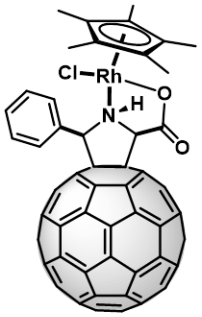

48

The product was obtained following the standard procedure as brown solid after flash chromatography, eluent DCM and DCM/MeOH (50:1 to 20:1) in 60% isolated yield.

5.6.3. racemic mixture of *cis*-[(η^6-cymene)Ru (Pyrrolidino[3,4:1,2][60]fullerene carboxylate)Cl] (49)

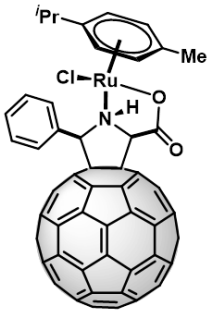

49

The product was obtained following the standard procedure as brown solid after flash chromatography, eluent DCM and DCM/MeOH (50:1) in 55% isolated yield.

5.7. Catalytic Reactions from Fullerene Hybrids

5.7.1. General Procedure for Ketones Reduction with Isopropanol

A suspension of racemic mixture of metallo-fulleropyrrolidines (**47**, **48** and **49**) ($1.6 \cdot 10^{-3}$ mmol, 0.5%), or iridium dimer ($1.6 \cdot 10^{-3}$ mmol, 0.5%), K_2CO_3 ($1.6 \cdot 10^{-3}$ mmol, 0.5%) and acetophenone (0.32 mmol, 1 eq.) in 2 mL of isopropanol was bubbled with argon for 15 min and then, refluxed for 18 hours. Once separated from the catalyst by mechanical means (centrifugation), the product was isolated by solvent evaporation and analyzed by spectroscopic techniques without any further purification.

Recycling Experiments

At the end of the process, the catalyst was precipitated at room temperature by adding methanol to the reaction mixture. The solution was centrifuged at 6000 rpm for 15 minutes (three times) and the catalyst residue was washed to completely remove any remaining products and/or reactants. The isolated solid was reused in a new reaction under identical reaction conditions, observing no change in the catalytic activity.

1-phenylethanol

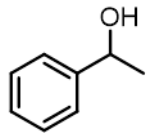

^{1}H NMR (300 MHz, 298 K, $CDCl_3$) δ: 7.38-7.24 (m, 5H), 4.87 (q, 1H, *J* = 6.5 Hz), 2.05 (br s, 1H), 1.48 (d, 1H, *J* = 6.5 Hz).

^{13}C NMR (75 MHz, 298 K, $CDCl_3$) δ: 145.8, 128.4, 127.4, 125.3, 70.3, 25.1.

1-pentanol

^{1}H NMR (300 MHz, 298 K, $CDCl_3$) δ: 3.64 (t, *J* = 6.7 Hz, 2H), 1.58 (m, 2H), 1.39-1.27 (m, 4H), 0.91 (m, 3H).

^{13}C NMR (75 MHz, 298 K, $CDCl_3$) δ: 63.10, 32.51, 27.92, 22.49, 14.04.

Cyclohexanol

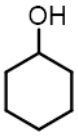

^{1}H NMR (300 MHz, 298 K, $CDCl_3$) δ: 3.62 (s, 1H), 1.90 (m, 2H), 1.72 (m, 2H), 1.25 (m, 6H).

^{13}C NMR (75 MHz, 298 K, $CDCl_3$) δ: 68.87, 40.60, 29.68, 26.71, 25.96.

Cyclohexylmethanol

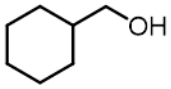

^{1}H NMR (300 MHz, 298 K, $CDCl_3$) δ: 3.42 (d, *J* = 6.0 Hz, 2H), 2.65-2.90 (m, 1H), 1.72-1.75 (m, 6H), 1.42-1.73 (m, 1H), 1.13-1.28 (m, 2H), 0.87-0.96 (m, 2H).

^{13}C NMR (75 MHz, 298 K, $CDCl_3$) δ: 68.87, 40.60, 29.68, 26.71, 25.96.

5.7.2. General Procedure for the *N*-alkylation of Amines with Alcohols by Hydrogen Borrowing Mechanism

N-alkylation was performed into a hermetically sealed vial (1.0 mL). A mixture of amine (1eq.), alcohol (1.2 eq.), K_2CO_3 (same equivalents as that of the catalyst) and catalyst in 0.5 mL of anhydrous toluene, once purged with argon for 10 minutes, was refluxed for 17 hours.

At the end of the process, the reaction mixture was cooled to room temperature and the catalyst was removed by centrifugation. Finally, solvent evaporation yielded the crude residue that was characterized by standard spectroscopic techniques.

***N*-alkylation of Amines with Secondary Alcohols**

In the case of secondary alcohols and amines the reaction was carried out in a ratio 1:1, in 0.1 mL of anhydrous toluene. The reaction mixture was heated at 130ºC and in some cases was needed to add $MgSO_4$ as dehydrating agent.

5.7.2.1. Synthesis of Cp*-Iridium prolinate (50)

The iridium complex **50** was prepared following the methodology described in the literature.[187]

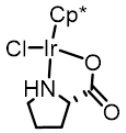

50

^{1}H NMR (300 MHz, 298 K, $CDCl_3$) δ: 3.40 (dd, *J* = 15.6 Hz, *J* = 15.3 Hz, 2H), 1.70 (s, 15H).

5.7.2.2. Synthesis of Amine Compounds

The amine compounds were prepared following the general procedure for the *N*-alkylation of amines with alcohols by hydrogen borrowing mechanism and showed identical spectroscopic properties to the described products.

***N*-(*p*-methoxybenzyl)aniline**

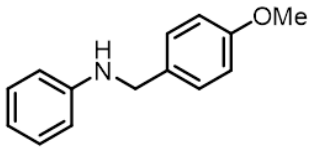

^{1}H NMR (300 MHz, 298 K, $CDCl_3$) δ: 7.25-7.10 (m, 4H), 6.85-6.56 (m, 5H), 4.19 (s, 2H), 3.88 (br, 1H), 3.74 (s, 3H).

_N_-cyclohexylaniline

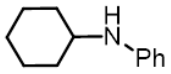

^{1}H NMR (300 MHz, 298 K, $CDCl_3$) δ: 7.17 (t, *J* = 7.9 Hz, 2H), 6.67 (t, *J* = 7.3 Hz, 1H), 6.60 (d, *J* = 7.7 Hz, 2H), 3.52 (s, 1H), 3.27 (tt, *J* = 10.2 Hz, 3.8 Hz, 1H), 2.06-2.09 (m, 2H), 1.78 (dt, *J* = 13.5 Hz, 3.9 Hz, 2H), 1.67 (dt, *J* = 12.8 Hz, 3.8 Hz, 1H), 1.34-1.43 (m, 2H), 1.22-1.28 (m, 1H).

_N_-(1-Methylheptyl)aniline

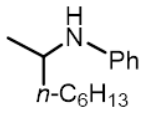

^{1}H NMR (300 MHz, 298 K, $CDCl_3$) δ: 7.05-7.11 (m, 2H), 6.55-6.59 (m, 1H), 6.47-6.50 (m, 2H), 3.36 (sext, *J* = 6.3 Hz, 1H), 3.22 (s, 1H), 1.53-1.57 (m, 2H), 1.16-1.44 (m, 8H), 1.09 (d, *J* = 6.3 Hz, 3H), 0.80 (t, *J* = 6.8 Hz, 3H).

_N_-(1-Ethylbutyl)aniline

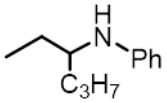

^{1}H NMR (300 MHz, 298 K, $CDCl_3$) δ: 7.15 (td, *J* = 8.7, 1.5 Hz, 2H), 6.64 (tt, *J* = 1.2 Hz, 7.2 Hz, 1H), 6.57 (dd, *J* = 1.2 Hz, 8.5 Hz, 1H), 3.46 (bs, 1H), 3.28 (quint, *J* = 6.0 Hz, 1H), 1.74–1.26 (m, 8H), 0.92 (t, *J* = 7.5 Hz, 3H), 0.89 (t, *J* = 7.2 Hz, 3H).

_N_-(4-Methoxybenzyl)-_N_-methylaniline

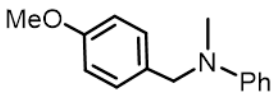

^{1}H NMR (300 MHz, 298 K, $CDCl_3$) δ: 7.18 (t, J=8.0 Hz, 2H), 7.11 (d, J=8.5 Hz, 2H), 6.81 (d, J=8.5 Hz, 2H), 6.73 (d, J=8.0 Hz, 2H), 6.68 (t, J=8.0 Hz, 1H), 4.41 (s, 2H), 3.71 (s, 3H), 2.92 (s, 3H).

***N*-(4-Methoxybenzyl)piperidine**

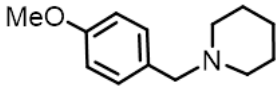

^{1}H NMR (300 MHz, 298 K, $CDCl_3$) δ: 7.22-7.33 (m, 2H), 6.87 (d, *J* = 8.6 Hz, 2H), 3.82 (s, 3H), 3.45 (s, 2H), 2.40 (br s, 4H), 1.3-1.68 (m, 6H).

***N*-cyclohexylbenzylamine**

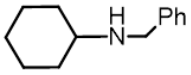

^{1}H NMR (300 MHz, 298 K, $CDCl_3$) δ: 7.33-7.19 (m, 5H), 3.80 (s, 2H), 2.53-2.43 (m, 1H), 1.93-1.89 (m, 2H), 1.75-1.70 (m, 2H), 1.63-1.59 (m, 1H), 1.35-1.04 (m, 6H).

5.7.3. General Procedure for Chirality and Hydrogen Transfer by Formate Dehydrogenation

A mixture of 2-acetylnaphthalene **50** (7 mg, 0.06 mmol) or 2-bromoacetyl pyrene **51** (3 mg, $9 \cdot 10^{-3}$ mmol), HCOONa (20 mg, 0.3 mmol) and optically pure metallo-fulleropyrrolidines (5%) in 0.14 mL of THF in the presence of two drops of water was stirred for 20 hours at room temperature. In some cases, silver fluoride was added to the reaction mixture. The *ee* values and yields were determined by HPLC.

HPLC conditions: chiral column: *ChiralPack IA*; solvents: Hexane/IPA (95:5); flow rate: 1.0 mL/min; λ= 280 nm; temperature: 25ºC.

2-(2-Bromo-1-hydroxy)ethylnaphthalene

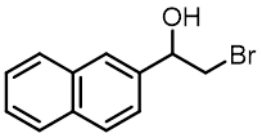

^{1}H NMR (300 MHz, 298K, $CDCl_3$) δ: 7.10-8.10 (m, 7H, Ar), 5.26 (dd, *J* = 7.6 Hz, 4.5 Hz, 1H, CH-OH), 3.50 (d, *J* = 4.5 Hz, 1H, CH_2-Br), 3.47 (d, *J* = 7.6 Hz, 1H, CH_2-Br), 2.80 (s, 1H, OH).

1-(2-bromo-1-hydroxy)ethylpyrene

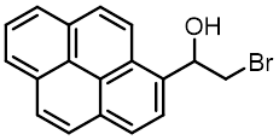

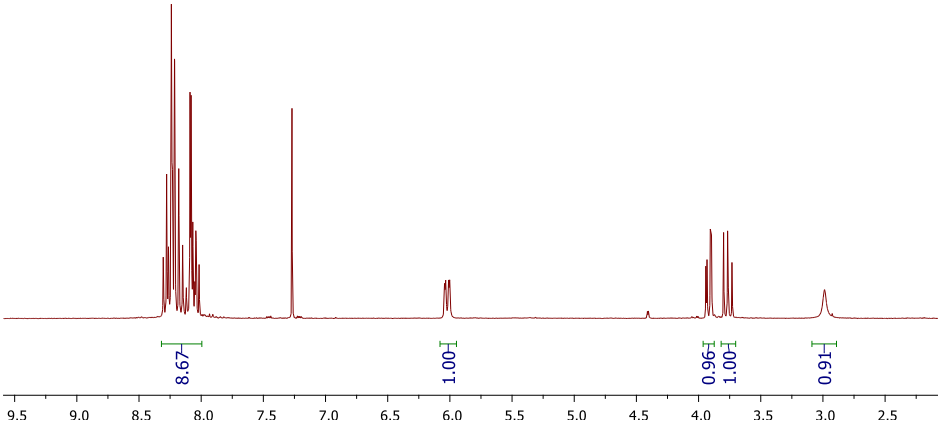

^{1}H NMR (300 MHz, 298K, $CDCl_3$) δ: 8.33-8.00 (m, 9H, Ar), 6.02 (dd, *J* = 9.6 Hz, 2.9 Hz, 1H, CH-OH), 3.92 (dd, *J* = 10.7 Hz, 2.9 Hz, 1H, CH_2-Br), 3.77 (dd, *J* = 10.7 Hz, 9.6 Hz, 1H, CH_2-Br), 2.99 (s, 1H, OH).

^{13}C NMR (75 MHz, 298K, $CDCl_3$) δ: 133.28, 131.43, 130.63, 128.48, 127.87, 127.75, 127.57, 126.29, 125.81, 125.54, 125.29, 125.11, 124.98, 124.89, 123.43, 121.80, 71.45 (CH-OH), 40.13 (CH_2-Br).

HRMS (ESI$^+$) $[M]^+$ m/z calculated for $C_{18}H_{13}BrO$: 324.0144; found: 324.0145.

5.8. Synthesis of Precursors

5.8.1 Synthesis of methyl 4-benzoylbutyrate (54)

To a solution of 4-benzoylbutyric acid (3 g, 15.6 mmol, 1 eq.) in methanol (40 mL), oxalyl chloride (2.97 g, 23 mmol, 1.5 eq.) was added and the reaction mixture was refluxed for 24 hours. The solvent was partially evaporated under vacuum and the residue was extracted into dichloromethane, washed with water/sodium bicarbonate, and dried with anhydrous $MgSO_4$. The solvent was removed under vacuum obtaining an oil in 90% yield.

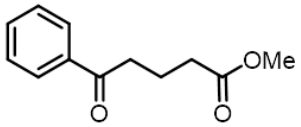

54

^{1}H NMR (300 MHz, 298 K, $CDCl_3$) δ: 7.98 (d, *J* = 8.1 Hz, 2H, Ar), 7.65 (m, 2H), 7.45 (m, 1H), 3.69 (s, 3H, OCH_3), 3.07 (t, *J* = 7.1 Hz, 2H), 2.46 (t, *J* = 7.1 Hz, 2H), 2.09 (q, *J* = 7.1 Hz, 2H).

^{13}C NMR (75 MHz, 298 K, $CDCl_3$) δ: 199.4, 173.7, 136.7, 133.1, 128.6, 128.0, 51.6, 37.4, 33.1, 19.3.

MS (ESI): m/z 206 [M+] calculated for $C_{21}H_{26}O_3$; experimental: m/z 207.

5.8.2. Synthesis of methyl 4-benzoylbutyrate *p*-tosylhydrazone (55)

A mixture of methyl 4-benzoylbutyrate **54** (2.25 g, 11 mmol, 1 eq.) and *p*-toluenesulfonyl hydrazide (3.17 g, 17 mmol, 1.5 eq.) in ethanol (50 mL) was refluxed overnight. After that, the reaction mixture was allowed to reach room temperature and the solvent was partially removed under vacuum. The mixture was introduced into an ice bath and immediately a precipitate was formed. It was filtered and washed with cold ethanol several times obtaining the final product in 90% yield.

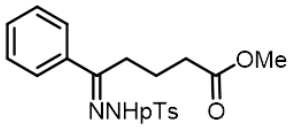

55

^{1}H NMR (300 MHz, 298 K, $CDCl_3$) δ: 9.3 (s, 1H, NH), 7.93 (d, *J* = 8.5 Hz, 2H, *o*-$HArSO_2$-), 7.66 (m, 2H, *o*-HAr), 7.34 (m, 3H), 7.28 (d, *J* = 8.5 Hz, 2H, *m*-$HArSO_2$-), 3.79 (s, 3H, OCH_3), 2.64 (m, 2H, $N{=}CCH_2$), 2.40 (s, 3H, -$ArCH_3$), 2.33 (t, *J* = 6 Hz, 2H, -CH_2CO_2R), 1.69 (m, 2H, -$CH_2CH_2CO_2R$).

^{13}C NMR (75 MHz, 298 K, $CDCl_3$) δ: 174.51, 173.43, 153.90, 156.98, 143.63, 143.95, 136.01, 132.45, 135.77, 135.08, 129.46, 129.36; 129.40, 128.25, 128.35, 127.73, 127.91, 126.06, 126.21, 52.00, 51.35, 32.01, 32.75, 25.70, 36.98, 21.38, 20.77, 20.92.

MS (ESI): m/z 374 [M+] calculated for $C_{19}H_{22}N_2O_4S$; found: 375.

Pf: 123-124 ºC

5.8.3. Synthesis of methyl 5-diazo-5-phenylpentanoate (56)

To a solution of *p*-tosylhydrazone **55** (9 mg, 0.03 mmol) in anhydrous toluene (4 mL), sodium (50-fold) was added and the reaction mixture was refluxed until the color turned red indicating the formation of the diazocompound **56**. Finally, the crude was filtered to remove the solid residues. The compound is highly unstable to light and was impossible to isolate. So, it must be immediately used in the same solution for the next step of synthesis.

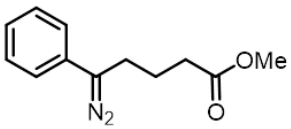

56

5.9. General Procedure of Alkylation Reactions of 4,4'-disubstituted Benzophenones

To a solution of 4,4'-dihydroxybenzophenone (2.14 g, 10 mmol, 1 eq.) in anhydrous DMF (50 mL), potassium carbonate (4.14 g, 30 mmol, 3 eq.), the corresponding halogenated derivative (2.3 eq.) and a spatula tip of sodium iodide were added under inert atmosphere. The mixture was refluxed for 48 hours and the crude was washed with 200 mL of HCl 1M, extracted into dichloromethane and finally washed with water and dried over anhydrous $MgSO_4$. The solvent was removed under reduced pressure and the crude was recrystallized to give a solid residue.

5.9.1. 4,4'-Bis(butoxy)benzophenone (64a)

Following the general alkylation procedure of 4,4'-disubstituted benzophenones, the synthesis of compound **64a** was carried out in 85% yield, using 1-bromobutane as the halogenated derivative.

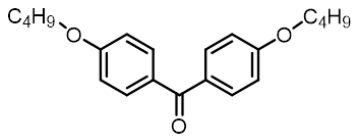

64a

^{1}H NMR (300 MHz, 298 K, $CDCl_3$) δ: 7.35 (d, 2H, *J* = 8.52 Hz, Ar), 6.94 (d, 2H, *J* = 8.52 Hz, Ar), 4.00 (t, 2H, *J* = 6.40 Hz, R-CH_2O), 1.82 (m, 2H, R-CH_2-R), 1.20-1.53 (m, 2H, R-CH_2-R), 0.89 (t, 3H, *J* = 7.40 Hz, CH_3-R).

^{13}C NMR (75 MHz, 298 K, $CDCl_3$) δ: 193.0, 162.4, 132.2, 130.5, 113.9, 68.1, 31.8, 20.3, 14.0.

MS (ESI): [M+] m/z calculated for $C_{21}H_{26}O_3$: 326; found: 327.

Pf: 110-111 ºC

5.9.2. 4,4'-Bis(hexyloxy)benzophenone (64b)

Following the general alkylation procedure of 4,4'-disubstituted benzophenones, the synthesis of compound **64b** was carried out in 86% yield using 1-bromohexane as the halogenated derivative.

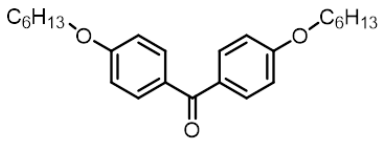

64b

^{1}H NMR (300 MHz, 298 K, $CDCl_3$) δ: 7.37 (d, 2H, *J* = 8.82 Hz, Ar), 6.94 (d, 2H, *J* = 8.82 Hz, Ar), 4.03 (t, 2H, *J* = 6.42 Hz, R-CH_2O), 1.72-1.82 (m, 2H, R-CH_2-R), 1.26-1.50 (m, 6H, R-CH_2-R), 0.93 (t, 3H, *J* = 7.55 Hz, CH_3-R) ppm.

^{13}C NMR (75 MHz, 298 K, $CDCl_3$) δ: 195.4, 162.4, 132.2, 130.5, 113.9, 68.2, 31.5, 29.1, 25.6, 22.5, 14.0.

MS (ESI): [M+] m/z calculated for $C_{25}H_{34}O_3$: 382; found: 383.

Pf: 105-106 ºC

5.10. General Procedure for the Synthesis of 4,4'-disubstituted benzophenone hydrazones

A solution of the corresponding 4,4´-disubstituted benzohydrazine **64a,b** (0.6 g, 1 eq.) and hydrazine monohydrated (12 eq.) in ethanol (40 mL) was refluxed for 2 days. The reaction mixture was gradually warmed to room temperature and the solvent was partially evaporated. Finally was added water and the mixture was cooled in an ice bath obtaining a white solid which was filtered and used without further purification.

5.10.1. 4,4'-Bis(butoxy)benzophenone hydrazone (65a)

Following the general procedure for the preparation of 4,4'-disubstituted benzohydrazines, the synthesis of compound **65a** was carried out in 60% yield.

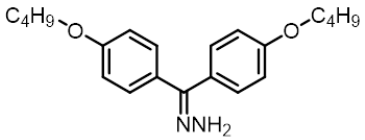

65a

^{1}H NMR (300 MHz, 298 K, $CDCl_3$) δ: 7.42 (d, 2H, *J* = 8.54 Hz, Ar), 7.23 (d, 2H, *J* = 8.54 Hz, Ar), 7.04 (d, 2H, *J* = 8.54 Hz, Ar), 6.83 (d, 2H, *J* = 8.54 Hz, Ar), 4.02 (t, 2H, *J* = 6.32 Hz, R-CH_2O), 3.96 (t, 2H, *J* = 6.32 Hz, R-CH_2O), 1.80 (q, 4H, *J* = 7.27 Hz, R-CH_2-R), 1.53 (m, 4H, R-CH_2-R), 1.03 (t, 3H, *J* = 7.34 Hz, CH_3-R), 0.99 (t, 3H, *J* = 7.34 Hz, CH_3-R).

^{13}C NMR (75 MHz, 298 K, $CDCl_3$) δ: 154.8, 144.2, 131.2, 129.5, 123.5, 67.5, 31.2, 20.0, 14.1.

MS (ESI): [M+] m/z calculated for $C_{21}H_{28}N_2O_2$: 340; found: 341.

Pf: 73-74 ºC

5.10.2. 4,4'-Bis(hexyloxy)benzophenone hydrazone (65b)

Following the general procedure for the preparation of 4,4'-disubstituted benzohydrazines, the synthesis of compound **65b** was carried out in 67% yield.

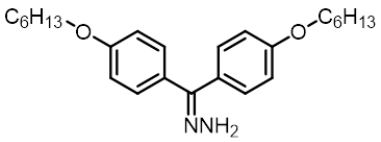

65b

^{1}H NMR (300 MHz, 298 K, $CDCl_3$) δ: 7.39 (d, 2H, *J* = 8.93 Hz, Ar), 7.22 (d, 2H, *J* = 8.93 Hz, Ar), 7.03 (d, 2H, *J* = 8.93 Hz, Ar), 6.81 (d, 2H, *J* = 8.93 Hz, Ar), 4.02 (t, 2H, *J* = 6.54 Hz, R-CH_2O), 3.95 (t, 2H, *J* = 6.54 Hz, R-CH_2O), 1.71-1.89 (m, 4H, R-CH_2-R), 1.29-1.54 (m, 12H, R-CH_2-R), 0.93 (t, 3H, *J* = 7.69 Hz, CH_3-R), 0.91 (t, 3H, *J* = 7.69 Hz, CH_3-R).

^{13}C NMR (75MHz, 298 K, $CDCl_3$) δ: 155.6, 143.2, 132.2, 128.3, 125.5, 68.7, 31.9, 29.2, 25.9, 21.7, 14.1.

MS (ESI): [M+] m/z calculated for $C_{25}H_{36}N_2O_2$: 396; found: 397.

Pf: 70-71 ºC

5.11. General Procedure for Diazocompounds

To a solution of the corresponding hydrazone **66a,b** (0.4 g, 1 eq.) in THF (40 mL), manganese dioxide (5.4 eq.) was added. The mixture was stirred at room temperature for 30 minutes in the dark and, then, was filtered on celite. The solvent was removed under vacuum obtaining the diazocompound as a purple solid that was used without further purification. These compounds are highly unstable to light and must be immediately used for the next step of synthesis.

5.11.1. Bis (4-butoxyphenyl)diazomethane (66a)

Following the general procedure for obtaining diazocompounds, the synthesis of compound **66a** was carried out in 88% yield.

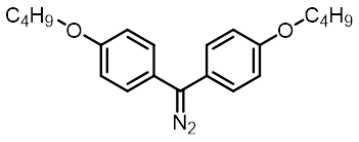

66a

5.11.2. Bis (4-hexyloxyphenyl)diazomethane (66b)

Following the general procedure for obtaining diazocompounds, the synthesis of compound **66b** was carried out in 87% yield.

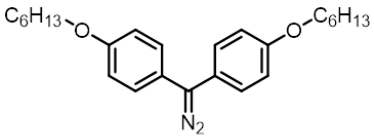

66b

5.12. General Procedure for [5,6]Fulleroids

5.12.1. Synthesis of [70]PCBM [5,6]Fulleroids

To a solution of diazocompound **56** in anhydrous toluene (4 mL) was added C_{70} (10 mg, 0.012 mmol, 1 eq.) under inert atmosphere. The mixture was stirred for 2 minutes at room temperature in the dark. The solvent was removed under vacuum and the crude was purified by silica-gel column chromatography using CS_2 as eluent to recover the unreacted C_{70}, and then, a mixture of solvents (toluene/hexane 8:2) to collect compounds **57**, **58** and **59** in 86% yield (based on recovered C_{70}). The [5,6]fulleroids were isolated by HPLC.

HPLC conditions: column: 5PYE; solvents: toluene/hexane/acetonitrile (60:36:4); flow: 0.5 mL/min; λ= 320 nm; temperature: 25ºC.

Compound 57: *a*-[5,6]PC_{71}BM

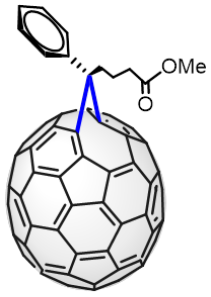

***a*-[5,6]-fulleroid**

57

^{1}H NMR (700 MHz, 298K, $CDCl_3$) δ: 8.48 (d, *J* = 7.1 Hz, 2H), 7.82-7.77 (m, 2H), 7.61-7.56 (m, 1H), 3.64 (s, 3H), 2.22 (m, 2H), 1.65 (m, 2H), 1.43 (m, 2H).

^{13}C NMR (175 MHz, 298 K, $CDCl_3$) δ: 173.1, 151.4, 151.1, 150.6, 150.5, 150.3, 150.0, 148.5, 148.4, 148.0, 147.9, 147.8, 147.7, 147.6, 147.4, 147.2, 147.0, 146.6, 146.5, 145.8, 145.0, 144.9, 144.7, 144.5, 144.4, 144.2, 143.4, 144.1, 142.7, 140.6, 138.9, 138.0, 134.2, 131.9, 132.3, 131.5, 131.1, 129.3, 128.6, 128.3, 127.6, 122.5, 54.2, 51.6, 37.3, 34.0, 20.1.

MS (MALDI TOF): [M^+] m/z calculated for $C_{82}H_{14}O_2$: 1030.099; found: 1030.053.

Compound 58: *b*-[5,6]PC$_{71}$BM

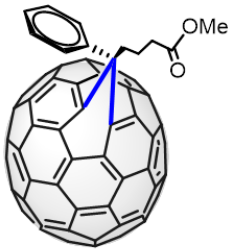

***b*-[5,6]-fulleroid**

58

^{1}H NMR (700 MHz, 298K, $CDCl_3$) δ: 7.99 (m, 2H), 7.58 (m, 2H), 7.47 (m, 1H), 3.71 (s, 3H), 2.22 (m, 2H), 1.58 (m, 2H), 1.44-1.40 (m, 2H).

The yield of compound **58** was too low to obtain a good quality ^{13}C NMR spectrum.

MS (MALDI TOF): [M^+] m/z calculated for $C_{82}H_{14}O_2$: 1030.099; found: 1030.167.

Compound 59: *c*-[5,6]PC$_{71}$BM

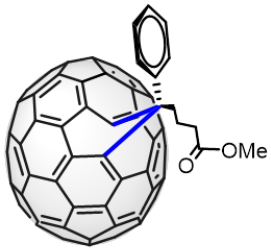

***c*-[5,6]-fulleroid**

59

Due to the small amount of compound **59**, the NMR characterization was not accurate enough for a proper assignation.

MS (MALDI TOF): [M^+] m/z calculated for $C_{82}H_{14}O_2$: 1030.099; found: 1030.120.

5.12.2. Synthesis of [70]DPM [5,6] Fulleroids

Diazocompound **66** (4mg, 0.012 mmol, 1 eq.) was added to a solution of [70]fullerene (10 mg, 0.012 mmol, 1 eq.) in toluene (4 mL). The mixture was stirred at room temperature for 2 min in the dark. Then, the solvent was removed under vacuum, and the crude product was purified by silica-gel column chromatography using CS_2 as eluent to recover the unreacted C_{70}, and a mixture of solvents (hexane/toluene 8:2) to collect compounds **67**, **68** and **69** (72% yield, based on recovered C_{70}) with a small fraction of the [6,6]closed derivatives **70** and **71**, (15% yield, based on recovered C_{70}).

HPLC conditions: column: Buckyprep; solvents: toluene/hexane/acetonitrile (60:36:4); flow: 0.5 ml/min; λ= 320 nm; temperature: 25ºC.

Compound 67: *a*-[5,6]-[70]DPM

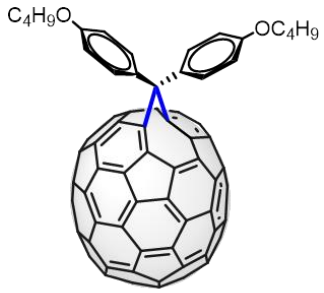

***a*-[5,6]-fulleroid**

67

^{1}H NMR (700 MHz, 298 K, $CDCl_3$) δ: 8.47 (d, *J* = 8.6 Hz, 2H), 7.77 (d, *J* = 8.9 Hz, 2H), 7.19 (dd, *J* = 23.1, 8.1 Hz, 2H), 6.82 (d, *J* = 8.9 Hz, 2H), 4.12 (t, *J* = 6.4 Hz, 2H), 3.91 (dd, *J* = 11.8, 5.3 Hz, 2H), 1.91-1.85 (m, 2H), 1.82-1.78 (m, 2H), 1.74 (dd, *J* = 14.7, 6.9 Hz, 2H), 1.49-1.46 (m, 2H), 1.10-1.06 (t, *J* = 7.4 Hz, 3H), 0.99 (t, *J* = 7.4 Hz, 3H).

^{13}C NMR (175 MHz, 298 K, $CDCl_3$) δ: 157.8, 152.0, 151.0, 150.6, 150.4, 148.5, 148.4, 148.0, 147.9, 147.8, 147.5, 147.3, 147.0, 146.5, 146.4, 146.3, 145.8, 144.8, 144.5, 144.4, 144.1, 144.0, 143.3, 142.8, 140.9, 140.8, 137.4, 134.0, 133.5, 132.4, 132.0, 131.3, 131.2, 130.3, 128.4, 123.8, 115.4, 114.7, 114.2, 67.8, 31.5, 19.5, 14.1.

MS (MALDI TOF) of compounds **67+68+69**: [M^+] m/z calculated for $C_{91}H_{26}O_2$: 1150.193; found: 1150.201.

Compound 68: *b*-[5,6]-[70]DPM

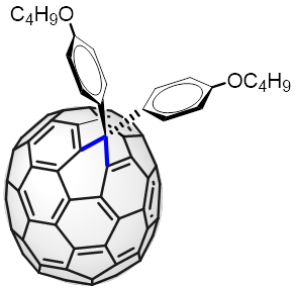

***b*-[5,6]-fulleroid**

68

^{1}H NMR (700 MHz, 298 K, $CDCl_3$) δ: 7.83 (d, *J* = 8.5 Hz, 2H), 7.46 (d, *J* = 8.7 Hz, 2H), 6.98 (d, *J* = 8.7 Hz, 2H), 6.65 (d, *J* = 8.7 Hz, 2H), 4.04 (t, *J* = 6.4 Hz, 2H), 3.81 (t, *J* = 6.4 Hz, 2H), 1.90-1.87 (m, 2H), 1.83-1.80 (m, 2H), 1.75-1.71 (m, 2H), 1.60 (m, 2H), 1.06 (t, *J* = 7.2 Hz, 3H), 0.92 (t, *J* = 7.2 Hz, 3H).

The yield of compound **68** was too low to obtain a good quality ^{13}C NMR spectrum.

Compound 69: *c*-[5,6]-[70]DPM

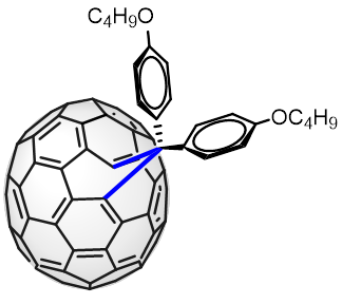

***c*-[5,6]-fulleroid**

69

The yield of compound **69** was too low to obtain a good quality ^{1}H NMR and ^{13}C NMR spectra.

MS (MALDI TOF) of compounds **67+68+69**: [M^+] m/z calculated for $C_{91}H_{26}O_2$: 1150.193; found: 1150.201.

5.13. General Procedure for [6,6]Methanofullerenes

5.13.1. Synthesis of *α*-[6,6]PCBM

To the solution of the diazocompound **56** was added C_{70} (10 mg, 0.012 mmol, 1 eq.) and the mixture was bubbled with argon for 15 minutes in a bath with dry ice and acetone (-78ºC). Finally was incident light wavelength 360 nm for 4 hours in the photoreactor. The solvent was removed under vacuum, and the crude was purified by silica-gel column chromatography using CS_2 as eluent to recover the unreacted C_{70}, and then, a mixture of solvents (toluene/hexane 8:2) to collect compound **60** in 86% yield (based on recovered C_{70}).

HPLC conditions: column: 5PYE; solvents: toluene/acetonitrile (1:1); flow: 1 ml/min; λ= 320 nm; temperature: 25ºC.

Compound 60: *α*-[6,6]PC_{71}BM

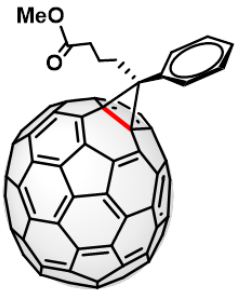

α-siteisomer

60

^{1}H NMR (700 MHz, 298 K, $CDCl_3$) δ: 7.91 (m, 2H, *o*-H Ar), 7.52 (m, 2H, *m*-H Ar), 7.43 (m, 1H, *p*-H Ar), 3.68 (s, 3H, -OCH_3), 2.49 (t, 2H, *J* = 7.6 Hz, R-CH_2-CO_2R), 2.17 (m, 2H, R-CH_2-R), 2.10 (m, 2H, -CH_2-CH_2-CO_2R).

^{13}C NMR (175 MHz, 298 K, $CDCl_3$) δ: 173.3, 155.9, 155.3, 152.2, 151.9, 151.5, 151.2, 151.1, 150.8, 150.5, 149.4, 149.2, 149.1, 148.5, 148.4, 148.3, 148.1, 147.9, 147.6, 147.5, 147.4, 147.0, 146.9, 146.3, 146.1, 145.8, 145.7, 144.9, 144.5, 144.1, 143.9, 143.8, 143.4, 143.3, 142.7, 141.7, 141.6, 140.2, 139.3, 138.9, 137.9, 137.3, 134.0, 132.8, 131.6, 130.8, 130.7, 128.6, 128.2, 71.9, 69.8, 51.7, 35.9, 34.1, 33.8, 32.0, 31.5, 30.2, 29.8, 29.5, 22.8, 21.7, 14.2.

FTIR (KBr, cm^{-1}) ν: 2923, 2854, 1742, 1429, 1266, 754, 606, 577.

MS (MALDI TOF): m/z calculated for $C_{82}H_{14}O_2$:1030.099; found: 1030.090.

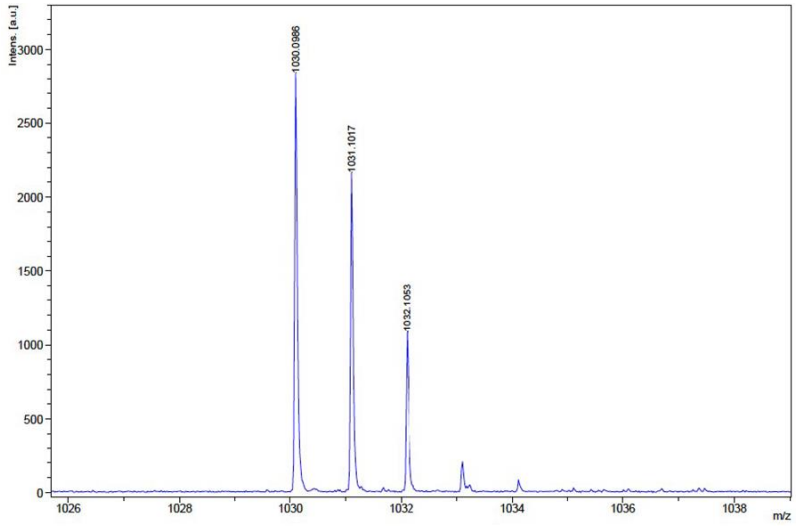

5.13.2. Synthesis of *α*-[6,6]DPM

Diazocompound **66a,b** (4 mg, 1 eq.) was added to a solution of [70]fullerene (10 mg, 0.012 mmol, 1 eq.) in dry toluene (4 mL). The mixture was bubbled with argon for 15 minutes in an ice-salt bath (-20ºC). Finally in the photoreactor was incident light wavelength 360 nm for 4 hours. The solvent was removed under vacuum, and the crude product was purified by silica-gel column chromatography using CS_2 as eluent to recover the unreacted C_{70}, and a mixture of solvents (hexane/toluene 8:2) to collect compound **70a,b** (72% yield, based on recovered C_{70}).

HPLC conditions: column: Buckyprep; solvents: toluene/acetonitrile (90:10); flow: 1 mL/min; λ= 320 nm; temperature: 25ºC.

Compound 70a: *α*-[6,6]DPM4

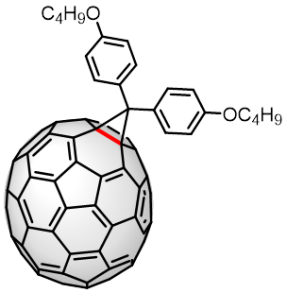

α-siteisomer

70a

^{1}H NMR (700 MHz, 298 K, $CDCl_3$) δ: 7.92 (d, 2H, *J* = 8.75 Hz, Ar), 6.92 (d, 2H, *J* = 8.75 Hz, Ar), 3.97 (t, 2H, *J* = 6.25 Hz, R-CH_2O), 1.78 (m, 2H, R-CH_2-R), 1.49-1.54 (m, 2H, R-CH_2-R), 0.99 (t, 3H, *J* = 7.50 Hz, CH_3-R).

^{13}C NMR (175 MHz, 298 K, $CDCl_3$) δ: 158.6, 155.7, 152.1, 151.5, 151.2, 150.9, 150.6, 149.4, 149.2, 149.1, 148.6, 148.5, 148.4, 148.3, 148.0, 147.5, 147.4, 146.9, 146.4, 146.1, 145.7, 145.5, 144.5, 143.9, 143.8, 143.3, 142.6, 141.7, 141.6, 140.0, 138.8, 133.9, 132.8, 131.8, 131.4, 130.8, 130.7, 130.6, 115.1, 114.7, 71.9, 69.8, 67.7, 40.9, 31.5, 19.5, 14.1.

FTIR (KBr, cm^{-1}) ν: 2924, 2857, 1508, 1461, 1427, 1245, 1174, 753, 605, 576.

MS (MALDI TOF): [M^+] m/z calculated for $C_{91}H_{26}O_2$: 1151.207; found: 1152.151.

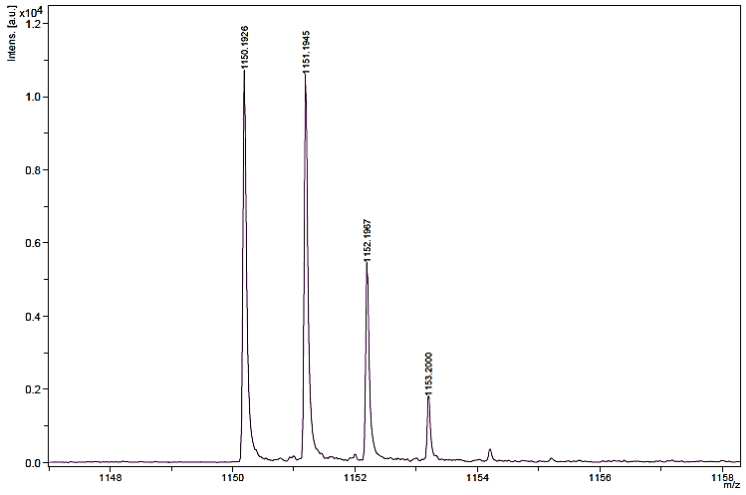

Compound 70b: *α*-[6,6]DPM6

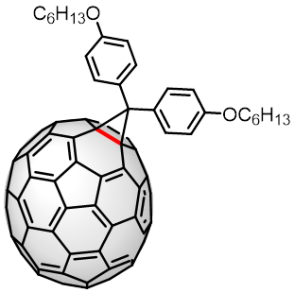

α-siteisomer

70b

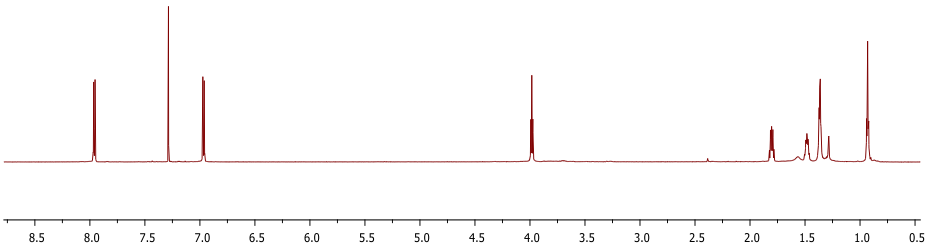

^{1}H NMR (700 MHz, 298 K, $CDCl_3$) δ: 7.80 (d, 2H, *J* = 8.64 Hz, Ar), 6.96 (d, 2H, *J* = 8.64 Hz, Ar), 3.97 (t, 2H, *J* = 6.51 Hz, R-CH_2O), 1.78 (m, 2H, R-CH_2-R), 1.42-1.56 (m, 6H, R-CH_2-R), 0.90 (t, 3H, *J* = 6.86 Hz, CH_3-R).

^{13}C NMR (175 MHz, 298 K, $CDCl_3$) δ: 158.6, 155.7, 152.0, 151.5, 151.2, 150.9, 150.5, 149.4, 149.2, 149.1, 148.6, 148.5, 148.4, 148.3, 148.1, 147.5, 147.4, 146.9, 146.4, 146.0, 145.7, 144.5, 143.9, 143.8, 143.3, 142.6, 141.6, 140.0, 138.9, 133.9, 132.8, 131.8, 131.4, 130.8, 130.7, 130.6, 114.7, 71.9, 69.8, 68.0, 40.9, 31.7, 29.7, 29.4, 25.9, 22.8, 14.2.

FTIR (KBr, cm^{-1}) ν: 2922, 2855, 1506, 1459, 1424, 1243, 1173, 732, 605, 576.

MS (MALDI TOF): [M^+] m/z calculated for $C_{95}H_{34}O_2$: 1206.256; found: 1207.259.

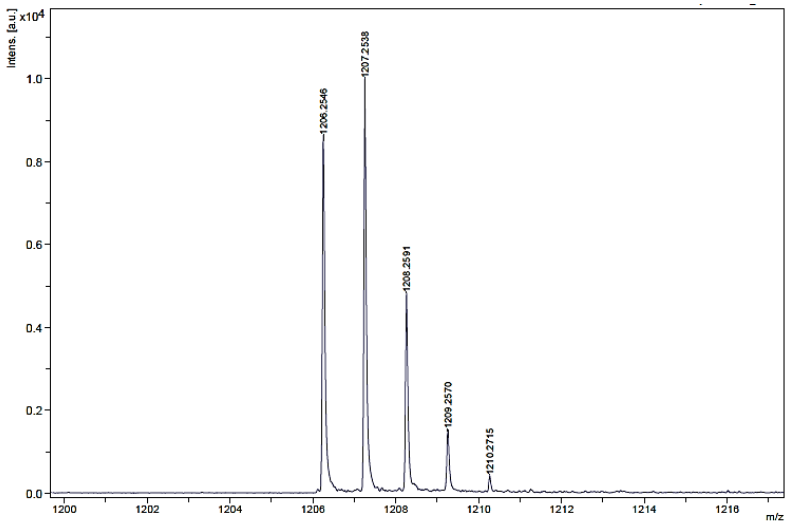

5.14. General Procedure for [6,6]Methanofullerenes from Sulfonium Salts

5.14.1.Synthesis of Methoxycarbonylphenylmethyl(dimethyl)sulfonium tetrafluoroborate (73)

To a solution of methyl α-Br-phenylacetate **72** (229 mg, 1 mmol, 1 eq.) and Me_2S (186 mg, 3 mmol, 3 eq.) in dichloromethane (2.5 mL) was added $AgBF_4$ (195 mg, 1mmol, 1 eq.) at 0ºC. The reaction mixture was stirred and gradually warmed to room temperature for 4 hours. After filtration through celite to remove the precipitate, the solvent was removed under reduced pressure. The residue was washed twice by decantation with hexane.

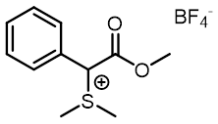

73

^{1}H NMR (300 MHz, 298 K, $CDCl_3$) δ: 7.42-7.55 (m, 5H, Ar), 5.83 (s, 1H, R-CHS-R), 3.84 (s, 3H, R-$COOCH_3$), 3.13 (s, 3H, R-S-CH_3R), 2.69 (s, 3H, R-S-RCH_3).

^{13}C NMR (75 MHz, 298 K, $CDCl_3$) δ: 166.6 131.5, 130.3, 129.6, 162.4, 126.4, 77.5, 63.5, 54.6, 26.3, 24.9, 22.1.

MS (ESI): [M+] m/z calculated for $C_{11}H_{15}O_2S$: 211.08; found: 211.0.

5.14.2. Synthesis of α-[70]Methanofullerene 74

To a solution of sulfonium salt **73** (8 mg, 0.012 mmol, 2 eq.) and C_{70} (5 mg, 0.006 mmol, 1 eq.) in *o*-DCB (2 mL), Et_3N (1.21 mg, 0.012 mmol, 2 eq.) was added at room temperature. The mixture was stirred for 10 minutes, and the solvent was removed under vacuum. The crude product was purified by silica-gel column chromatography using CS_2 as eluent to remove unreacted C_{70}, and then a mixture of solvents (toluene/hexane 8:2) to obtain the product in 70% yield (based on recovered C_{70}).

HPLC conditions: column: 5PYE; solvents: toluene/acetonitrile (1:1); flow: 1 mL/min; λ= 320 nm; temperature: 25ºC.

Compound 74: *α*-[6,6]methanofullerene

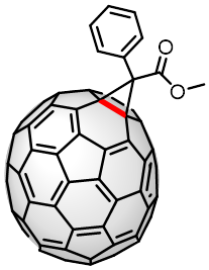

α-siteisomer

74

^{1}H NMR (700 MHz, 298 K, $CDCl_3$) δ: 8.09 (d, 2H, *J* = 7.5 Hz, Ar), 7.54 (t, 2H, *J* = 7.6 Hz, Ar), 7.49 (t, 1H, *J* = 7.4 Hz, Ar), 3.93 (s, 3H).

^{13}C NMR (175 MHz, 298 K, $CDCl_3$) δ: 166.6, 155.5, 155.3, 151.9, 151.8, 151.5, 151.2, 151.1, 150.9, 150.8, 150.6, 150.5, 149.4, 149.2, 149.1, 148.6, 148.5, 148.4, 148.1, 147.7, 147.6, 147.5, 147.4, 147.0, 146.9, 146.4, 145.9, 145.8, 144.9, 144.6, 144.4, 144.0, 143.9, 143.7, 143.6, 143.5, 142.7, 141.9, 141.8, 141.4, 141.2, 140.3, 139.7, 138.3, 137.2, 134.0, 133.8, 132.8, 132.7, 131.9, 130.9, 130.8, 130.7, 129.4, 128.9, 69.2, 67.8, 53.7, 40.5, 29.9.

MS (MALDI TOF): [M^+] m/z calculated for $C_{79}H_8O_2$: 988.052; found: 989.073.

5.15. Synthesis of β-methanofullerenes

To a solution of methyl α-Br-phenylacetate **72** (5.5 mg, 0.024 mmol, 1 eq.) in a mixture *o*-DCB/DMF (0.8 mL/2 mL), DBU (3.6 mg, 0.024 mmol, 1 eq.) and 5 minutes later C_{70} (20 mg, 0.024 mmol, 1 eq.) were added. The reaction mixture was stirred for 5 minutes, and the solvent was removed under vacuum. The crude product was purified by silica-gel column chromatography using CS_2 as eluent to remove unreacted C_{70}, and then a mixture of solvents (toluene/hexane 8:2) to obtain the products in 35% yield.

HPLC conditions: column: 5PYE; solvents: toluene/acetonitrile (1:1); flow: 1 mL/min; λ= 320 nm; temperature: 25ºC.

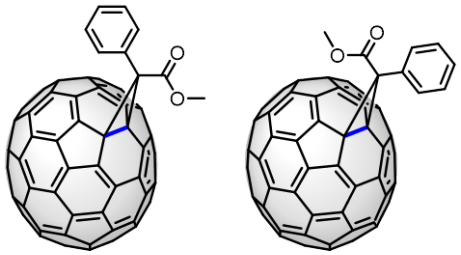

76 β-siteisomers **77**

^{1}H NMR (700 MHz, 298 K, $CDCl_3$) δ: 7.98 (d, 2H, *J* = 7.0 Hz, Ar), 7.56-7.60 (m, 2H, Ar), 7.43-7.45 (m, 2H, Ar), 7.20-7.24 (m, 3H, Ar), 3.96 (s, 3H, CH_3-CO_2), 3.60 (s, 3H, CH_3-CO_2).

^{13}C NMR (175 MHz, 298 K, $CDCl_3$) δ: 151.4, 151.3, 149.9, 149.8, 149.7, 149.6, 149.3, 149.2, 149.1, 148.9, 148.8, 148.7, 148.6, 148.5, 148.4, 148.3, 148.2, 148.1, 147.9, 147.3, 147.2, 147.1, 147.0, 146.9, 146.8, 146.2, 146.0, 145.9, 145.8, 145.6, 145.5, 145.4, 145.3, 144.9, 144.8, 144.7, 144.6, 144.4, 144.3, 144.2, 144.0, 143.9, 143.6, 143.5, 143.3, 143.2, 143.1, 143.0, 142.1, 141.9, 141.7, 141.6, 141.5, 141.4, 140.9, 140.8, 140.0, 139.9, 138.9, 133.5, 132.7, 132.4, 132.2, 132.1, 132.0, 131.9, 131.8, 131.7, 131.3, 131.0, 130.6, 129.5, 129.4, 129.1, 129.0, 128.9, 128.5, 127.9, 127.7, 127.6, 127.2, 127.1, 123.7, 62.9, 53.7, 53.3, 42.6, 29.9, 22.9, 14.4.

MS (MALDI TOF): [M^+] m/z calculated for $C_{79}H_8O_2$: 988.052; found: 989.073.

Compounds 61 and 62: β-[6,6]$PC_{71}BM$

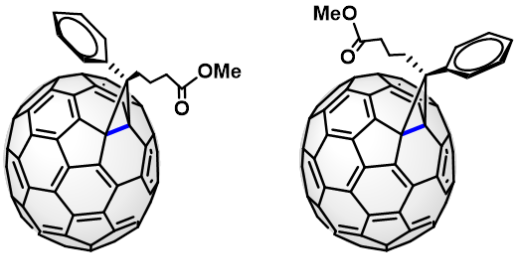

61 β-siteisomers **62**

Mayor β-[6,6]$PC_{71}BM$:

^{1}H NMR (700 MHz, 298K, $CDCl_3$) δ: 7.80 (d, *J* = 7.4 Hz, 2H), 7.58 (t, *J* = 6.8 Hz, 2H), 7.24 (d, *J* = 5.7 Hz, 1H), 3.54 (d, *J* = 1.3 Hz, 3H), 2.57-2.51 (m, 2H), 2.20 (t, *J* = 7.4 Hz, 2H), 2.08-1.99 (m, 2H).

Minor β-[6,6]$PC_{71}BM$:

^{1}H NMR (700 MHz, 298K, $CDCl_3$) δ: 7.54-7.50 (m, 2H), 7.48-7.45 (m, 2H), 7.43 (d, *J* = 7.5 Hz, 1H), 3.54 (d, *J* = 1.3 Hz, 3H), 2.51-2.46 (m, 2H), 2.15-2.09 (m, 2H), 1.88-1.79 (m, 2H).

^{13}C NMR (175 MHz, 298K, $CDCl_3$) of the mixture of **61** and **62**, δ: 14.3, 21.7, 22.2, 33.5, 33.6, 33.8, 35.3, 37.4, 51.4, 51.6, 65.3, 65.6, 127.0, 127.7, 127.8, 127.9, 128.3, 128.3, 128.6, 130.5, 131.2, 131.2, 131.5, 131.6, 131.8, 132.2, 132.2, 132.5, 136.6, 138.0, 139.7, 140.0, 141.2, 141.5, 141.7, 141.8, 142.5, 142.6, 142.7, 142.8, 143.1, 143.5, 144.1, 144.2, 144.3, 144.5, 144.6, 144.8, 144.9, 145.3, 145.5, 145.6, 145.8, 145.9, 146.3, 146.5, 146.8, 147.1, 147.2, 147.9, 148.1, 148.2, 148.2, 148.3, 148.6, 148.8, 149.1, 149.2, 149.3, 149.4, 149.4, 148.5, 149.5, 149.6, 149.7, 149.8, 149.9, 150.0, 151.2, 151.4, 153.2, 172.8, 173.1.

MS (MALDI TOF) of compounds **61+62**: [M^+] m/z calculated for $C_{82}H_{14}O_2$: 1030.099; found: 1030.093.

5.16. Synthesis of α-iminoester Methyl (*E*)-*N*-[(*p*-methoxyphenyl)methylene]glycinate (78)

α-iminoester **78** was synthesized according to the procedure described in the literature which showed identical spectroscopic properties.[177]

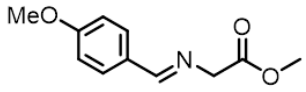

78

^{1}H NMR (300 MHz, 298 K, $CDCl_3$) δ: 8.09 (s, 1H), 7.62 (d, *J* = 8.4 Hz, 2H), 6.82 (d, *J* = 8.4 Hz, 2H), 4.27 (s, 2H), 3.71 (s, 3H), 3.66 (s, 3H).

5.17. General Procedure for the Synthesis of Enantiomerically Pure Endohedral [60]fulleropyrrolidines

A mixture of metal salt (0.0028 mmol, 0.12 eq.) and optically pure chiral ligand (0.0025 mmol, 0.1 eq.) in dry toluene (7 mL) was stirred for 45 min. at room temperature. Then, α-iminoester **78** (0.028 mmol, 1.2 eq.) was added to the solution. Finally, a small amount of Et_3N (in the case of the *trans*-isomers) and a sample composed by C_{60}:HF@C_{60} in a ratio (12:88) (0.025 mmol, 1 eq.) or C_{60}:H_2O@C_{60} in a ratio (25:75) were added. The mixture was stirred at room temperature for 2 hours for *trans* isomers, and cooled to -15°C for 2 hours for *cis* isomers. Afterwards, it was quenched with a saturated ammonium chloride solution (10 mL). The mixture was extracted with toluene (3 x 7 mL), and the combined extracts were washed with brine (10 mL). The organic layer was dried over $MgSO_4$ and the solvent was evaporated under vacuum. Finally, the crude product was purified by silica-gel column chromatography using CS_2 as eluent (recovering unreacted fullerenes) and a mixture of hexane/chloroform (1:1) to obtain the desired product.

5.17.1. Synthesis of HF@*cis*-(2*R*)-Methoxycarbonyl-(5*R*)-(*p*-methoxyphenyl)pyrrolidino[3,4:1,2][60]fullerene (79b) and HF@*cis*-(2*S*)-Methoxycarbonyl-(5*S*)-(*p*-methoxyphenyl)pyrrolidino[3,4:1,2][60]fullerene (80b)

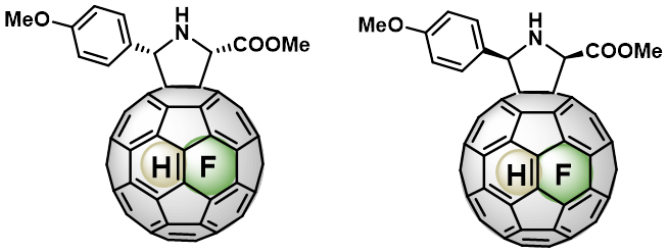

79b *(2R, 5R)* **80b** *(2S, 5S)*

The enantiopure products were obtained following the standard procedure in 55% isolated yield, using (*R,R*)-BPE as chiral ligand and Ag(OAc) as metallic salt for compound **79b** and (*R*)-FeSulPhos as chiral ligand and $Cu(OAc)_2$ as metallic salt for compound **80b**.

HPLC conditions: chiral column: *Pirkle Covalent* (*R,R*) *Whelk-02*; solvents: hexane/methanol (97:3); flow rate: 0.5 mL/min; λ= 320 nm; temperature: 25ºC. t_R(2*R*, 5*R*) = 39.9 min, t_R(2*S*, 5*S*) = 44.5 min.

^{1}H NMR (700 MHz, 298 K, $CDCl_3$) δ: 7.72 (d, *J* = 8.7 Hz, 2H), 6.98 (d, *J* = 8.7 Hz, 2H), 5.84 (d, *J* = 10.2 Hz, 1H), 5.66 (d, *J* = 9.6 Hz, 1H), 3.92 (s, 3H), 3.83 (s, 3H), -5.81 (d, *J* = 505.8 Hz, 1H).

FTIR (KBr, cm^{-1}) ν: 2924, 2854, 1514, 1462, 1258, 799, 744, 607.

HRMS (MALDI TOF): [M+] m/z calculated for $C_{71}H_{14}NO_3F$: 947.0958; found: 948.1031.

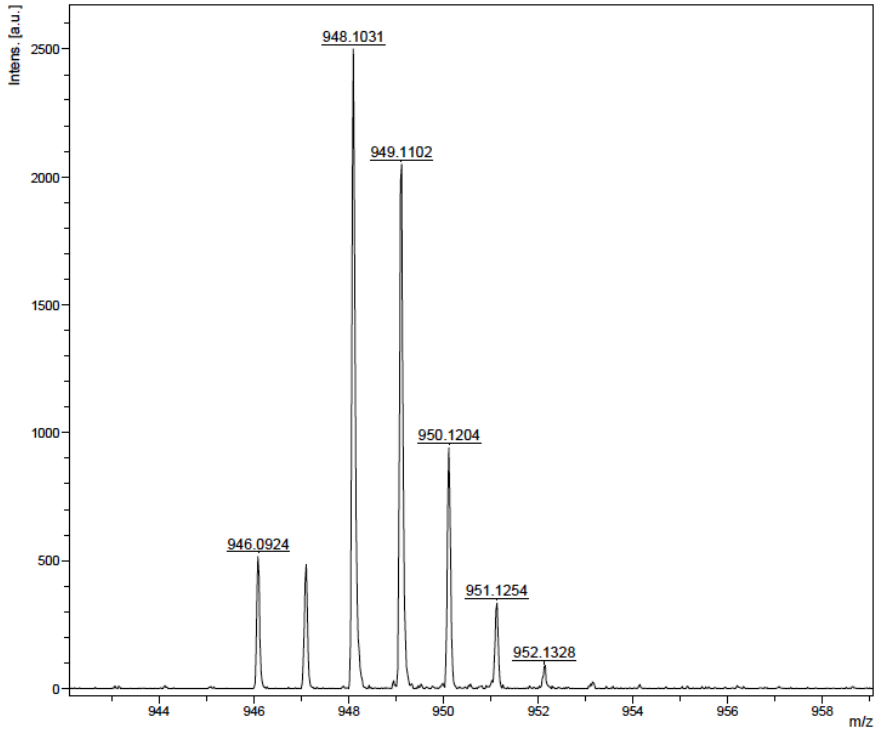

5.17.2. Synthesis of HF@*trans*-(2*R*)-Methoxycarbonyl-(5*S*)-(*p*-methoxyphenyl)pyrrolidino[3,4:1,2][60]fullerene (81b) and HF@*trans*-(2*S*)-Methoxycarbonyl-(5*R*)-(*p*-methoxyphenyl)pyrrolidino[3,4:1,2][60]fullerene (82b)

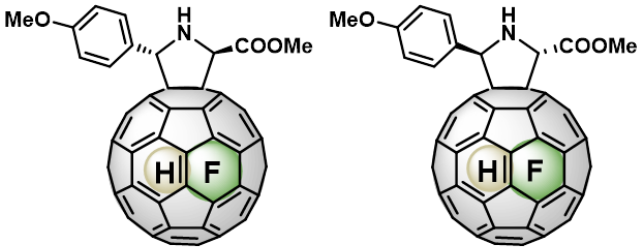

81b (2*R*, 5*S*) **82b (2*S*, 5*R*)**

The enantioenriched products were obtained following the standard procedure in 50% isolated yield, using (*R*)-DTBM-SegPhos as chiral ligand and $Cu(OTf)_2$ as metallic salt for compound **81b** and (*S*)-DTBM-SegPhos and $Cu(OTf)_2$ for compound **82b**.

HPLC conditions: chiral column: *ChiralPack IC*; solvents: hexane/methanol (97:3); flow rate: 0.5 mL/min; λ= 320 nm; temperature: 25ºC. t_R(2*R*, 5*S*) = 26.9 min, t_R(2*S*, 5*S*) = 80.6 min.

^{1}H NMR (700 MHz, 298 K, $CDCl_3$) δ: 7.80 (d, *J* = 8.7 Hz, 2H), 6.96 (d, *J* = 8.7 Hz, 2H), 6.52 (s, 1H), 5.83 (s, 1H), 3.94 (s, 3H), 3.83 (s, 3H), -5.88 (d, *J* = 506.0 Hz, 1H).

FTIR (KBr, cm^{-1}) ν: 2923, 2853, 1513, 1461, 1255, 751, 609.

HRMS (MALDI TOF): [M+] m/z calculated for $C_{71}H_{14}NO_3F$: 947.0958; found: 948.0993.

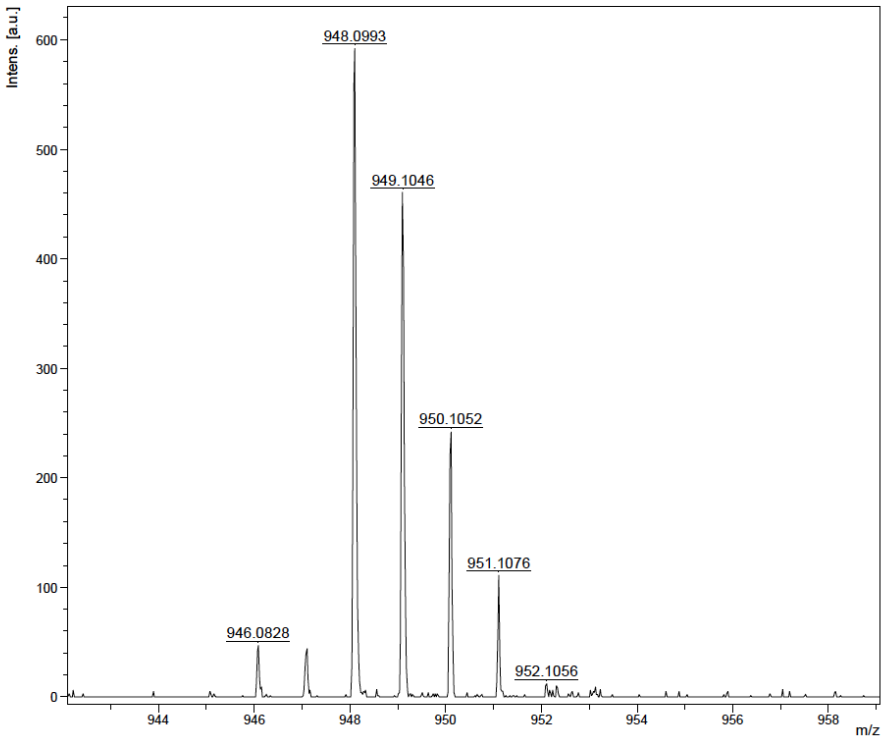

5.17.3. Synthesis of H_2O@*cis*-(2*S*)-Methoxycarbonyl-(5*S*)-(*p*-methoxyphenyl)pyrrolidino[3,4:1,2][60]fullerene (83b)

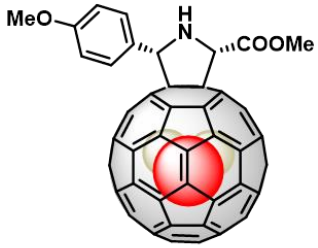

83b *(2S, 5S)*

The enantiopure products were obtained following the standard procedure in 55% isolated yield, using (*R*)-FeSulPhos as chiral ligand and $Cu(OAc)_2$ as metallic salt for compound **83b**.

HPLC conditions: chiral column: *Pirkle Covalent* (*R,R*) *Whelk-02*; solvents: hexane/methanol (97:3); flow rate: 1.25 mL/min; λ= 320 nm; temperature: 25ºC. t_R(2*R*, 5*R*) = 24.0 min, t_R(2*S*, 5*S*) = 28.1 min.

^{1}H NMR (700 MHz, 298 K, $CDCl_3$) δ: 7.77 (d, *J* = 8.6 Hz, 2H), 7.00 (d, *J* = 8.6 Hz, 2H), 5.94 (s, 1H), 5.77 (s, 1H), 3.96 (s, 3H, CH_3O), 3.85 (s, 3H, $COOCH_3$), -7.87 (s, 2H, $H_2O@C_{60}$) ppm.

HRMS (MALDI TOF): $[M+H]^+$ m/z calculated for $C_{71}H_{16}NO_4$: 946.1079; found: 946.1091.

5.17.4. Synthesis of H_2O@*trans*-(2*S*)-Methoxycarbonyl-(5*R*)-(*p*-methoxyphenyl)pyrrolidino[3,4:1,2][60]fullerene (84b)

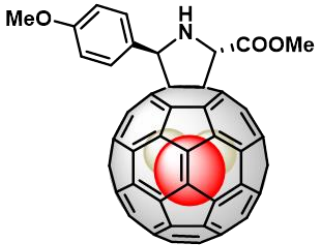

84b (2*S*, 5*R*)

The enantioenriched products were obtained following the standard procedure in 49% isolated yield, using (*S*)-DTBM-SegPhos as chiral ligand and $Cu(OTf)_2$ as metallic salt for compound **84b**.

HPLC conditions: chiral column: *Pirkle Covalent* (*R,R*) *Whelk-02*; solvents: hexane/methanol (97:3); flow rate: 1.25 mL/min; λ= 320 nm; temperature: 25ºC. t_R(2*S*, 5*R*) = 15.9 min, t_R(2*S*, 5*S*) = 17.6 min.

^{1}H NMR (700 MHz, 298 K, $CDCl_3$) δ: 7.81 (d, *J* = 8.4 Hz, 2H), 6.98 (d, *J* = 8.4 Hz, 2H), 6.54 (s, 1H), 5.85 (s, 1H), 3.96 (s, 3H, CH_3O), 3.84 (s, 3H, $COOCH_3$), -7.87 (s, 2H, $H_2O@C_{60}$).

HRMS (MALDI TOF): $[M+H]^+$ m/z calculated for $C_{71}H_{16}NO_4$: 946.1079; found: 946.1092.

5.18. *Cis-trans* Isomerization Reaction

Three solutions of (2*S*,5*S*)-*cis* **80a**, (2*S*,5*S*)-*cis* **80b** and (2*S*,5*S*)-*cis* **83b** in chlorobenzene/acetonitrile 1:1, were prepared at the same time and with exactly the same molar concentration (0.4 mM). They were stirred at 25ºC and the reaction progress was analyzed every 24h by HPLC. (The same experiment was repeated at 30ºC and 40ºC).

HPLC conditions: Buckyprep Waters; solvents: toluene/hexane/acetonitrile (20:70:10); flow rate: 0.5 ml/min; λ= 320 nm; temperature: 25ºC.

CONCLUSIONS

6. CONCLUSIONS

1. Synthesis of Chiral Fullerene/Metal Hybrids

We have carried out the synthesis of a new family of chiral fullerene–metal hybrids namely, iridium, rhodium, and ruthenium pyrrolidino[3,4:1,2][60]fullerene half-sandwich complexes, with a good control over the four new stereogenic centers.

For the first time, chiral fullerene/metal hybrids with a configurationally stable stereogenic metal center, have been synthesized. The stereochemical outcome of the four chiral centers stems from the chiral catalysts employed and the diastereoselective addition of the metal complexes used.

The presence of a repulsive interaction between the lone pair of the chloride ligand and the π-electrons of the adjacent phenyl ring, as well as the stabilizing CH-π interaction between two methyl groups of the Cp^* ligand and the phenyl substituent lead to an exclusive isomer avoiding epimerization processes at the metal.

The stereodivergent control in fullerene derivatives endowed with a chiral metal atom represents a new progress in the synthesis of chiral fullerenes. This easy methodology paves the way toward application of these new fullerene–metal hybrid systems, which are of interest in their own right but are also potential catalysts for a variety of stereochemical reactions.

2. Catalytic Activity of Chiral Fullerene/Metal Hybrids

The novel C_{60}-based catalysts showed high efficiencies in fundamental hydrogen transfer reactions such as the reduction of ketones with isopropanol as hydrogen donor solvent and the *N*-alkylation of amines with alcohols. Remarkably, the use of iridium complexes resulted to be significantly more efficient showing excellent conversion values with low catalyst loadings. Specifically, the hybrid catalysts have shown a remarkable efficiency due to a synergic effect found between the metals and the carbon cage.

Moreover present important advantages compared to other catalysts. In particular, those merged from acting as a molecular homogeneous catalyst with those of heterogeneous catalysts. Considering the solubility of these hybrid

catalysts, products are easily isolated and the catalyst recovered by mechanical means and reused in the same conditions.

Enantioenriched metal-fullerene hybrids have also proven their ability in hydrogen and chirality transfer in ketones reduction. In this regard, the use of sodium formate as the hydrogen donor and rhodium-based hybrids under mild experimental conditions afforded the best results with *ee* values as high as 90%. Interestingly, since the chiral fullerene/metal hybrids are prepared with a control of the stereogenic centers, both alcohols (*R* and *S*) resulting from the ketone reduction, are obtained at will.

Although a lot of chemistry has been carried out with fullerenes, to the best of our knowledge, this is the first time in which fullerene derivatives are directly involved in a catalytic process.

3. Selectivity in Higher Fullerenes

We have described a new approach for selectively obtaining the elusive [5,6]-open derivatives as the principal product of the reaction. Three [70]PCBM-type [5,6]-fulleroids, as well as their analogues of [70]DPM, were formed with a high degree of selectivity. UV-vis spectroscopy and CV electrochemical data clearly confirm their [5,6]-fulleroid nature.

Furthermore, [5,6]-fulleroids could be easily transformed to the respective [6,6]-methanofullerenes by photochemical isomerization. Based on the isomers obtained, the nature of the precursors [5,6]-fulleroids was unambiguously assigned.

A most appealing experimental finding was that the chemical reactivity of the obtained [5,6]-fulleroids was strongly dependent of the position on the fullerene cage (a > b > c > d), thus following a similar trend to that found for the thermal reactivity in pristine [70]fullerene (α > β > γ > δ).

On the other hand, we have developed a new methodology based on mild conditions such as, low temperature and light irradiation, for a site-selective control on [70]fullerene.

In this regard, we have successfully prepared, isolated, and characterized [70]fullerene derivatives with a remarkable high isomeric purity in two different systems, namely α-[70]PCBM and α-[70]DPM (including the X-ray

structure). This unprecedented approach avoids time- and solvent-consuming HPLC separations that are usually employed to obtain these products.

4. Pure Siteisomers on [70]Fullerene for OPV

To demonstrate the correlation between isomeric purity and device performance, some organic devices were fabricated with two different fullerene samples, from pure α-[70]PCBM and its isomeric mixture. According to our preliminary results, α-siteisomer showed better efficiency but no significant differences in the photovoltaic parameters were observed.

5. Effect of the HF on the Chemical Reactivity of HF@C_{60}

We have carried out the first chemical modification on the recently reported HF@C_{60} endohedral by 1,3-dipolar cycloaddition on the fullerene cage. We have also studied the isomerization process from the optically pure (2*S*,5*S*)-*cis*-pyrrolidino[60]fullerene to the (2*S*,5*R*)-*trans*-pyrrolidino[60]fullerene and it has been compared with the empty C_{60} and $H_2O@C_{60}$.

Interestingly, the incarcerated HF molecule contributes to increase the isomerization rate through a weak hydrogen bonding assistance without affecting the final *cis*-*trans* ratio or promoting the loss of enantioselective control through the retro-cycloaddition reaction.

The experimental findings reveal that the two endohedral fullerenes present the highest isomerization rates $H_2O@C_{60}$ > HF@C_{60} > C_{60}, which confirms that the encapsulated molecule plays a significant role in the zwitterionic intermediate stability and, therefore, in the kinetics of the process.

REFERENCES

7. REFERENCES

1) H. W. Kroto, J. R. Heath, S. C. O'Brien, R. F. Curl, R. E. Smalley, *Nature*, **1985**, *318*, 162.

2) W. Krätschmer, L. D. Lamb, K. Fostiropoulos, D. R. Huffman, *Nature*, **1990**, *347*, 354.

3) a) Multi-wall carbon nanotubes: S. Iijima, *Nature*, **1991**, *354*, 56. Single-wall carbon nanotubes: b) S. Iijima, T. Ichihashi, *Nature*, **1993**, *363*, 603. c) D. S. Bethune, C. H. Klang, M. S. de Vries, G. Gorman, R. Savoy, J. Vasquez, R. Beyers, *Nature*, **1993**, *363*, 605.

4) a) K. S. Novoselov, A. K. Geim, S. V. Morozov, D. Jiang, Y. Zhang, S. V. Dubonos, I. V. Grigorieva, A. A. Firsov, *Science*, **2004**, *306*, 666. b) A. K. Geim, K. S. Novoselov, *Nat. Mater.*, **2007**, *6*, 183.

5) J. L. Delgado, M. A. Herranz, N. Martín, *J. Mater. Chem.*, **2008**, *18*, 1417.

6) a) T. Akasaka, S. Nagase, *Endofullerenes: A New Family of Carbon Clusters*, Ed. Kluver Academic Publishers, Dordrecht, The Netherlands, **2002**. b) L. Dunsch, S. Yang, *Small*, **2007**, *3*, 1298. c) M. N. Chaur, F. Melin, A. L. Ortíz, L. Echegoyen, *Angew. Chem. Int. Ed.*, **2009**, *48*, 7514.

7) S. Iijima, M. Yudasaka, R. Yamada, S. Bandow, K. Suenaga, F. Kokai, K. Takahashi, *Chem. Phys. Lett.*, **1999**, *309*, 165.

8) D. Ugarte, *Nature*, **1992**, *359*, 707.

9) D. Larcher, J-M. Tarascon, *Nat. Chem.*, **2015**, *7*, 19.

10) Z. Zhang, L. Wei, X. Qin, Y. Li, *Nano Energy*, **2015**, *15*, 490.

11) A. J. Heeger, *Adv. Mater.*, **2014**, *26*, 10.

12) N. Martín, *Adv. Energy Mater.*, **2016**, 1601102.

13) a) S. Navalon, A. Dhakshinamoorthy, M. Alvaro, H. García, *Chem. Rev*., **2014**, *114*, 6179. b) D. R. Dreyer, C. W. Bielawski, *Chem. Sci*., **2011**, *2*, 1233. c) D. S. Su, S. Perathoner, G. Centi, *Chem. Rev*., **2013**, *113*, 5782. d) C. Su, K. P. Loh, *Acc. Chem. Res*., **2013**, *46*, 2275. e) J. Pyun, *Angew. Chem. Int. Ed*., **2011**, *50*, 46. f) X. Liu, L. Dai, *Nat. Rev. Mater*., **2016**, *1*, 16064.

14) A. Tiwari, S. Titinchi, Advanced Catalytic Materials, Wiley, **2015**.

15) M. Boronat, A. Corma, *Journal of Catalysis*, **2011**, *284*, 138.

16) R. Schloegl, *Advances in Catalysis*, **2013**, *56*, 103.

17) a) D. Haag, H. H. Kung, *Top. Catal*., **2014**, *57*, 762. b) C. J. Shearer, A. Cherevan, D. Eder, *Adv. Mater*., **2014**, *26*, 2295. c) X. K. Kong, C. L. Chen, Q. W. Chen, *Chem. Soc. Rev*., **2014**, *43*, 2841.

18) N. F. Goldshleger, A. P. Moravsky, *Russ. Chem. Rev*., **1997**, *66*, 323.

19) Y. Xu, M. Kraft, R. Xu, *Chem. Soc. Rev*., **2016**, *45*, 3039.

20) a) D. R. Dreyer, H.-P. Jia, C. W. Bielawski, *Angew. Chem. Int. Ed*., **2010**, *49*, 6813. b) C. Huang, C. Li, G. Shi, *Energy Environ. Sci.*, **2012,** *5*, 8848.

21) a) C. S. Yannoni, P. P. Bernier, D. S. Bethune, G. Meijer, J. R. Salem, *J. Am. Chem. Soc*., **1991**, *113*, 3190. b) M. S. Dresselhaus, G. Dresselhaus, P. C. Eklund, Sience of Fullerenes and Carbon Nanotubes, Academic Press, San Diego, **1996**.

22) R. C. Haddon, *Acc. Chem. Res*., **1992**, *25*, 127.

23) T. G. Schmalz, W. A. Seitz, D. J. Klein, G. E. Hite, *Chem. Phys. Lett*., **1986**, *130*, 203.

24) H. W. Kroto, *Nature*, **1987**, *329*, 529.

25) H. Ajie, M. M. Alvarez, S. J. Anz, R. D. Beck, F. Diederich, K. Fostiropoulos, D. R. Huffman, W. Krätschmer, Y. Rubin, K. E. Shriver, D. Sensharma, R. L. Whetten, *J. Phys. Chem*., **1990**, *94*, 8630.

26) D. M. Guldi, *Chem. Commun*., **2000**, *5*, 321.

27) D. M. Guldi, M. Prato, *Acc. Chem. Res*., **2000,** *33*, 695.

28) N. Martín, L. Sánchez, B. Illescas, I. Pérez, *Chem. Rev*., **1998,** *98*, 2527.

29) a) C. A. Reed, R. D. Bolskar, *Chem. Rev*., **2000**, *100*, 1075. b) A. D. J. Haymet, *Chem. Phys. Lett*., **1985**, *122*, 421. c) P. D. Hale, *J. Am. Chem. Soc*., **1986**, *108*, 6087.

30) a) F. Arias, Q. Xie, Y. Wu, Q. Lu, S. R. Wilson, L. Echegoyen, *J. Am. Chem. Soc*., **1994**, *116*, 6388. b) P.-M. Allemand, A. Koch, F. Wudl, Y. Rubin, F. Diederich, M. M. Alvarez, S. J. Anz, R. L. Whetten, *J. Am. Chem. Soc*., **1991**, *113*, 1050.

31) R. E. Haufler, J. Conceicao, L. P. F. Chibante, Y. Chai, N. E. Byrne, S. Flanagan, M. M. Haley, S. C. O'Brien, C. Pan, *J. Phys. Chem*., **1990**, *94*, 8634.

32) Q. Xie, E. Pérez-Cordero, L. Echegoyen, *J. Am. Chem. Soc*., **1992**, *114*, 3978.

33) L. Echegoyen, L. E. Echegoyen, *Acc. Chem. Res*., **1998**, *31*, 593.

34) a) T. Suzuki, Q. Li, K. C. Khemani, F. Wudl, Ö. Almarsson, *Science*, **1991**, *254*, 1186. b) D. M. Guldi, N. Martín, M. A. Herranz, L. Echegoyen, Chapter 9 ¨Fullerenes: From Synthesis to Optoelectronic Properties¨, Kluwer Academic Publishers, Dordrecht, The Netherlands, **2002**.

35) R. C. Haddon, L. E. Brus, K. Raghavachari, *Chem. Phys. Lett*., **1986**, *125*, 459.

36) Q. Xie, F. Arias, L. Echegoyen, *J. Am. Chem. Soc*., **1993**, *115*, 9818.

37) H. Imahori, Y. Sakata, *Eur. J. Org. Chem*., **1999**, *1999*, 2445.

38) a) M. S. Meier, R. G. Bergosh, M. E. Gallagher, H. P. Spielmann, Z. Wang, *J. Org. Chem*., **2002**, *67*, 5946. b) A. Hirsch, *Top. Curr. Chem*., **1999**, *199*, 1. b) A. Hirsch, *Top. Curr. Chem*., **1999**, *199*, 1.

39) J. Nossal, R. K. Saini, L. B. Alemany, M. Meier, W. E. Billups, *Eur. J. Org. Chem*., **2001**, 4167.

40) F. Cataldo, S. Iglesias-Groth, *Fulleranes: The Hydrogenated Fullerenes*, Eds., Springer: Dordrecht, The Netherlands, **2010**.

41) R. M. Baum, *Chem. Eng. News*, **1993**, *22*, 8.

42) R. Taylor, *J. Chem. Soc. Perkin Trans*, **1994**, *2*, 2497.

43) C. C. Henderson, P. A. Cahill, *Science*, **1993**, *259*, 1885.

44) M. S. Meier, P. S. Corbin, V. K. Vance, M. Clayton, M. Mollman, M. Poplawska, *Tetrahedron Lett*., **1994**, *35*, 5789.

45) L. Becker, T. P. Evans, J. L. Bada, *J. Org. Chem*., **1993**, *58*, 7630.

46) A. S. Lobach, A. A. Perov, A. I. Rebrov, O. S. Roschupkina, V. A. Tkacheva, A. N. Stepanov, *Russ. Chem. Bull*., **1997**, *46*, 641.

47) A. D. Darwish, A. K. Abdul-Sada, G. J. Langley, H. W. Kroto, R. Taylor, D. R. M. Walton, *Synth. Met*., **1996**, *77*, 303.

48) A. D. Darwish, A. K. Abdul-Sada, G. J. Langley, H. W. Kroto, R. Taylor, D. R. M. Walton, *J. Chem. Soc. Perkin Trans*., **1995**, *2*, 2359.

49) M. Maggini, G. Scorrano, M. Prato, *J. Am. Chem. Soc*., **1993**, *115*, 9798.

50) a) N. Tagmatarchis, M. Prato, *Synlett*, **2003**, 768. b) M. Prato, M. Maggini, *Acc. Chem. Res*., **1998**, *31*, 519.

51) Although fulleropyrrolidines is usually used, the IUPAC name for these compounds is pyrrolidino[3,4:1,2][60]fullerene.

52) a) P. A. Liddell, D. Kuciauskas, J. P. Sumida, B. Nash, D. Nguyen, A. L. Moore, T. A. Moore, D. Gust, *J. Am. Chem. Soc*., **1997**, *119*, 1400. b) L. Sánchez, M. Sierra, N. Martín, A. J. Myles, T. J. Dale, J. Rebek, W. Seitz, D. M. Guldi, *Angew. Chem. Int. Ed*., **2006**, *45*, 4637.

53) a) J. L. Segura, E. Priego, N. Martín, C. Luo, D. M. Guldi, *Org. Lett*., **2000**, *2*, 4021. b) N. Martín, L. Sánchez, D. M. Guldi, *Chem. Commun*., **2000**, 113. c) M. Segura, L. Sánchez, N. Martín, J. De Mendoza, D. M. Guldi, *Org. Lett*., **2003**, *5*, 557. d) S. González, N. Martín, J. De Mendoza, D. M. Guldi, *Chem. Eur. J*., **2003**, *9*, 2457. e) F. Giacalone, J. L. Segura, N. Martín, D. M. Guldi, *J. Am. Chem. Soc*., **2004**, *126*, 5340. f) F. Giacalone, J. L. Segura, N. Martín, J. Ramey, D. M. Guldi, *Chem. Eur. J*., **2005**, *11*, 4819.

54) a) N. Martín, M. Altable, S. Filippone, A. Martín-Domenech, L. Echegoyen, C. M. Cardona, *Angew. Chem. Int. Ed*., **2006**, *45*, 110. b) O. Lukoyanova, C. M. Cardona, M. Altable, S. Filippone, A. M. Domenech, N. Martín, L. Echegoyen, *Angew. Chem. Int. Ed*., **2006**, *45*, 7430. c) S. Filippone, M. Izquierdo, A. Martín-Domenech, S. Osuna, M. Solá, N. Martín, *Chem. Eur. J*., **2008**, *14*, 5198.

55) a) N. Martín, F. Giacalone, Eds., *Fullerene Polymers. Synthesis, Properties and Applications*, Wiley-VCH, **2009**. b) F. Langa, J.-F. Nierengarten, Eds., *Fullerenes. Principles and Applications*, RSC, Cambridge, Reino Unido, **2011**. c) N. Martín, J. F. Nierengarten, Eds., *Supramolecular Chemistry of Fullerenes and Carbon Nanotubes*, Wiley-VCH, **2012**.

56) N. N. P. Moonen, C. Thilgen, L. Echegoyen, F. Diederich, *Chem. Commun*., **2000**, 335.

57) S. Sinbandhit, J. Hamelin, *J. Chem. Soc. Chem. Commun*., **1977**, 768.

58) N. Martín, M. Altable, S. Filippone, A. Martín-Domenech, R. Martínez-Álvarez, M. Suárez, M. E. Plonska-Brzezinska, O. Lukoyanova, L. Echegoyen, *J. Org. Chem*., **2007**, *72*, 3840.

59) N. Martín, J. L. Segura, F. Wudl, "New Concepts in Diels-Alder Cycloadditions to Fullerenes" in *Fullerenes: From Synthesis to Optoelectronic Properties*, Chapter 3, D. M. Guldi, N. Martín Eds., Kluver Academic Publishers, Dordrecht, Holland, **2002**.

60) J. L. Segura, N. Martín, *Chem. Rev*., **1999**, *99*, 3199.

61) F. Diederich, L. Isaacs, D. Philp, *Chem. Soc. Rev*., **1994**, 243.

62) a) T. Ohno, N. Martín, B. Knight, F. Wudl, T. Suzuki, H. Yu, *J. Org. Chem*., **1996**, *61*, 1306. b) M. H. Hall, H. Lu, P. B. Shevlin, *J. Am. Chem. Soc*., **2001**, *123*, 1349. c) A. B. Smith III, R. M. Strongin, L. Brard, G. T. Furst, W. J. Romanow, K. G. Owens, R. C. King, *J. Am. Chem. Soc*., **1993**, *115*, 5829. d) A. B. Smith III, R. M. Strongin, L. Brard, G. T. Furst, W. J. Romanow, K. G. Owens, R. J. Goldschmidt, R. C. King, *J. Am. Chem. Soc*., **1995**, *117*, 5492. e) L. Isaacs, A. Wehrsig, F. Diederich, *Helv. Chim. Acta*, **1993**, *76*, 1231. f) G. Schick, A. Hirsch, *Tetrahedron*, **1998**, *54*, 4283.

63) a) C. A. Merlic, H. D. Bendorf, *Tetrahedron Lett*., **1994**, *35*, 9529. b) T. S. Fabre, W. D. Treleaven, T. D. McCarley, C. L. Newton, R. M. Landry, M. C. Saraiva, R. M. Strongin, *J. Org. Chem*., **1998**, *63*, 3522. c) N. Dragoe, H. Shimotani, J. Wang, M. Iwaya, A. de Bettencourt-Días, A. Balch, K. Kitazawa, *J. Am. Chem. Soc*., **2001**, *123*, 1294. d) M. Yamada, T. Akasaka, S. Nagase, *Chem. Rev*., **2013**, *113*, 7209.

64) C. Bingel, *Chem. Ber*., **1993**, *126*, 1957.

65) a) F. Wudl, *Acc. Chem. Res*., **1992**, *25*, 157. b) S. Shi, K. C. Khemani, Q. Li, F. Wudl, *J. Am. Chem. Soc*., **1992**, *114*, 10656. c) M. Prato, A. Bianco, M. Maggini, G. Scorrano, C. Toniolo, F. Wudl, *J. Org. Chem*., **1993**, *58*, 5578. d) R. Sijbesma, G. Srdanov, F. Wudl, J. A. Castoro, C. Wilkins, S. H. Friedman, D. L. Decamp, G. L. Kenyon, *J.*

Am. Chem. Soc., **1993**, *115*, 6510. e) T. Suzuki, Q. Li, K. C. Khemani, F. Wudl, O. Almarsson, *J. Am. Chem. Soc*., **1992**, *114*, 7300. f) M. Prato, V. Lucchini, M. Maggini, E. Stimpfl, G. Scorrano, M. Eiermann, T. Suzuki, F. Wudl, *J. Am. Chem. Soc*., **1993**, *115*, 8479. g) J. Osterodt, M. Nieger, P.-M. Windschief, I. Vogtle, *Chem. Ber*., **1993**, *126*, 2331. h) S. R. Wilson, Y. Wu, *J. Chem. Soc. Chem. Commun.*, **1993**, 784. i) M. Prato, T. Suzuki, F. Wudl, V. Lucchini, M. Maggini, *J. Am. Chem. Soc*., **1993**, *115*, 7876. j) J.-F. Nierengarten in *Fullerenes: From Synthesis to Optoelectronic Properties*, Chapter 2, D. M. Guldi, N. Martín, Eds., Kluver Academic Publishers, Dordrecht, Holland, **2002**.

66) R. F. Haldimann, F.-G. Klarner, F. Diederich, *Chem. Commun*., **1997**, 237.

67) A. Skiebe, A. Hirsch, *J. Chem. Soc. Chem. Commun*., **1994**, 335.

68) J. Osterodt, A. Zett, F. Vögtle, *Tetrahedron*, **1996**, *52*, 4949.

69) G. Bertrand, *Carbene Chemistry: From Fleeting Intermediates to Powerful Reagents*, Ed. Marcel Dekker, New York, **2002**.

70) W. R. Bamford, T. S. Stevens, *J. Chem. Soc*., **1952**, 4735.

71) a) R. A. J. Janssen, J. C. Hummelen, F. Wudl, *J. Am. Chem. Soc*., **1995**, 117, 544.

72) a) W. Yan, S. M. Seifermann, P. Pierrat, S. Bräse, *Org. Biomol. Chem*., **2015**, *13*, 25. b) T. M. Figueira-Duarte, J. Clifford, V. Amendola, A. Gegout, J. Olivier, F. Cardinal, M. Meneghetti, N. Armaroli, J. F. Nierengarten, *Chem. Commun*., **2006**, 2054.

73) A. Muñoz, D. Sigwalt, B. M. Illescas, J. Luczkowiak, L. Rodríguez-Pérez, I. Nierengarten, M. Holler, J. Remy, K. Buffet, S. P. Vincent, J. Rojo, R. Delgado, J. Nierengarten, N. Martín, *Nat. Chem.*, **2016**, *8*, 50.

74) a) J. M. Hawkins, A. Meyer, *Science*, **1993**, *260*, 1918. b) R. C. Haddon, G. E. Scuseria, R. E. Smalley, *Chem Phys Lett*., **1997**, *38*,

168. c) J. M. Hawkins, A. Meyer, M. A. Solow, *J. Am. Chem. Soc*., **1993**, *115*, 7499.

75) a) R. C. Haddon, *Science*, **1993**, *261*, 1545.

76) F. Cozzi, W. H. Powell, C. Thilgen, *Pure Appl. Chem*., **2005**, *77*, 843.

77) *Molecular Orbitals and Organic Chemical Reactions*, I. Fleming, Ed., Wiley: Chichester, U.K., **2010**.

78) E. E. Maroto, A. de Cózar, S. Filippone, A. Martín-Domenech, M. Suárez, F. P. Cossío, N. Martín, *Angew. Chem. Int. Ed*., **2011**, *50*, 6060.

79) M. Wienk, J. M. Kroon, W. J. H. Verhees, J. Krol, J. C. Hummelen, P. Van Haal, R. A. J. Janssen, *Angew. Chem. Int. Ed*., **2003**, *42*, 3371.

80) a) M. R. Cerón, M. Izquierdo, Y. Pi, S. L. Atehortúa, L. Echegoyen, *Chem. Eur. J*., **2015**, *21*, 7881. b) M. R. Cerón, M. Izquierdo, A. Aghabali, A. J. Valdez, K. B. Ghiassi, M. M. Olmstead, A. L. Balch, F. Wudl, L. Echegoyen, *J. Am. Chem. Soc*., **2015**, *137*, 7502. c) R. Tao, T. Umeyama, T. Higashino, T. Koganezawa, H. Imahori, *ACS Appl. Mater. Interfaces*, **2015**, *7*, 16676. d) M. R. Cerón, M. Izquierdo, A. Aghabali, S. P. Vogel, M. M. Olmstead, A. L. Balch, L. Echegoyen, *Carbon*, **2016**, *105*, 394.

81) C. Thilgen, I. Gosse, F. Diederich, *Top. Stereochem.*, **2003**, *23*, 1.

82) C. Thilgen, F. Diederich, *Chem. Rev*., **2006,** *106*, 5049.

83) R. Ettl, I. Chao, F. Diederich, R. L. Whetten, *Nature*, **1991**, *353*, 149.

84) T. Nishimura, K. Tsuchiya, S. Ohsawa, K. Maeda, E. Yashima, Y. Nakamura, J. Nishimura, *J. Am. Chem. Soc*., **2004**, *126*, 11711.

85) Z. Zhu, D. I. Schuster, M. E. Tuckerman, *Biochemistry*, **2003**, *42*, 1326.

86) S. H. Friedman, P. S. Ganapathi, Y. Rubin, G. L. Kenyon, *J. Med. Chem*., **1998**, *41*, 2424.

87) Y. Hizume, K. Tashiro, R. Charvet, Y. Yamamoto, A. Saeki, S. Seki, T. Aida, *J. Am. Chem. Soc*., **2010**, *132*, 6628.

88) Y. Wang, J. Xu, Y. Wang, H. Chen, *Chem. Soc. Rev*., **2013**, *42*, 2930.

89) B. Illescas, N. Martín, J. Poater, M. Solà, G. P. Aguado, R. M. Ortuño, *J. Org. Chem*., **2005**, *70*, 6929. b) A. Bianco, M. Maggini, G. Scorrano, C. Toniolo, G. Marconi, C. Villani, M. Prato, *J. Am. Chem. Soc*., **1996**, *118*, 4072. c) J.-F. Nierengarten, V. Gramlich, F. Cardullo, F. Diederich, *Angew. Chem. Int. Ed*., **1996**, *35*, 2101.

90) F. Djojo, A. Hirsch, *Chem. Eur. J*., **1998**, *4*, 344.

91) a) C. Nájera, J. M. Sansano, *Angew. Chem. Int. Ed*., **2005**, *44*, 6272. b) J. Adrio, J. C. Carretero, *Chem. Commun*., **2011**, *47*, 6784. c) S. Cabrera, R. Gómez Arrayas, J. C. Carretero, *J. Am. Chem. Soc*., **2005**, *127*, 16394.

92) a) A. S. Gothelf, K. V. Gothelf, R. G. Hazell, K. A. Jørgensen, *Angew. Chem. Int. Ed*., **2002**, *41*, 4236. b) Y. Oderaotoshi, W. Cheng, S. Fujitomi, Y. Kasano, S. Minakata, M. Komatsu, *Org. Lett*., **2003**, *5*, 5043.

93) a) D. J. Denhart, D. A. Griffith, C. H. Heathcock, *J. Org. Chem*., **1998**, *63*, 9616. b) P. R. Sebahar, R. M. Williams, *J. Am. Chem. Soc*., **2000**, *122*, 5666.

94) S.-H. Wu, W.-Q. Sun, D.-W. Zhang, L.-H. Shu, H.-M. Wu, J.-F. Xu, X.-F. Lao, *J. Chem. Soc. Perkin Trans*., **1998**, *1*, 1733.

95) D. Pantarotto, A. Bianco, F. Pellarini, A. Tossi, A. Giangaspero, I. Zelezetsky, J.-P. Briand, M. Prato, *J. Am. Chem. Soc*., **2002**, *124*, 12543.

96) S. Filippone, E. E. Maroto, A. Martín-Domenech, M. Suárez, N. Martín, *Nat. Chem*., **2009**, *1*, 578.

97) E. E. Maroto, S. Filippone, A. Martín-Domenech, M. Suárez, N. Martín, *J. Am. Chem. Soc*., **2012**, *134*, 12936.

98) E. E. Maroto, S. Filippone, M. Suárez, R. Martínez-Álvarez, A. de Cózar, F. P. Cossío, N. Martín, *J. Am. Chem. Soc*., **2014**, *136*, 705.

99) J. Marco-Martínez, S. Reboredo, M. Izquierdo, V. Marcos, J. L. López, S. Filippone, N. Martín, *J. Am. Chem. Soc*., **2014**, *136*, 2897.

100) a) R. A. Mosey, J. S. Fisk, J. J. Tepe, *Tetrahedron: Asymmetry*, **2008**, *19*, 2755. b) N. M. Hewlett, C. D. Hupp, J. J. Tepe, *Synthesis*, **2009**, *17*, 2825.

101) S. Peddibhotla, J. J. Tepe, *J. Am. Chem. Soc*., **2004**, *126*, 12776.

102) a) A. D. Melhado, M. Luparia, F. D. Toste, *J. Am. Chem. Soc*., **2007**, *129*, 12638. b) A. D. Melhado, G. W. Amarante, Z. J. Wang, M. Luparia, F. D. Toste, *J. Am. Chem. Soc*., **2011**, *133*, 3517.

103) a) B. List, *Chem. Rev*., **2007**, *107*, 5413. b) D. W. C. MacMillan, *Nature*, **2008**, *455*, 304. c) B. Bertelsen, K. A. Jørgensen, *Chem. Soc. Rev*., **2009**, *38*, 2178. d) E. N. Jacobsen, D. W. C. MacMillan, *Proc. Natl. Acad. Sci. USA*, **2010**, *107*, 20618. e) B. List, Asymmetric Organocatalysis, In Topics in Current Chemistry; Springer-Verlag: Berlin Heidelberg, **2010**.

104) J. Marco-Martínez, V. Marcos, S. Reboredo, S. Filippone, N. Martín, *Angew. Chem. Int. Ed*., **2013**, *52*, 5115.

105) B. F. O. Donovan, P. B. Hitchcock, M. F. Meidine, H. W. Kroto, R. Taylor, D. R. M. Walton, *Chem. Commun*., **1997**, 81.

106) a) D. Enders, O. Niemeier, A. Henseler, *Chem. Rev*., **2007**, *107*, 5606. b) X. Bugaut, F. Glorius, *Chem. Soc. Rev*., **2012**, *41*, 3511. c) S. J. Ryan, L. Candish, D. W. Lupton, *Chem. Soc. Rev*., **2013**, *42*, 4906.

107) A. L. Balch, M. Olmstead, *Chem. Rev*., **1998**, *98*, 2123.

108) a) P. J. Fagan, J. C. Calabrese, B. Malone, *Science*, **1991**, *252*, 1160. b) L.-C. Song, G.-F. Wang, P.-C. Liu, Q.-M. Hu, *Organometallics*, **2003**, *22*, 4593. c) L.-C. Song, G.-A. Yu, F.-H. Su, Q.-M. Hu, *Organometallics*, **2004**, *23*, 4192.

109) a) H. Nagashima, A. Nakaota, Y. Saito, M. Kato, T. Kawanishi, K. Itoh, *J. Chem. Soc. Chem. Commun.*, **1992**, 377. b) L.-C. Song, G.-A. Yu, H.-T. Wang, F.-H. Su, Q.-M. Hu, Y.-L. Song, Y.-C. Gao, *Eur. J. Inorg. Chem.*, **2004**, 866. c) L.-C. Song, F.-H. Su, Q.-M. Hu, E. Grigiotti, P. Zanello, *Eur. J. Inorg. Chem.*, **2006**, 422.

110) a) A. L. Balch, J. W. Lee, B. C. Noll, M. Olmstead, *Inorg. Chem.*, **1993**, *32*, 55. b) A. V. Usatov, K. N. Kudin, E. V. Voronstov, L. E. Vinogradova, Y. N. Novikov, *J. Organomet. Chem.*, **1996**, *522*, 147.

111) a) A. L. Balch, V. J. Catalano, J. W. Lee, *Inorg. Chem.*, **1991**, *30*, 3980. b) A. V. Usatov, E. V. Martynova, F. M. Dolgushin, A. S. Peregudov, M. Y. Antipin, Y. N. Novikov, *Eur. J. Inorg. Chem.*, **2002**, 2565. c) A. L. Balch, V. J. Catalano, J. W. Lee, M. Olmstead, S. R. Parkin, *J. Am. Chem. Soc.*, **1991**, *113*, 8953. d) A. L. Balch, A. S. Ginwalla, B. C. Noll, M. M. Olmstead, *J. Am. Chem. Soc.*, **1994**, *116*, 2227.

112) D. M. Thompson, M. Jones, M. C. Baird, *Eur. J. Inorg. Chem.*, **2003**, 175.

113) H. Song, K. Lee, J. T. Park, M.-G. Choi, *Organometallics*, **1998**, *17*, 4477.

114) a) K. Lee, H.-F. Hsu, J. R. Shapley, *Organometallics*, **1997**, *16*, 3876. b) D. M. Guldi, G. M. A. Rahman, R. Marczak, Y. Matsuo, M. Yamanaka, E. Nakamura, *J. Am. Chem. Soc.*, **2006**, *128*, 9420.

115) M. Sawamura, Y. Kuninobu, M. Toganoh, Y. Matsuo, M. Yamanaka, E. Nakamura, *J. Am. Chem. Soc.*, **2002**, *124*, 9354.

116) L.-C. Song, J.-T. Liu, Q.-M. Hu, L.-H. Weng, *Organometallics*, **2000**, *19*, 1643.

117) a) M. Maggini, A. Karlsson, G. Scorrano, G. Sandonà, G. Farnia, M. Prato, *J. Chem. Soc. Chem. Commun*., **1994**, 589. b) M. Iyoda, F. Sultana, S. Sasaki, H. Butenschön, *Tetrahedron Lett*., **1995**, *36*, 579. c) D. Guldi, M. Maggini, G. Scorrano, M. Prato, *J. Am. Chem. Soc*., **1997**, *119*, 974. d) B. Illescas, N. Martín, *J. Org. Chem*., **2000**, *65*, 5728.

118) a) J. D. Crane, P. B. Hitchcok, H. W. Kroto, R. Taylor, D. R. M. Walton, *J. Chem. Soc., Chem. Commun*., **1992**, 1764. b) J. D. Crane, P. B. Hitchcok, *J. Chem. Soc*., *Dalton Trans*., **1993**, 2537. c) M. M. Olmstead, D. A. Costa, K. Maitra, B. C. Noll, S. L. Phillips, P. M. Van Calcar, A. L. Balch, *J. Am. Chem. Soc*., **1999**, *121*, 7090. d) P. D. W. Boyd, C. A. Reed, *Acc. Chem. Res*., **2005**, *38*, 235.

119) N. Martín, M. Altable, S. Filippone, A. Martín-Domenech, *Chem. Commun*., **2004**, 1338.

120) a) N. Martín, M. Altable, S. Filippone, A. Martín-Domenech, *Chem. Commun*., **2004**, 1338. b) N. Martín, M. Altable, S. Filippone, A. Martín-Domenech, A. Poater, M. Solá, *Chem. Eur. J*., **2005**, *11*, 2716.

121) A. R. Tuktarov, V. V. Korolev, U. M. Dzhemilev, *Russian J. Org Chem*., **2010**, *46*, 588.

122) E. Sulman, V. Matveeva, N. Semagina, I. Yanov, V. Bashilov, V. Sokolov, *J. Mol. Cat. A: Chemical*, **1999**, *146*, 257.

123) J. B. Claridge, R. E. Douthwaite, M. L. Green, R. M. Lago, S. C. Tsang, A. P. E. York, J. Mol. *Catal*., **1994**, *89*, 113.

124) R. Malhotra, D. F. McMillen, D. S. Tse, D. C. Lorents, R. S. Ruoff, D. M. Keegan, *Energ. Fuel*, **1993**, *7*, 685.

125) C. Rüchardt, M. Gerst, J. Ebenhoch, H-D. Beckhaus, E. E. B. Campbell, R. Tellgmann, H. Schwarz, T. Weiske, S. Pitter, *Angew. Chem. Int. Ed*., **1993**, *32*, 584.

126) J. Nossal, R. K. Saini, A. K. Sadana, H. F. Bettinger, L. B. Alemany, G. E. Scuseria W. E. Billups, M. Saunders, A. Khong, R. Weisemann, *J. Am. Chem. Soc*., **2001**, *123*, 8482.

127) C. Rüchardt, M. Gerst, J. Ebenhoch, H.-D. Beckhaus, E. E. B. Campbell, R. Tellgman, H. Schwarz, T. Weiske, S. Pitter, *Angew. Chem. Int. Ed*., **1993**, *32*, 584.

128) P. Chen, X. Wu, J. Lin, K. L. Tan, *Science*, **1999**, *285*, 91.

129) L. Baojun X. Zheng, *J. Am. Chem. Soc*., **2009**, *131*, 16380.

130) a) T. Akasaka, F. Wudl, S. Nagase, *Chemistry of Nanocarbons*, Wiley-Blackwell, London, **2010**. b) X. Lu, T. Akasaka, S. Nagase, *Chem. Comm*., **2011**, *47*, 5942.

131) M. Yamada, T. Akasaka, S. Nagase, *Acc. Chem. Res*., **2010**, *43*, 92.

132) X. Lu, T. Akasaka, S. Nagase, *Chem. Commun*., **2012**, *47*, 5942.

133) A. Rodríguez-Fortea, A. L. Balch, J. M. Poblet, *Chem. Soc. Rev*., **2011**, *40*, 3551.

134) L. Dunsch, S. Yang, *Small*, **2007**, *3*, 1298.

135) S. Stevenson, M. A. Mackey, M. A. Stuart, J. P. Phillips, M. L. Easterling, C. J. Chancellor, M. M. Olmstead, A. L. Balch, *J. Am. Chem. Soc*., **2008**, *130*, 11844.

136) Y. Chai, T. Guo, C. Jin, R. E. Haufler, L. P. F. Chibante, J. Fure, L. Wang, J. M. Alford, R. E. Smalley, *J. Phys. Chem*., **1991**, *95*, 7564.

137) L. Feng, T. Tsuchiya, T. Wakahara, T. Nakahodo, Q. Piao, Y. Maeda, T. Akasaka, T. Kato, K. Yoza, E. Horn, N. Mizorogi, S. Nagase, *J. Am. Chem. Soc*., **2006**, *128*, 5990.

138) a) Y. Murata, M. Murata, K. Komatsu, *J. Am. Chem. Soc*., **2003**, *125*, 7152. b) K. Komatsu, M. Murata, Y. Murata, *Science*, **2005**, *307*, 238.

139) Y. Morinaka, F. Tanabe, M. Murata, Y. Murata, K. Komatsu, *Chem. Commun*., **2010**, *46*, 4532.

140) K. Kurotobi, Y. Murata, *Science*, **2011**, *333*, 613.

141) a) Y. Rubin, *Chem. Eur. J*., **1997**, *3*, 1009. b) G. Schick, T. Jarrosson, Y. Rubin, *Angew. Chem. Int. Ed*., **1999**, *38*, 2360.

142) a) M. R. Cerón, M. Izquierdo, M. Garcia-Borràs, S. S. Lee, S. Stevenson, S. Osuna, L. Echegoyen, *J. Am. Chem. Soc*., **2015**, *137*, 11775. b) M. Yamada, T. Wakahara, T. Nakahodo, T. Tsuchiya, Y. Maeda, T. Akasaka, K. Yoza, E. Horn, N. Mizorogi, S. Nagase, *J. Am. Chem. Soc*., **2006**, *128*, 1402. c) M. Yamada, M. Okamura, S. Sato, C. I. Someya, N. Mizorogi, T. Tsuchiya, T. Akasaka, T. Kato, S. Nagase, *Chem. Eur. J*., **2009**, *15*, 10533. d) M. Izquierdo, M. R. Cerón, M. M. Olmstead, A. L. Balch, L. Echegoyen, *Angew. Chem. Int. Ed*., **2013**, *52*, 11826.

143) E. E. Maroto, M. Izquierdo, M. Murata, S. Filippone, K. Komatsu, Y.Murata, N. Martín, *Chem. Commun*., **2014**, *50*, 740.

144) E. E. Maroto, J. Mateos, M. Garcia-Borràs, S. Osuna, S. Filippone, M. A. Herranz, Y. Murata, M. Solà, N. Martín, *J. Am. Chem. Soc*., **2015**, *137*, 1190.

145) A. Krachmalnicoff, R. Bounds, S. Mamone, S. Alom, M. Concistrè, B. Meier, K. Kouřil, M. E. Light, M. R. Johnson, S. Rols, A. J. Horsewill, A. Shugai, U. Nagel, T. Rõõm, M. Carravetta, M. H. Levitt, R. J. Whitby, *Nat. Chem*., **2016**, *8*, 953.

146) N. Armaroli, V. Balzani, *Angew. Chem. Int. Ed*., **2007**, *46*, 52.

147) D. M. Chapin, C. S. Fuller, G. L. Pearson, *J. Appl. Chem*., **1954**, *25*, 676.

148) M. T. Rispens, A. Meetsma, R. Rittberger, C. J. Brabec, N. S. Sariciftci, J. C. Hummelen, *Chem. Commun*., **2003**, 2116.

149) a) J. L. Delgado, P.-A. Bouit, S. Filippone, M. A. Herranz, N. Martín, *Chem. Commun*., **2010**, *46*, 4853. b) G. Dennler, M. C. Scharber, C. J. Brabec, *Adv. Mater*., **2009**, *21*, 1323. c) B. Kippelen, J.-J. Brédas, *Energy Environ. Sci*., **2009**, *2*, 251. d) B. C. Thompson, J. M. J. Fréchet, *Angew. Chem. Int. Ed*., **2008**, *47*, 58.

150) a) G. Yu, J. Gao, J. C. Hummelen, F. Wudl, A. J. Heeger, *Science*, **1995**, *270*, 1789. b) S. Gunes, H. Neugebauer, S. Sariciftci Niyazi, *Chem Rev*., **2007**, *107*, 1324.

151) a) L.-M. Chen, Z. Hong, G. Li, Y. Yang, *Adv. Mater*., **2009**, *21*, 1434. b) M. T. Dang, L. Hirsch, G. Wantz, J. D. Wuest, *Chem. Rev*., **2013**, *113*, 3734.

152) H. Hoppe, N. S. Sariciftci, *J. Mater. Chem*., **2004**, *19*, 1924.

153) S. E. Shaheen, C. J. Brabec, N. S. Sariciftci, F. Padinger, T. Fromherz, J. C. Hummelen, *Appl. Phys. Lett.*, **2001**, *78*, 841.

154) C. J. Brabec, A. Cravino, D. Meissner, N. S. Sariciftci, T. Fromherz, M. T. Rispens, L. Sánchez , J. C. Hummelen, *Adv. Funct. Mater*., **2001**, *11*, 374.

155) L. J. A. Koster, V. D. Mihailetchi, P. W. M. Blom, *Appl. Phys. Lett*., **2006**, *88*, 052104.

156) a) F. Zhang, W. Mammo, L. M. Andresson, S. Admassie, M. R. Andresson, O. Inganäs, *Adv. Mater*., **2006**, *18*, 2169. b) O. Inganäs, F. Zhang, M. R. Andersson, *Acc. Chem. Res*., **2009**, *42*, 1731.

157) J. C. Hummelen, B. W. Knight, F. LePeq, F. Wudl, J. Yao, C. L. Wilkins, *J. Org. Chem*., **1995**, *60*, 532.

158) G. Yu, J. Gao, J. C. Hummelen, F. Wudl, A. J. Heeger, *Science*, **1995**, *270*, 1789.

159) a) F. Padinger, R. S. Rittberger, N. S. Sariciftci, *Adv. Funct. Mater*., **2003**, *13*, 85. b) P. Schilinsky, C. Waldauf, C. J. Brabec, *Appl. Phys. Lett*., **2002**, *81*, 3885.

160) T. J. Prosa, M. J. Winokur, M. M. Moulton, P. Smith, A. J. Heeger, *Macromolecules*, **1992**, *25*, 4364.

161) D. Fernández, A. Viterisi, J. W. Ryan, F. Gispert-Guirado, S. Vidal, S. Filippone, N. Martín, E. Palomares, *Nanoscale*, **2014**, *6*, 5871.

162) a) I. Riedel, E. von Hauff, J. Parisi, N. Martín, F. Giacalone, V. Diakonov, *Adv. Funct. Mater*., **2005**, *15*, 1979. b) A. Sánchez-Díaz, M. Izquierdo, S. Filippone, N. Martín, E. Palomares, *Adv. Funct. Mater*., **2010**, *20*, 2695.

163) S. Backer, K. Sivula, D. F. Kavulak, J. M. J. Fréchet, *Chem. Mater*., **2007**, *19*, 2927.

164) J. W. Arbogast, C. S. Foote, *J. Am. Chem. Soc*., **1991**, *113*, 886.

165) S. H. Park, A. Roy, S. Beaupré, S. Cho, N. Coates, J. S. Moon, D. Moses, M. Leclerc, K. Lee, A. J. Heeger, *Nat. Photonics*, **2009**, *3*, 297.

166) F. B. Kooistra, V. D. Mihailetchi, L. M. Popescu, D. Kronholm, P. W. M. Blom, J. C. Hummelen, *Chem. Mater*., **2006**, *18*, 3068.

167) J. Zhao, Y. Li, G. Yang, K. Jiang, H. Lin, H. Ade, W. Ma, H. Yan, *Nat. Energy*, **2016**, *1*, 15027.

168) A. Kojima, K. Teshima, Y. Shirai, T. Miyasaka, *J. Am. Chem. Soc*., **2009**, *131*, 6050.

169) N. J. Jeon, J. H. Noh, W. S. Yang, Y. C. Kim, S. Ryu, J. Seo, S. I. Seok, *Nature*, **2015**, *517*, 476.

170) K. Wojciechowski, T. Leijtens, S. Siprova, C. Schlueter, M. T. Hçrantner, J. T.-W. Wang, C.-Z. Li, A. K. Y. Jen, T.-L. Lee, H. J. Snaith, *J. Phys. Chem. Lett*., **2015**, *6*, 2399.

171) a) C. L. Chochos, N. Tagmatarchis, V. G. Gregoriou, *RSC Adv*., **2013**, *3*, 7160. b) Y.-J. Hwang, B. A. E. Courtright, A. S. Ferreira, S. H. Tolbert, S. A. Jenekhe, *Adv. Mater*., **2015**, *27*, 4578.

172) J. Y. Jeng, Y. F. Chiang, M. H. Lee, S. R. Peng, T. F. Guo, P. Chen, T. C. Wen, *Adv. Mater*., **2013**, *25*, 3727. b) O. Malinkiewicz, A. Yella, Y. H. Lee, G. M. Espallargas, M. Grätzel, M. K. Nazeeruddin, H. J. Bolink, *Nat. Photon*., **2014**, *8*, 128.

173) a) M.-F. Lo, Z.-Q. Guan, T.-W. Ng, C.-Y. Chan, C.-S. Lee, *Adv. Funct. Mater*., **2015**, *25*, 1213.

174) a) V. V. Bashilov, P. V. Petrovskii, V. L. Sokolov, F. M. Dotgushin, A. L. Yanovsky, Y. T. Struchkov, *Russ. Chem. Bull*., **1996**, *45*, 1207. b) V. I. Sokolov, V. V. Bashilov, F. M. Dolgushin, N. V. Abramova, K. K. Babievsky, A. G. Ginzburg, P. V. Petrovskii, *Tetrahedron Lett*., **2009**, *50*, 5347. c) V. V. Bashilov, P. V. Petrovskii, V. I. Sokolov, *Russ. Chem. Bull*., **1993**, *42*, 392.

175) a) E. B. Bauer, *Chem. Soc. Rev*., **2012**, *41*, 3153. b) C. Tian, L. Gong, E. Meggers, *Chem. Commun*., **2016**, *52*, 4207. c) C. Ganter, *Chem. Soc. Rev*., **2003**, *32*, 130. d) H. Brunner, *Angew. Chem. Int. Ed*., **1999**, *38*, 1194.

176) D. Carmona, M. P. Lamata, F. Viguri, E. San José, A. Mendoza, F. J. Lahoz, P. García-Orduña, R. Atencio, L. A. Oro, *J. Organomet. Chem*., **2012**, *717*, 152.

177) A. López-Pérez, J. Adrio, J. C. Carretero, *Angew. Chem. Int. Ed*., **2009**, *48*, 340.

178) S. H. Wu, W. Q. Sun, D. W. Zhang, L. H. Shu, H. M. Wu, J. F. Xu, X. F. Lao, *J. Chem. Soc. Perkin Trans*, **1998**, *1*, 1733.

179) E. E. Maroto, M. Izquierdo, S. Reboredo, J. Marco-Martínez, S. Filippone, N. Martín, *Acc. Chem. Res*., **2014**, *47*, 2660.

180) H. Brunner, *Angew. Chem. Int. Ed*., **1983**, *22*, 897.

181) M. Nishio, M. Hirota, Y. Umezawa, The CH/π Interaction: Evidence, Nature, and Consequences, Wiley, **1998**.

182) E. R. Johnson, S. Keinan, P. Mori-Sánchez, J. Contreras-García, A. J. Cohen, W. Yang, *J. Am. Chem. Soc*., **2010**, *132*, 6498.

183) a) L. A. Oro, C. Claver, *Iridium Complexes in Organic Synthesis*, Wiley, **2009**. b) O. Saidi, J. M. J. Williams, P. G. Andersson, *Iridium Catalysis*, **2011**.

184) M. Kitamura, R. Noyori, *Ruthenium in Organic Synthesis*, Wiley-VCH Verlag GmbH & Co. KGaA, **2005**.

185) H. Yang, X. Cui, X. Dai, Y. Deng, F. Shi, *Nat. Commun*., **2015**, *6*, 6478.

186) a) M. H. S. A. Hamid, P. A. Slatford, J. M. J. Williams, *Adv. Synth. Catal*., **2007**, *349*, 1555. b) G. Guillena, D. J. Ramón, M. Yus, *Chem. Rev*., **2010**, *110*, 1611. c) G. E. Dobereiner, R. H. Crabtree, *Chem. Rev*., **2010**, *110*, 681.

187) A. Wetzel, S. Wöckel, M. Schelwies, M. K. Brinks, F. Rominger, P. Hofmann, M. Limbach, *Org. Lett*., **2013**, *15*, 266.

188) a) X. G. Li, X. F. Wu, W. P. Chen, F. Hancock, F. King, J. L. Xiao, *Org. Lett*., **2004**, *6*, 3321. b) X. F. Wu, X. G. Li, F. King, J. L. Xiao, *Angew. Chem*. **2005**, *117*, 3473, *Angew. Chem. Int. Ed*., **2005**, *44*, 3407. c) X. F. Wu, D. Vinci, T. Ikariya, J. L. Xiao, *Chem. Commun*. **2005**, 4447. d) X. H. Li, J. Blacker, I. Houson, X. F. Wu, J. L. Xiao, *Synlett* **2006**, 1155. e) X. F. Wu, J. K. Liu, X. H. Li, A. ZanottiGerosa, F. Hancock, D. Vinci, J. W. Ruan, J. L. Xiao, *Angew. Chem. Int. Ed*., **2006**, *45*, 6718. f) X. F. Wu, J. K. Liu, D. D. Tommaso, J. A. Iggo, C. R. A. Catlow, J. Bacsa, J. L. Xiao, *Chem. Eur. J*., **2008**, *14*, 7699.

189) a) A. B. III Smith, R. M. Strongin, L. Brard, G. T. Furst, W. J. Romanow, K. G. Owens, R. J. Goldschmidt, *J. Chem. Soc., Chem. Comm.*, **1994**, 2187. b) A. F. Kiely, R. C. Haddon, M. S. Meier, J. P. Selegue, C. Pratt Brock, B. O. Patrick, G. W. Wang, Y. Chen, *J. Am. Chem. Soc.*, **1999**, *121*, 7971. c) T. Sternfeld, C. Thilgen, R. E. Hoffman, M. R. Colorado Heras, F. Diederich, F. Wudl, L. T. Scott, J. Mack, M. Rabinovitz, *J. Am. Chem. Soc.*, **2002**, *124*, 5734.

190) C. Hadad, Z. Syrgiannis, A. Bonasera, M. Prato, *Eur. J. Org. Chem.*, **2015**, *7*, 1423.

191) H. Kitamura, K. Kokubo, T. Oshima, *Org. Lett.*, **2007**, *9*, 4045.

192) M. S. Meier, M. Poplawska, A. L. Compton, J. P. Shaw, J. P. Selegue, T. F. Guarr, *J. Am. Chem. Soc.*, **1994**, *116*, 7044.

193) T. Oshima, H. Kitamura, T. Higashi, K. Kokubo, N. J. Seike, *Org. Chem.*, **2006**, *71*, 2995.

194) M. Izquierdo, M. R. Cerón, M. M. Olmstead, A. L. Balch, L. Echegoyen, *Angew. Chem., Int. Ed.*, **2013**, *52*, 11826.

195) T. Tada, Y. Ishida, K. Saigo, *J. Org. Chem.*, **2006**, *71*, 1633.

196) T. Ito, T. Iwai, F. Matsumoto, K. Hida, K. Moriwaki, Y. Takao, T. Mizuno, T. Ohno, *Synlett.*, **2013**, *24*, 1988.

197) D. Mühlbacher, M. Scharber, M. Morana, Z. Zhu, D. Waller, R. Gaudiana, C. Brabec, *Adv. Mater.*, **2006**, *18*, 2884.

198) a) W. W. H. Wong, J. Subbiah, J. M. White, H. Seyler, B. Zhang, D. J. Jones, A. B. Holmes, *Chem. Mater.*, **2014**, *26*, 1686. b) R. Tao, T. Umeyama, K. Kurotobi, H. Imahori, *ACS Appl. Mater. Interfaces*, **2014**, *6*, 17313.

199) a) X. Meng, G. Zhao, Q. Xu, Z. a. Tan, Z. Zhang, L. Jiang, C. Shu, C. Wang, Y. Li, *Adv. Funct. Mater.*, **2014**, *24*, 158. b) W. W. Wong, J.

Subbiah, J. M. White, H. Seyler, B. Zhang, D. J. Jones, A. B. Holmes, *Chem. Mater*., **2014**, *26*, 1686.

200) F. Zhao, X. Meng, Y. Feng, Z. Jin, Q. Zhou, H. Li, L. Jiang, J. Wang, Y. Li, C. Wang, *J. Mater. Chem. A*, **2015**, *3*, 14991.

201) Y. H. Liu, J. B. Zhao, Z. K. Li, C. Mu, W. Ma, H. W. Hu, K. Jiang, H. R. Lin, H. Ade, H. Yan, *Nat. Commun*., **2014**, *5*, 5293.

202) T. Umeyama, T. Miyata, A. C. Jakowetz, S. Shibata, K. Kurotobi, T. Higashino, T. Koganezawa, M. Tsujimoto, S. Gélinas, W. Matsuda, S. Seki, R. H. Friend, H. Imahori, *Chem. Sci*., **2016**, *8*, 181.

203) S. Dai, X. Zhang, W. Chen, X. Li, Z. Tan, C. Li, L. Deng, X. Zhan, M. Lin, Z. Xing, T. Wen, R. Ho, S. Xie, R. Huanga, L. Zhenga, *J. Mater. Chem. A*, **2016**, *4*, 18776.

204) D. Feller, K. A. Peterson, *Theochem*., **1997**, *400*, 69.

205) G. A. Dolgonos, G. H. Peslherbe, *Phys. Chem. Chem. Phys*., **2014**, *16*, 26294.

206) S. Aroua, M. Garcia-Borràs, S. Osuna, Y. Yamakoshi, *Chem. Eur. J*., **2014**, *20*, 14032.

207) D. D. Perrin, I. F. Amariego, D. R. Perrin, *Purification of laboratory Chemicals*, Pergamon Press, Oxford, **1980**.